NASA-CR-165,571

NASA Contractor Report 165571

NASA-CR-165571
19830004181

BENCHMARK NOTCH TEST FOR LIFE PREDICTION

P. A. Domas

General Electric Company
Cincinnati, Ohio

and

W. N. Sharpe and M. Ward

Louisiana State University
Baton Rouge, Louisiana

and

J. F. Yau

General Electric Company
Cincinnati, Ohio

LIBRARY COPY

NOV 24 1982

LANGLEY RESEARCH CENTER
LIBRARY, NASA
HAMPTON, VIRGINIA

October 1982

Prepared for

NATIONAL AERONAUTICS AND SPACE ADMINISTRATION
Lewis Research Center
Under Contract NAS3-22522

PREFACE

This technical program was conducted in a joint effort by the General Electric Aircraft Engine Business Group and Louisiana State University under Contract NAS3-22522.

The Technical Managers were Dr. P. A. Domas (General Electric) and Dr. W. N. Sharpe (Louisiana State University). Mr. J. A. McKenzie was General Electric Program Manager.

Mr. M. Ward conducted the notch experiments as part of his Master of Science Program at Louisiana State University. Dr. J. F. Yau conducted the analytical strain analysis studies at General Electric.

Mr. J. Jortner developed the plotting routines at LSU and Mr. C. Capsis (GE) designed the test specimen and adapted the initial test system.

Drs. J. Laflen and D. Corbly wrote the Technical Proposal for this program and their creative thinking led to its initial planning and implementation.

N83-12451#

TABLE OF CONTENTS

TABLE OF CONTENTS (Concluded)

1.0 SUMMARY

A comprehensive set of local notch root strain measurements for a variety of load patterns in an Inconel 718 notch specimen at 649° C (1200° F) was obtained and documented using the laser Interferometric Strain Displacement Gage (ISDG). The ISDG was successfully adapted to the high-temperature measurements in this typical Ni-base superalloy and was shown to have a relative uncertainty of ±3% of the measured strain with an additional uncertainty of ±150 microstrain.

Measurements were made for six load patterns including continuous cyclic, creep and cyclic with tensile and comprehensive hold periods on flat, double-notch bars with an elastic stress concentration factor of 1.9.

Pedigree tensile and cyclic stress-strain data were also generated at 649° C and employed in a simple Neuber analysis to obtain analytic predictions for comparisons to test results. A modified Neuber approach and a limited finite-element study were also compared to the data.

A smooth bar specimen subjected to the notch root strain history recorded from a continuously cycled notch bar was also used to obtain stress behavior data for comparison to the predictions.

The Neuber analysis predicted the first cycle notch root behavior very well on the basis of hysteresis loop comparison when the notch root strain rate stress-strain response curve was used. The stabilized cyclic loops were not well predicted even when cyclic softening had stabilized. The modified Neuber equation (corrected for stress redistribution due to plasticity) and the finite-element analysis improved the cyclic correlation but did not totally resolve the problem.

The smooth bar test using the notch root strain history control shed additional light on this in that the maximum monotonic and stable cyclic stresses were well predicted by Neuber (as was the minimum stable cyclic stress) while the minimum monotonic (first cycle unload) was not. This suggests that kinematic-hardening assumptions may be incorrect for the early cyclic transition period.

The utility of the computerized data acquisition and storage system associated with the ISDG was demonstrated by examining cyclic history dependent parameters (e.g., loop area) on a cycle-by-cycle basis. These parameters were used to assess data quality as well as behavioral trends, and have potential for extension to life prediction application. The hysteresis loop elastic loading slope was used to predict notch root crack initiation which was confirmed by posttest microscopy.

The program objectives of generation of benchmark notch data in a turbine disk alloy at elevated temperature and comparison to a Neuber analysis were met. Significant implications for future model development were determined.

2.0 INTRODUCTION

2.1 THE NEED FOR A BENCHMARK TEST

Aircraft gas turbine engine components are subjected to severe stress, temperature, and environmental conditions. In these components, local stress raisers (e.g., notches, boltholes, welds, fillet radii) are very often life limiting areas in that low cycle fatigue failures generally initiate in these critical regions. Economic and reliability demands have prompted inordinate effort in development of analytic methods to first predict stresses and strains in these complex geometry regions and, ultimately, predict the low cycle fatigue life for components containing these necessary design features. These analytical developments have apparently been successful since numerous techniques (most notably in the form of finite-element computer models) have evolved. There remains, however, the need to check or verify these analytical methodologies against actual experimental data measurements. This is not a simple task. Most stress concentration regions in gas turbine engines are geometrically very small, eliminating many conventional extensometry methods for strain measurement. Further, conditions of interest include long times at elevated temperatures (near 649° C), eliminating conventional strain gage measurement methods. The laser Interferometric Strain Displacement Gage was recognized as having the potential to accomplish this demanding task and was employed in this program.

The overall objective of this program was the generation, measurement, and documentation of the actual strains incurred at the root of a discontinuity in cyclically loaded test samples subjected to inelastic deformation at high temperature where creep deformations readily occur. A secondary objective was to perform an analysis of the steady-state cyclic stress-strain response at the root of the discontinuity in the tested samples for comparison to the measured results.

A nickel-base gas turbine disk alloy (Inconel 718) was chosen for this program; however, the analysis and measurement methodologies are directly applicable to other materials as well, including blade and combustor alloys. Additional needless complications arising from material instability,

anisotropy, and extensive localized oxidation damage were avoided by choosing Inconel 718. These effects can be addressed in follow-on efforts. Test cycle elements known to be highly influential in complex cycle fatigue damage have been included.

Data from this program provide a unique data base for ascertaining the degree of correlation between measurements and available cyclic elastic-plastic-creep finite-element analysis computer programs.

These results will substantially impact high-technology design where notch fatigue life is the predominant component service life limitation and viable experimentally measured data have been lacking.

2.2 MORE GENERAL CONSIDERATIONS

One of the goals of solid mechanics is to enable the designer to predict the behavior of complicated structures from the material properties determined in simple tests. The most obvious example is design based on strength. Given the material properties from a simple one-dimensional test, the designer can predict failure of three-dimensional structures or components using the distortion energy theory. A more recent example is fracture mechanics in which material properties determined from compact tension or three-point bending tests are used to predict fracture in complicated geometries.

The interplay between analytical and experimental solid mechanics is vividly demonstrated in the development of stress concentration factors as a design tool over 60 years ago. Here again, the elastic properties from one-dimensional tests are used in computing the strains in complicated geometries. The analysis demonstrating the effect was available, but a new experimental tool - photoelasticity - was needed to verify that analysis and to determine stress concentration factors in components too complicated to analyze.

These same ideas carry over into design based on plastic yielding and also on fatigue. The Neuber relation is an analytical way of accounting for plastic yielding at stress concentrations, and it has been extended to fatigue predictions at stress concentrations. All of this work is in its infancy, having started approximately 15 years ago. But the subject of concern here -

low cycle fatigue behavior at stress concentrations at high temperature - has barely been born. The work reported herein is the first evaluation of the simple Neuber approach and a sophisticated finite-element code using experimental data taken from a stress concentration at high temperature. In analogy to photoelasticity, a new experimental technique - the interferometric strain displacement gage - was required to provide the data.

2.3 REVIEW OF EXPERIMENTAL TECHNIQUES

The measuring of cyclic elastic-plastic strains at the root of a notch in a high-temperature environment requires a versatile technique. The technique must be able to measure local strains in a high-strain gradient region. This requires a measuring system gage length which is small in comparison with the strain gradient region. The measuring technique must also be capable of measuring strain at a rate rapid enough to accurately obtain the cyclic response of the specimen. This requires either a continuous strain measuring device or the ability to measure at discrete points within a continuous load cycle. A third requirement of an acceptable measuring technique is that it cannot be adversely affected by a high-temperature environment.

Monotonic elastic-plastic strains occurring at a stress concentration have been accurately measured using a variety of techniques. A photodot technique was employed by Merrill (Reference 1) to measure plastic strains occurring around a hole in a flat plate. A photoelastic coating method was utilized by Dixon (Reference 2) while Durelli and Sciammarella (Reference 3) used the Moire method. These methods all yielded accurate results for the monotonic case, but are not suited for the cyclic case.

The measuring of cyclic elastic-plastic strains occurring at a stress concentration was first attempted by Griffith (Reference 4). He used electromagnetic strain gages with a gage length of 12.7 mm (0.5 in.). This large gage length required the use of specimens which were 1473 mm x 610 mm (58 in. x 24 in.) with a 102 mm (4 in.) diameter hole in the center to maintain a large ratio between the size of the stress concentration and the gage length of the measuring system. The accuracy of Griffith's measurements was considered to

be within ±7.5%. A similar large-scale specimen was used by Carroll, et al. (References 5, 6, 7). A specially designed strain transducer was used in "super-scale" aluminum specimens containing a 50 mm (2.0 inch) diameter center hole to monitor complex strain histories. Crews and Hardrath (Reference 8) employed electric resistance strain gages with gage lengths of 1.59 mm (0.0625 in.). Crews reported a problem in maintaining the integrity of the bond between the gage and specimen throughout the duration of the test. Leis, et al. (Reference 9), taking advantage of the improved technology in resistance strain gages, employed gages with gage lengths of 0.38 mm (0.015 in.). This smaller gage allowed for the use of smaller specimens, but the problem encountered by Crews was still prevalent.

The interferometric strain displacement gage was utilized by Bofferding (Reference 10) to measure cyclic strains at notch roots. This method, unlike the resistance strain gage, does not measure strain continuously, but measures very rapidly at discrete points within a continuous load cycle. The ISDG has a gage length which is typically 0.1 mm (0.004 in.) and is a noncontacting laser-based measuring system.

Guillot (Reference 11) extended the ISDG measuring system to measure cyclic elastic-plastic strains in notch roots of aluminum and steel specimens at 149° C (300° F) and 260° C (500° F), respectively.

One of the purposes of this study was to measure and document elastic-plastic strains in the root of a notch under a variety of load patterns at a test temperature of 649° C (1200° F). The specimen material to be tested was Inconel 718, a superalloy used in the aircraft turbine industry. This was accomplished utilizing the ISDG measuring system previously developed. The ISDG is fully described in this report, as are the results from each test.

2.4 REVIEW OF ANALYTIC TECHNIQUES

Analytic determination of stresses and strains in stress concentration regions has been widely studied. Often, elastic stress concentration factors, K_t (ratio of local stress to stress away from the concentration), have been determined for design use. For the case of purely elastic stresses (low K_t

and/or applied load), closed form solutions of many notched, holed, and filleted structural geometries have been carried out by Neuber (Reference 12) and Savin (References 13 and 14). Finite-element computer techniques and photoelasticity are also widely used. Peterson (Reference 15) has tabulated many of these results in convenient graphical form.

For larger K_t's and higher stresses, an elastic-plastic analysis that accounts for local notch root yielding is necessary since linear elastic assumptions no longer apply. Neuber (Reference 16) has presented an analytical approximate means for determining local stresses and strains for cases beyond the yield point. Since this method has been widely used (References 17 through 20), it was selected for evaluation in this program and will be discussed in detail in this report. Other empirical methods such as the Stowell-Hardrath-Ohman (Reference 21) secant modulus approach have been used and modified (Reference 22) to obtain acceptable stress-strain predictions for various cases. More recently, however, elastic-plastic finite-element methods have been employed to determine local plastic stress and strain fields (References 5, 23, and 24). Because of modelling versatility, this approach appears to offer the most promise to provide a reliable means for expedient solution of complicated notch geometry stress and strain distributions. Socie (Reference 25), for example, has developed and demonstrated the viability of a two-dimensional finite-element model that not only modeled cyclic notch root behavior but also accounted for cyclic plasticity and residual stresses and strains due to a growing fatigue crack.

Analytical predictions of notch root stress and strain for the specimens in this program were made using a Neuber-based model. Some additional analyses utilizing an elastic-plastic-creep finite-element code (Reference 26) were also made.

2.5 PROGRAM ORGANIZATION

This program combined the resources of the General Electric Company and Louisiana State University. The General Electric Company utilized extensive analytical capability and computational facilities to conduct the analytical tasks in the program. In addition, based on extensive aircraft engine turbine

disk alloy experience, a large material data base, and substantial material behavior understanding, General Electric provided for the procurement of material and test specimen manufacture in accord with high aircraft engine industry standards.

The notched root strain measurement tasks were conducted by Dr. W.N. Sharpe and Mr. M. Ward of Louisiana State University. The ISDG and associated minicomputer-controlled system for fringe motion monitoring are highly suited for the measurement tasks in this program. The measurement facilities developed by Dr. Sharpe at LSU offered an excellent and highly viable approach to precisely measuring local notch root strains.

The approach consisted of a five-phase effort as shown diagrammatically in Figure 1. Task I was a material and specimen procurement phase that included final detail design of a suitable double-notch specimen. In Task II, the ISDG system was adapted to and checked against the measurement requirements for the program. Task III was the testing phase wherein both pedigree and benchmark notch tests were conducted. The pedigree data were used to conduct a detailed modified Neuber notch analysis in Task IV. And finally, measurements of notch root strain using the ISDG system were documented and compared to the analysis in Task V. A Task VI effort covering formal report presentation is also shown.

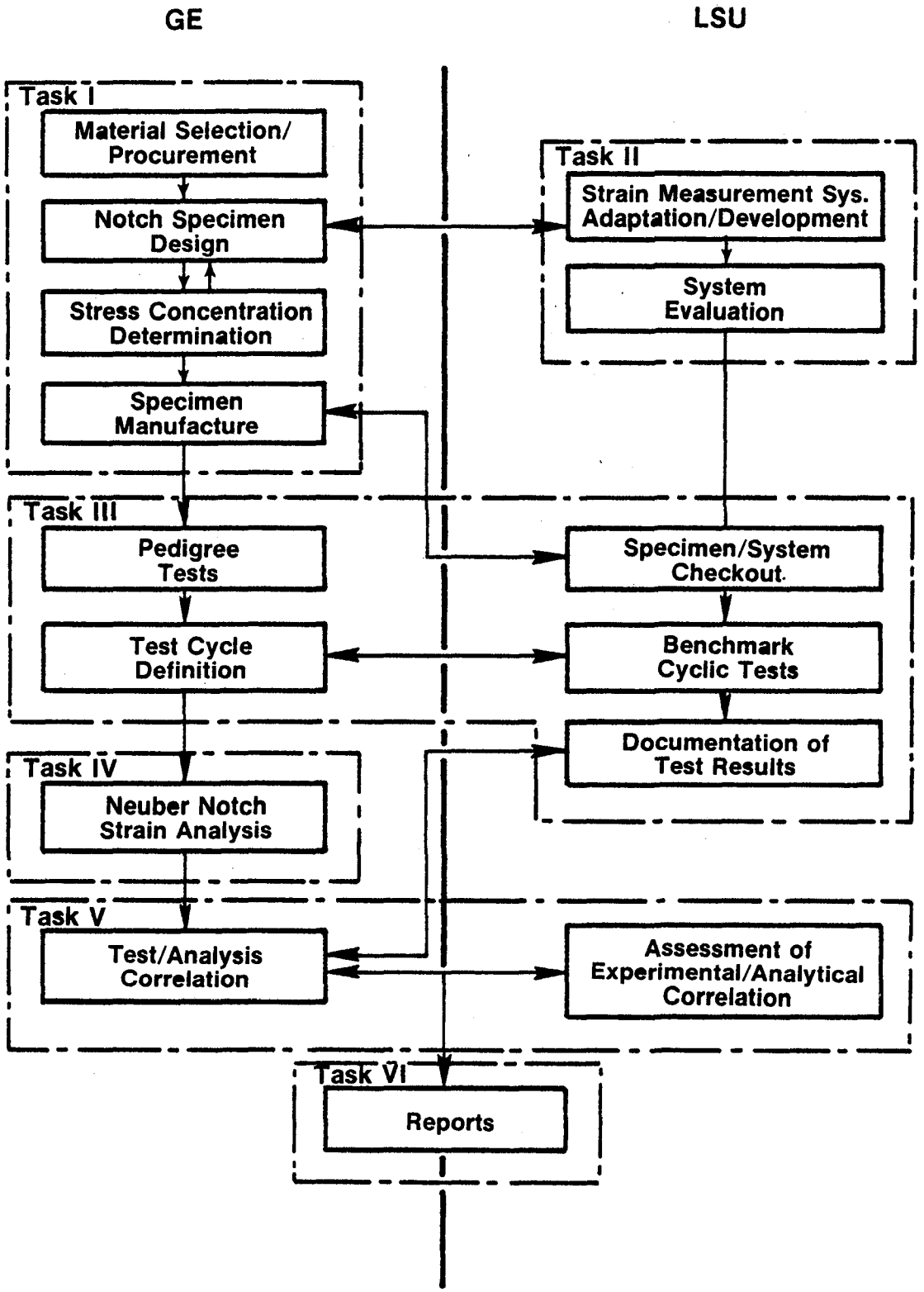

Figure 1. Technical Effort Flow Chart.

3.0 TASK I - MATERIAL AND SPECIMEN CHARACTERIZATION

In this section the rationale for material choice and the material and specimen specifications is presented.

3.1 MATERIAL SELECTION

The material used in this program was Inconel 718, a nickel-base superalloy widely used in current production gas turbine engines. This alloy is primarily used in turbine disk applications at temperatures approaching 649° C (1200° F).

An important material selection consideration, due to the objective of measuring highly localized strains, is microstructural homogeneity. A homogeneous and isotropic material is required in order that continuum mechanics analyses can be evaluated against these benchmark experimental results. For these reasons, a fine, equiaxed grain size is needed. Thermal mechanical processing parameters were available for Inconel 718 which would result in the desired microstructure. Consideration of the gage length of the strain measurement system indicated that an ASTM 9-11 grain size was desirable. This results in 6-12 grains on the average in the gage length. This grain size is achievable in Inconel 718, and the material used in this study was processed to obtain this microstructure.

In an effort to avoid material waste, bar stock was used as the test specimen material form. This material was heat treated to simulate disk forging properties.

Sixteen hundred and thirty-eight newtons (368 lb) of Inconel 718 25.4 mm (1.0 in.) OD centerless ground bar stock material were received from ATEK Metals Company, Woodlawn, Ohio. The material is from Teledyne ALLvac Heat No. S108. Vendor-supplied composition and certification test results are listed in Table I along with specification minimum and typical average properties. The material is well within specification and appears to have approximately average mechanical properties.

Table I. Vendor-Supplied Certification Properties.

Inconel 718, 25.4 mm (1.0 in.) diameter centerless ground bar stock Teledyne ALLvac heat No. S108, Spec. B50TF15AS-10, ATEK No. AT802370

a. Composition (Weight Percent)

Element	Specification	Vendor	Element	Specification	Vendor
Al	0.3-0.7	0.49	Mn	0.35 Max.	0.16
B	0.006 Max.	0.004	Mo	2.80-3.30	2.93
C	0.02-0.08	0.042	Ni	50.0-55.0	52.08
Cb+Ta	4.75-5.50	5.14	P	0.015 Max.	0.004
Co	1.0 Max.	0.53	S	0.015 Max.	0.002
Cr	17.0-21.0	17.42	Si	0.35 Max.	0.10
Cu	0.30 Max.	0.05	Ti	0.75-1.15	1.05
Fe	15.0-21.0	Bal.			

b. Mechanical Properties

Source	Temperature °C	Temperature °F	UTS MPa	UTS ksi	0.2% YS MPa	0.2% YS ksi	Elongation, %	RA, %	Hard. R_c
Vendor	21	70	1413	205	1152	167	21.2	41.2	43.5
Spec.	70	21	1241	180	1034	150	12.0	15.0	38-48
Typ. Avg.	21	70	1386	201	1165	169	18.0	30.0	---
Vendor	649	1200	1152	167	960	139	21.8	48.3	44
Spec.	649	1200	1000	145	862	125	10.0	15.0	38-48
Typ. Avg.	649	1200	1110	161	972	141	19.0	35.0	---

c. Stress Rupture*

Source	Temperature °C	Temperature °F	Stress MPa	Stress ksi	Life, hr	Elongation, %	RA, %
Vendor	649	1200	759	110	89.1	25.8	---
Spec.	649	1200	689	100	25 min	>5.0	---

d. Grain Size

Vendor: Avg. ASTM 10
Spec. Avg. < ASTM 4 with Max. ASTM 2

*Smooth 6.35 mm (0.25 in.) nominal diameter bar.

It was planned to heat treat the as-received (annealed) material to standard forging specifications. There was concern, however, about potential undesirable grain growth during the solution heat treatment. To evaluate this, random samples were removed and heat treated to the two schedules in Table II. The first is the standard (C50TF6) forging specification heat treatment and includes a solutioning cycle. The second treatment eliminates the solution cycle.

Table II. Heat Treat Schedules Evaluated on Small Samples of Inconel 718 Bar Stock Heat S108.

Treatment No. 1 (Standard C50TF6 Specification)

968° C (1775 °F) - 1 hr - He Quench plus
718° C (1325° F) - 8 hr - Furnace Cool 38° C (100° F)/hr
to 621° C (1150° F) - 8 hr - Air Cool to Room Temperature

Treatment No. 2 (Nonstandard)

718° C (1325° F) - 8 hr - Furnace Cool 38° C (100° F)/hr
to 621° C (1150° F) - 8 hr - Air Cool to Room Temperature

The optical micrographs in Figure 2 show the resulting microstructures. The nonstandard treatment had excessive δ (Ni_3Cb) phase at the grain boundaries. The standard treatment had a representative forging structure with small (ASTM 10) grain size confirming no undesirable grain growth occurs. The remainder of the material was heat treated to the standard forging specification.

Table III details the allocation of the material. Sufficient material was purchased to provide a 1100 N (250 lb) stockpile as well as the listed quantity of specimens. Only the specimen material was heat treated. The stockpile material remains in the as-received annealed condition*.

*Small quantities of this material are available to other researchers. Inquiries should be directed to the NASA Project Manager at the address provided in Section 5.3.

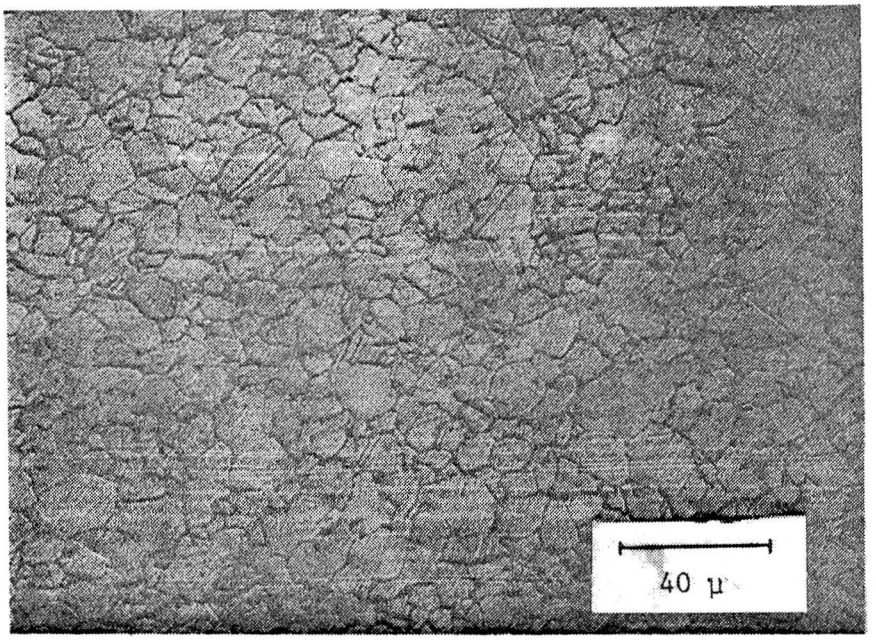

500x

(a) Heat Treat No. 1, Solution and Age (Spec B50TF15)

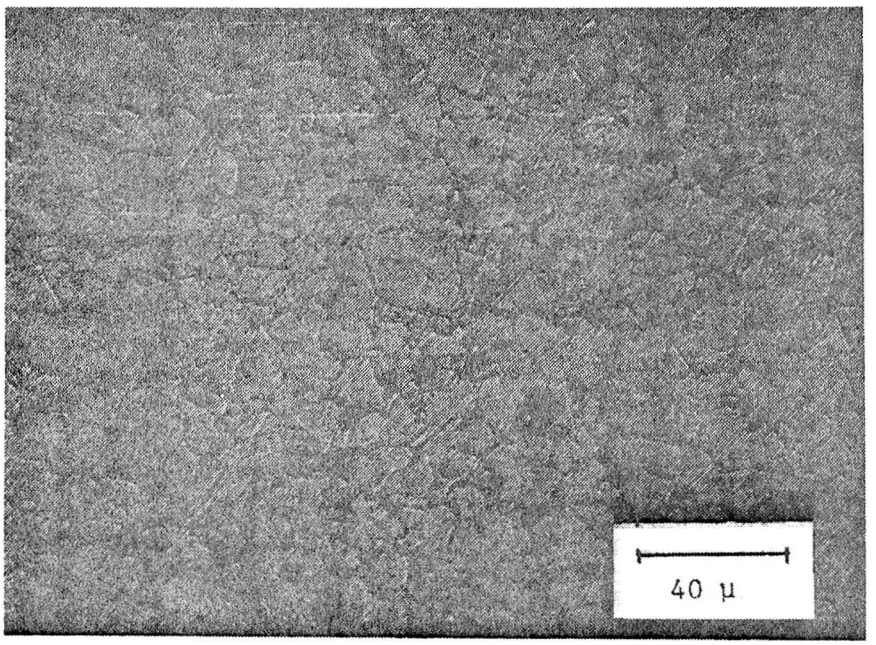

500x

(b) Heat Treat No. 2, No Solution, Age Only

Figure 2. Optical Micrographs of Inconel 718 1-Inch Diameter Bar Stock, Teledyne ALLvac Heat No. S108. ASTM Grain Size 10.

Table III. Material Allocation.

Specimen Type	Drawing No.	Quantity	Test Description
Tensile	4013195-002	16	8 - Tensile Pedigree
			8 - Creep Pedigree
Low Cycle Fatigue	401195-202	16	8 - LCF Pedigree
			4 - Cyclic $\sigma - \varepsilon$
			4 - ε-Control to measured notch ε
Flat Double Notch ($K_t = 1.90$)	CAP 111280P01	14	12 - Benchmark Tests
			2 - System Checkout
Flat No Notch ($K_t = 1.0$)	CAP 111280P02	1	1 - System Checkout

25.4 mm - Centerless Ground Inconel 718 Bar Stock Requirements

Tensile - 95.3 mm × 16 = 1524 mm = 1.52 m (5 ft)

LCF - 139.7 mm × 16 = 2235 mm = 2.24 m (7.5 ft)

Notch - 266.7 mm × 15 = 4000 mm = 4.0 m (13 ft)

plus Heat Treat(1) Assessment = 305 mm (1.0 ft)

plus Stockpile (1100 N) = 29.3 m (96.0 ft)

(1)Heat Treat to ASTM 9-11 Grain Size (C50TF6 Forging Specification).

3.2 PEDIGREE TESTING

To assess material pedigree, a series of standard tensile and rupture tests was conducted. In addition, to acquire data needed for notch strain analysis, cylic stress-strain curve data were also obtained.

3.2.1 Tensile and Rupture Testing

Tensile and creep-rupture pedigree assessment specimens were manufactured to the dimensions and specifications shown in Figure 3. The specimens were manufactured by Metcut Research Associates, Cincinnati, Ohio. The tests were conducted in the Material and Process Technology Laboratories at General Electric.

Table IV tabulates the results of four tensile tests (two each at 21° C and 649° C) and four creep-rupture tests (all at 649° C). Also shown in the table for comparison are average standard results for forged Inconel 718.

At 21° C, the average results of the two tensile pedigree tests agree fairly well with average forging properties. Yield strength is about 40 MPa (6 ksi) lower and ultimate strength about 20 MPa (3 ksi) higher than average. Ductility for the benchmark material is moderately higher.

At 649° C, the benchmark material is 13-55 MPa (2-8 ksi) higher in strength level and much more ductile (by nearly a factor of two) than standard material. This is thought to be the result of the very fine (ASTM 10) grain size in the bar stock.

Creep rupture results from Table IV are also plotted in Figure 4 for a comparison to a standard curve. The results indicate essentially average rupture life at 649° C (1200° F).

The creep behavior of the four specimens is shown in Figure 5 on a plot of creep strain versus time. These results are further detailed and compared to previous (standard) data in Figures 6, 7, and 8 and show time to specific inelastic strain levels as a function of stress. In general, the material exhibits essentially average creep response.

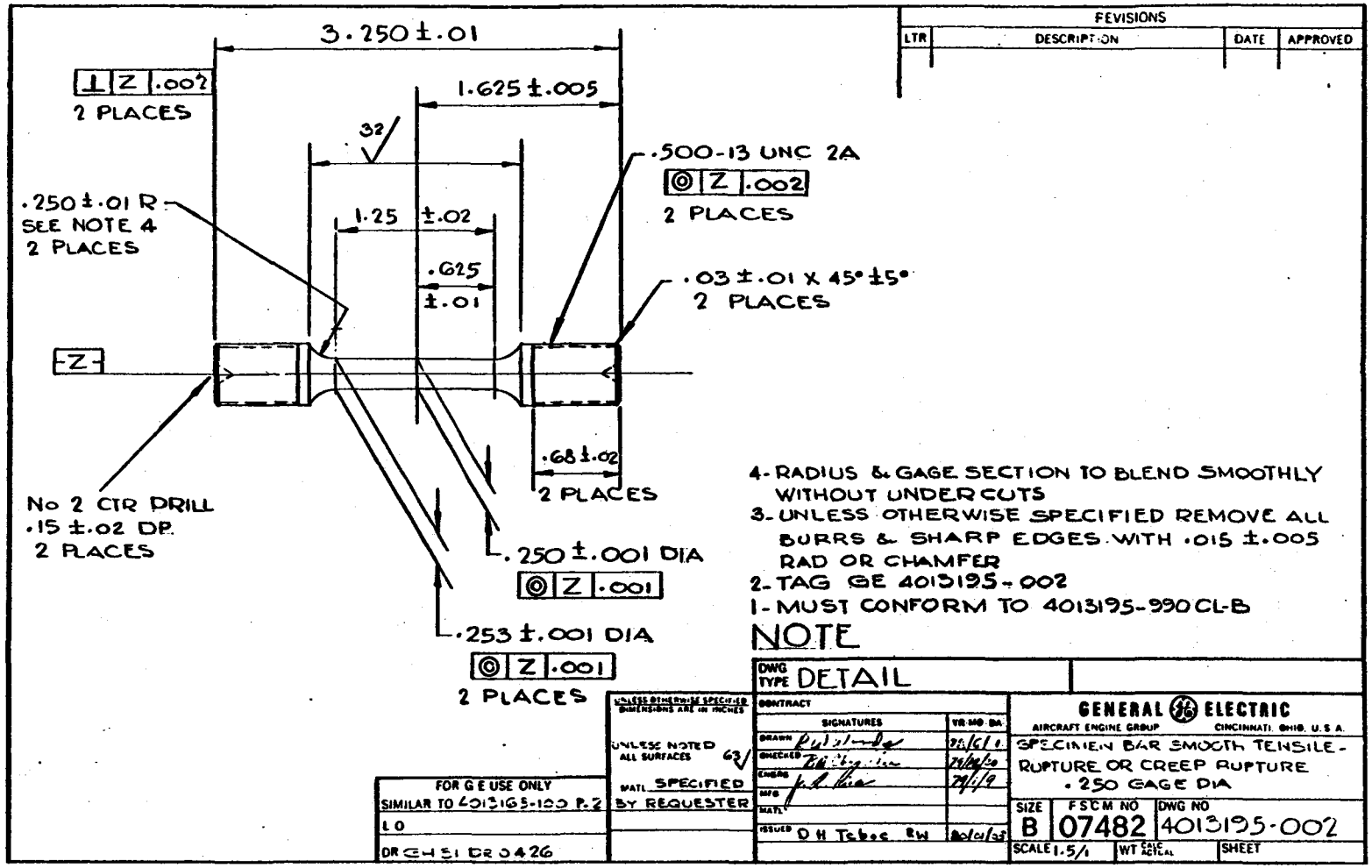

Figure 3. Tensile and Creep Rupture Pedigree Test Specimens.

Table IV. NASA Benchmark Notch Test Program, Pedigree Specimen Test Results.

(Inconel 718 Bar Stock, Heat Treated to Forging Specification, Heat No. S108)

Tensile

Spec. No.	Temperature °C	Temperature °F	0.02% YS MPa	0.02% YS ksi	0.2% YS MPa	0.2% YS ksi	UTS MPa	UTS ksi	RA, %	Elongation, %
11	21	70	1000	145	1156	168	1396	203	43	19
10	21	70	994	144	1123	163	1378	200	44	21
Average	21	70	997	145	1140	165	1387	201	44	20
Average Standard*	21	70	1034	150	1178	171	1364	198	31	17
7	649	1200	845	123	974	141	1140	165	51	22
2	649	1200	843	122	984	143	1151	167	66	27
Average	649	1200	844	123	979	142	1145	166	59	24
Average Standard*	649	1200	830	121	961	140	1091	158	26	16

Creep Rupture:

Spec. No.	Temperature °C	Temperature °F	Stress MPa	Stress ksi	Measured hr to Rupture	Average Standard* hr to Rupture
12	649	1200	551	80	1583	1600
4	649	1200	689	100	131	160
6	649	1200	758	110	92	50
1	649	1200	827	120	26	15

*C50TF6 Specification

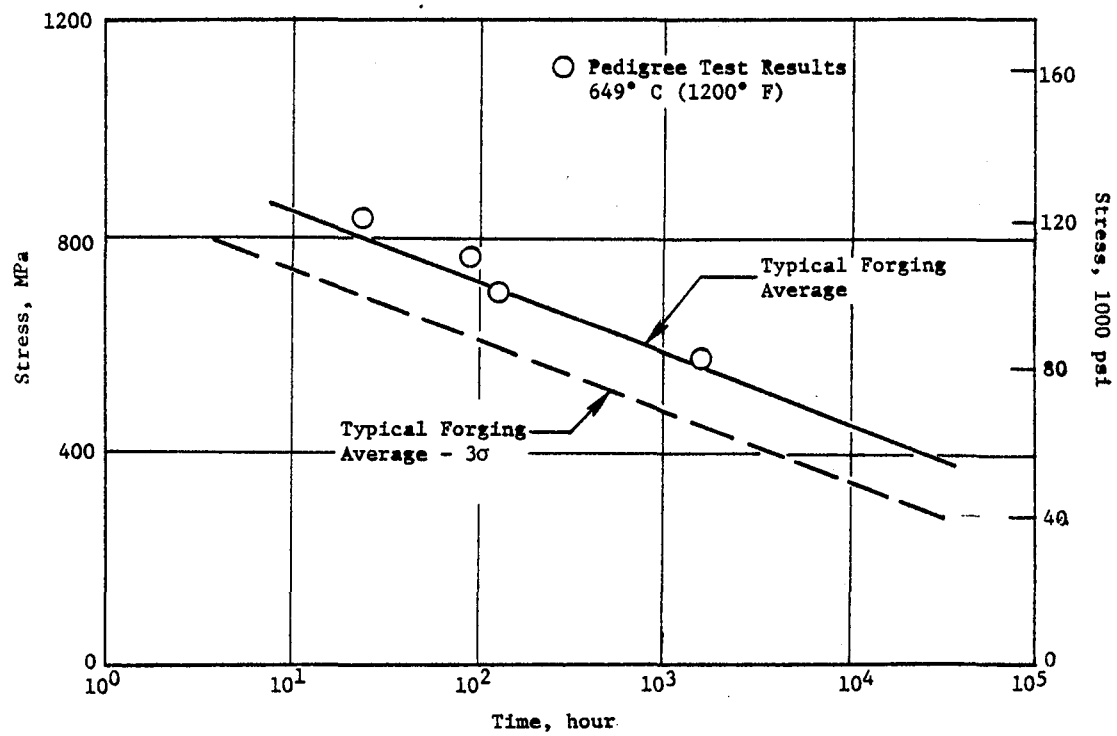

Figure 4. Isothermal Creep Rupture Tests Results, Inconel 718 Bar Stock, Heat Treated to Forging Specifications (C50TF6CLB), 649° C (1200° F), Heat Number S108.

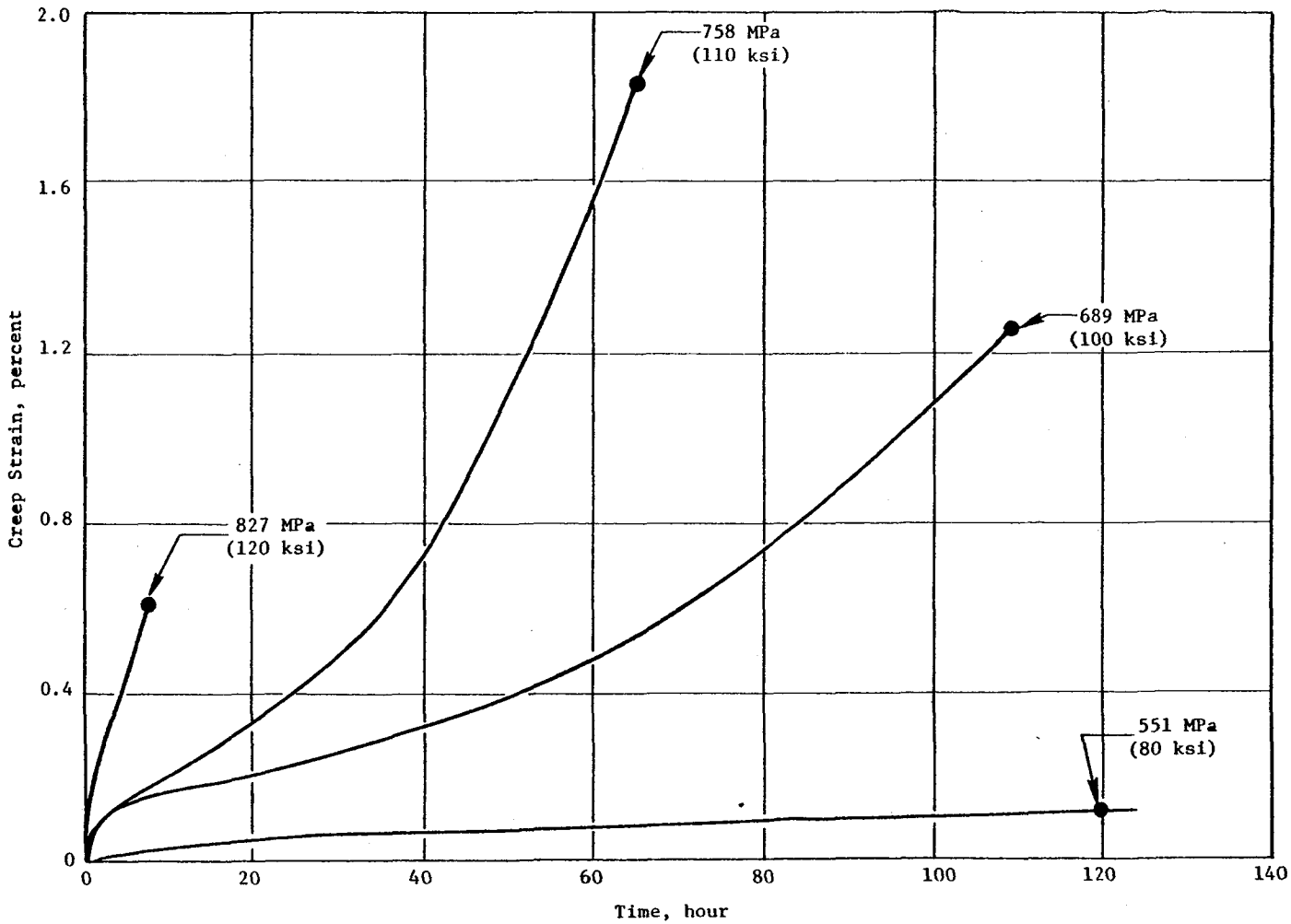

Figure 5. Creep Strain Versus Time for Several Test Stress Levels, Inconel 718 Bar Stock Heat Number S108, 649° C (1200° F).

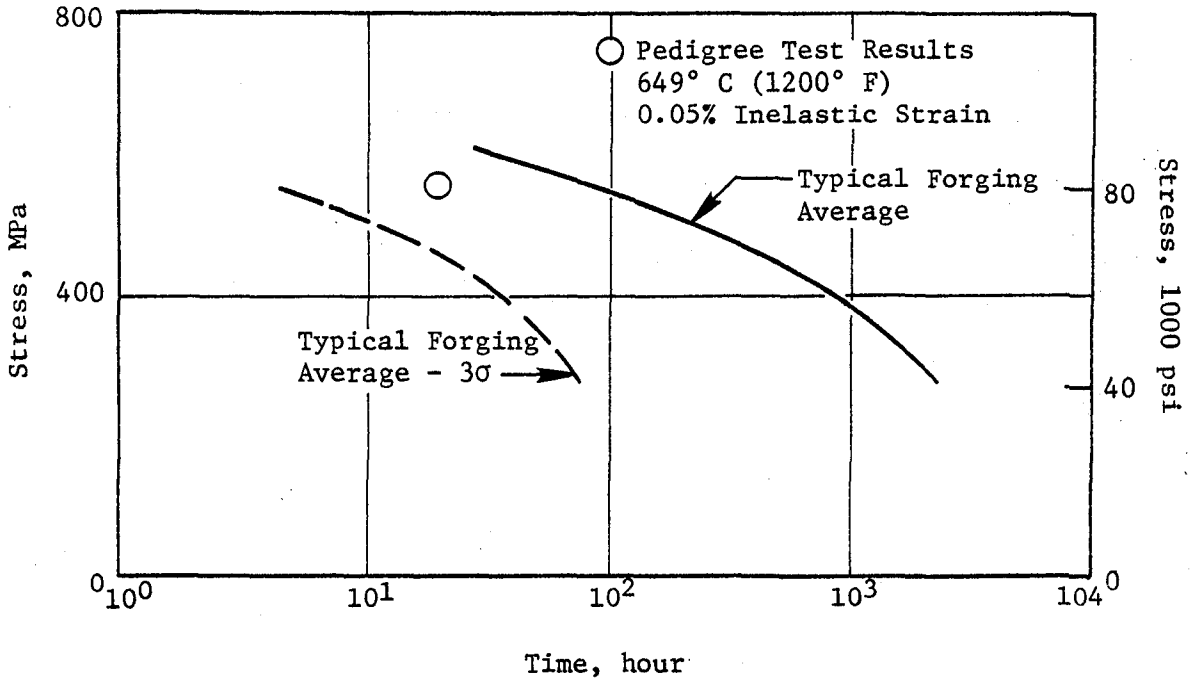

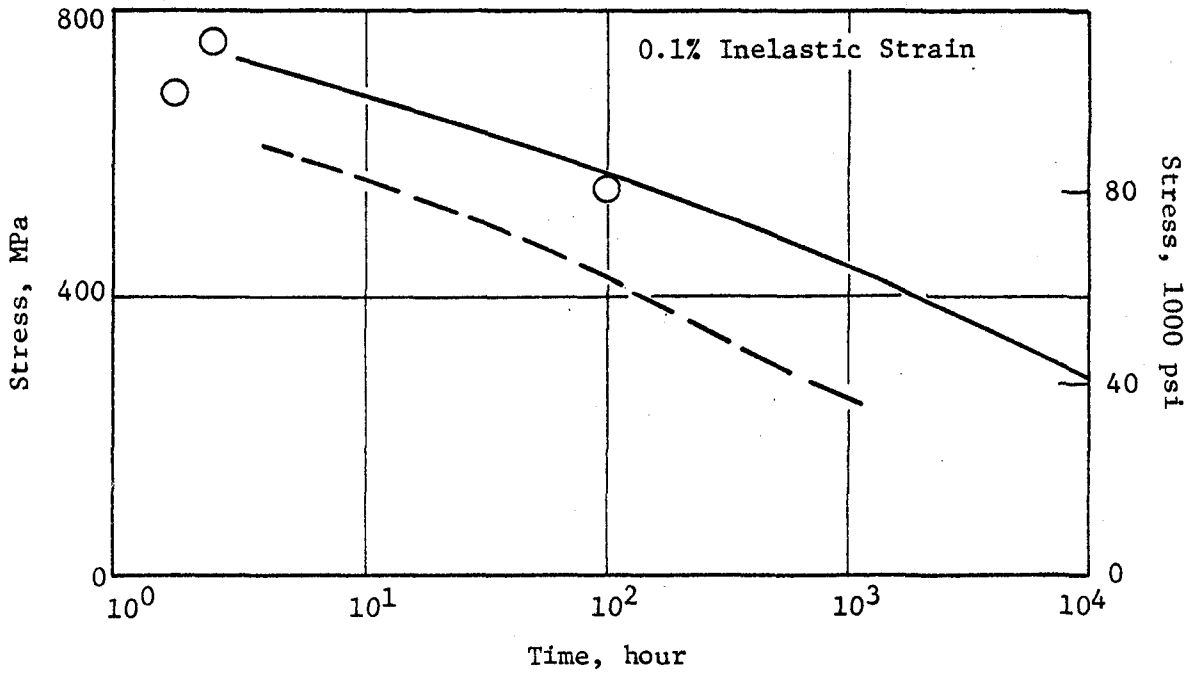

Figure 6. Time to Specific Inelastic Strain Levels, Inconel 718 Bar Stock, Heat Treated to Forging Specifications.

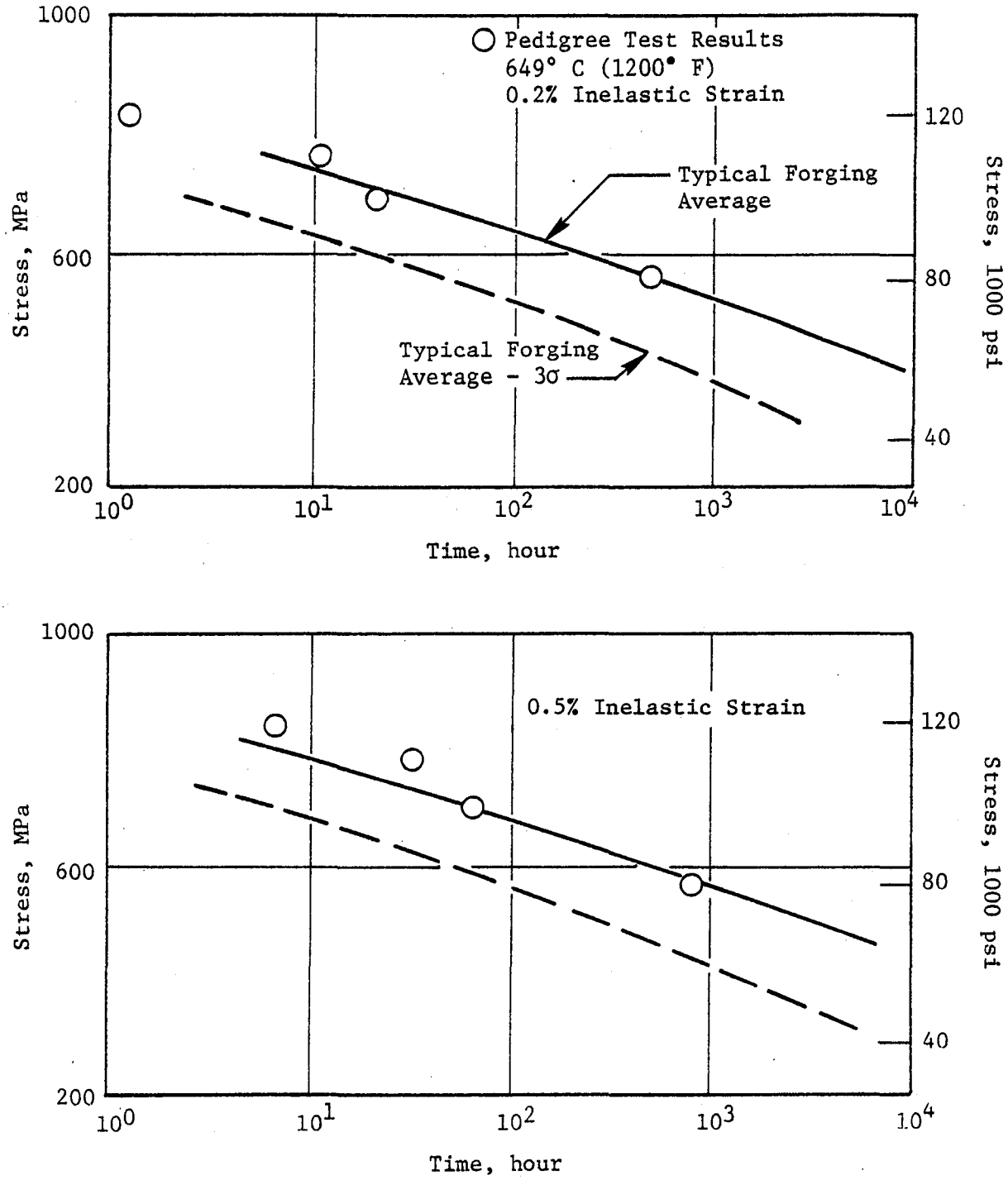

Figure 7. Time to Specific Inelastic Strain Levels, Inconel 718 Bar Stock, Heat Treated to Forging Specifications.

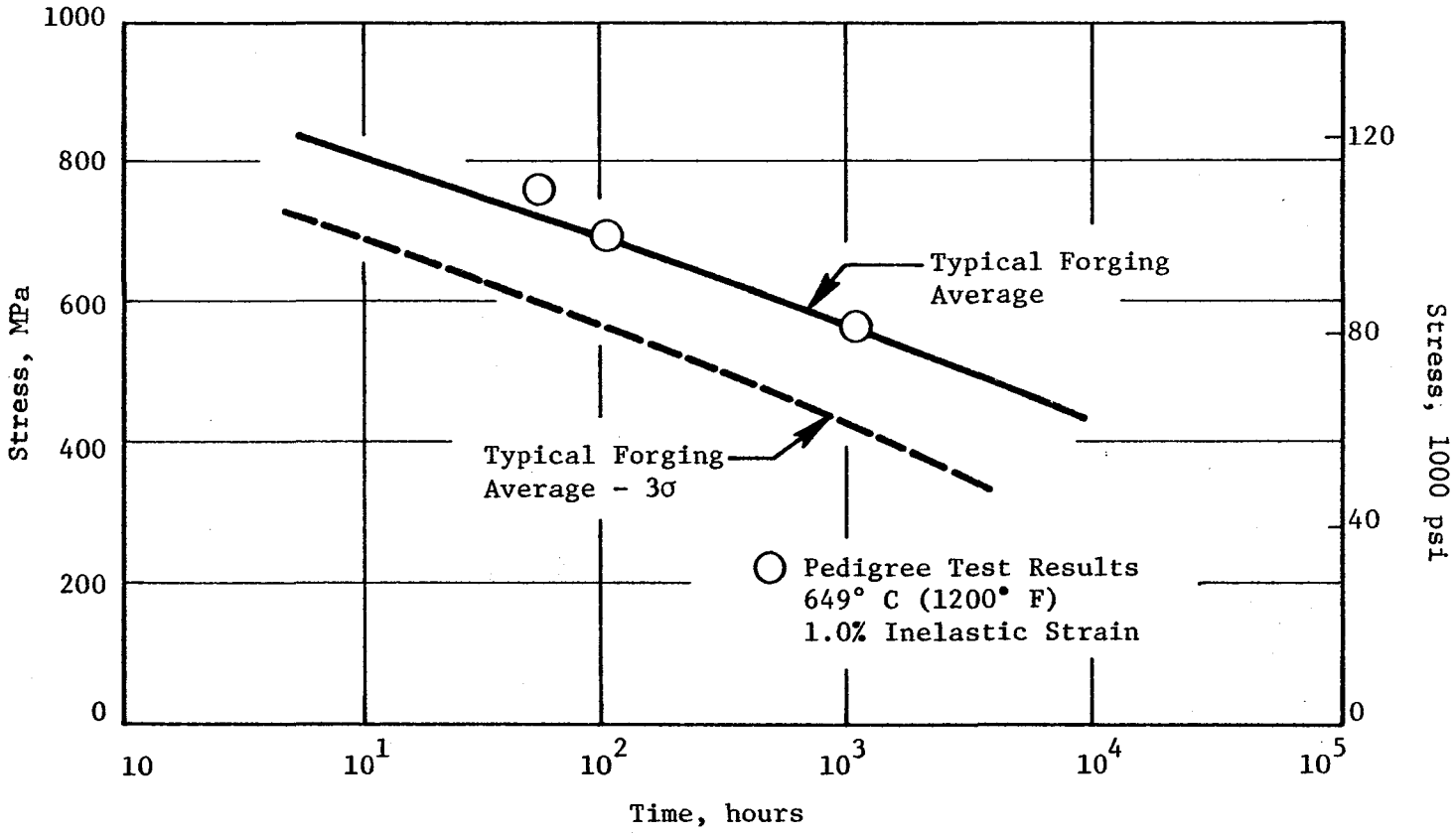

Figure 8. Time to Specific Inelastic Strain Levels, Inconel 718 Bar Stock, Heat Treated to Forging Spec. (C50TF6).

3.2.2 Cyclic Stress-Strain Curve Generation

Six cyclic stress-strain tests using longitudinal strain control low cycle fatigue test specimens (Figure 9) were used to characterize the cyclic material response. The specimens were manufactured and tested by Metcut Research Associates.

The cyclic stress-strain curve is of interest because many materials alter their deformation behavior after repeated loading. The material can harden, soften, or remain neutral. The bulk of the change is estimated to take place in approximately the first 20% of life, with only small changes taking place after that (Reference 27). However, for convenience and uniformity, the stable cyclic curve is usually defined at half life, $N_f/2$.

There is, however, no universal agreement on the exact definition of the cyclic stress-strain curve nor on the test procedure to obtain it. The most common technique involves plotting the locus of the tips of the stable stress-strain loops from several specimens subjected to different levels of completely reversed constant strain amplitudes. Because of the estimated rapid achievement of steady-state strain conditions, test efficiency can be improved by cycling each specimen to several levels of applied strain; this is shown in Figure 10a.

An alternate technique is shown in Figure 10b, where a triangular strain cycle with constant maximum strain is combined with a varying maximum strain to obtain a triangular wave shape with an increasing-decreasing amplitude. Another possible approach is to halt any of the cyclic tests at specimen half life and conduct a monotonic test.

It should be noted that the cyclic techniques are all based on testing experience at $R_\varepsilon = -1$ (R_ε = minimum strain/maximum strain). In an $R_\varepsilon = -1$ test, the material undergoes fully reversed loading about a mean strain of zero, resulting in load-displacement records that are essentially axisymmetric about the origin. The specimens do frequently develop a small, less than 34 MPa (5 ksi), compressive mean stress, however. Potential mean stress effects under other conditions were recognized by recommendations that multiple strain level tests be conducted using a high-to-low load sequence to eliminate the mean stress.

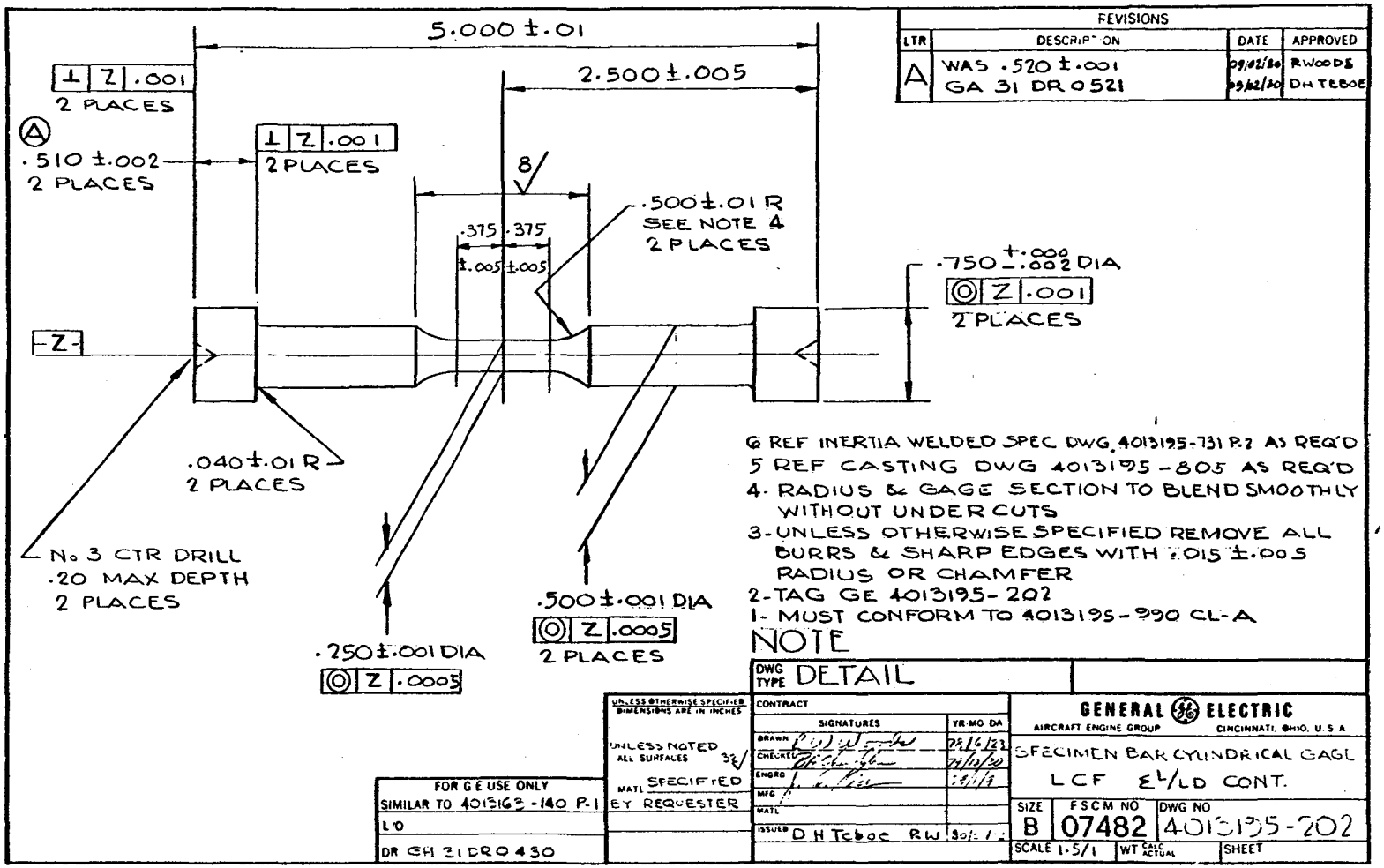

Figure 9. Longitudinal Strain Control Low Cycle Fatigue Test Specimens Used for Cyclic Stress - Strain Curve Generation.

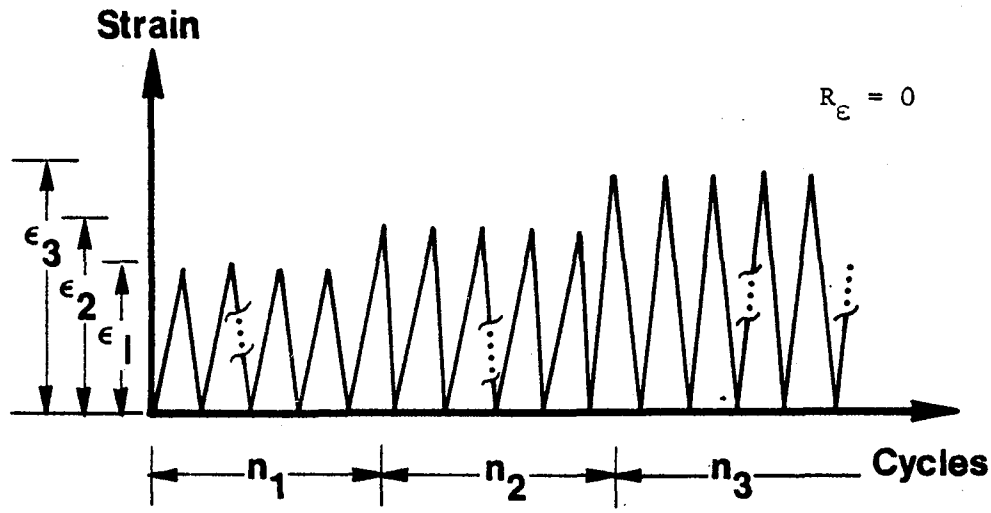

(a) Blocks of Constant Applied Strain Amplitude.

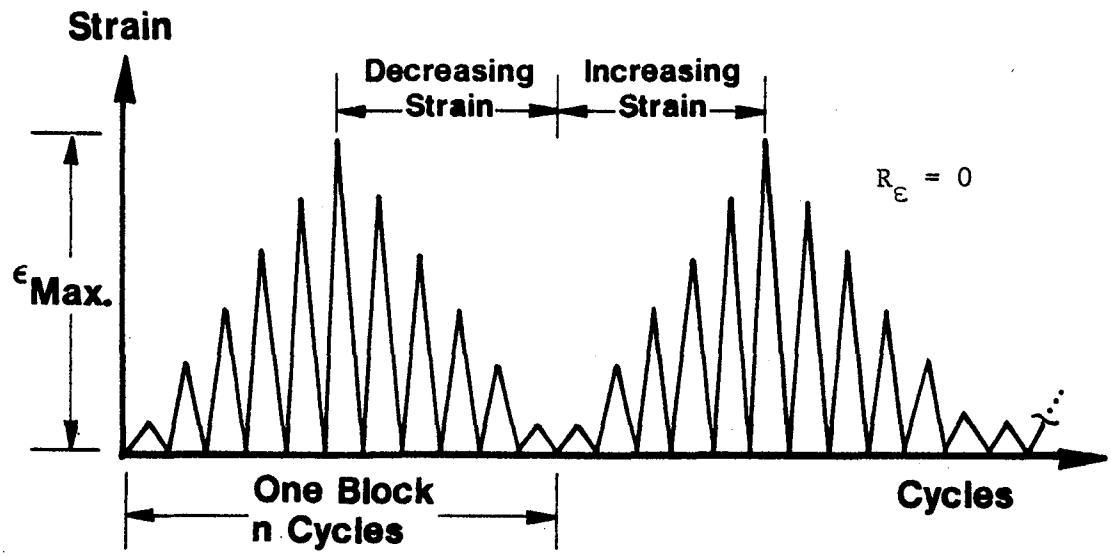

(b) Increasing-Decreasing Applied Strain Amplitude.

Figure 10. Cyclic Strain Patterns.

When a constant strain amplitude test is performed, a single point, i.e., $\Delta\varepsilon$, versus $\Delta\sigma$, on the cyclic curve is obtained for each test. However, if the increasing-decreasing blocks of Figure 10b are used, then, for $R_\varepsilon = -1$, the entire cyclic curve can be obtained from a single test. Because engine disk conditions frequently do not correspond to $R_\varepsilon = -1$ conditions, much of the current LCF work is conducted under $R_\varepsilon = 0$ conditions. Unlike $R_\varepsilon = -1$, the hysteresis loops obtained during a constant strain amplitude test and the loop at the corresponding strain range in the increasing-decreasing test mode are not the same.

In other words, this means that even when the increasing-decreasing amplitude technique is used, the entire cyclic curve cannot be obtained from a single test for $R_\varepsilon = 0$. At most, four or five points can be obtained from a multiple strain level test (Figure 10a) and only a single point on the curve is obtained when a constant maximum strain range is used. If we define the cyclic (or loop) amplitude as half the total stress range of the hysteresis loop, the cyclic amplitude can be determined as a function of strain range, regardless of the test condition. It should be independent of R ratio, as it describes the cyclic hardening/softening which is a material property. On the other hand, the mean stress, as has been indicated, depends on the test condition. Thus the cyclic stress-strain curve, as defined by the loop tips, depends on the R ratio.

Cook (Reference 28) has defined the "complete" cyclic stress-strain curve as the locus of the hysteresis loop tips rather than the loop amplitude which includes the influence of mean stress.

For this program, recognizing a dependence on strain rate, tests were run for $R_\varepsilon = -1$ and $R_\varepsilon = 0$ at controlled strain rates of 5%, 20%, and 100%/minute. All tests were done at 649° C. An incremental step-loading procedure, wherein an initial strain level is imposed, the specimen cycled to approximately one-quarter of its life, a second (higher) level is imposed, the specimen cycled to one-half life and so on to failure, was employed. Four steps were used in each test with a triangular waveform. For each step, stress and strain ranges were determined on the most nearly stabilized hysteresis loop in the block. It was anticipated that stabilization would occur in the allotted

block times. The first step was the only one, however, where stabilization did occur. In the other steps, the loops were nearly stable but were continuing to show small changes when the next block was started.

Monotonic stress-strain curves were also obtained at strain rates of 1%/minute and 20%/minute.

A summary of the stress-strain data obtained for this program is given in Table V.

Figure 11 shows the stress-strain response in terms of alternating stress and alternating plastic strain. Assuming a relation:

$$\sigma_{alt} = A\,(\varepsilon_{P_{alt}})^{n}$$

the A and n values in Table V were determined. In general the slope of these curves is near the expected value of ~0.1. For the 20%/minute, $R_\varepsilon = -1$, curve the lowest stress-strain point appears to be in error (at least in relation to the other data trends). This point has been ignored in constructing the curves of Figure 11.

Figure 12 compares cyclic stress-strain curves based on hysteresis loop amplitudes for these strain rates with $R_\varepsilon = -1$. Consistent data trends are observed. A strong strain rate dependence is shown with the higher rates having lower stress for a given strain.

Comparisons between the various curves are also shown in Figure 13. There is considerable scatter as evidenced by comparing the two $R_\varepsilon = 0$ cyclic curves. The complete stress strain curves represent the maximum stress and strain points in the hysteresis loops. The trend of the complete curve towards the cyclic curve is typical and illustrates that for small strain there is a stable mean stress present.

For reference, detailed test data are presented in Table VI.

Table V. Cyclic Stress-Strain Curve Parameters, Inconel 718, Heat Treated to Forging Specifications, 649° C (1200° F).

Type(1)	A(2) Ratio	R Ratio	$\dot{\epsilon}$ %/min	E(3)		A(4)		n(4)	C_c(5)
				X10^3 MPa	X10^6 psi	X10^3 MPa	ksi		
C	∞	-1	5.0	155	22.5	1.4	202.3	0.108	0.986
C	∞	-1	20.0	165	23.9	1.1 (1.3)(6)	157.6 (188.7)	0.083 (0.110)	0.993 (0.995)
C	∞	-1	100.0	158	22.9	1.1	156.6	0.092	0.995
C	1.0	0	20.0	165	24.0	1.4	196.6	0.121	0.998
C	1.0	0	20.0	164	23.8	1.4	197.7	0.106	0.999
M	---	---	1.0	161	23.4	1.2	166.9	0.054	0.997
M	---	---	20.0	164	23.8	1.4	210.0	0.063	0.995

(1)M-Monotonic; C-Cyclic

(2)A ratio = Alternating Strain/Mean Strain

(3)E measured at $N_f/2$ (Average for multistep tests)

(4)Strength Coefficient, A, and Strain-Hardening Exponent, n

(5)Correlation coefficient for straight-line curve fits

(6)Values in parentheses were determined without the results of the first load step.

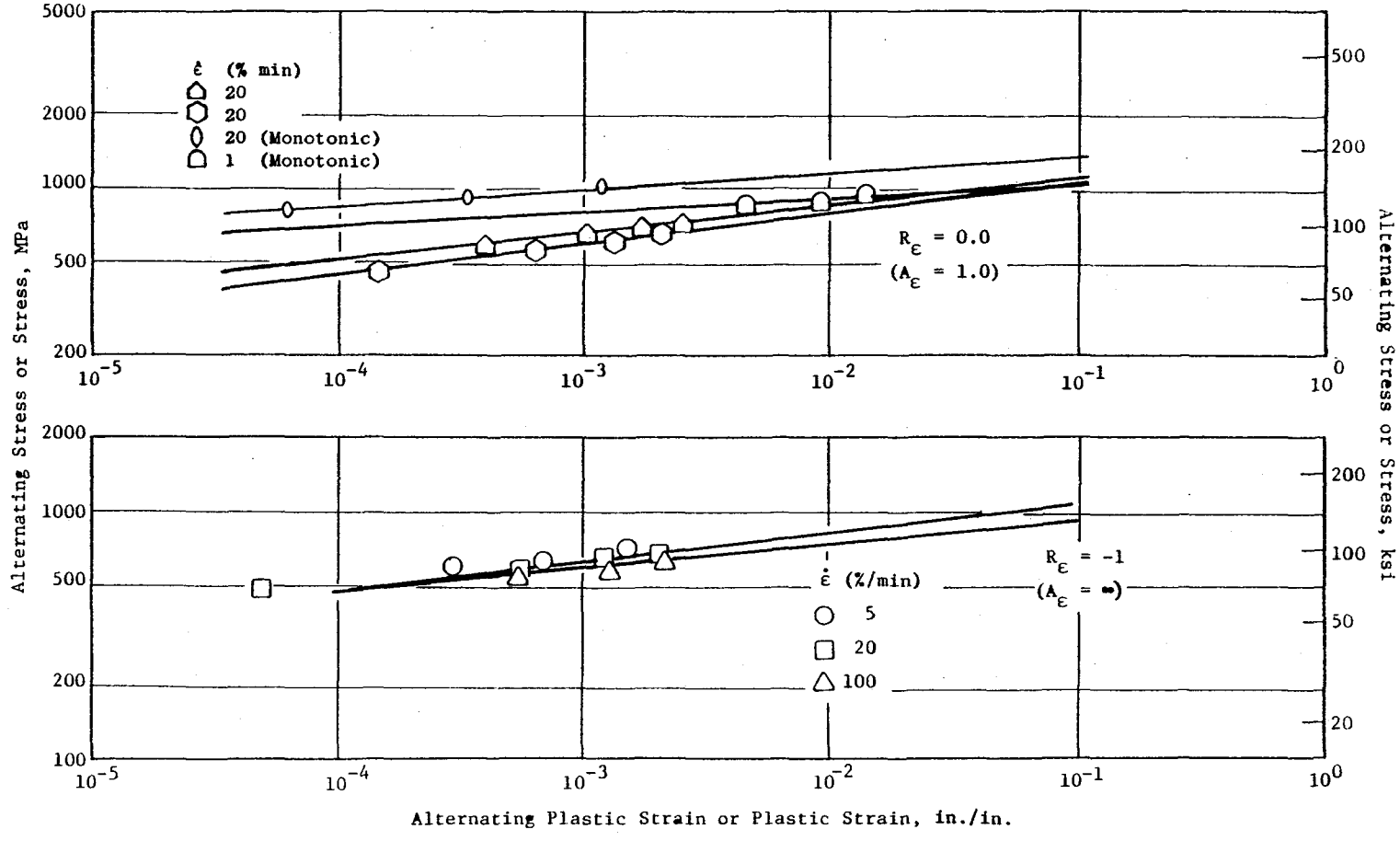

Figure 11. Cyclic Stress-Strain Curves - Inconel 718 Bar, 649° C (1200° F).

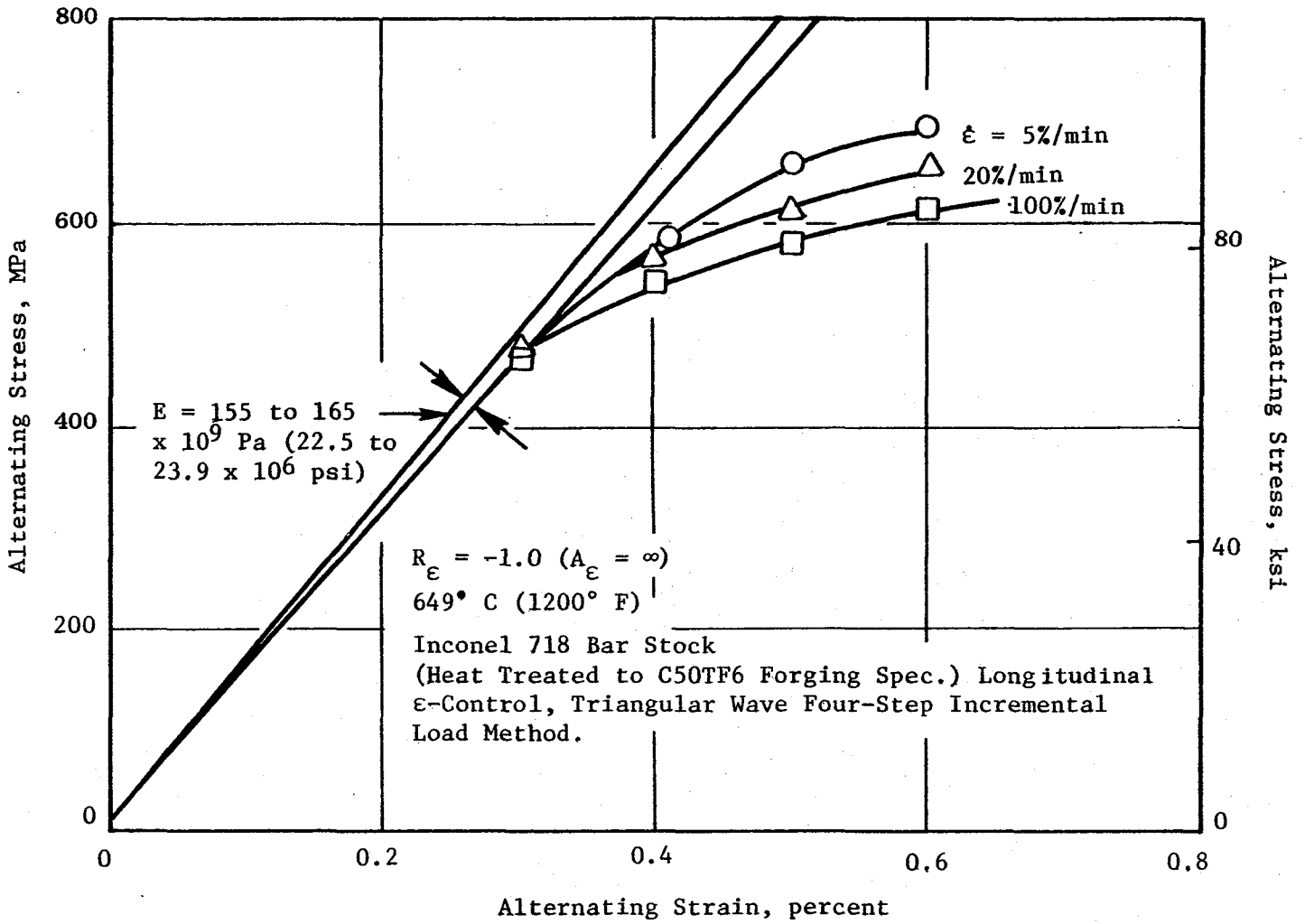

Figure 12. Cyclic Stress-Strain Curves Benchmark Notch Fatigue Program.

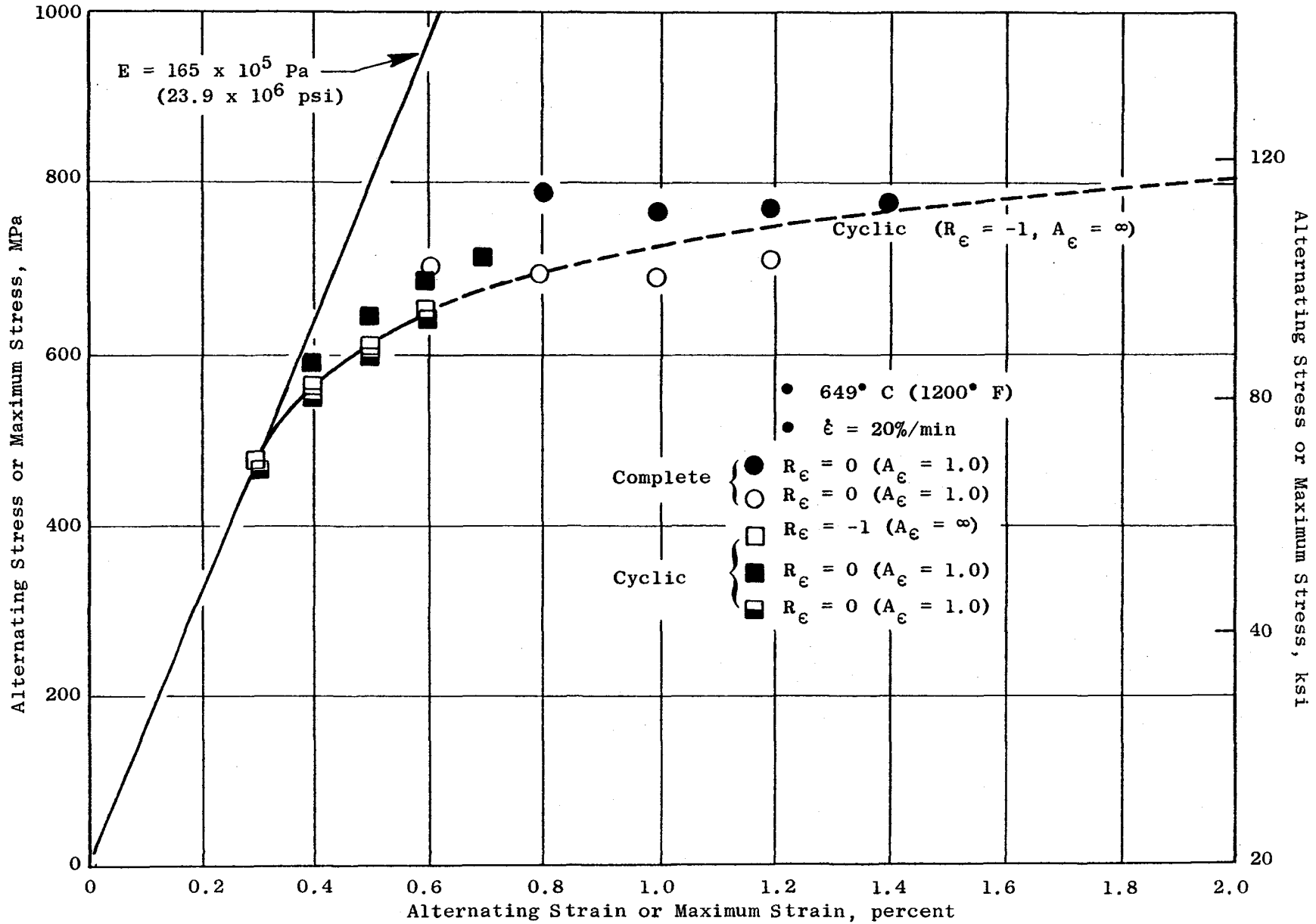

Figure 13. Cyclic Stress-Strain Curves - Inconel 718 Bar, H.T. to Forging Spec.

Table VI. NASA Benchmark Notch Fatigue Program Cyclic Stress-Strain Curve Test Results.

Inconel 718 Bar Stock, Heat Treated to Forging Specification (C50TF6), Heat No. S108
Four Step Incremental Test, Triangular Waveform, 649° C (1200° F).

Test No. 1: $R_\varepsilon = -1$ ($A_\varepsilon = \infty$) - Cyclic
(Spec. No. 1) $\dot{\varepsilon} = 5\%/min$

Step No.	N Cycles	N^1 Cycles	$\Delta\sigma$ MPa	$\Delta\sigma$ ksi	$\Delta\varepsilon_T$ %	$\Delta\varepsilon_e$ %	$\Delta\varepsilon_p$ %	$\Delta\sigma/2$ MPa	$\Delta\sigma/2$ ksi	$\Delta\varepsilon/2$ %
1	10,000	9,975	927.4	134.5	0.60	0.6	0.0	464.0	67.3	0.30
2	1,500	1,490	1174.2	170.3	0.81	0.75	0.06	587.5	85.2	0.41
3	400	137	1323.8	192.0	1.00	0.86	0.14	661.9	96.0	0.50
4	100	90	1398.3	202.8	1.20	0.90	0.30	699.2	101.4	0.60

Test No. 2: $R_\varepsilon = -1$ ($A_\varepsilon = \infty$) - Cyclic
(Spec No. 3) $\dot{\varepsilon} = 20\%/min$

1	10,000	9,995	961.9	139.5	0.60	0.59	0.01	481.3	69.8	0.30
2	1,500	1,490	1143.9	165.9	0.80	0.69	0.11	572.3	83.0	0.40
3	400	390	1238.3	179.6	1.00	0.75	0.25	619.9	89.8	0.50
4	100	98	1321.1	191.6	1.20	0.80	0.40	660.5	95.8	0.60

Test No. 3: $R_\varepsilon = -1$ ($A_\varepsilon = \infty$) - Cyclic
(Spec. No. 2) $\dot{\varepsilon} = 100\%/min$

1	10,000	2,650	926.7	134.4	0.59	0.59	0.0	463.3	67.2	0.295
2	1,500	1,450	1087.3	157.7	0.80	0.69	0.11	544.0	78.9	0.40
3	400	350	1165.3	169.0	1.00	0.74	0.26	582.6	84.5	0.50
4	100	95	1232.1	178.7	1.20	0.78	0.42	616.4	89.4	0.60

$\Delta\varepsilon_T$ - Total Strain Range
$\Delta\varepsilon$ - Elastic Strain Range
$\Delta\varepsilon_p$ - Plastic Strain Range
$\Delta\sigma$ - Stress Range
R_ε - Minimum Strain/Maximum Strain
A_ε - Alternating Strain/Mean Strain
$\dot{\varepsilon}$ - Strain Rate (Frequency Controlled to Maintain Strain Rate)
N - Cycles in a Given Step
N^1 - Cycle where Data was Calculated

Table VI. NASA Benchmark Notch Fatigue Program Cyclic Stress-Strain Curve Test Results. (Concluded)

Step No.	N Cycles	N^1 Cycles	$\Delta\sigma$ MPa	$\Delta\sigma$ ksi	$\Delta\varepsilon_T$ %	$\Delta\varepsilon_e$ %	$\Delta\varepsilon_p$ %	$\Delta\sigma/2$ MPa	$\Delta\sigma/2$ ksi	$\Delta\varepsilon/2$ %
Test No. 4: $R_\varepsilon = 0$ ($A_\varepsilon = 1.0$) - Cyclic (Spec. No. 4) $\dot{\varepsilon} = 20\%/min$										
1	10,000	9,995	941.2	136.5	0.60	0.57	0.03	470.9	68.3	0.3
2	1,500	1,495	1112.9	161.4	0.80	0.67	0.13	556.4	80.7	0.4
3	400	399	1212.8	175.9	1.00	0.73	0.27	606.8	88.0	0.5
4	100	95	1301.1	188.7	1.20	0.78	0.42	650.9	94.4	0.6
Test No. 5: $R_\varepsilon = 0$ ($A_\varepsilon = 1.0$) - Cyclic (Spec No. 5) $\dot{\varepsilon} = 20\%/min$										
1	1,500	1,490	1188.7	172.4	0.80	0.72	0.08	594.3	86.2	0.4
2	500	495	1307.3	189.6	1.00	0.79	0.21	653.6	94.8	0.5
3	200	195	1392.8	202.0	1.20	0.85	0.35	696.4	101.0	0.6
4	100	98	1448.0	210.0	1.40	0.88	0.52	724.0	105.0	0.7
Test No. 6: Monotonic (Spec. No. 6) $\dot{\varepsilon} = 1\%/min$										
1	Load Only	---	916.3	132.9	2.0	0.57	1.43	---	---	---
Test No. 7: Monotonic (Spec. No. 24) $\dot{\varepsilon} = 20\%/min$										
1	Load Only	---	943.2	136.8	0.68	0.58	0.11	---	---	---

3.2.3 Elastic Modulus

In order to assess measured notch root strains in the elastic regime, it is necessary to have accurate modulus of elasticity (E) values. An understanding of the potential variability in measured E values is also important for separating strain measurement errors from material property variations. Table VII summarizes the values of E obtained from the cyclic stress-strain curve tests and shows comparisons to Standard Inconel 718 forging dynamic E values. The moduli for the benchmark material tests agree well with standard forging dynamic moduli.

3.3 NOTCH SPECIMEN DESIGN

The benchmark notch specimen design for this program is shown in Figure 14. This design was the culmination of considerations that included the need for:

- An elastic stress concentration factor (K_t) representative of typical engine components - K_t approximately 1.9
- A notch geometry that permits a clear path for incoming and reflected laser beams - a shallow surface notch
- A cross-sectional area compatible with the load cell capacity and the need to obtain plasticity and creep behavior at the notch root
- Adequate buckling restraint to allow substantial compressive loading
- Approximate plane stress conditions at the notch root so as to provide for uniaxial straining in the measurement direction - thin gage section
- Sufficient length to provide clearance between the grip faces for a furnace with optical ports for the laser beams - 254 mm (10 in.) long
- Precise specimen alignment - buttonhead design
- Minimal material cost and waste - bar stock, round grip ends.

The flared gage section evolved with the need to obtain the highest K_t from the 25.4 mm bar stock while preserving the shallow notch geometry. There was also a desire to keep the mass at the ends of the specimen as low as possible to avoid undue bending of the thin gage section during handling. The specimens were shipped in plastic tubes as a further precaution.

Table VII. Comparison of Elastic Modulus (E) Measurements - Inconel 718, Bar, Heat Treated to Forging Spec. (x 10^9 Pa [x 10^6 psi]).

Test[1]	$\dot{\varepsilon}$ (%/min)	R Ratio	21° C (70° F) 1st Cycle	649° C (1200° F) 1st Cycle	649° C (1200° F) $N_f/2$
1	5.0	-1	201.3 (29.2)	155.8 (22.6)[3]	155.1 (22.5)
2	100.0	-1	198.6 (28.8)	157.0 (22.78)	157.6 (22.85)
3	20.0	-1	203.4 (29.5)	162.9 (23.63)	164.4 (23.85)
4	20.0	0	204.1 (29.6)	164.7 (23.88)	165.5 (24.00)
5	20.0	0	207.5 (30.1)	164.4 (23.85)	164.3 (23.83)
6	1.0	—	204.8 (29.7)	161.3 (23.4)	—
7	20.0	—	—	164.1 (23.8)	—
	Avg.		203.3 (29.48)	161.5 (23.42)	161.4 (23.41)
	Std. Dev.		3.0 (0.44)	3.6 (0.53)	4.7 (0.68)
	Maximum		207.5 (30.10)	164.7 (23.88)	165.5 (24.00)
	Minimum		201.3 (29.20)	155.8 (22.60)	155.1 (22.50)
	Range		6.2 (0.90)	8.8 (1.28)	10.3 (1.50)
	Range (% of Mean)		3.1	5.5	6.4
	Handbook[2] Avg. Std. Dynamic		200.0 (29.0)	162.0 (23.5)	162.0 (23.5)
	Min. Std. Dynamic		193.7 (28.1)	155.8 (22.6)	155.8 (22.6)
	Std. Std. Dev.		2.1 (0.3)	2.1 (0.3)	2.1 (0.3)

[1]Cyclic Stress-Strain Tests

[2]GE Material Handbook

[3]Values are average of four measurements for multistep tests.

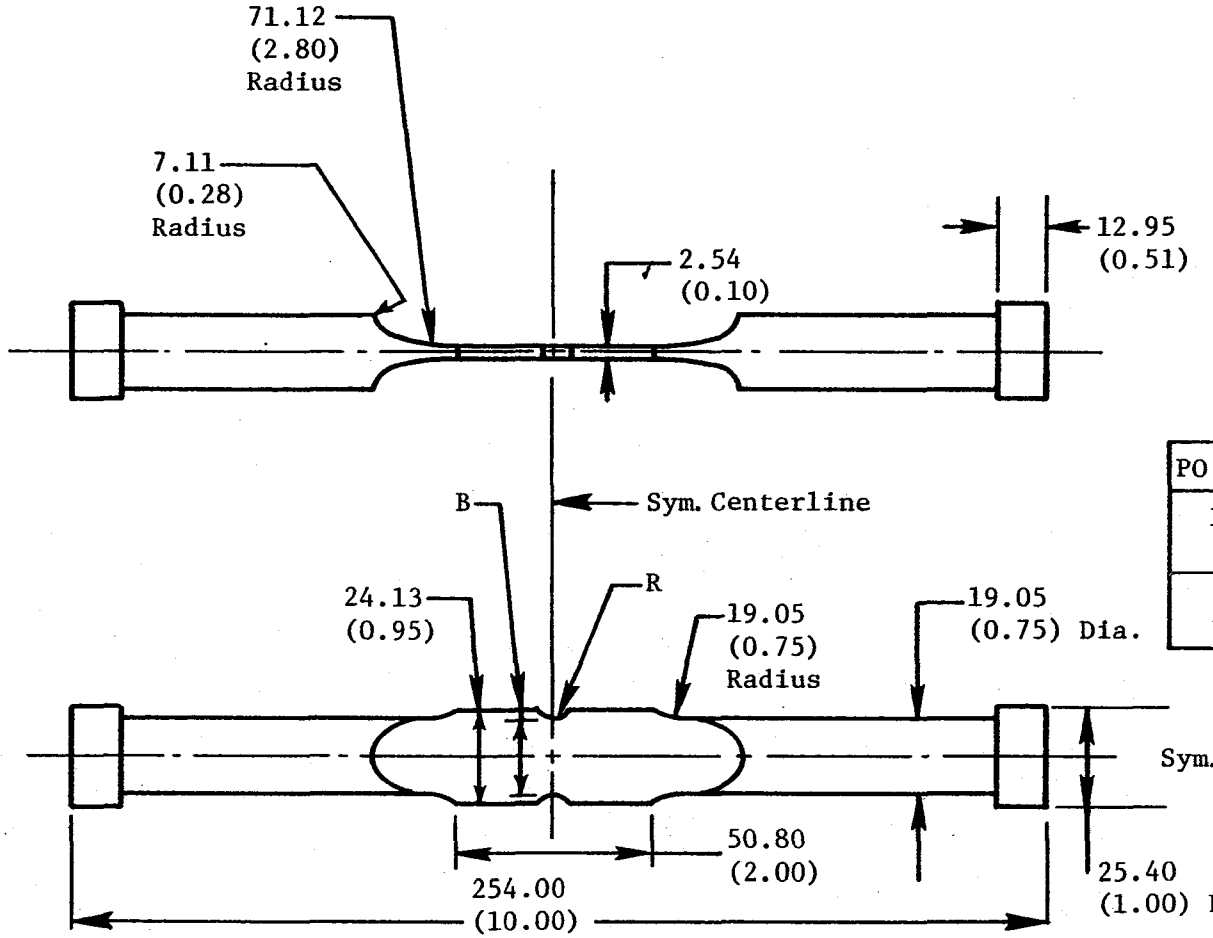

PO No.	B	R
1	17.958 (0.707)	4.902 (0.193)
2	24.13 (0.95)	-

• Dimensions in mm (inches)

Figure 14. Benchmark Notch Specimen CAP111280 (K_t = 1.9).

The gage section surfaces were final machined by low stress grinding methods to avoid unwanted residual stress effects. Some additional notch surface preparation was also done (Section 4.4) to prepare the surface for ISDG measurement.

The specimens were machined at Metcut Research Associates. Detailed measurements of the as-received specimens showed them to be within tolerance.

3.4 NOTCH SPECIMEN STRESS CONCENTRATION DETERMINATION

Although the relative simplicity of the notch specimen allows a good estimate of the K_t to be made from Peterson (Reference 15), the importance of this value in the Neuber analysis necessitated the inclusion of an elastic finite-element analysis of the final design.

Three finite-element models were employed. Two three-dimensional models were run at General Electric. A third, independent two-dimensional model, was run at LSU. The General Electric models will be described first followed by comparison to LSU results. The first model was a three-dimensional model of the specimen gage section only, Figure 15. This model was of 1/8 of the gage section, recognizing the three-fold symmetry. When initial notch measurements were made, they suggested that the gage section only model inadequately described the stress distribution resulting from the flared specimen design.

The second model was therefore expanded to include the entire flat-to-round transition section as shown in Figure 16. Again, 1/8 of the specimen was modeled. (It was later determined that in the initial tests the hardness tester indentations for the ISDG were not centered at the notch root which led to inaccurate measurements. The adequacy of the first mesh was subsequently verified by the second model.)

The models used eight-noded isoparametric brick elements in the CYANIDE elastic-plastic-creep computer code. A nominal net section stress of 689.5 MPa (100 ksi) was applied to both models.

- First Mesh of Gage Section Only

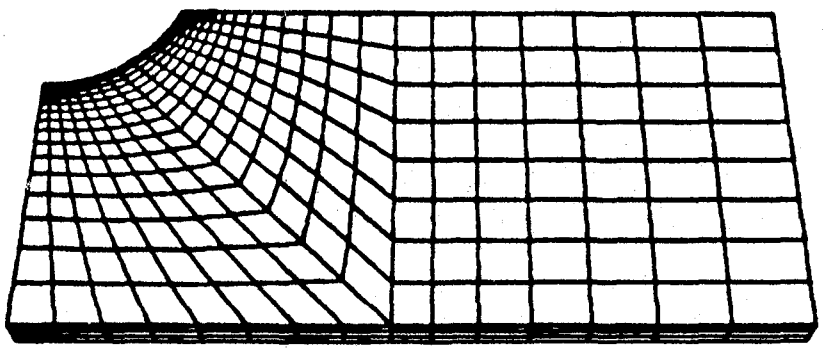

Figure 15. Three-Dimensional Finite-Element Model of 1/8 of the Benchmark Notch Fatigue Specimen.

- Second Mesh Including Transition Region

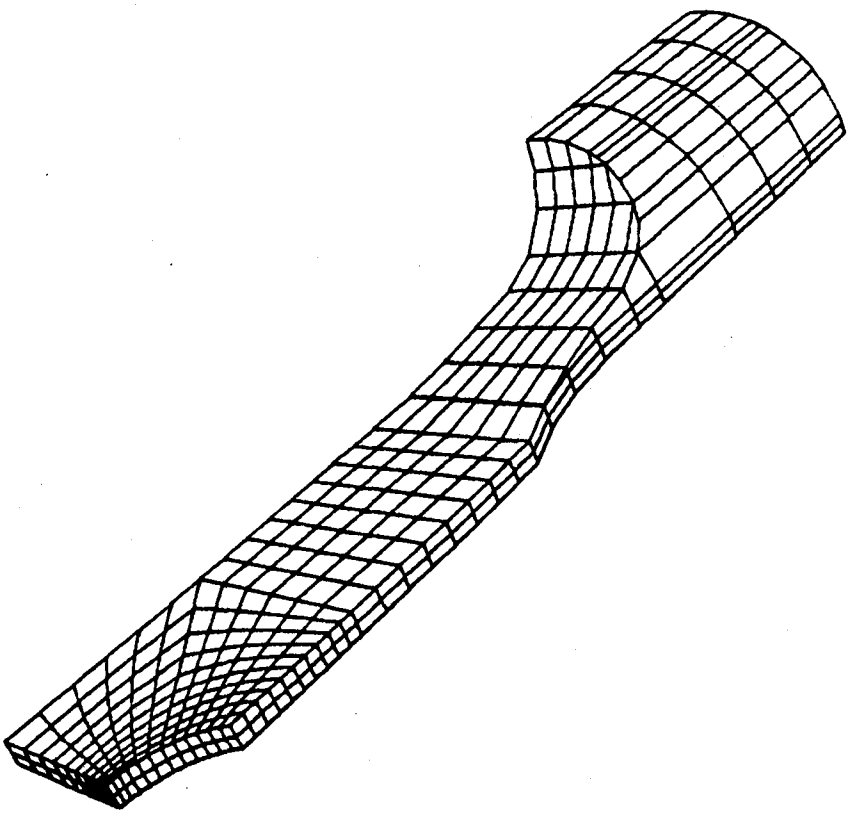

Figure 16. Three-Dimensional Finite-Element Mesh Pattern of 1/8 of the Benchmark Notch Fatigue Specimen.

There are several means of determining K_t from the finite-element results. Calculated stress and strains are output at element centroids. By plotting element centroid stresses versus distance from surface, an extrapolation to the specimen surface can be made. This is done in Figure 17 for results from the model of only the gage section. An extrapolated value of $K_t = 1.94$ is predicted compared to Peterson's 1.9. Since there are uncertainties in the extrapolation procedure, it is possible to employ actual element centroid stresses for K_t determination, providing the element size is small. The determination of a sufficiently small size is, however, again problematical. One can also estimate K_t by using surface nodal point displacements to calculate surface stress. Table VIII summarizes the various K_t's obtained by applying these methods to the two models. The two models predict consistent K_t's when extrapolated to the surface; however, the more coarse elements in the second model place the centroids further from the surface predicting lower K_t's for the other methods.

Figure 18 shows the predicted axial stress distribution across the specimen thickness (Model 1, gage section only). A very small through-thickness variation at the notch surface is shown, confirming an essentially plane stress specimen design.

An independent two-dimensional finite-element code (developed at LSU) was also used to compare to the above results. Figure 19 shows excellent correlation among the different approaches on an axial strain versus distance from notch root graph.

Finally, as also shown in Figure 19, strain measurements using resistance strain gages (RSG) applied across the minimum section of the specimen confirmed the basic trends. Gages 0.79 mm (0.031 in.) long by 0.81 mm (0.032 in.) wide, spaced 2.03 mm (0.08 in.) on centers were applied across the full net section. As the notch root was approached the RSG gave low results, probably due to an averaging over a relatively large area by the RSG.

Accepting the finer mesh of the original model (Model 1) as the best model and recognizing accuracy limitations, a value of $K_t = 1.9$ was accepted for the benchmark specimen and used for all subsequent data reduction.

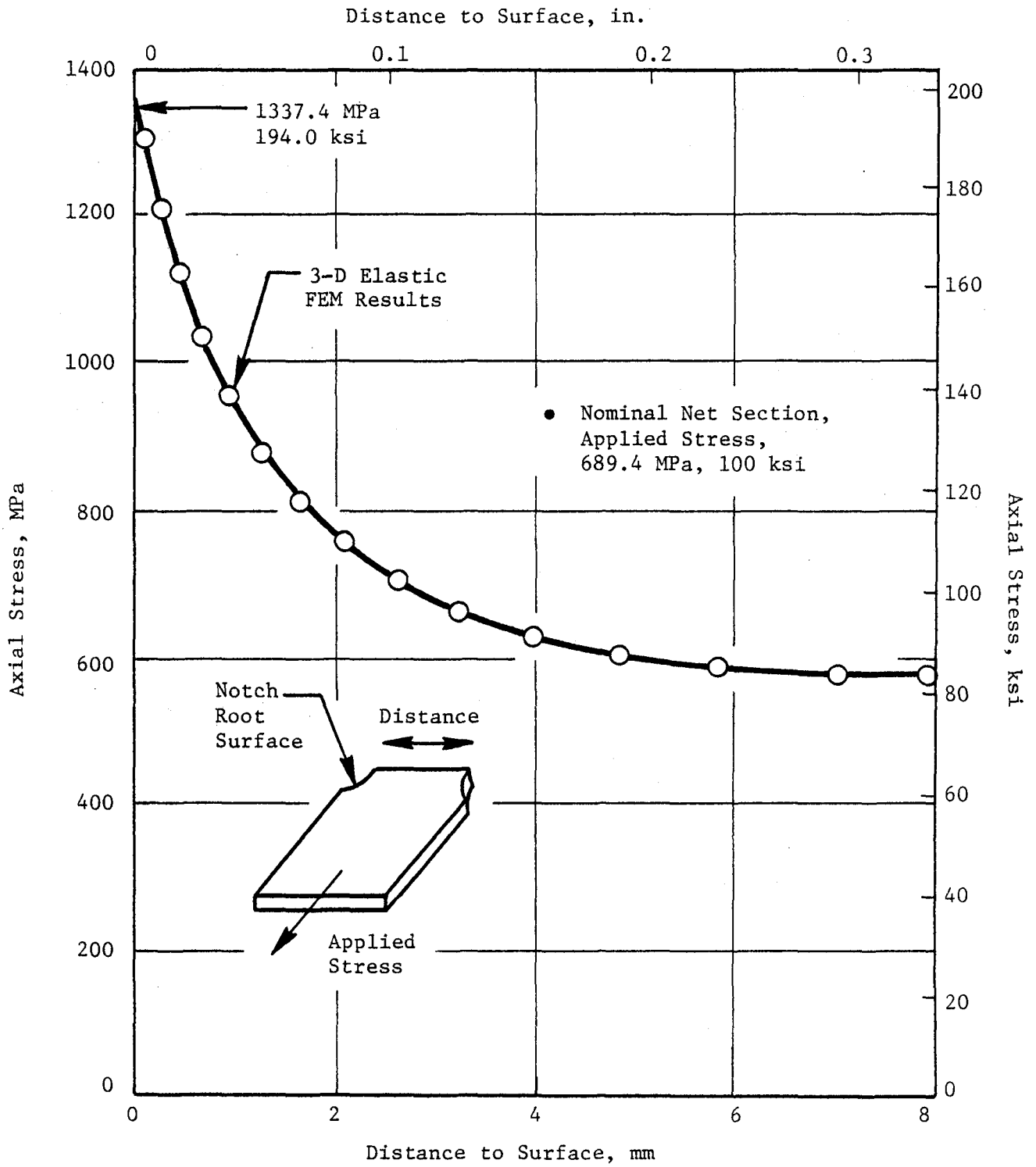

Figure 17. Axial Stress Versus Distance from Surface. CYANIDE Predicted Using Gage Only Model (Model No. 1).

Table VIII. Stress Concentration Factors for the Benchmark Notch Specimen Determined by Several Methods.

Source	K_t
Peterson[1]	1.90
Finite Element Models	
Extrapolated to Surface	
Gage Only - Model 1	1.94
Complete Bar - Model 2	1.94
Centroid of Surface Element	
Gage Only - Model 1	1.88
Complete Bar - Model 2	1.78
Calculated from Surface Deflection	
Gage Only - Model 1	1.89
Complete Bar - Model 2	1.83

[1]Peterson, R.E., Stress Concentration Factors, Wiley, 1974.

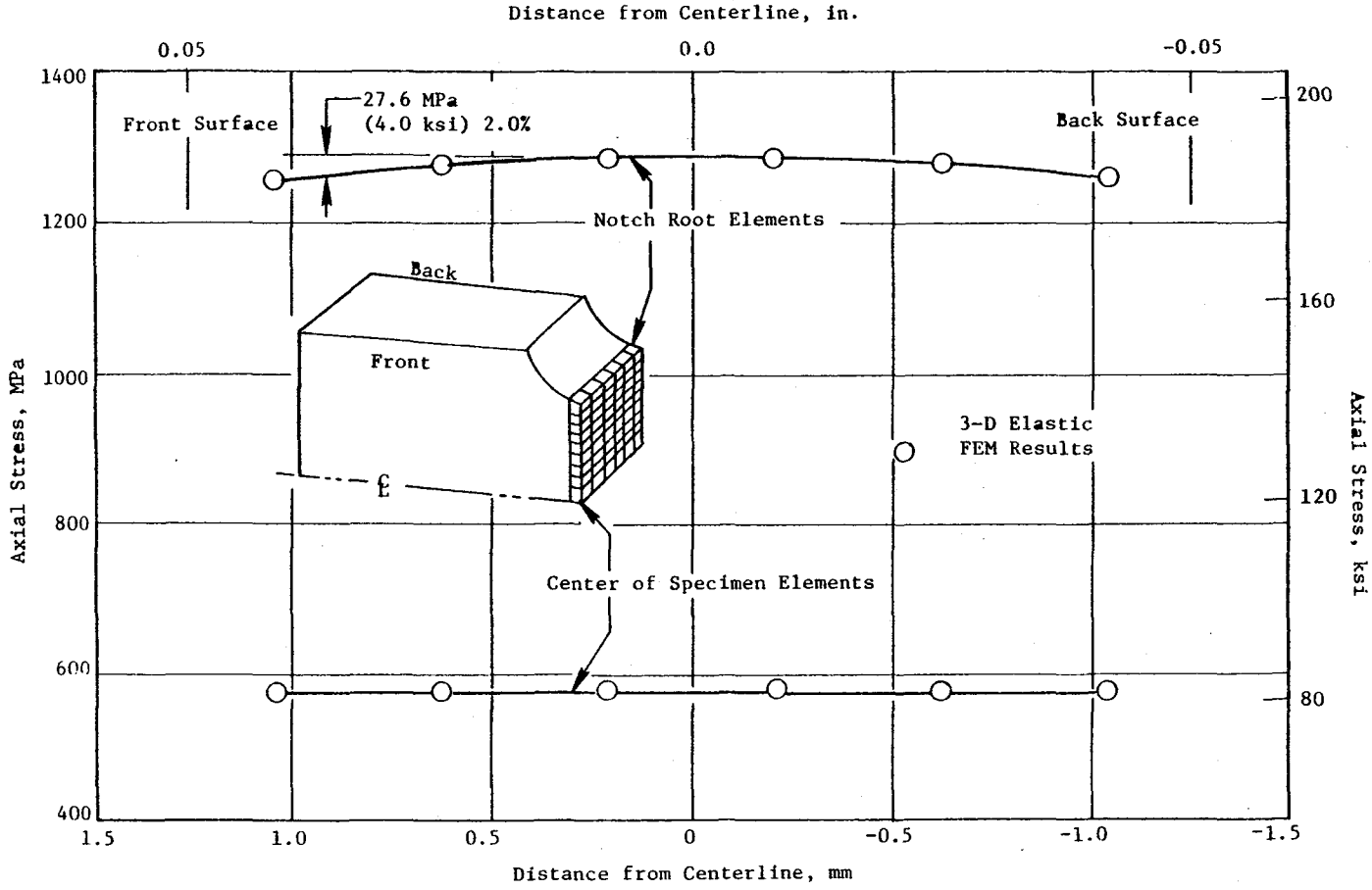

Figure 18. Through-Thickness Elastic Axial Stress Distribution for Benchmark Specimen as Predicted by 3-D Finite-Element Model.

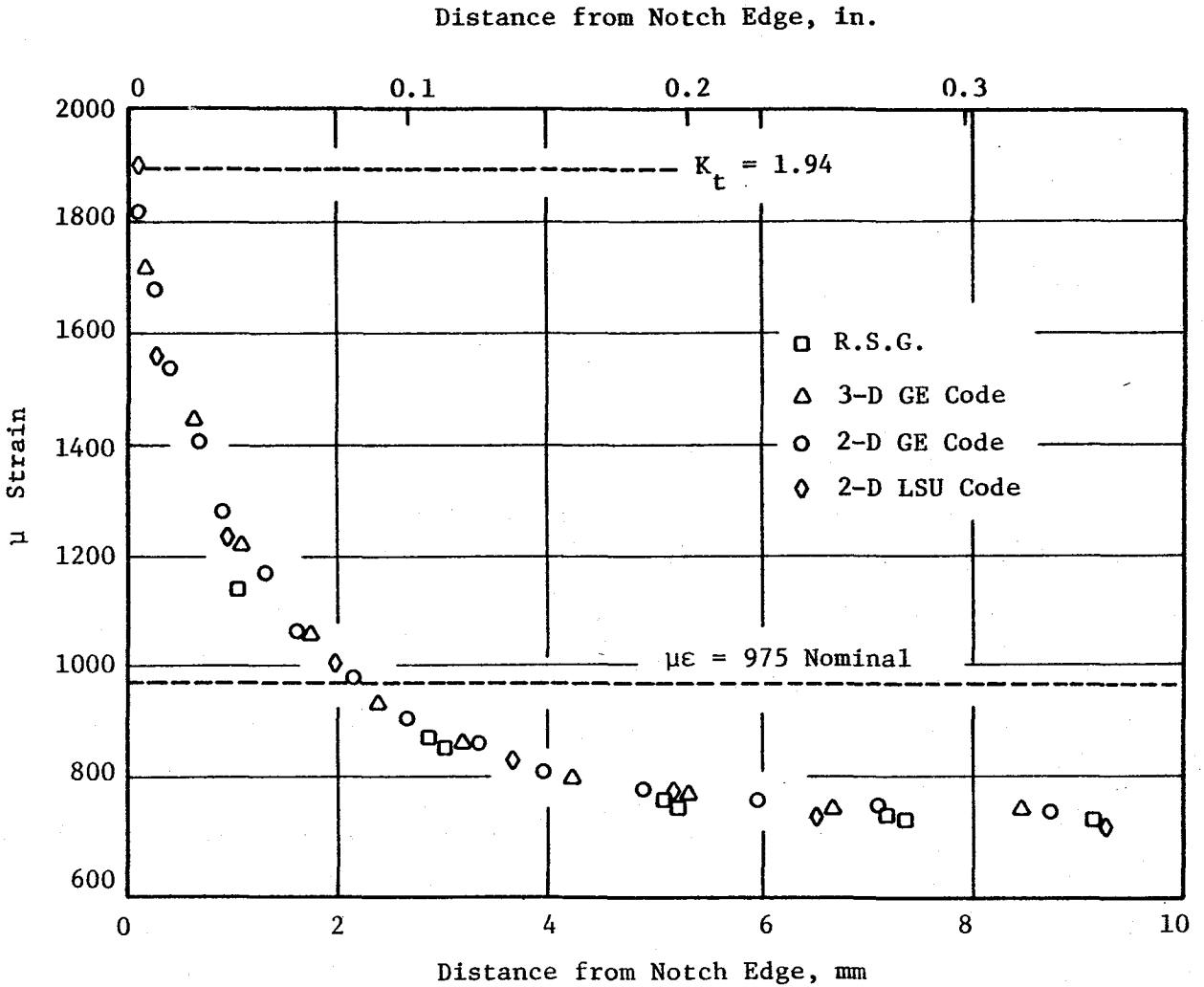

Figure 19. Comparison of Finite-Element Model Stress Predictions to Resistance Strain Gage Measurements.

4.0 TASK II - STRAIN MEASUREMENT SYSTEM ADAPTATION/DEVELOPMENT

The interferometric strain displacement gage measuring system was in place at LSU and being used for similar fatigue strain measurements on an NSF-sponsored program. Two substantial improvements to the system were accomplished on the current NASA program - an upgrade of the fringe measuring equipment and development of a new measurement strategy. The old fringe measuring equipment consisted of photomultiplier tubes (PMT) over 10 years old and homemade amplifiers. Also, the servocontrolled mirrors were not temperature controlled. Both of these problems were solved with the purchase of new tubes, mirrors, mirror control units, and amplifiers. The new strategy switched from scanning several fringes to following the minimum of a single fringe; this increased the testing rate by a factor of 2.5.

This section describes the system as it now exists and as it was applied to these particular specimens. The basics of the ISDG are first briefly presented and then followed by a detailed system description. Details of the instrumentation capabilities are given in the remaining sections which include some preliminary tests.

4.1 BASICS OF THE ISDG MEASUREMENT SYSTEM

The ISDG is a laser-based measuring system which measures relative displacement between two small indentations. These indentations are applied with a Vicker's hardness tester. The indentations generally measure from 15 to 25 microns on a side with center-to-center spacing ranging from 50 to 400 microns. Figure 20 shows a typical set of indentations.

The indentations are illuminated with highly coherent monochromatic laser light, causing two diffraction patterns to form. These diffraction patterns overlap, creating interference fringe patterns on either side of the laser beam, Figure 21. As the distance between the indentations (d) changes, the fringes move. The phase difference between two interfering rays of light is $d*\sin\alpha$, where α is the angle between the incident laser beam and the rays in question. Whenever the following relation is satisfied,

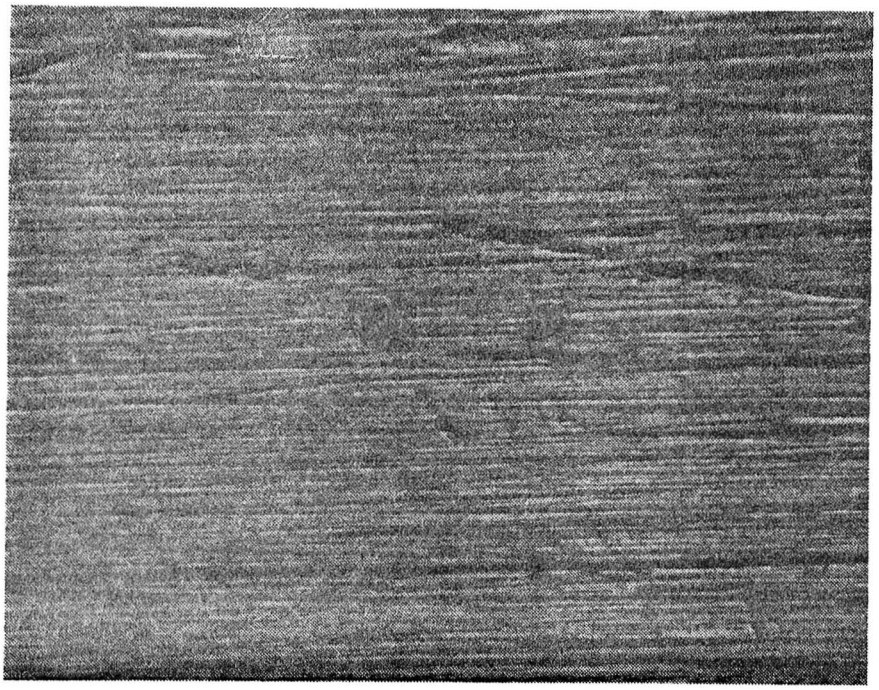

Figure 20. Photomicrograph of Indentations in Root of Notch. The Centers of the Indents are 100 Micrometers Apart. 200X.

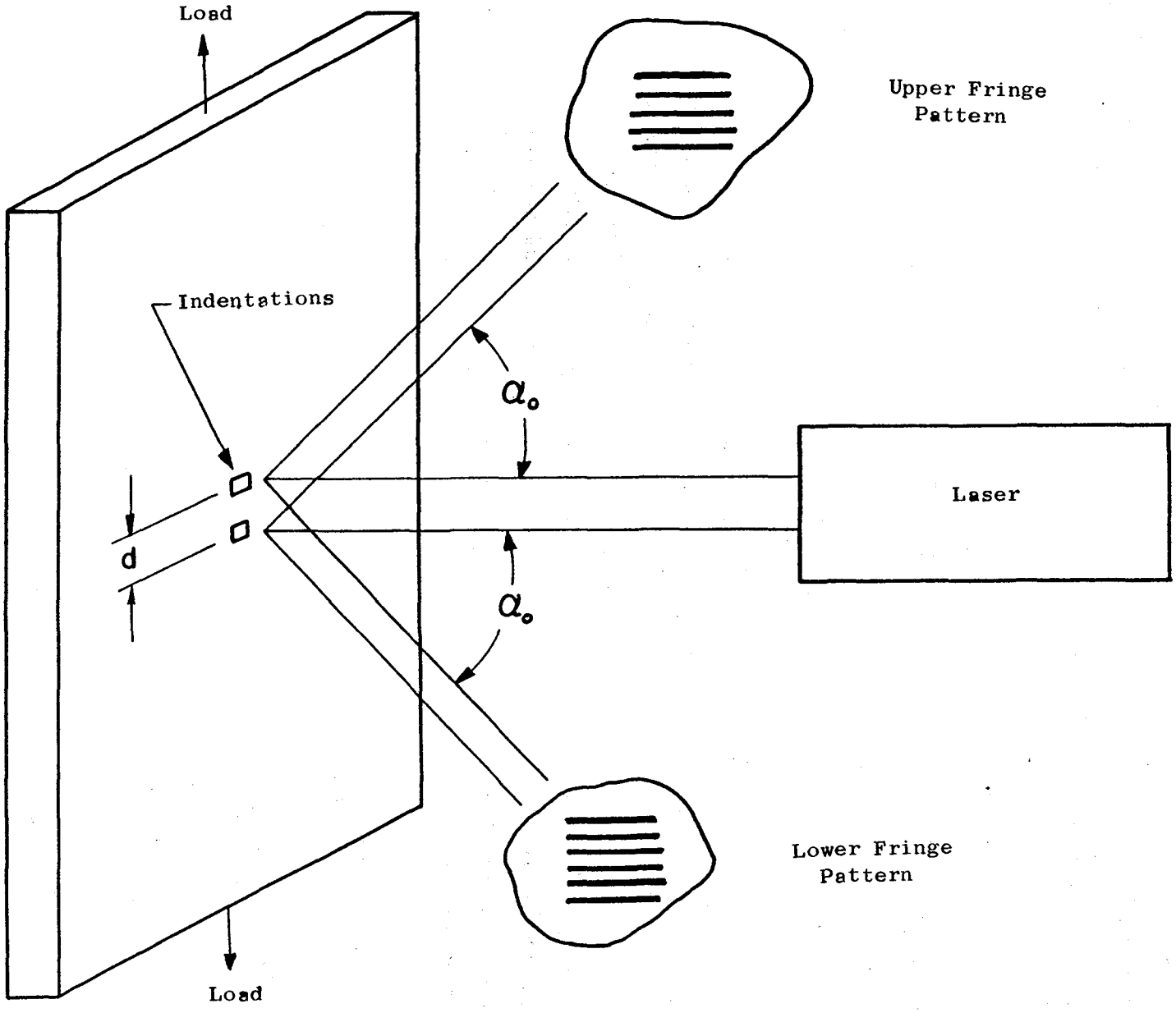

Figure 21. Schematic of the ISDG.

$$d \sin \alpha = M\lambda \qquad M = 0, \pm 1, \pm 2, \ldots \tag{1}$$

where λ denotes the wavelength of the laser light, the light rays interfere constructively, generating bright fringes.

If one observes the fringe pattern from a fixed observation point, α_o, while the indentations move relative to each other, the fringes will move past this point. The strain, $\delta d/d_o$, is given by:

$$\varepsilon = \frac{\delta d}{d_o} = \frac{\lambda}{d_o \sin \alpha_o} \delta M \tag{2}$$

δM denotes the number of fringes, or fraction thereof, passing the observation point.

Rigid body motion of the specimen will also cause the fringes to move. If the testing machine is carefully aligned, the rigid body motion can be sufficiently eliminated except for motion in the direction of the applied load. The fringe patterns on both sides of the laser beam will both move equally in the direction of the rigid body motion. If one defines positive fringe motion to be toward the laser beam, a simple average of the two fringe pattern motions will eliminate this rigid body effect. So in practice, strain is measured by:

$$\varepsilon = \frac{\delta M_1 + \delta M_2}{2} \frac{\lambda}{d_o \sin \alpha_o} \tag{3}$$

4.2 MEASUREMENT AND TEST SYSTEM

This research adapted a measurement system previously developed by Guillot (Reference 11) to satisfy the particular needs of this work. The basic system consists of a minicomputer in communication with various analog devices. A schematic of the system is shown in Figure 22.

The methodology followed by this measurement system is as follows: As the fringe patterns move in correlation with the relative displacement of the indentations, a predetermined minimum on each channel is tracked by the computer. This is accomplished by sending a computer-generated, 60-step ramp to

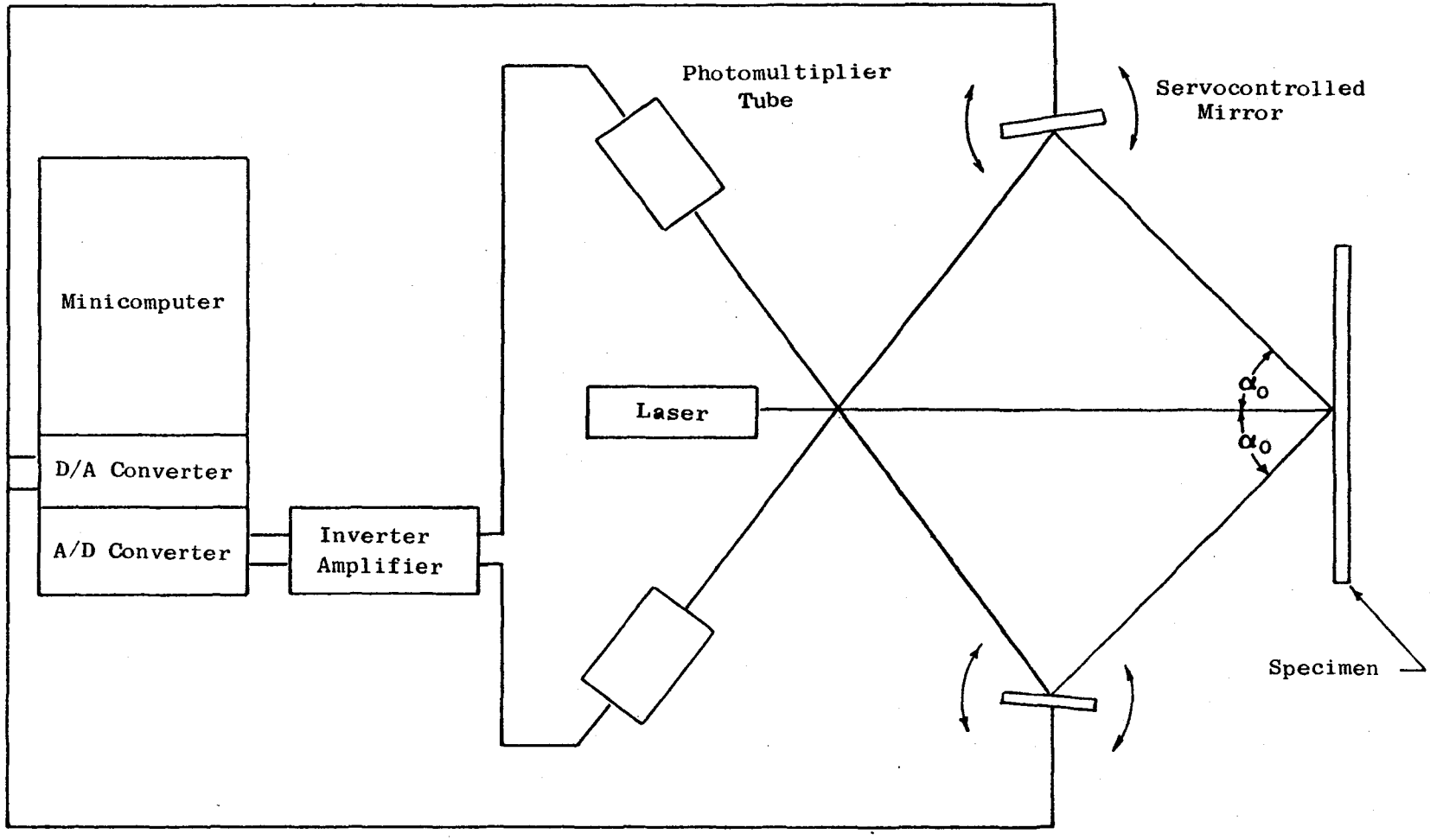

Figure 22. Schematic of the Minicomputer-Controlled ISDG System.

the servocontroller, causing each mirror to rotate about its axis. The total angular rotation of the mirror is adjusted via the gain control on the servocontroller to scan only the "trough" region surrounding the predetermined minimum of each fringe pattern. The fringe pattern is swept over a narrow slit over the photomultiplier tube face. Figure 23 shows a typical fringe pattern with the trough region identified. At each one of the 60 increments of the mirrors constituting a sweep, the photomultiplier tubes sample the fringe intensities and relay their electric analogs to the minicomputer via an inverting amplifier. Typically, the minicomputer averages the 60 intensities recorded per channel with a six point sliding average routine to mask any noise present and then locates the new minimum intensity locations for each channel using a simple comparison loop. The next mirror sweep will now be centered about this new minimum. The total fringe displacement is determined by subtracting this new minimum location from the original minimum location prior to any load on the specimen. The total fringe displacement is then multiplied by the appropriate constant to determine strain. This entire process takes 100 milliseconds to generate 1 data point. Normally, 60 data points are gathered per cycle; therefore, one cycle takes 6 seconds. At the end of each cycle, the 60 strain and corresponding load values are stored on a flexible diskette to be inspected after the test is completed. A simple flow chart of the Fortran program controlling the measuring system is presented in Figure 24.

The minicomputer employed by this measurement system is a Digital Equipment Corporation MINC system. The system prior to this work included four A/D's, four DAC's, a VT105 graphics terminal, an RX02 flexible diskette storage device, and a DEC LA120 line printer. Additional accessory equipment purchased from other funding sources was added during the course of this work and includes a DEC RL01 solid disk control unit, a Houston Instruments digital plotter, and a software upgrade package. The old system utilized the MINC operating system with BASIC as the only programmed language available. The upgrade package has extended the capabilities of the system to include Fortran IV and MACRO (a hexidecimal-based assembly language) when utilizing the RT-11 operating system now available. This operating system allows keypad editing of programs as well as easy file manipulations. In addition, various laboratory, statistical, and graphics subroutines are now available.

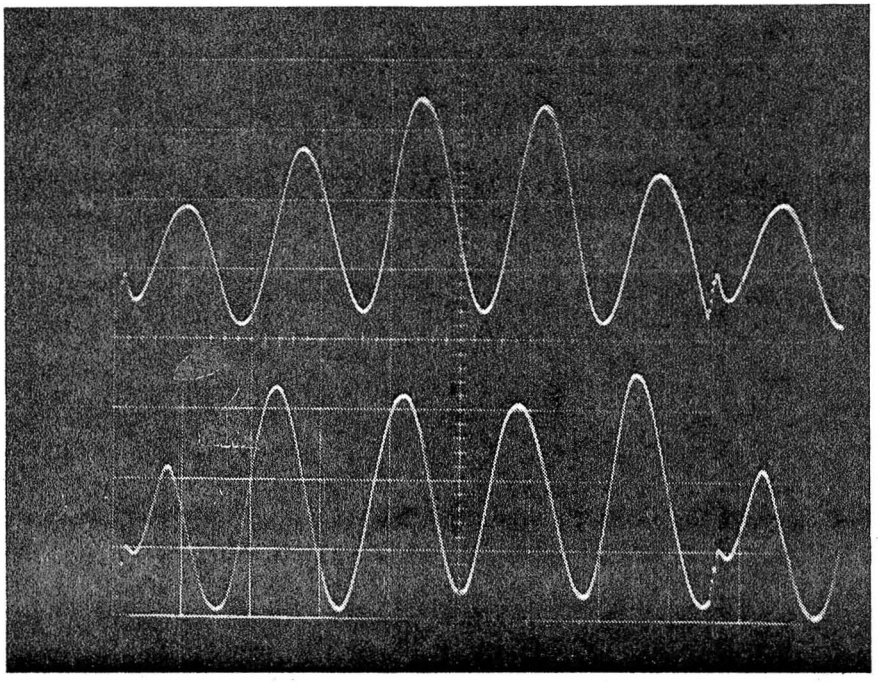

(a) Photo of Typical Output for one Sweep of the Fringe Pattern. The Sweep is Approximately 8 1/2 Divisions Long, and the Vertical Scale is 1 Volt Per Division.

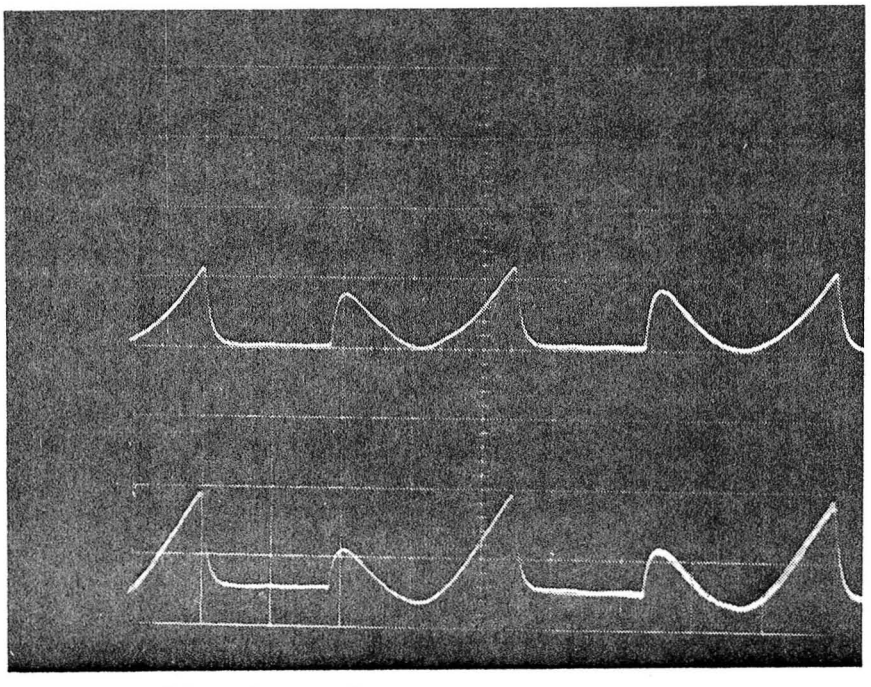

(b) Photo of a Typical Output When the Scanning Mirror is "Locked On" to a Minimum. The Horizontal Sweep is 20 Milliseconds Per Division and the Vertical is 1 Volt Per Division.

Figure 23. Typical Output of the ISDG.

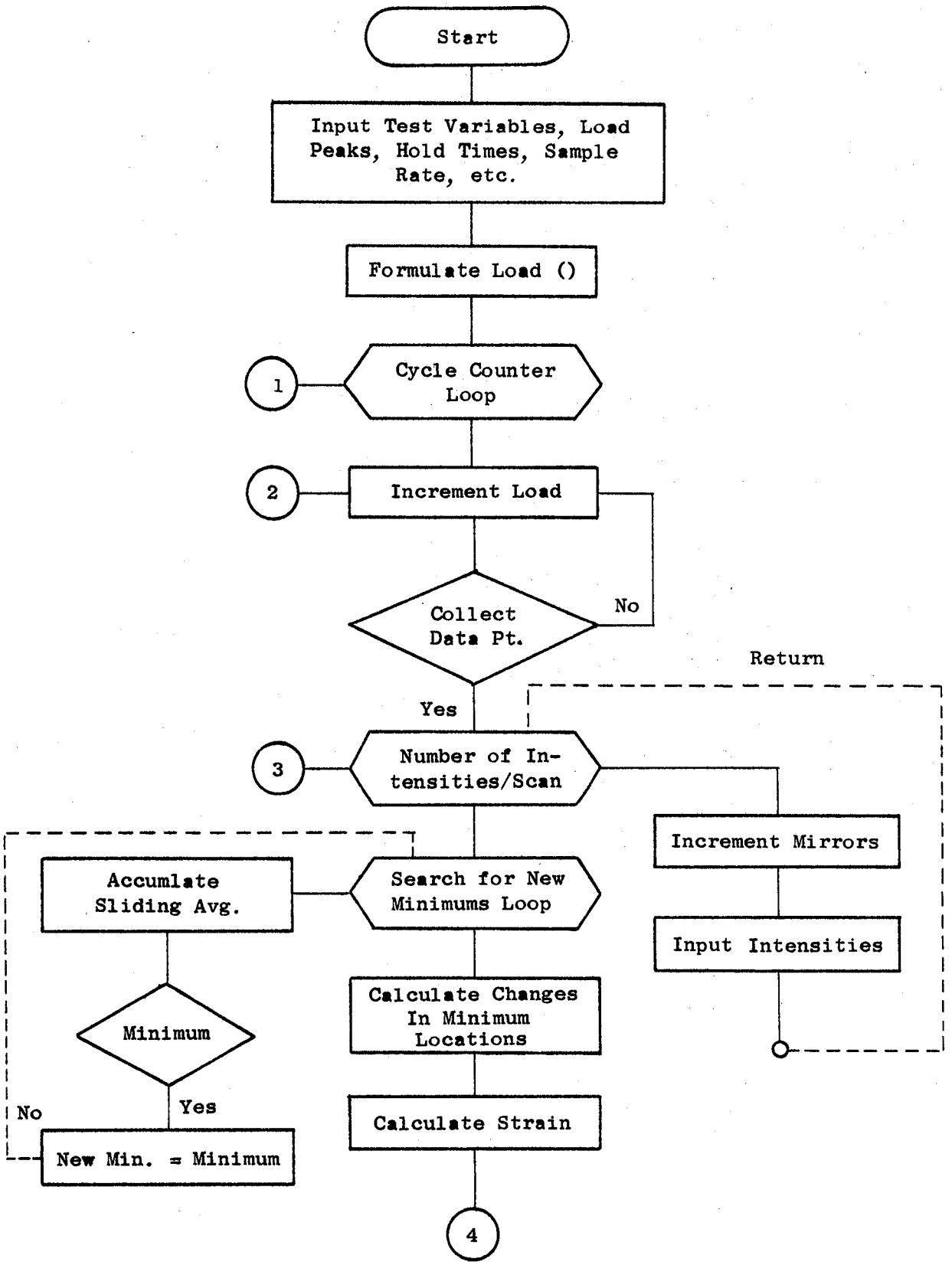

Figure 24. Flow Chart Data Acquistion Strategy.

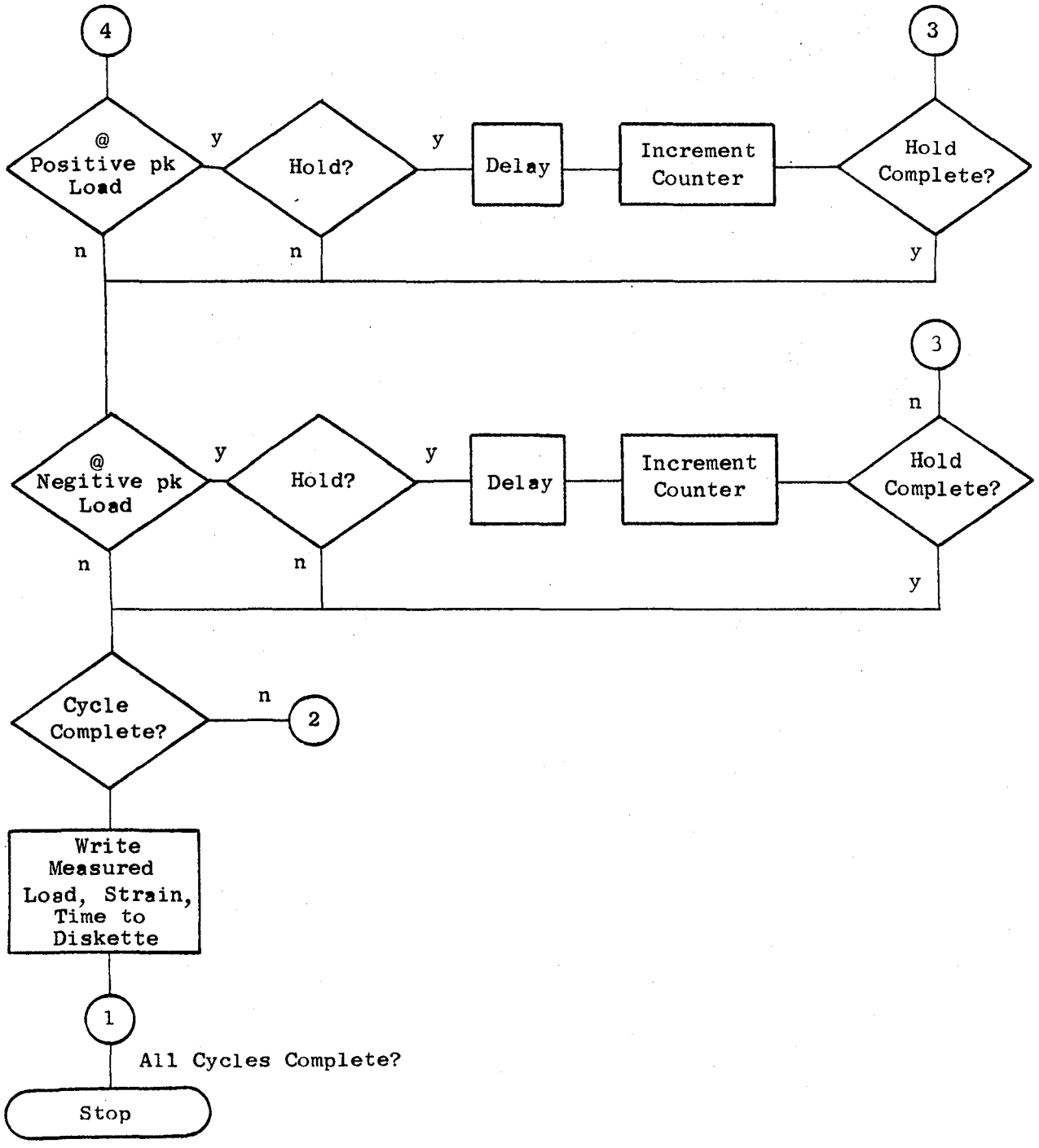

Figure 24. Flow Chart Data Acquisition Strategy (Concluded).

The optical scanners and control units utilized were purchased with NASA funds received for this project. These scanners are General Scanning Inc., Model G-100PDT, temperature compensated units. The temperature compensation feature of these scanners minimizes the electrical drift associated with temperature variations. The corresponding control units are also products of General Scanning and are Model CCX101. Each control unit has external gain and offset control knobs, which permit accurate adjustment of location and sweep range of each scanner.

The 13.5 volts DC required by the RCA photomultiplier tubes and associated power supplies, Parts No. 4840 and PF1042, respectively, is supplied by a Tektronix Model 501-2 rack-mounted power supply. Since the electrical analog of the fringe intensity created by the photomultiplier tube is normally on the order of 10 millivolts and inverted, a Tektronix Model 502 inverter/amplifier unit is used to condition the electrical signal to be within ±5 volts as required by the A/D's of the minicomputer. The photomultiplier tubes, power supply, and inverter/amplifiers were all purchased with NASA funds made available by this contract.

An MTS electrohydraulic, closed-loop test system with a 10-ton load cell is the central component of the experimental system. The minicomputer generated the command signal which controlled the MTS load applied to the test specimens. A photograph of the test system is presented in Figure 25.

The notched low cycle fatigue specimens, as well as the corresponding grips, were supplied by General Electric.

The grips were water-cooled to maintain the MTS load cell temperature below 66° C (150° F). Figure 26 exhibits a photograph of a specimen in the grips. A detailed alignment procedure, as outlined in General Electric Specification TP40-75, was followed to align the load train. This procedure required the grip faces to be within ±0.0127 mm (±0.0005 in.) parallel with the load frame base. The concentricity between the upper and lower grips was established using precision dowel pins, a Thomson linear motion bushing, and precision dial indicators. The concentricity tolerance was also ±0.0127 mm (±0.0005 in.).

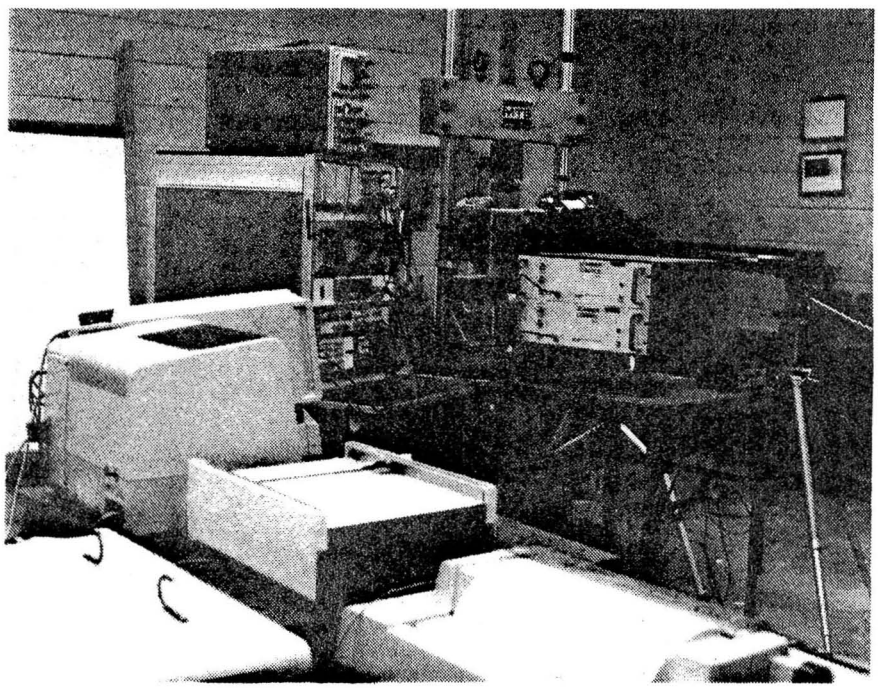

Figure 25. Photograph of Entire Lab Setup.

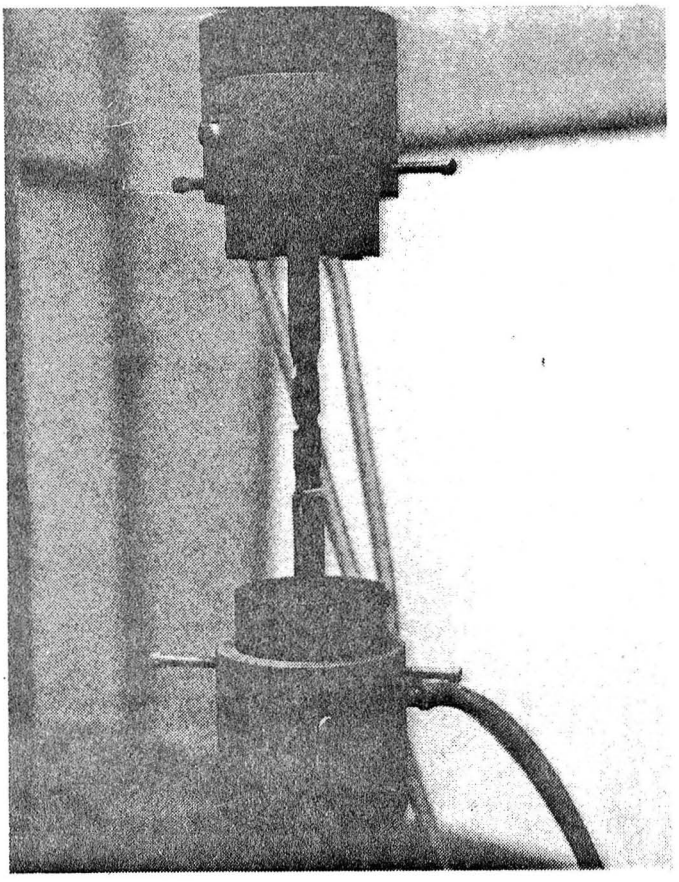

Figure 26. Photograph of Specimen in Water-Cooled Grips.

After aligning the load train to these specifications, an alignment verification process as outlined in ASTM STD E466 was pursued. This process is summarized as follows: bending strains in a specimen should be measured via a minimum of four strain gages uniformly spaced around the periphery of the specimen and whose center points lie in a common transverse plane. The percent bending is then computed as

$$\% \text{ bending} = [(S_{max} - S_{avg})/S_{avg}] * 100 \quad (4)$$

The result must be less than or equal to 5% to verify acceptable alignment of the system. Following this process with four strain gages on a smooth specimen, a percent bending of 2.2% was recorded, thus verifying the load train was aligned well within specification.

The furnace was designed and constructed at LSU specifically for the specimen and grips utilized in this work, Figure 27. Thermcraft (Winston-Salem, North Carolina) electric heating elements providing 1320 watts of power were embedded in insulating fire brick, which in turn was surrounded by an aluminum shell. Passages, which were sealed at both ends with quartz plates, were cut in the front of the furnace to allow the ISDG access to the specimen. Three passages were required - one for the incident laser beam and two for the reflecting interference fringe patterns. In preparation for the test program, six thermocouples were affixed to a notched specimen at various locations to ascertain the temperature distribution of the specimen at 649° C (1200° F). A large thermal gradient was noted in the vertical direction resulting from the water-cooled grips; however, the test section was maintained at 649° C ±16° (1200° F ±2°) (Figure 28).

4.3 EVALUATION BASED ON SMOOTH SPECIMEN

Various measurement system specifications were evaluated using an unnotched, or "smooth" specimen. These specifications include hysteresis, linearity, resolution, and frequency response. Figure 29 is a plot of microstrain measured by a resistance strain gage versus microstrain measured by the ISDG. No hysteresis is apparent; the linearity of the measurement system is also well established. However, Section 4.6 gives a more complete

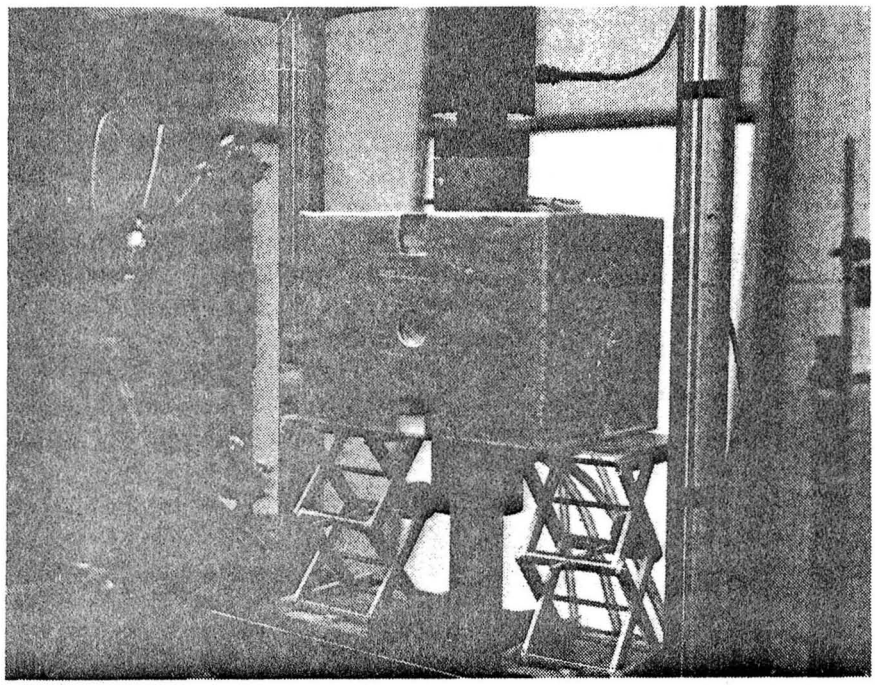

Figure 27. Photograph of Furnace Mounted Around Specimen in Test Machine.

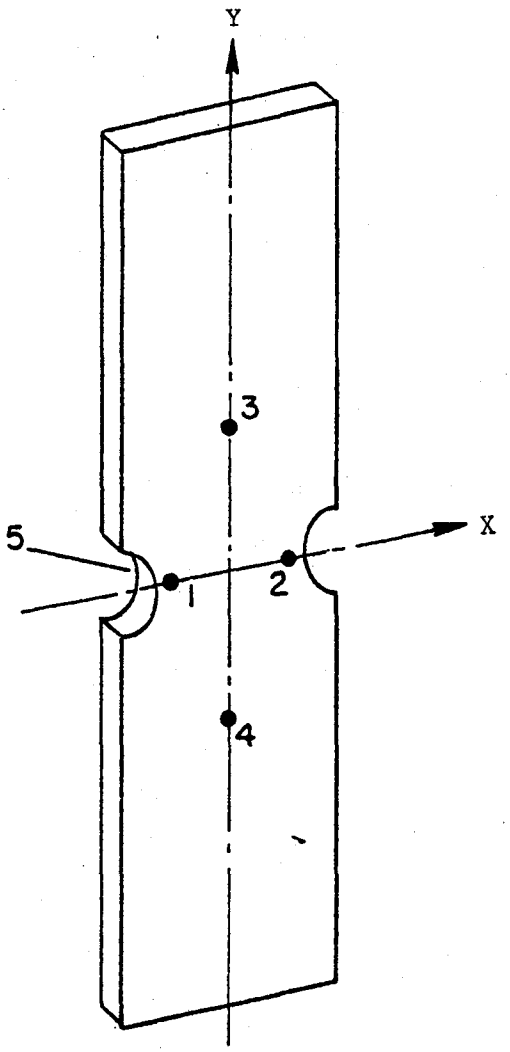

Thermocouple No.	Y-X Location mm	(in.)	Temperature ° C	(° F)
1	0, -6.35	(0, -0.25)	648	(1199)
2	0, +6.35	(0, +0.25)	649	(1201)
3	19.05, 0	(+0.75, 0)	638	(1180)
4	-19.05, 0	(-0.75,0)	604	(1120)
5	0, 0	(0, 0) Back	649	(1200)

Figure 28. Schematic of Measured Temperature Distribution.

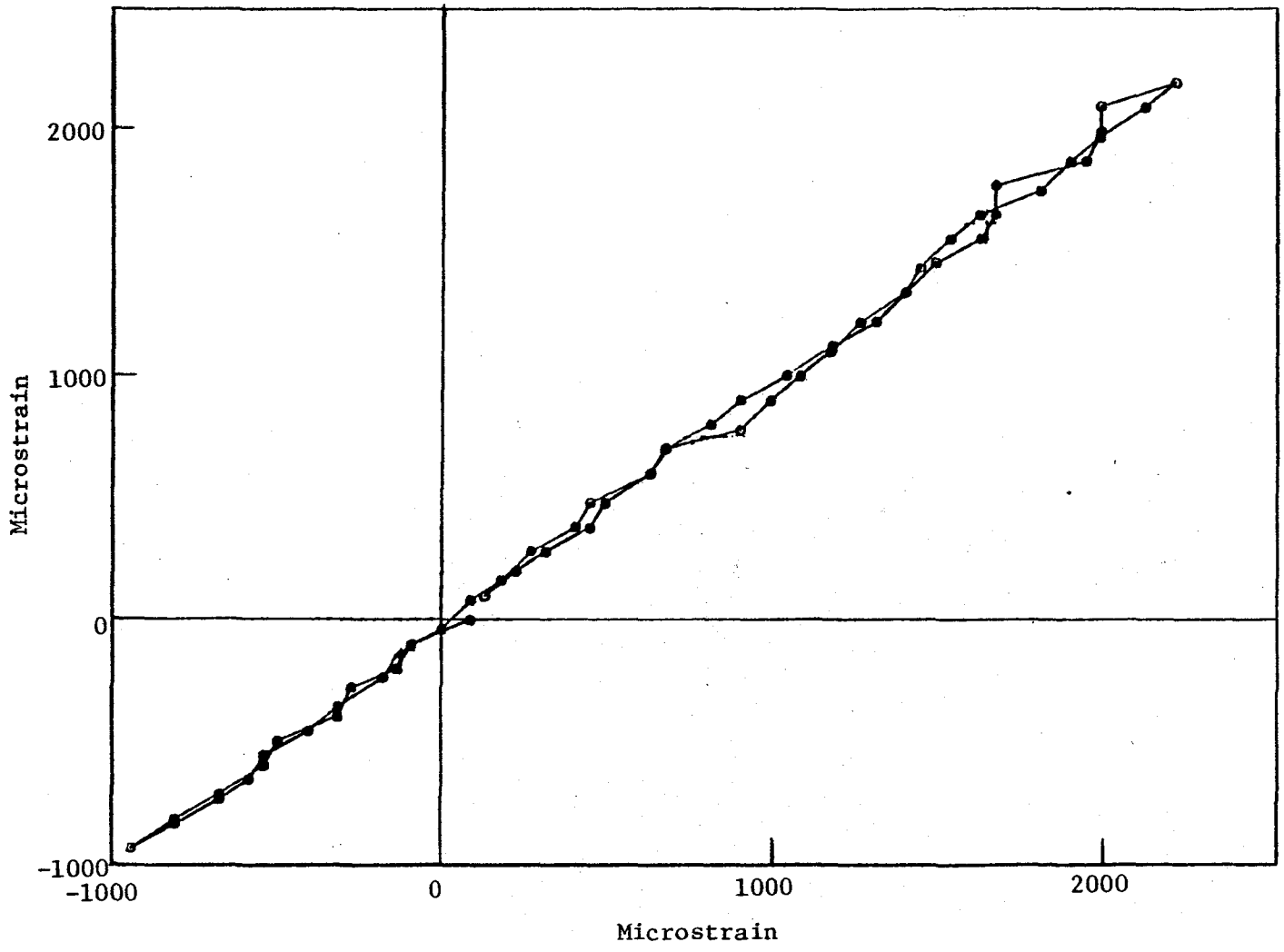

Figure 29. Plot of ISDG Versus RSG for Smooth Calibration Test at Room Temperature.

evaluation of the relative uncertainty of a measurement. The resolution of the ISDG is dependent on several test variables; these are fringe spacing (δM), indentation spacing (d), and the angle between the incident laser beam and the interference fringe pattern (α). Typically, the resolution of the ISDG is 55 microstrain. This corresponds to a 1-bit change in the D/A controlling the mirror position, using characteristic values for the test variables. The frequency response of the ISDG during a continuous cycle load condition equals 0.1667 Hz or 10 cpm. This could be increased slightly by measuring 40 discrete points per cycle instead of 60.

4.4 NOTCH SPECIMEN PREPARATION

Since the ISDG is a noncontacting measuring system, most problems associated with high temperature measurements are alleviated. One problem, however, remains: surface oxidation occurring at high temperatures can effectively blot out the indentations, causing the required fringe patterns to become obscure. This phenomenon is apparent in Inconel 718 at approximately 593° C (1100° F). Since the test measurements were to be made at 649° C (1200° F), a surface preparation method was devised which extended the measurable temperature range adequately. The procedure is quite simple. The notch root is first polished with 600-grit sandpaper in a direction parallel with the major axis of the specimen. The specimen is then cleansed with soap and water, acetone, and methanol, respectively. Once the specimen has been polished and cleaned, it is placed in the furnace and heated at 649° C (1200° F) for approximately 30 minutes. When the specimen is removed from the furnace, a thick oxide layer will have formed in the notch root, as shown in Figure 30. The notch root is now lightly buffed with a wet felt wheel to remove most of the oxide, but not all of it. This last step is quite crucial because a thin oxide layer seems to "seal" the surface prohibiting any further oxide formation, while a thick oxide layer is nonreflective. After buffing the notch root to the desired effect, the indentations are embedded 100 microns (0.004 in.) apart in the root of the notch using a Vicker's hardness tester with a vernier traveling base. A photomicrograph of a prepared specimen prior to testing is shown in Figure 31.

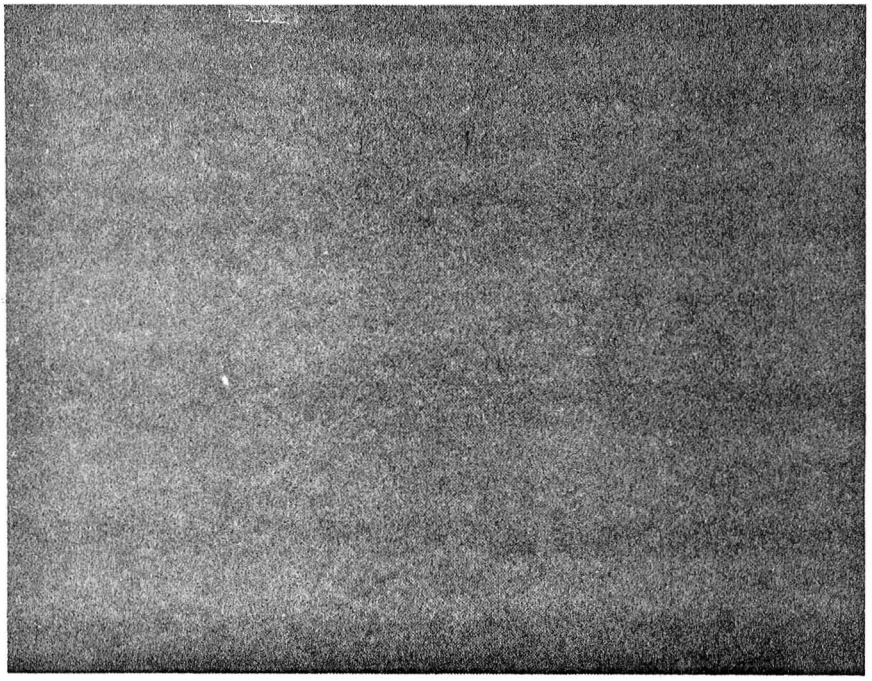

50X

Figure 30. Photomicrograph Showing Heavy Oxide in Root of Notch After Preoxidation of 649° C (1200° F).

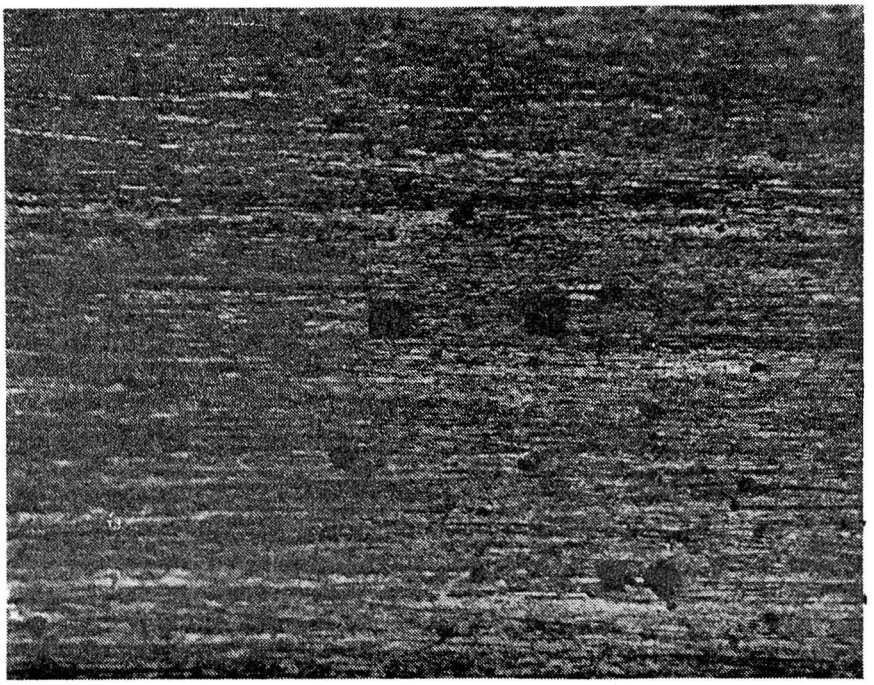

Figure 31. Photomicrograph Showing Root of Notch After Light Polish and Indent Application. 200X.

4.5 PRELIMINARY TEST RESULTS

Prior to testing of the six benchmark specimens, four specimens were tested to identify any unforeseen problems that might occur under actual test conditions. The specimen log for these tests is presented below.

Spec. No.	Test No.	Load Range N (lb)	Test Duration	Load Pattern
0	0A	35,600 - 21,360 (8,000 - 4,800)	2 cycles	Continuous Cycle
	0B	25,187 - 15,103 (5,660 - 3,394)	880 cycles	Continuous Cycle
7	1	25,187 - 15,103 (5,660 - 3,394)	1000 cycles	Continuous Cycle
	2A	29,886 - 17,933 (6,716 - 4,030)	1000 cycles	Continuous Cycle
	2B	35,600 - 21,360 (8,000 - 4,800)	38 cycles	Continuous Cycle
6	3	29,886 - 17,933 (6,716 - 4,030)	180 cycles	2-Minute Tension Hold
5	4	29,886 (6,716)	7 minutes	Creep
	5	29,886 - 37,380 (6,716 - 8,400)	6.9 hours	Creep

Six different load patterns comprise the actual benchmark program; these are described in detail in Section 5.1. However, it was felt that all "bugs" in the measured system had been located and corrected after tests using three typical load patterns: continuous tension-compression, cyclic with 2-minute tension hold, and creep.

A problem which was unveiled during Test No. 0A was related to the large amount of rigid body motion resulting from the relatively high tensile load applied to the specimen. The rigid body motion occurring under a 35,600 N (8000 lb) tension load moved the two indentations out of the effective diameter of the laser beam, thus obliterating the necessary fringe patterns. This problem was solved by moving the laser farther away from the specimen.

This allowed the laser beam to disperse to an effective diameter approximately two times the previous diameter. The intensity of the laser beam striking the indentations was reduced by this solution, but the remaining intensity was still large enough to produce the PMT signals which could be amplified to an acceptable range.

Test No. 0B through Test No. 3 were all successfully conducted. However, a peculiar characteristic was noticed when the data were analyzed. All of the strain data recorded seemed to be lower than expected, even the elastic strain values. It was concluded an error was present in the measuring system or procedure. Upon close inspection of Specimen No. 5, it was noted that the indentations were not placed at the root of the notch, Figure 32. A further investigation of all the specimens revealed this to be a common problem. As a result of these misplaced indentations, the stress concentration factor utilized in analysis (K_t = 1.9) was inappropriately high; thus the strain data recorded was less than that predicted. This problem was alleviated prior to the benchmark tests by a more careful indentation application procedure. A photomicrograph of the notch region of each benchmark specimen was also taken after applying the indentations to confirm their location at the root of the notch.

4.6 MEASUREMENT SYSTEM EVALUATION

An error analysis of the strain measured by the ISDG for the notched specimen at 649° C (1200° F) is conducted below.

Recall that λ in Equations 1 through 3 is the wavelength of the laser light and thus introduces no error to the measurement theory; d is the distance between the two indentations. This can be measured to within 0.2 micron using the microscope available. Since 100 microns is a typical value for d, this imposes an error of 0.2%; α is the angle between the incident laser beam and the reflecting fringe patterns. This angle can be determined to within 1.5°. Using a typical value for α equal to 41°, an error of 3% is introduced for the $\sin(\alpha)$ term. The error associated with measuring the fringe motion $\delta M1$ and $\delta M2$ is derived from the quality of the fringe patterns. When the fringes are bright and the speckles distributed smoothly, the fringes have good quality and the analog signal is smooth - making it easy to identify a

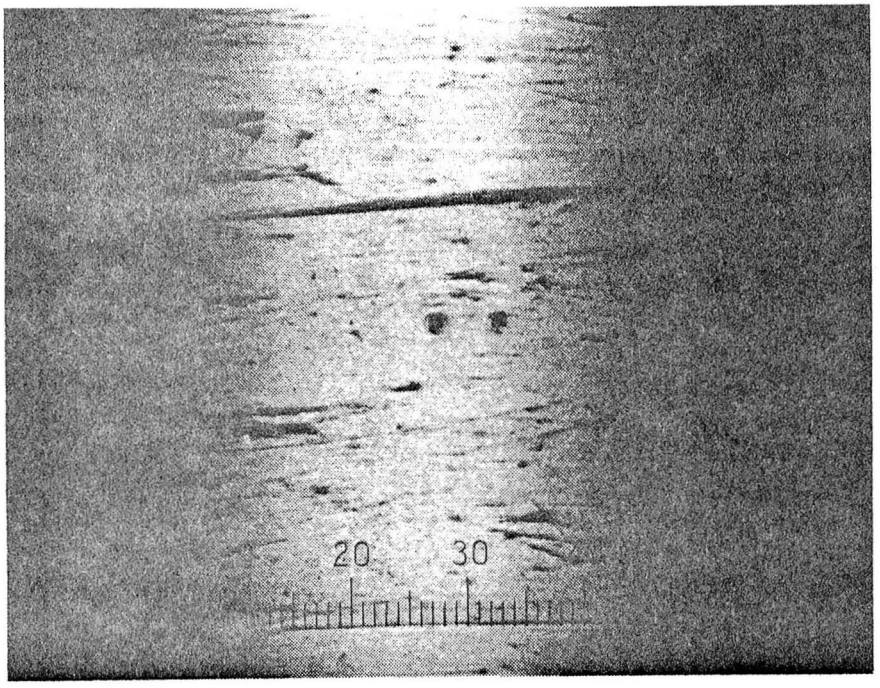

Figure 32. Photomicrograph of Misplaced Indents. 50X.

minimum. During the test, the indentations and their surrounding area can change reflectivity which can make the speckles nonuniform and the analog signal ragged. This behavior was found to be independent of strain level; therefore, the possible error should not be thought of as a percent error, but rather, as an error band. This value was determined from data collected over a 2-hour duration at 649° C (1200° F) with no load applied to the specimen. The drift of the measuring system was also established from these data. Figure 33 presents these data with the resulting error band evident. The band width is 300 microstrain. The total drift recorded was approximately -250 microstrain. In conclusion, the relative uncertainty of the ISDG measured strain values is determined to be ±3%, with an additional uncertainty of ±150 microstrain. The first uncertainty comes from the calibration constant, and the second comes from uncertainty in locating the fringe minimums. For example, a measured strain of 1.5% would have an uncertainty of 450 + 150 microstrain or ±600 microstrain total.

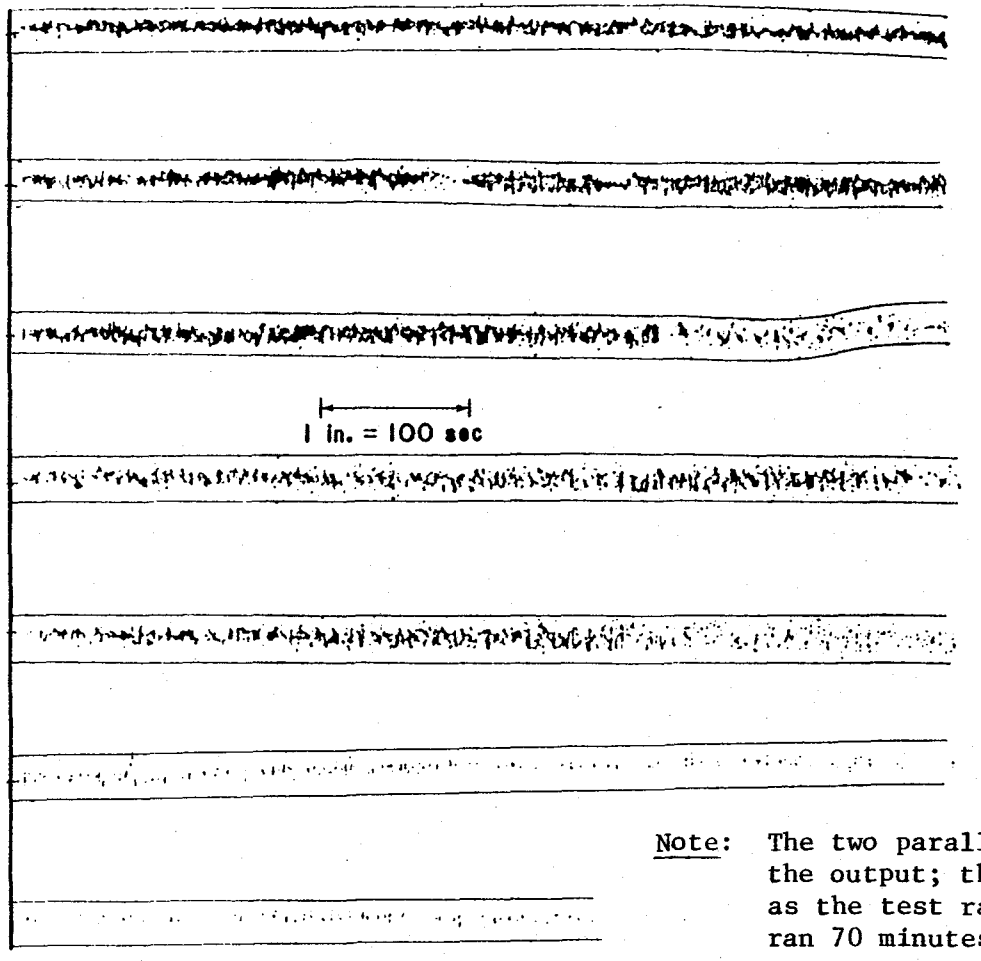

Note: The two parallel lines encompass the output; the ink pen dried up as the test ran. The total test ran 70 minutes.

Figure 33. Plot of ISDG Output Versus Time at 649° C (1200° F) and Zero Load.

5.0 TASK III - TESTING PROGRAM

5.1 LOAD PATTERN DEFINITION

The benchmark test program consists of six different load patterns, see Figure 34. Each test was conducted with the notch region of the specimen maintained at 649° C (1200° F). The duration of each test was determined by either cracks developing on the specimen surface or by the tension strain limitation of the measurement system, approximately 1.6%.

5.2 BENCHMARK NOTCH BAR TEST RESULTS

5.2.1 Load Pattern I (Continuous Cycle = 0.167 Hz)

Specimen No. 1 was tested using this load pattern. The test specifications are presented below:

Spec. No.	Test No.	Load Range (N)	Load Range (lb)	No. of Cycles
1	6	25,187 - 15,103	5660 - 3394	1000
	7	29,886 - 17,933	6716 - 4030	884

Test Nos. 6 and 7 were conducted on two different days, with the specimen allowed to cool between each test. In addition, any offset present at the completion of Test No. 6 is not accounted for in Test No. 7. Cycle Nos. 1, 500, and 1000 for Test No. 6 are presented in Figures 35 through 37. The results of Test No. 7 are presented in Figures 38 through 40. Cycle No. 884, Test No. 7, is the last cycle recorded; however, upon inspection of the specimen after the test was completed, it was noted that a crack had grown to a substantial length, Figure 41. Consequently, the last few cycles do not represent valid plastic strain measurements. Analyzing the hysteresis loop areas of Test Nos. 6 and 7 reveals a sudden change occurring at approximately the 700th cycle of Test No. 7. It is felt that this depicts the point where the crack opening displacement substantially affects the data. Plots of the loop area versus cycle of Test Nos. 6 and 7 are presented in Figures 42 and 43*.

*Loop area was calculated for each cycle by utilizing a trapezoidal integration scheme that traversed the 60 data points and summated or subtracted appropriate areas under the load-strain locus.

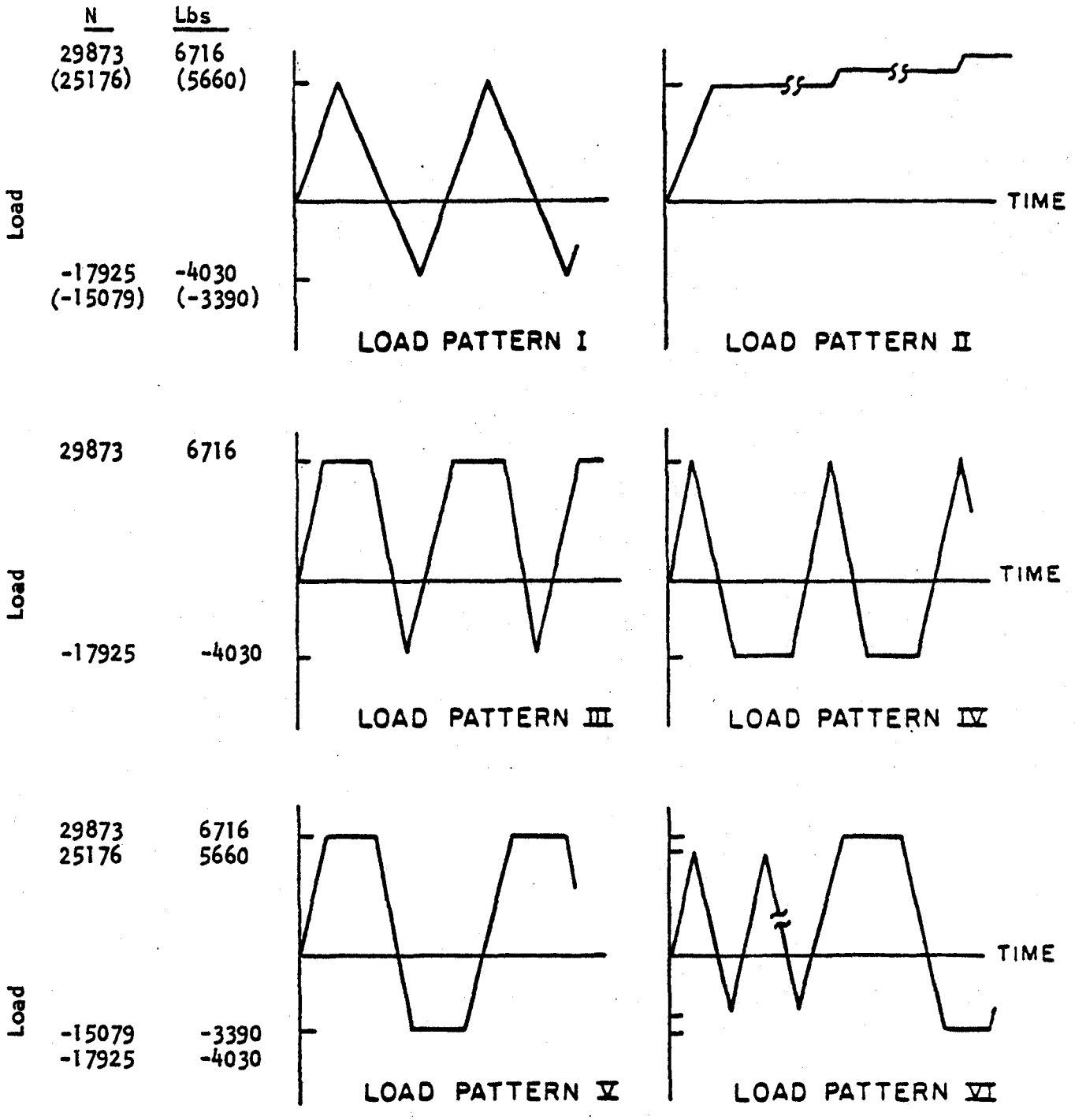

Figure 34. Load Spectra.

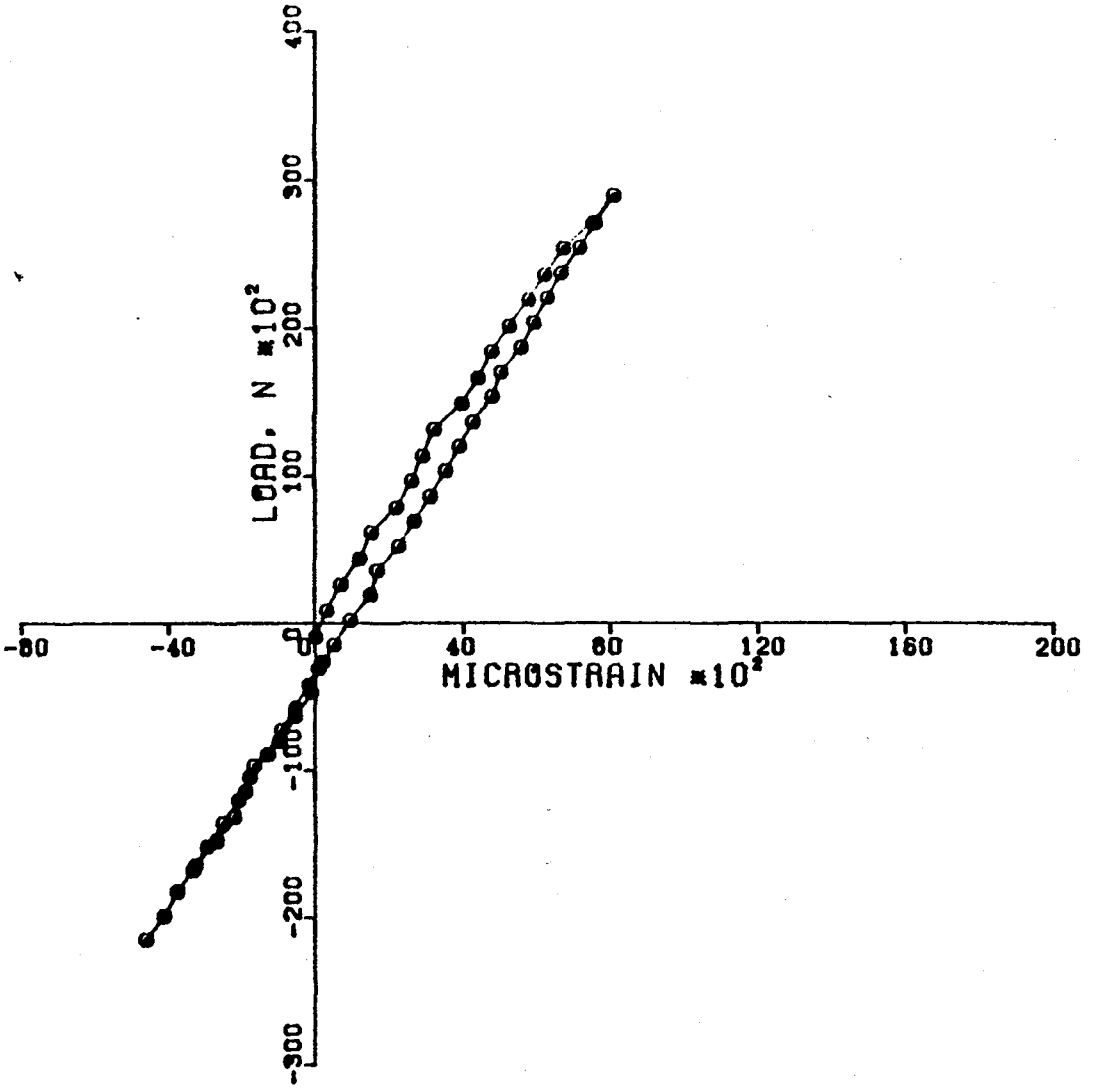

Figure 35. Cycle 1, Test 6, Continuous Fatigue.

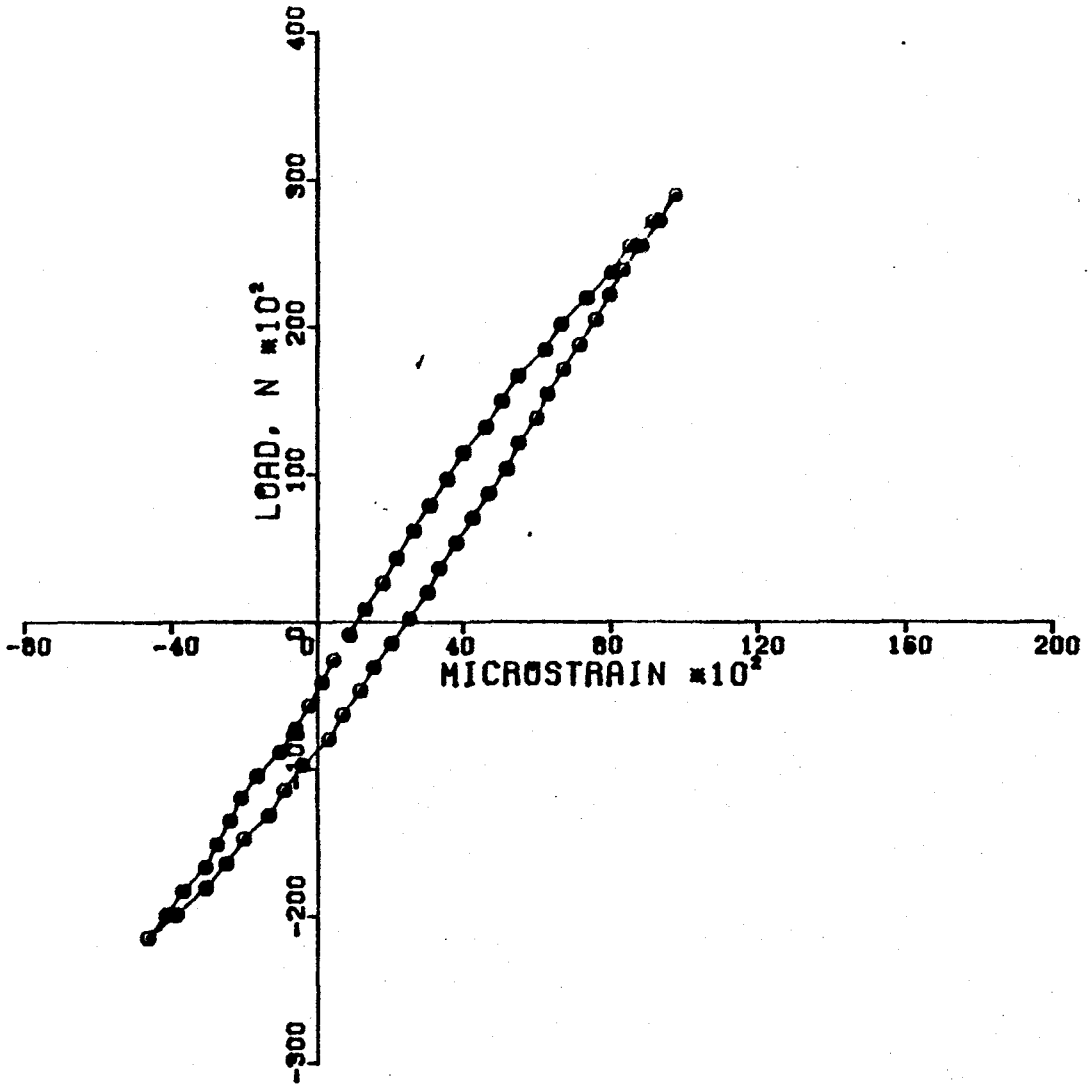

Figure 36. Cycle 500, Test 6, Continuous Fatigue.

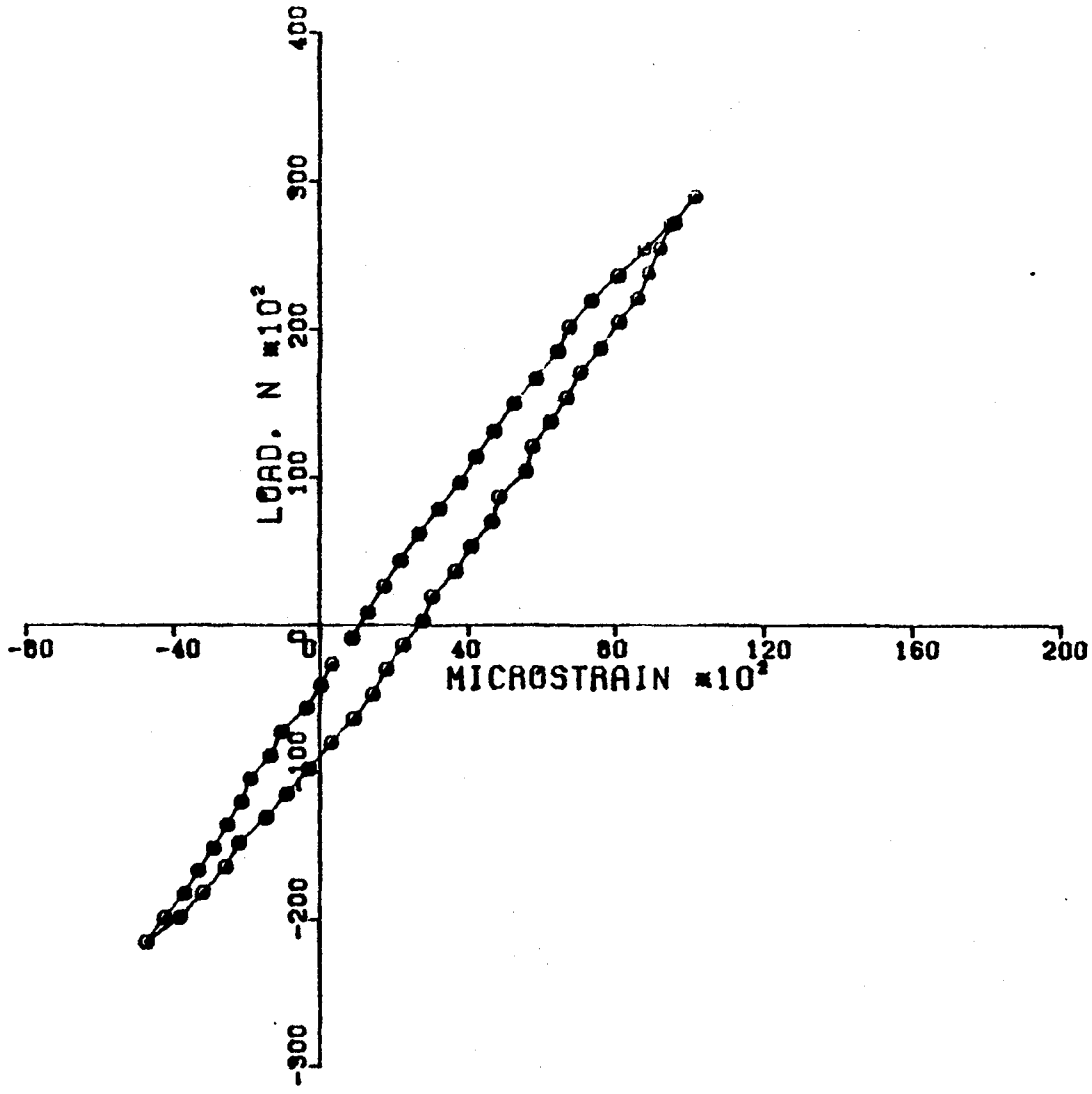

Figure 37. Cycle 1000, Test 6, Continuous Fatigue.

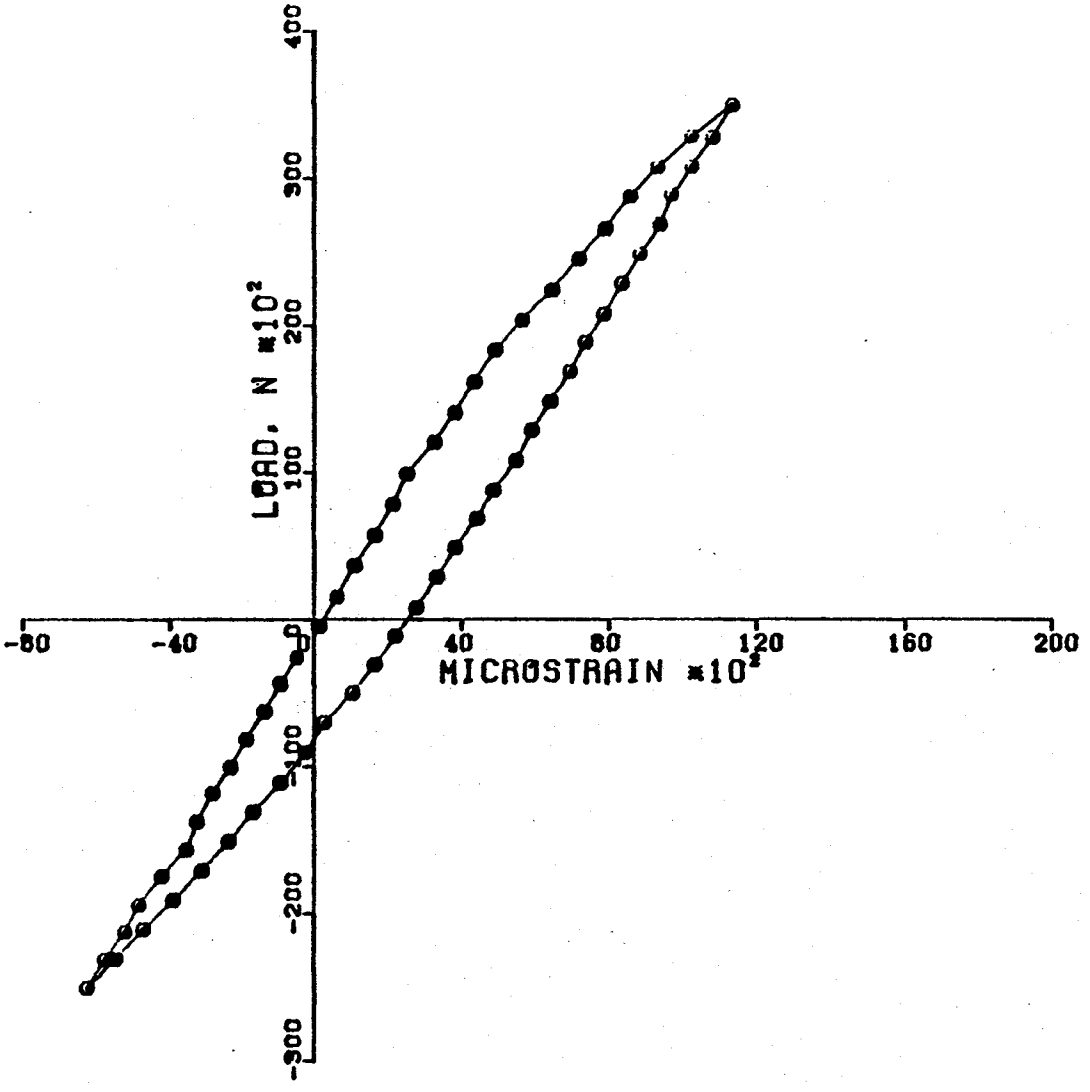

Figure 38. Cycle 1, Test 7, Continuous Fatigue.

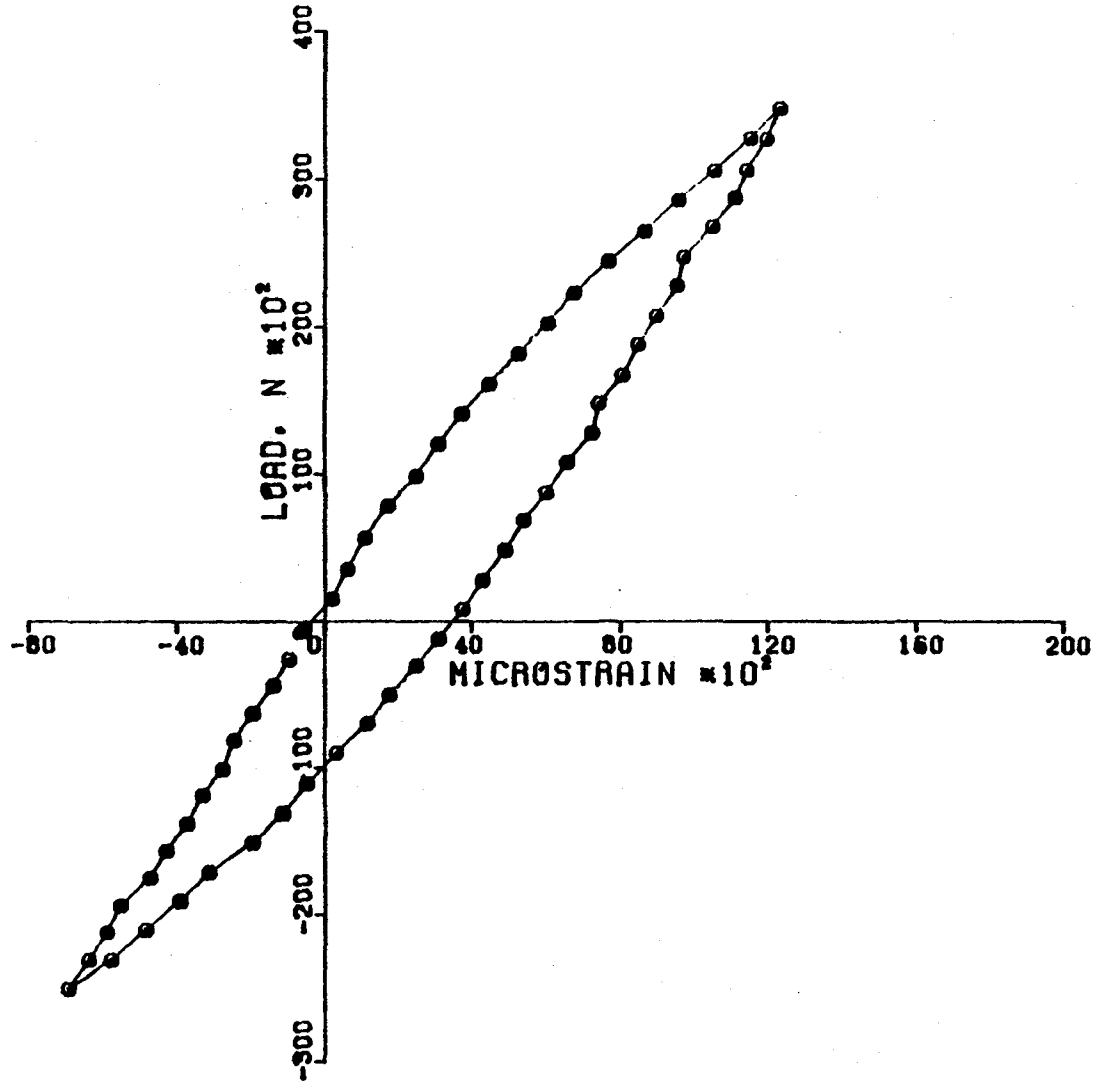

Figure 39. Cycle 500, Test 7, Continuous Fatigue.

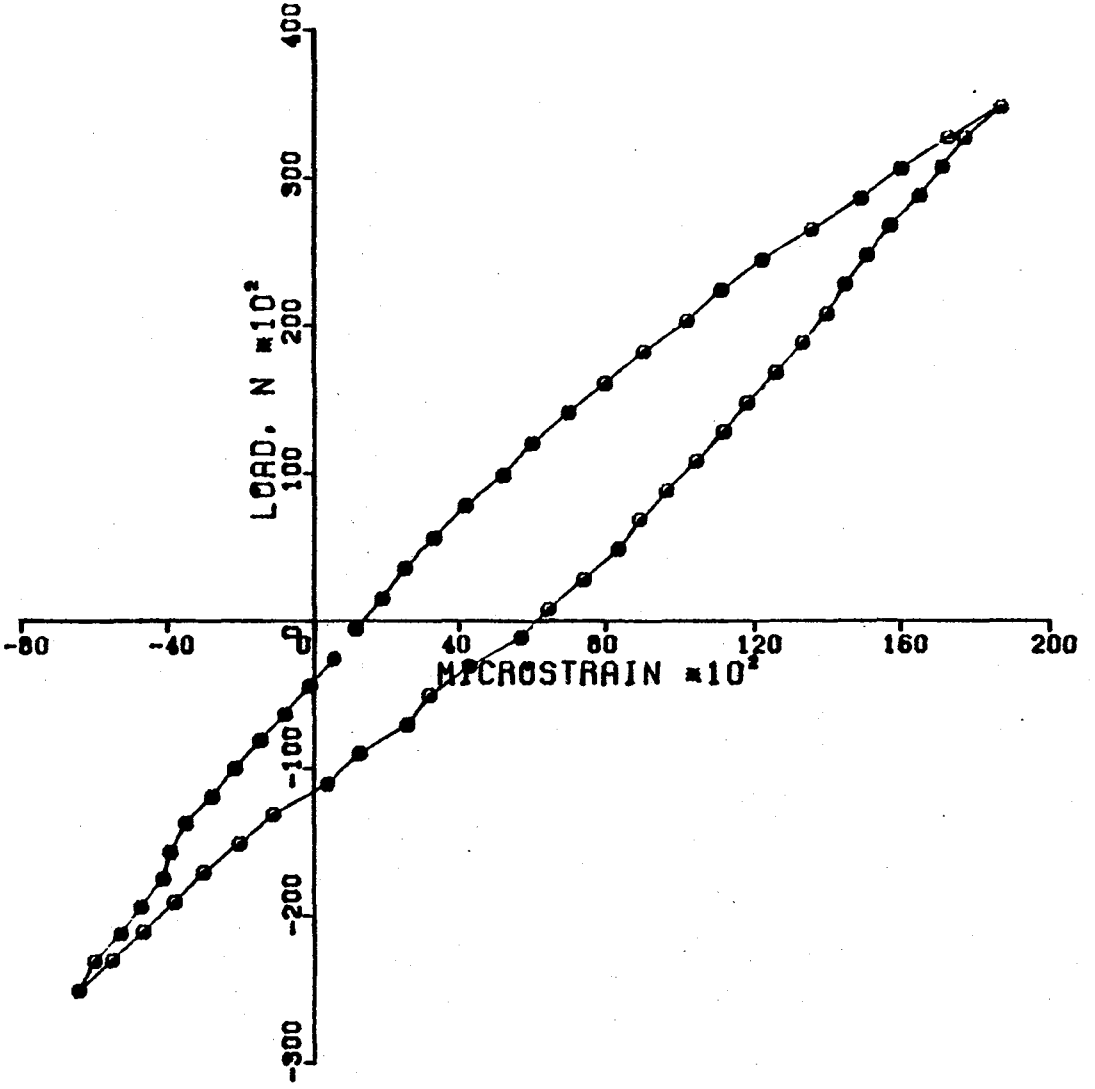

Figure 40. Cycle 884, Test 7, Continuous Fatigue.

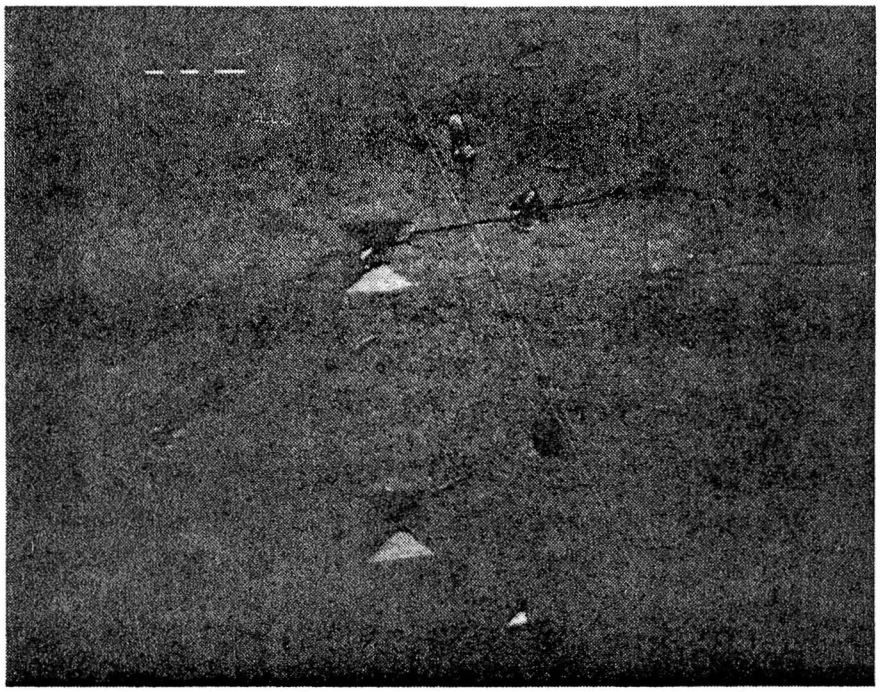

Figure 41. SEM Photo of Specimen No. 1 After Tests 6 and 7. 350X. Note the Crack Through the Indentation.

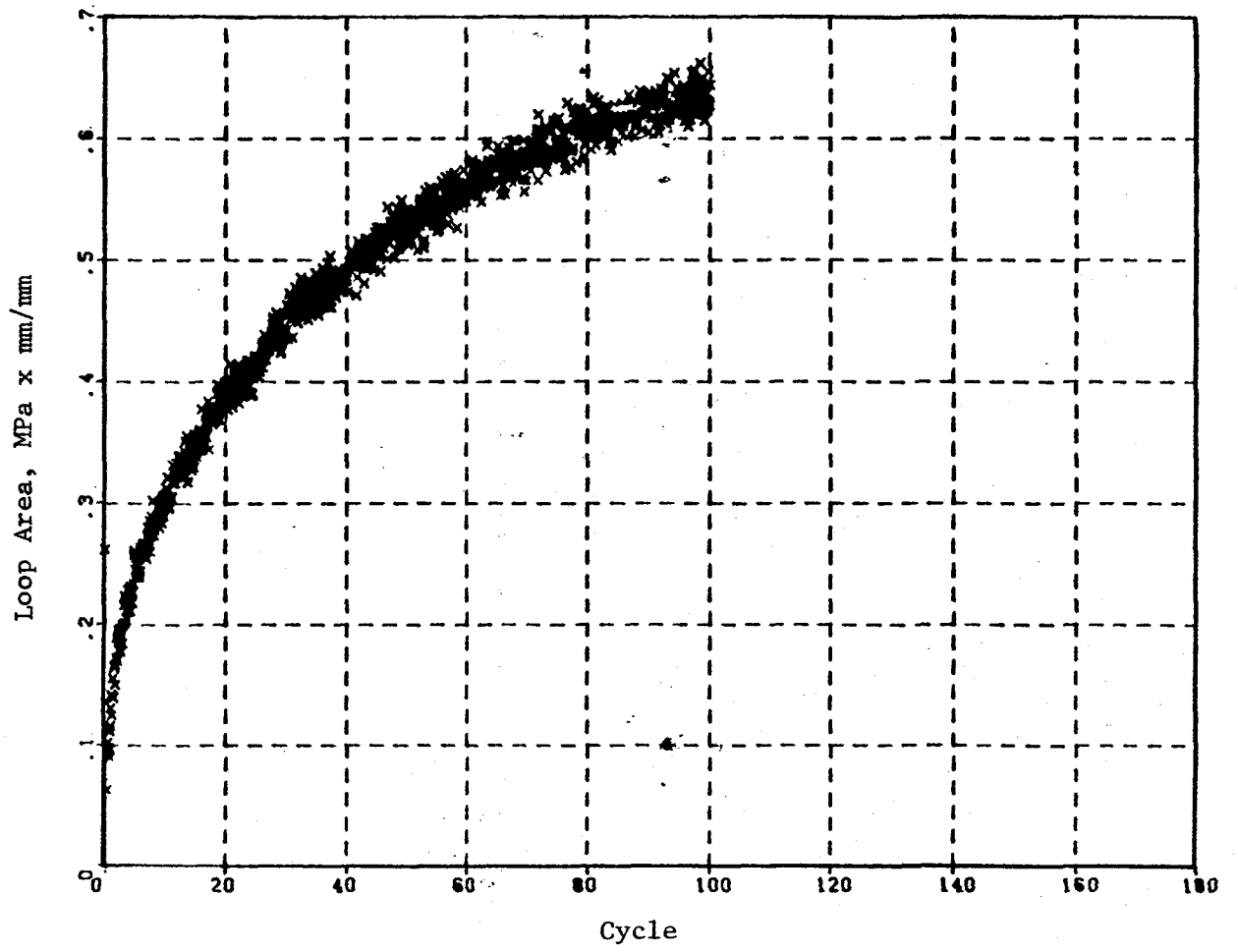

Figure 42. Loop Area Versus Cycles for Test 6.

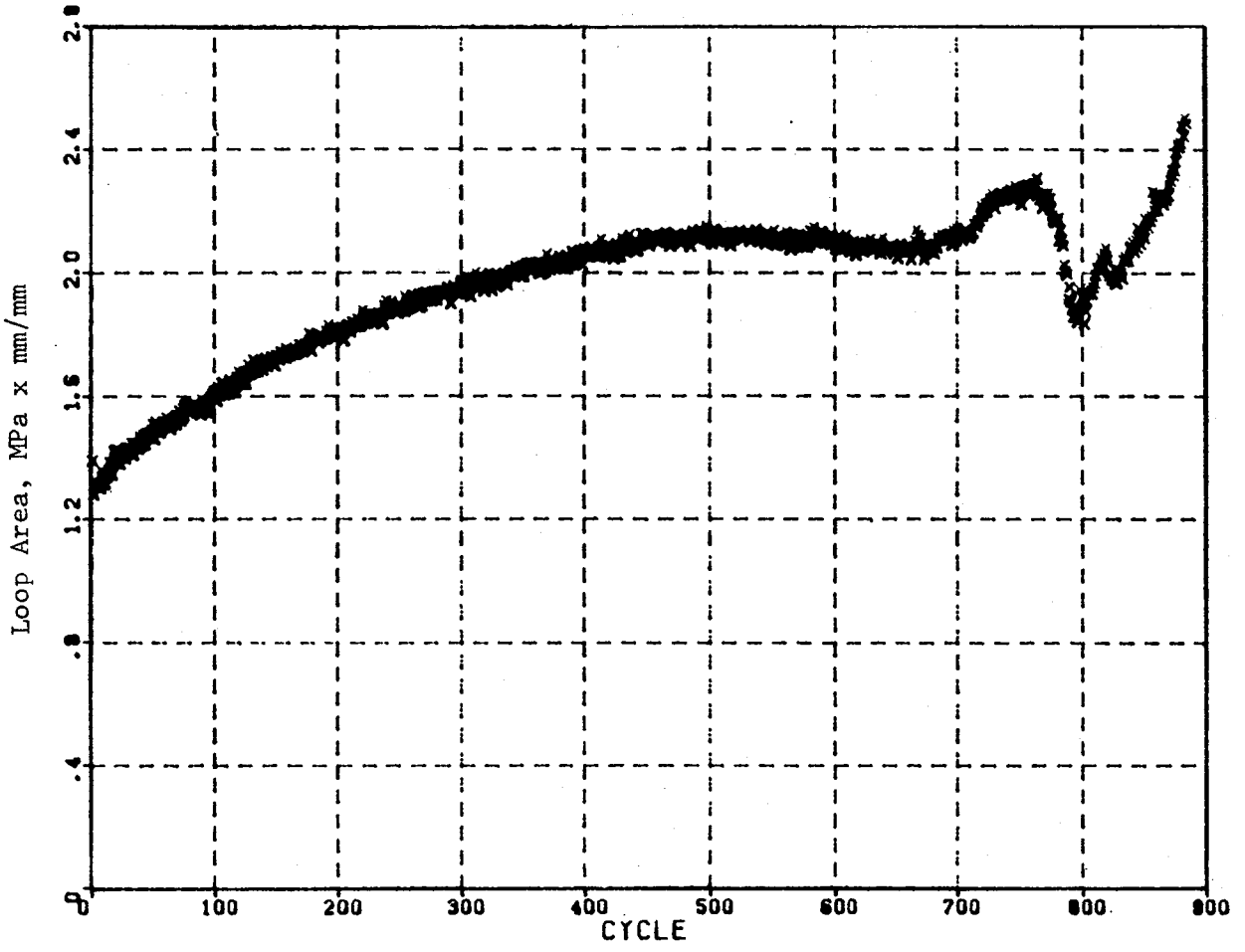

Figure 43. Loop Area Versus Cycles for Test 7.

5.2.2 Load Pattern II (Creep)

Specimen No. 9 was subjected to the test specifications presented below.

Spec. No.	Test No.	Load Range (N)	Load Range (lb)	Time (hr)
9	12A	29,886 - 34,087	6716 - 7660	5.1
	12B	34,087 - 35,600	7660 - 8000	2.0

The results of Test No. 12A are shown in Figure 44. The load was incremented 5 times as shown. The increases of load were made manually with a control potentiometer on the MTS system. This explains the slight changes in the magnitude of the load increases. Test No. 12A was ended prematurely when a measurement system "spike" caused the ISDG to lose contact with the interference fringe patterns. When this occurred, the specimen was unloaded for approximately 15 minutes in order to relocate the fringes. Test No. 12B was then immediately begun. The results of 12B are presented in Figure 45. The initial strain occurring at a 34,087 N (7660 lb) load is much lower than that previously measured, implying that some recovery took place during the unloading of the specimen. A photomicrograph of the specimen at the completion of Test No. 12B reveals no surface crack formation, Figure 46.

5.2.3 Load Pattern III (Tension Hold)

Specimen No. 11 was tested using the specifications shown below:

Spec. No.	Test No.	Load Range (N)	Load Range (lb)	No. of Cycles
11	10	29,886, -17,933	6716, -4030	384

The hold time at the tensile load limit equaled 2 minutes. During this hold period 30 data points were measured at equal intervals by the ISDG to determine the creep effect. The test history is shown in Figures 47 through 49. As can be seen in these figures, the creep effect is present but not very large. The measured strain values seem to have a positive drift as the test progressed. This is consistent with the results of Load Patterns V and VI, where 2-minute hold times were employed at both the compression and tension limits. This drift is thus postulated to be a material characteristic rather than a measuring system error.

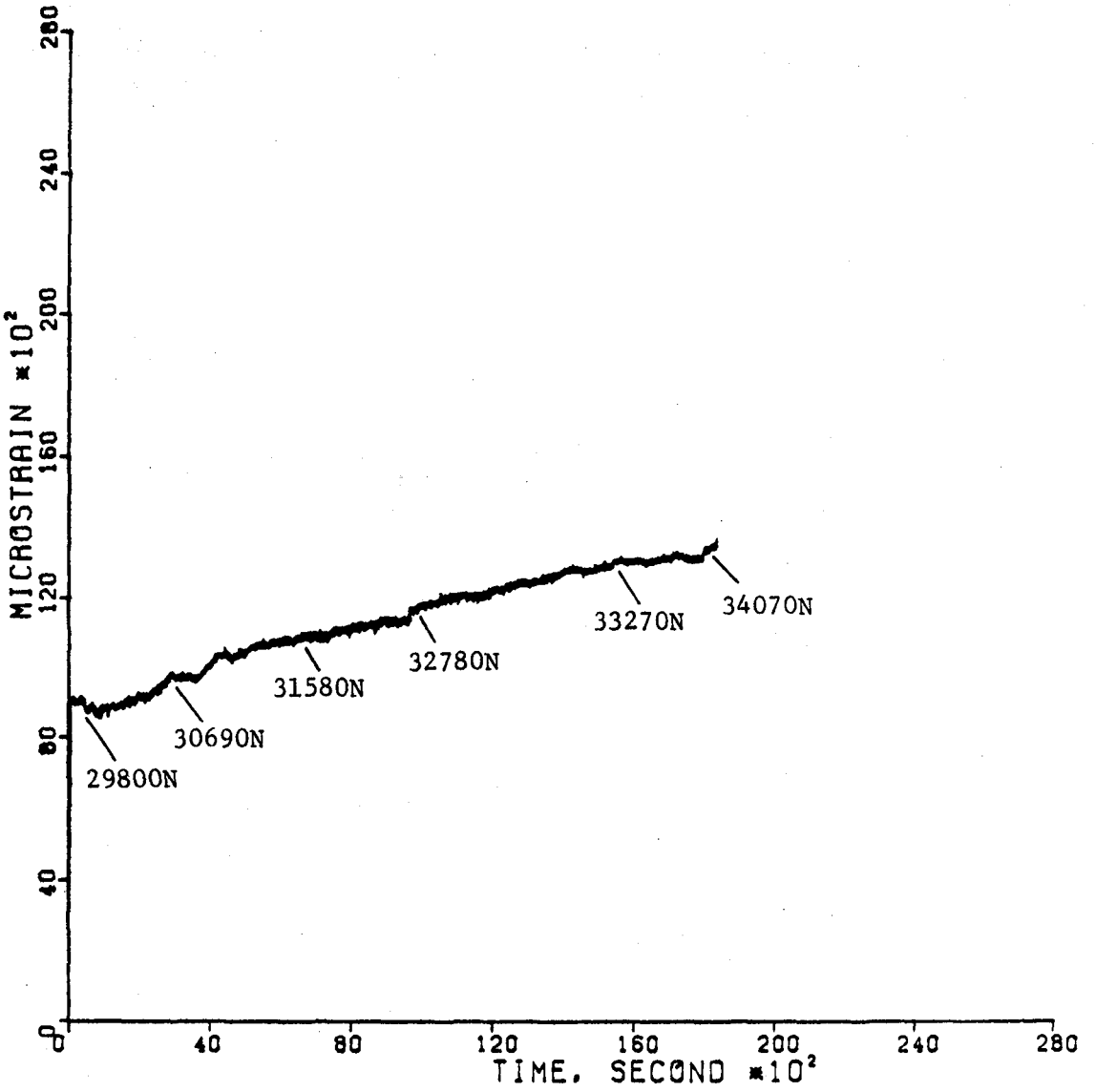

Figure 44. Creep Strain for Test 12A - Initial Test.

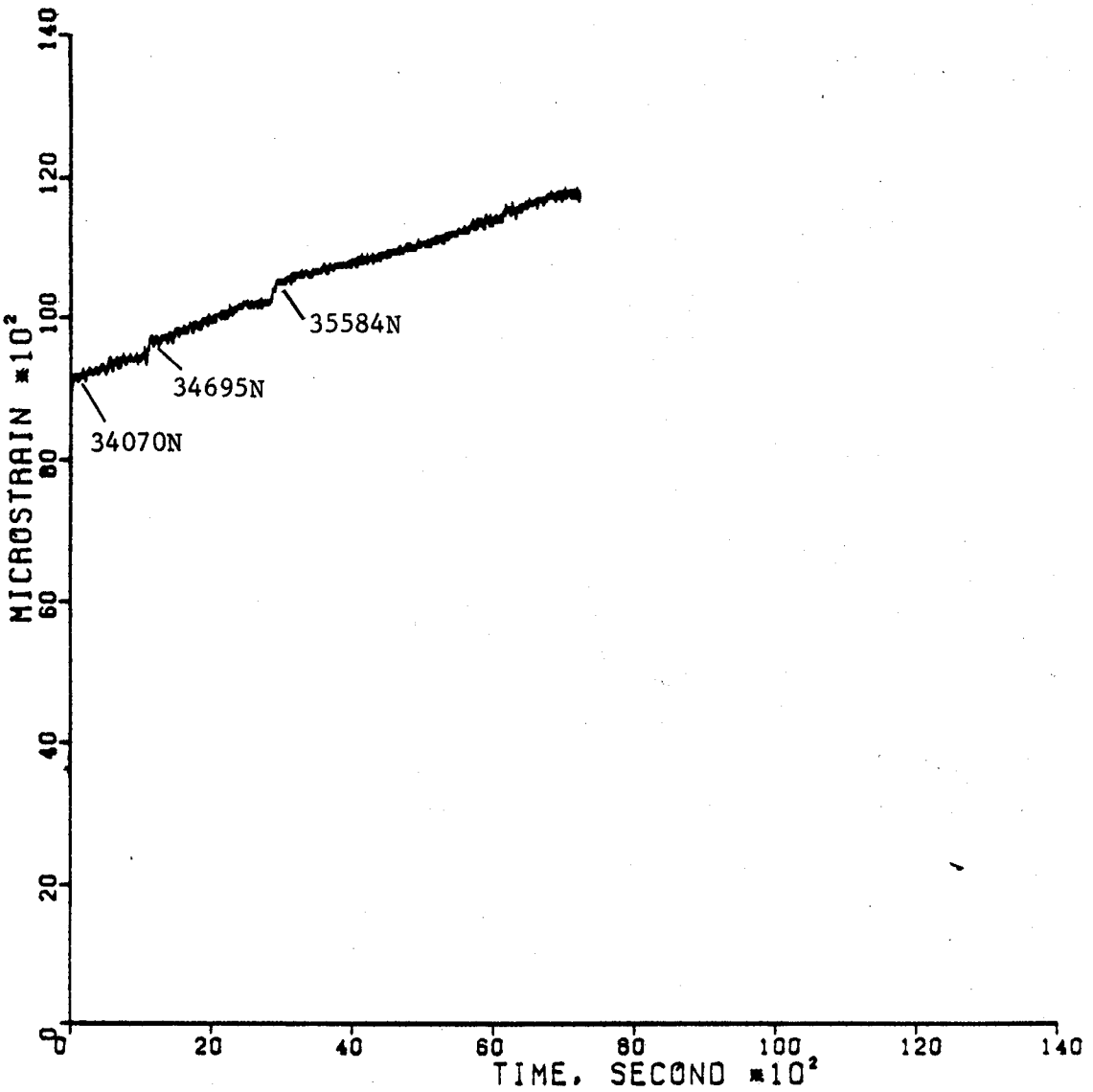

Figure 45. Creep Strain for Test 12B - Restarted Test.

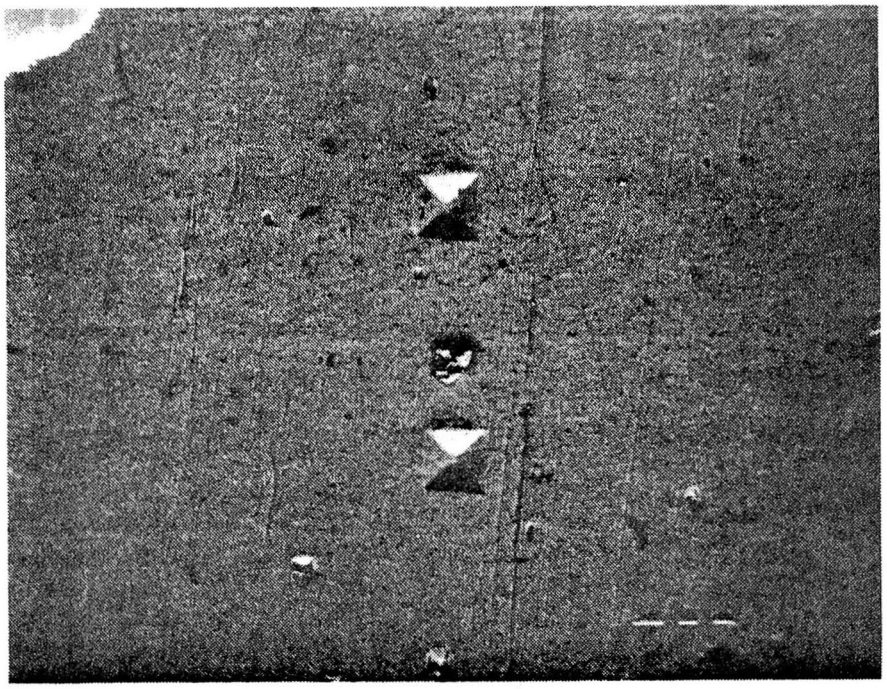

Figure 46. SEM Photo of Specimen No. 9 After Test 12.

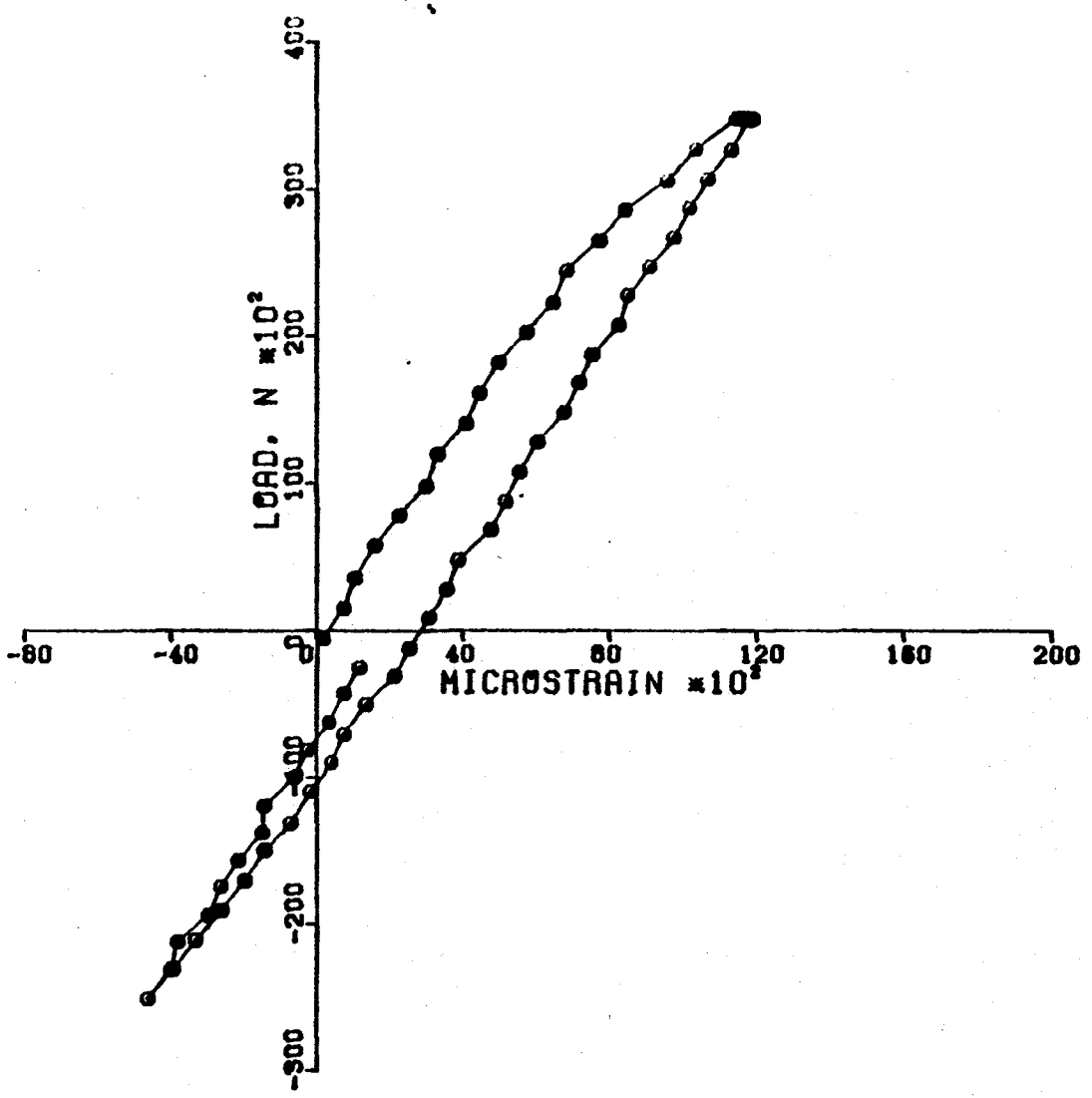

Figure 47. Cycle 1, Test 10, Tension Hold.

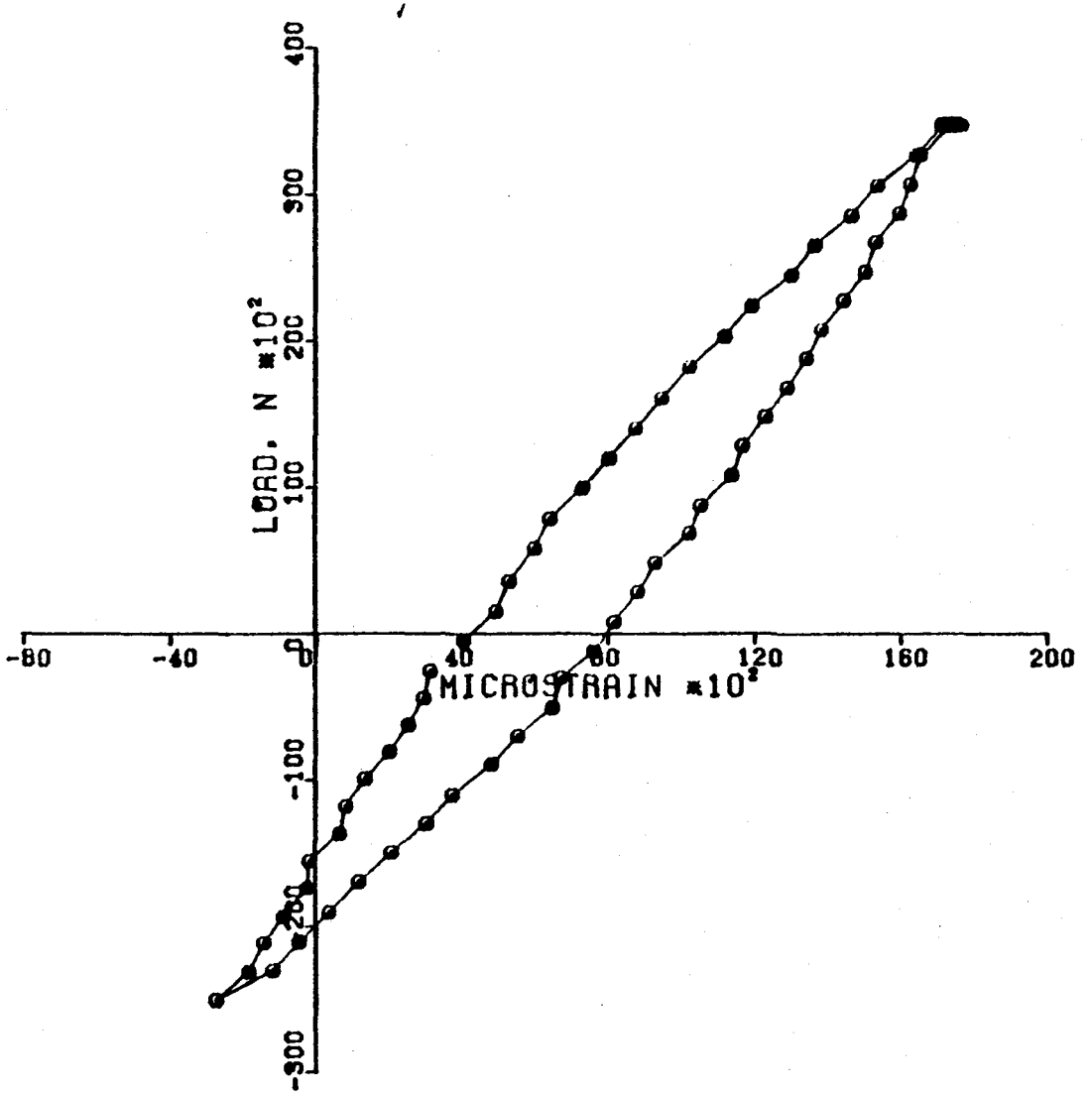

Figure 48. Cycle 200, Test 10, Tension Hold.

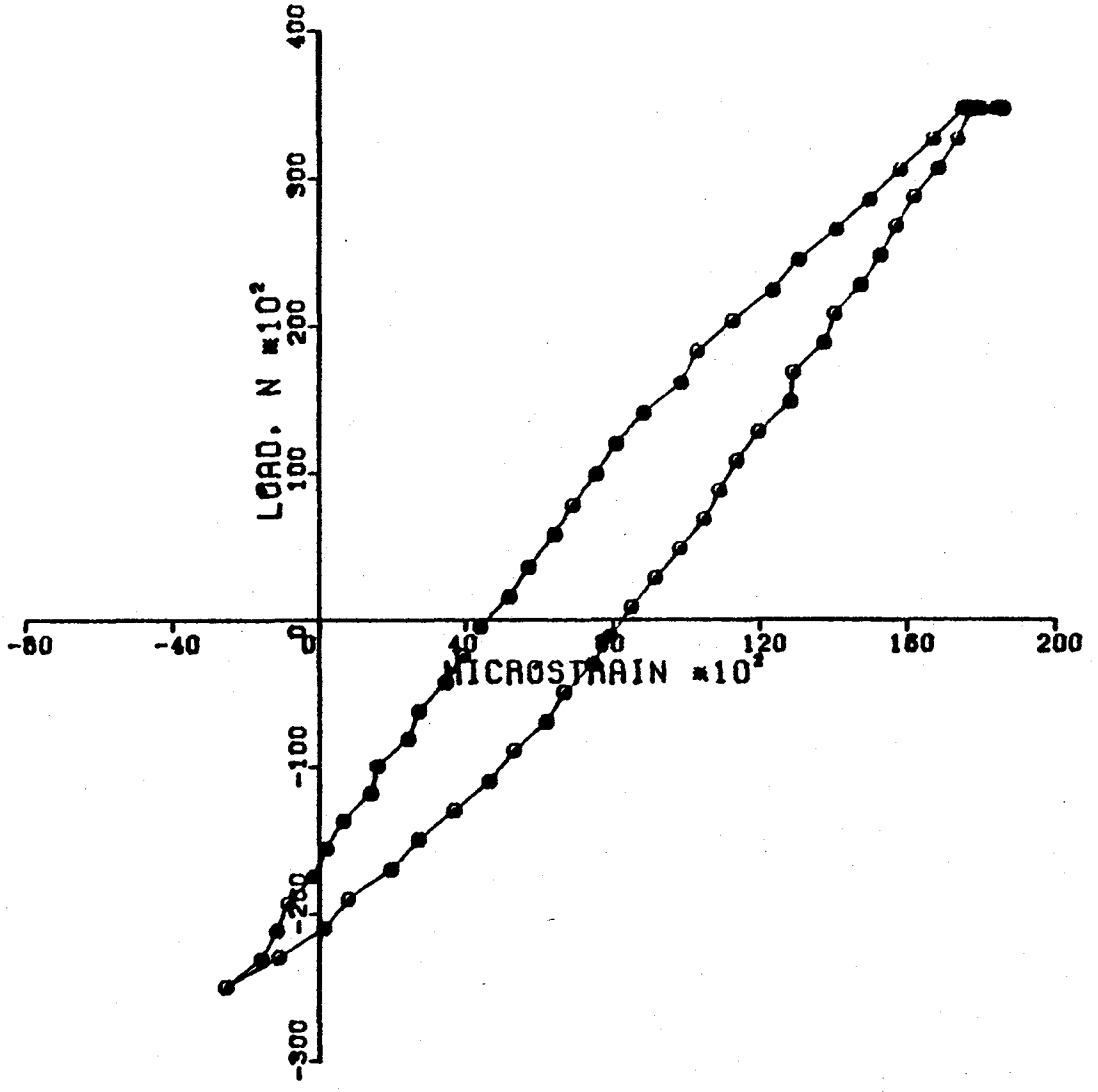

Figure 49. Cycle 380, Test 10, Tension Hold.

At the conclusion of the test, very small surface cracks could be seen in the notch root, Figure 50. It is felt that these cracks have not substantially altered the plastic strain values recorded. A plot of loop area versus cycles does not reveal abnormalities, Figure 51.

5.2.4 Load Pattern IV (Compression Hold)

Specimen No. 8 was tested using this load pattern according to the specifications below.

Spec. No.	Test No.	Load Range (N)	Load Range (lb)	No. of Cycles
8	8	29,886, -17,933	6716, -4030	345

A 2-minute hold duration was employed at the compression limit, with 30 data points collected as before. Figures 52 through 55 depict the results of this test. Cycle No. 325 reveals a rough hysteresis loop with much experimental scatter. This breakdown of the uniformity of the loop began on approximately Cycle No. 240. A plot of the loop area versus cycle reveals this clearly, Figure 56. A SEM photomicrograph of the specimen after the test was completed depicts a large amount of surface deformation in the notch root, Figure 57.

5.2.5 Load Pattern V (Tension/Compression Hold)

Specimen No. 12 was tested using this load pattern as follows.

Spec. No.	Test No.	Load Range (N)	Load Range (lb)	No. of Cycles
12	9	29,886, -17,933	6716, -4030	253

A 2-minute hold time was employed at both the tension and compression limits. The results of this test are shown in Figures 58 through 60. A slight positive drift in the recorded strain is evident as previously noted. The plot of loop area versus cycle discloses an abnormal effect starting at Cycle 150, Figure 61. An ensuing SEM photomicrograph divulged surface flaws of a nature similar to those formed in Specimen No. 8, Figure 62.

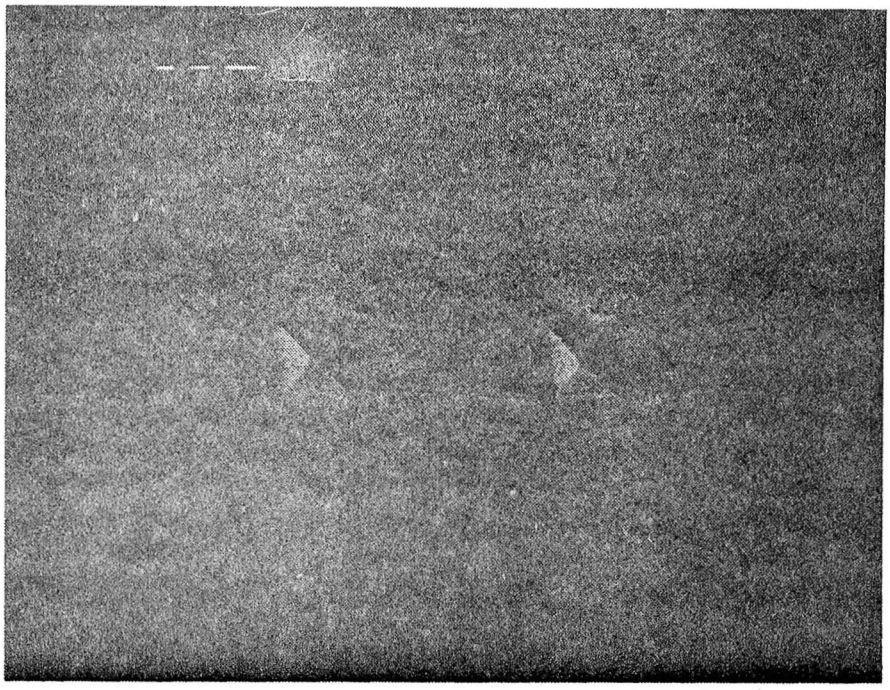

Figure 50. SEM Photo of Specimen No. 11 After Test 10.

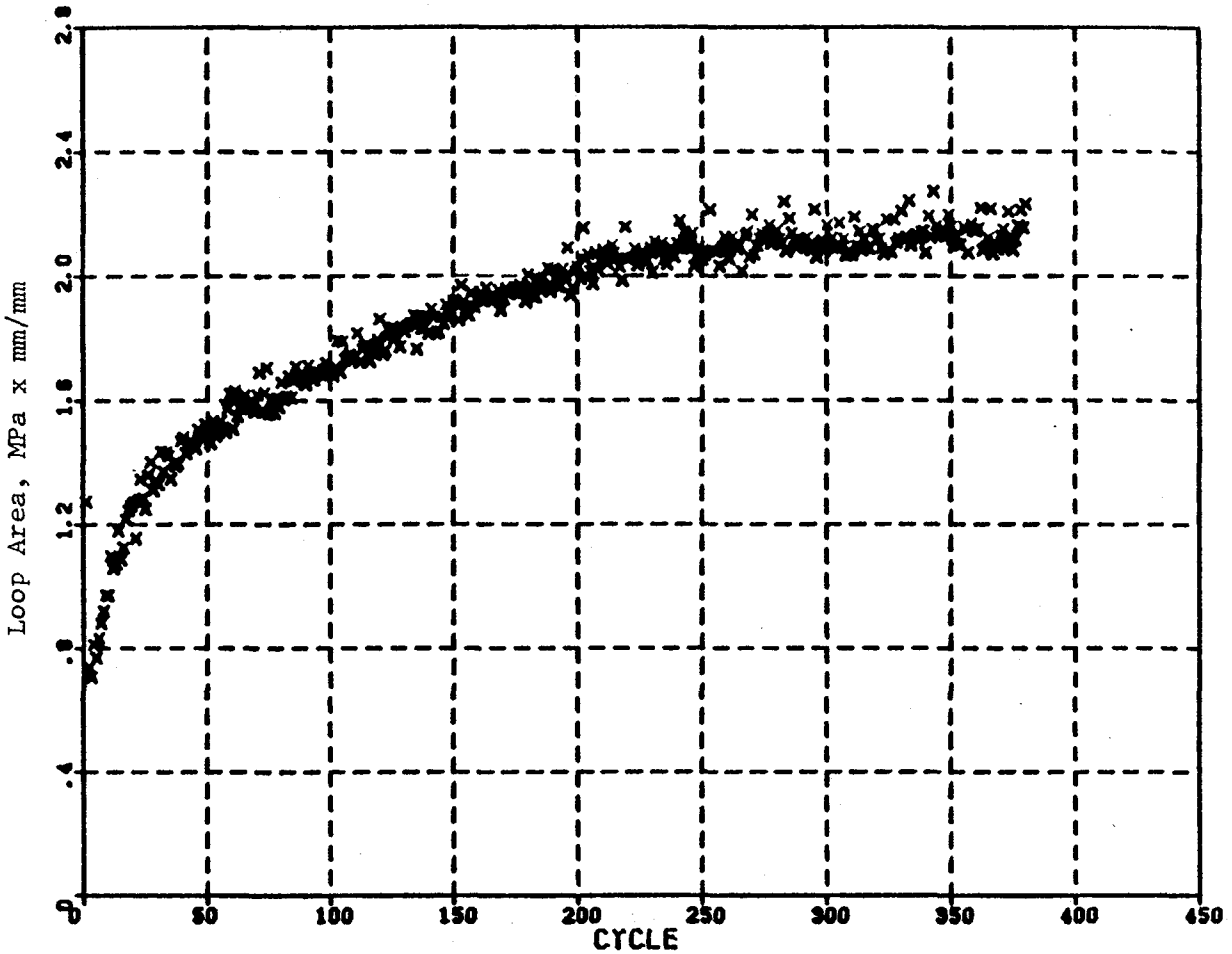

Figure 51. Loop Area Versus Cycles for Test 10.

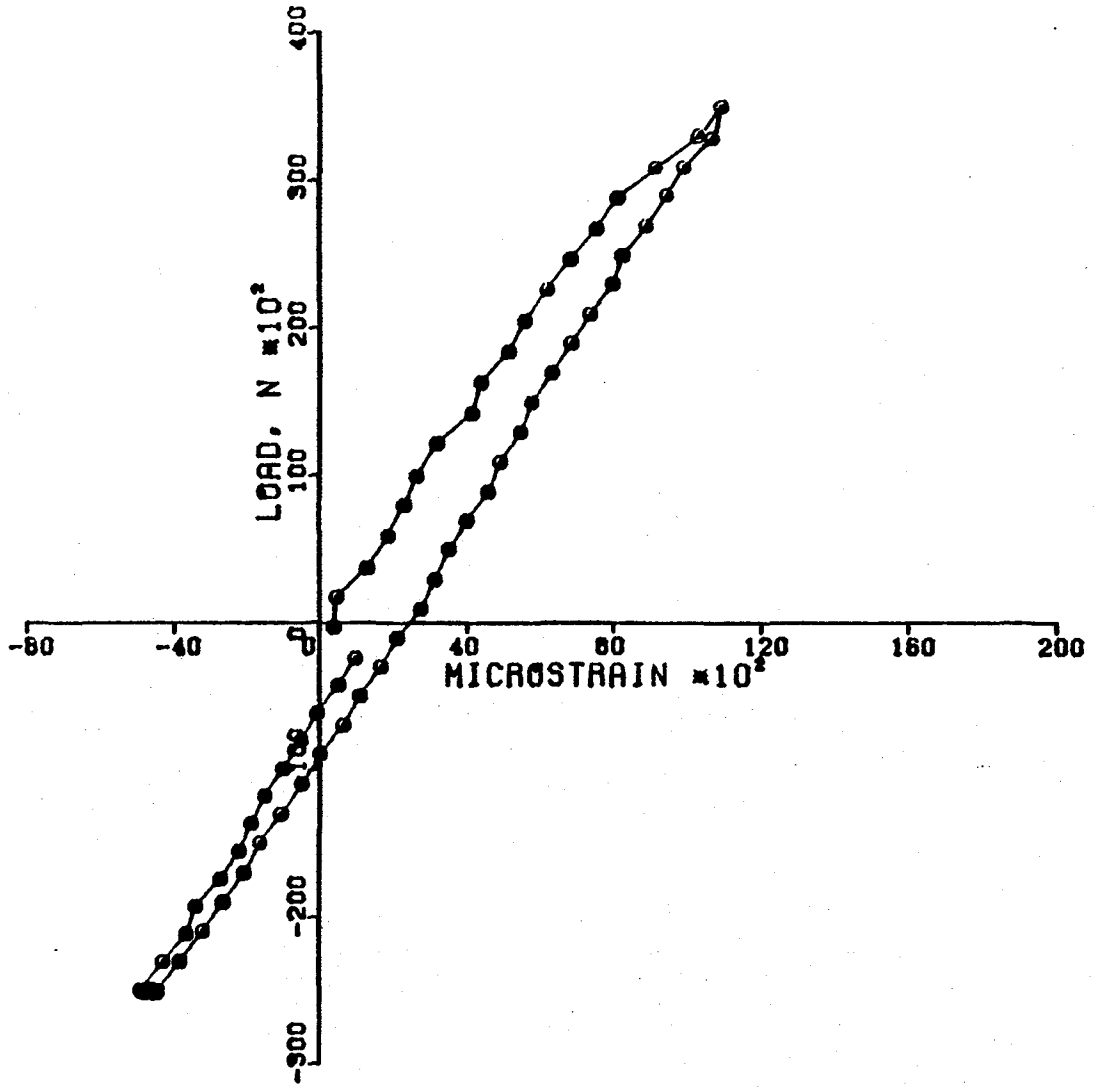

Figure 52. Cycle 1, Test 8, Compression Hold.

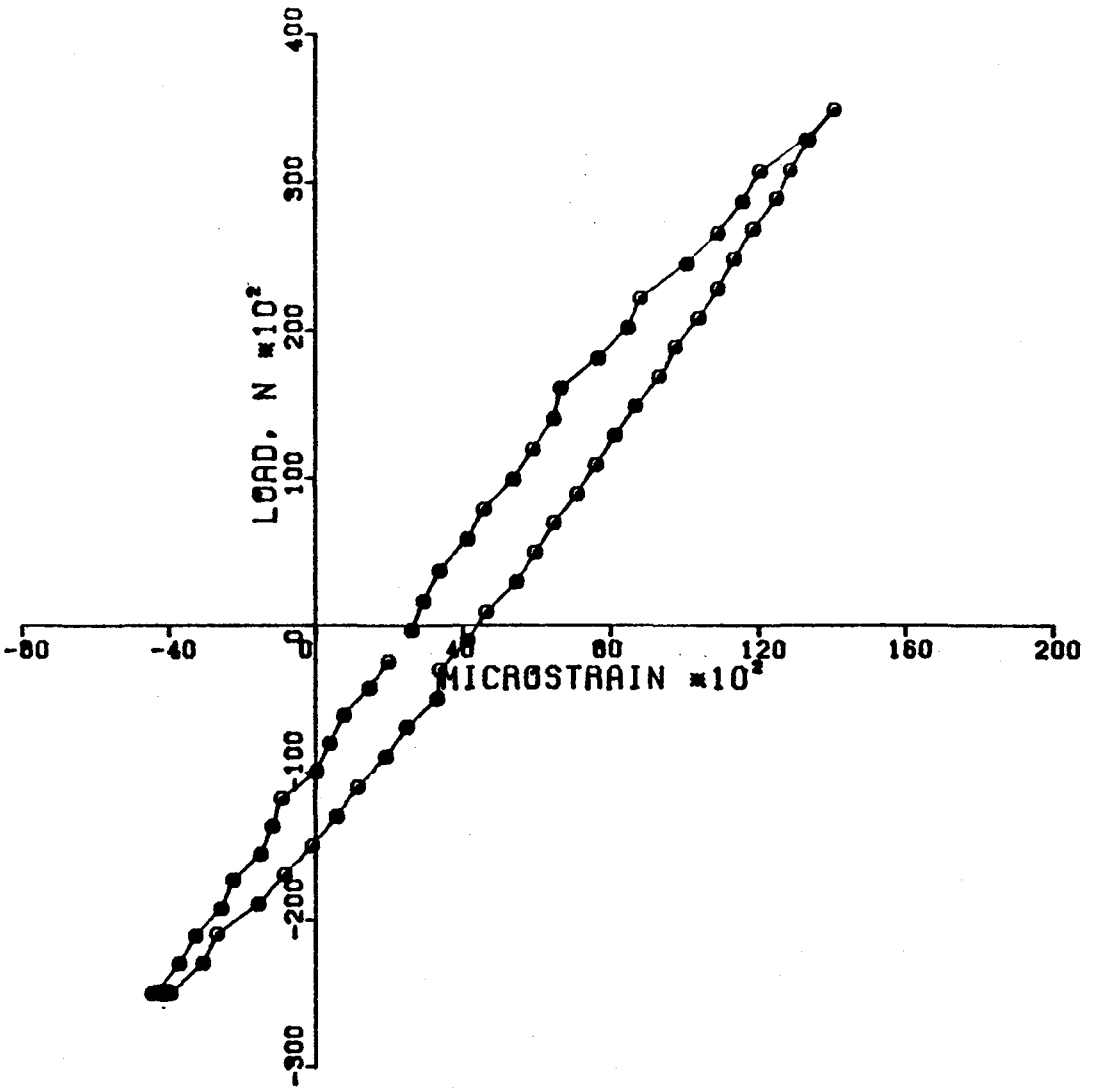

Figure 53. Cycle 100, Test 8, Compression Hold.

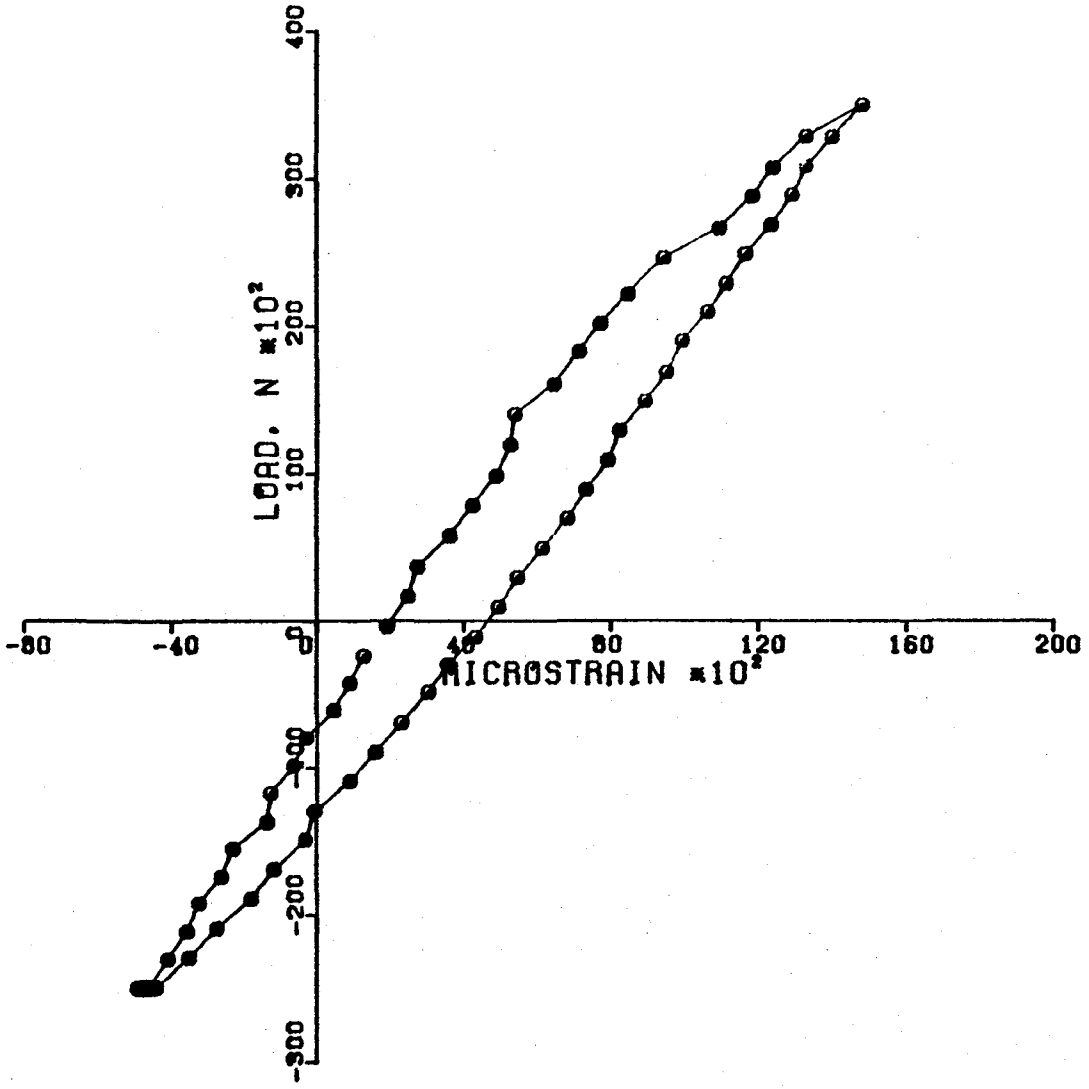

Figure 54. Cycle 220, Test 8, Compression Hold.

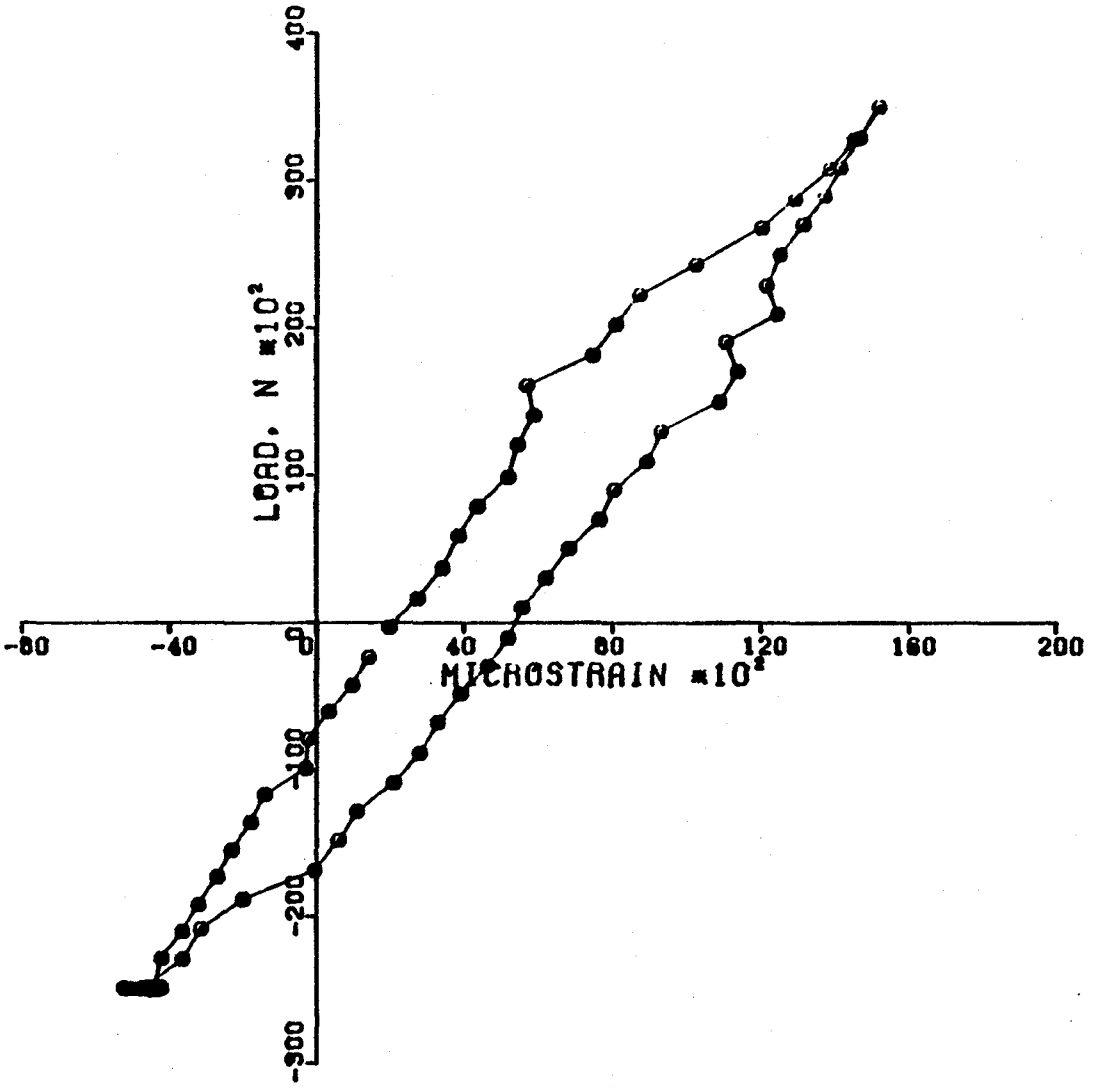

Figure 55. Cycle 325, Test 8, Compression Hold.

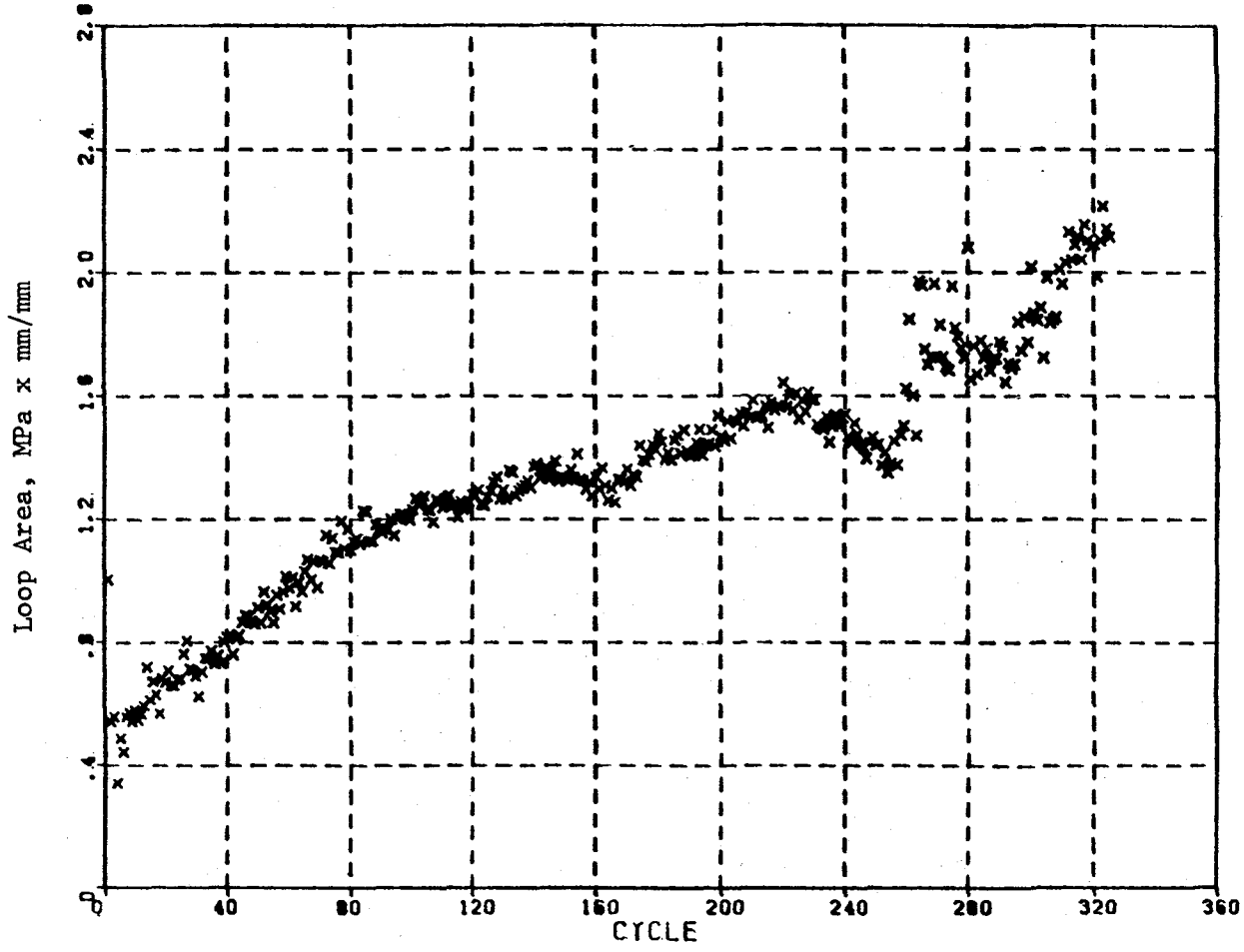

Figure 56. Loop Area Versus Cycles for Test 8.

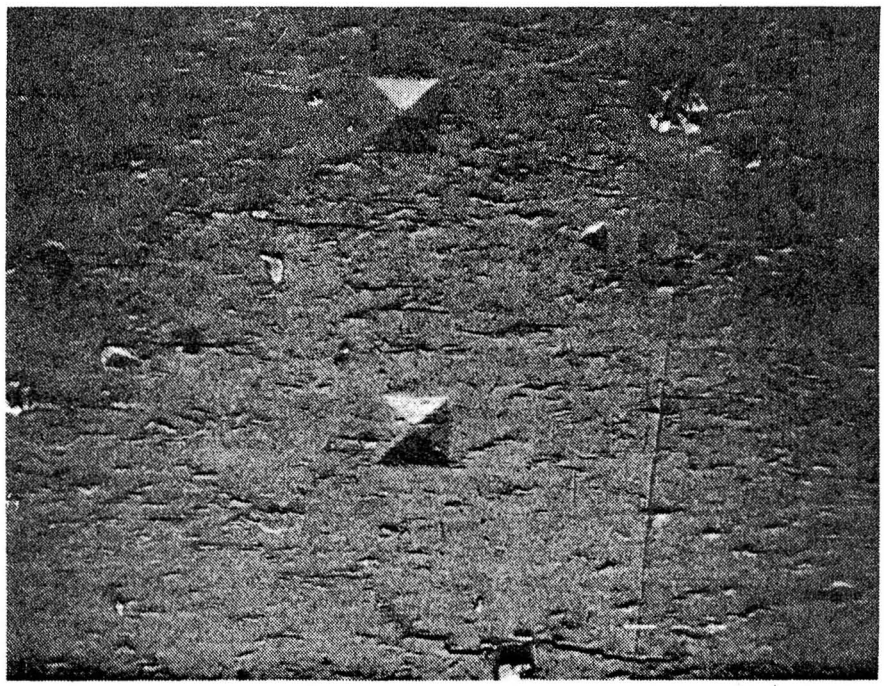

Figure 57. SEM Photo of Specimen No. 8 After Test No. 8. Note the Carbides at Several of the Larger Crack Origins.

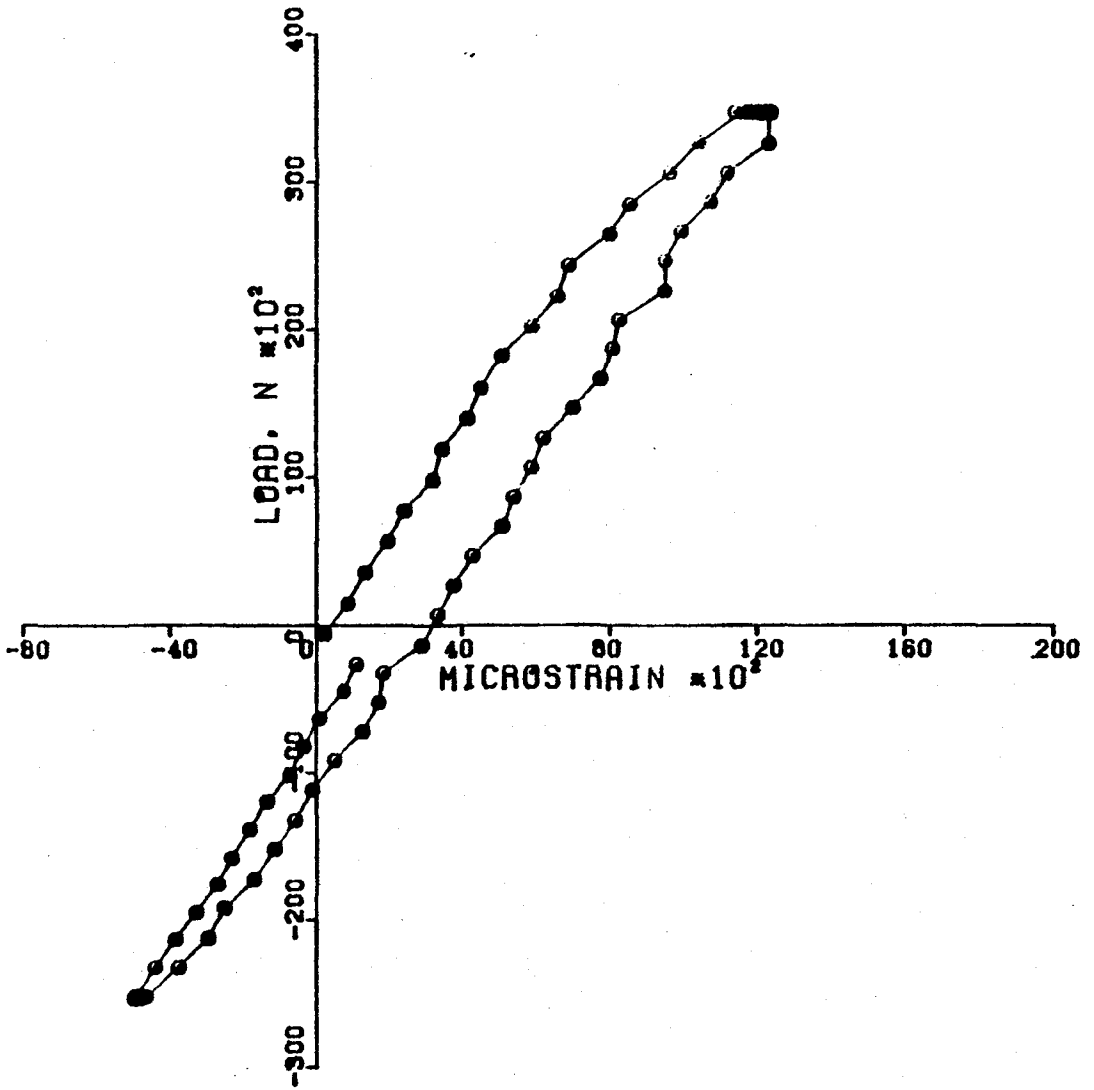

Figure 58. Cycle 1, Test 9, Tension/Compression Hold.

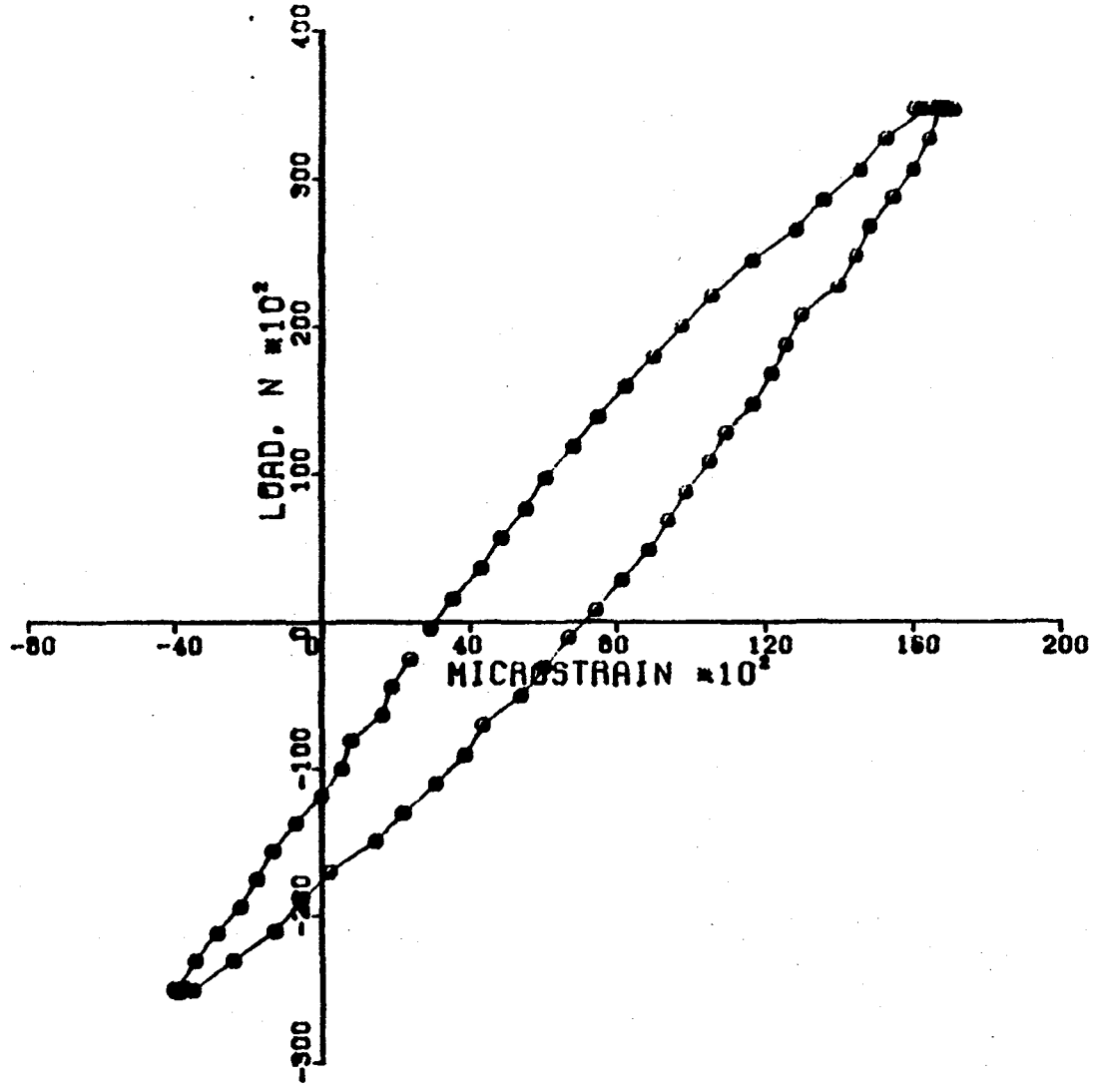

Figure 59. Cycle 120, Test 9, Tension/Compression Hold.

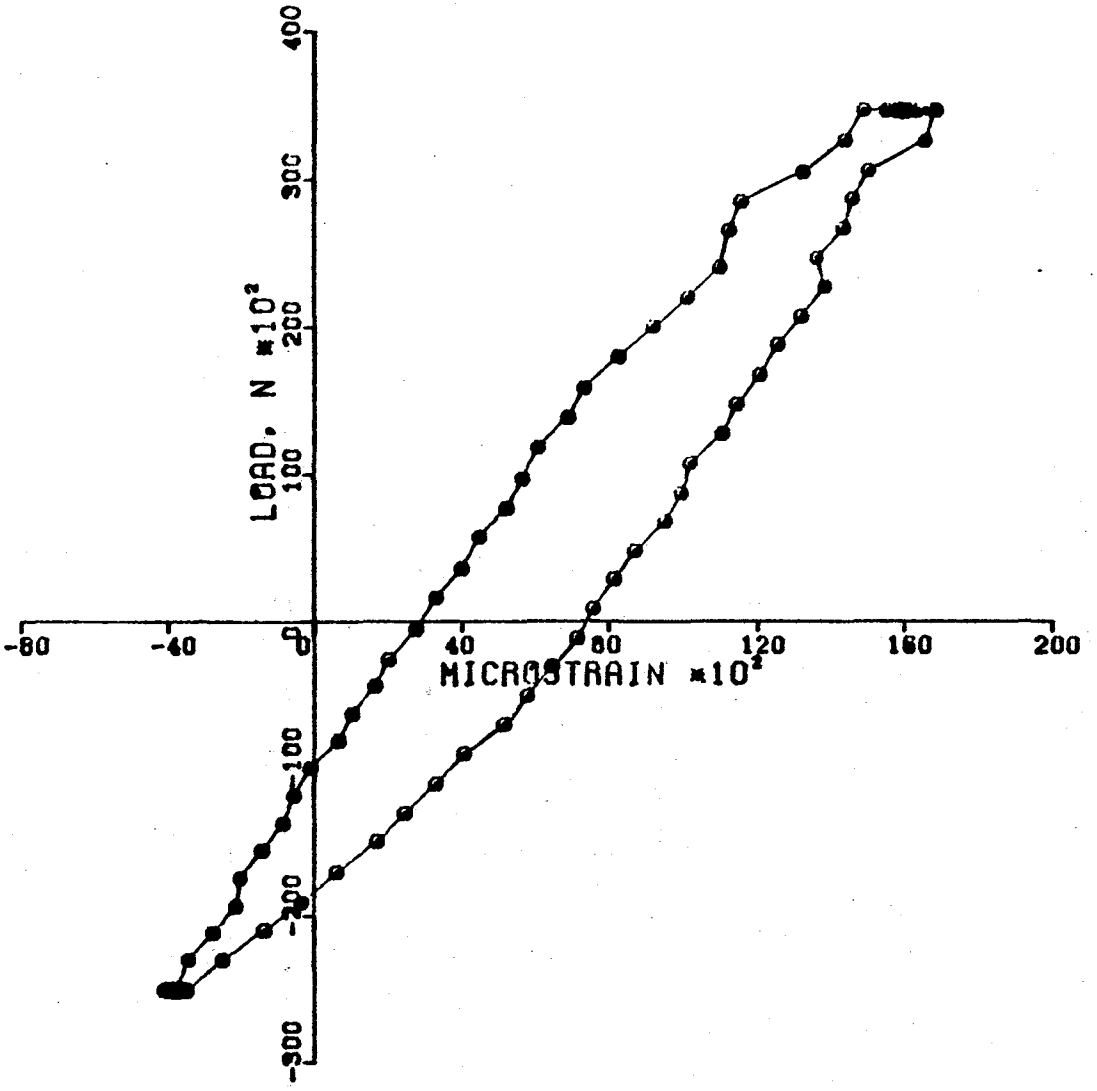

Figure 60. Cycle 253, Test 9, Tension/Compression Hold.

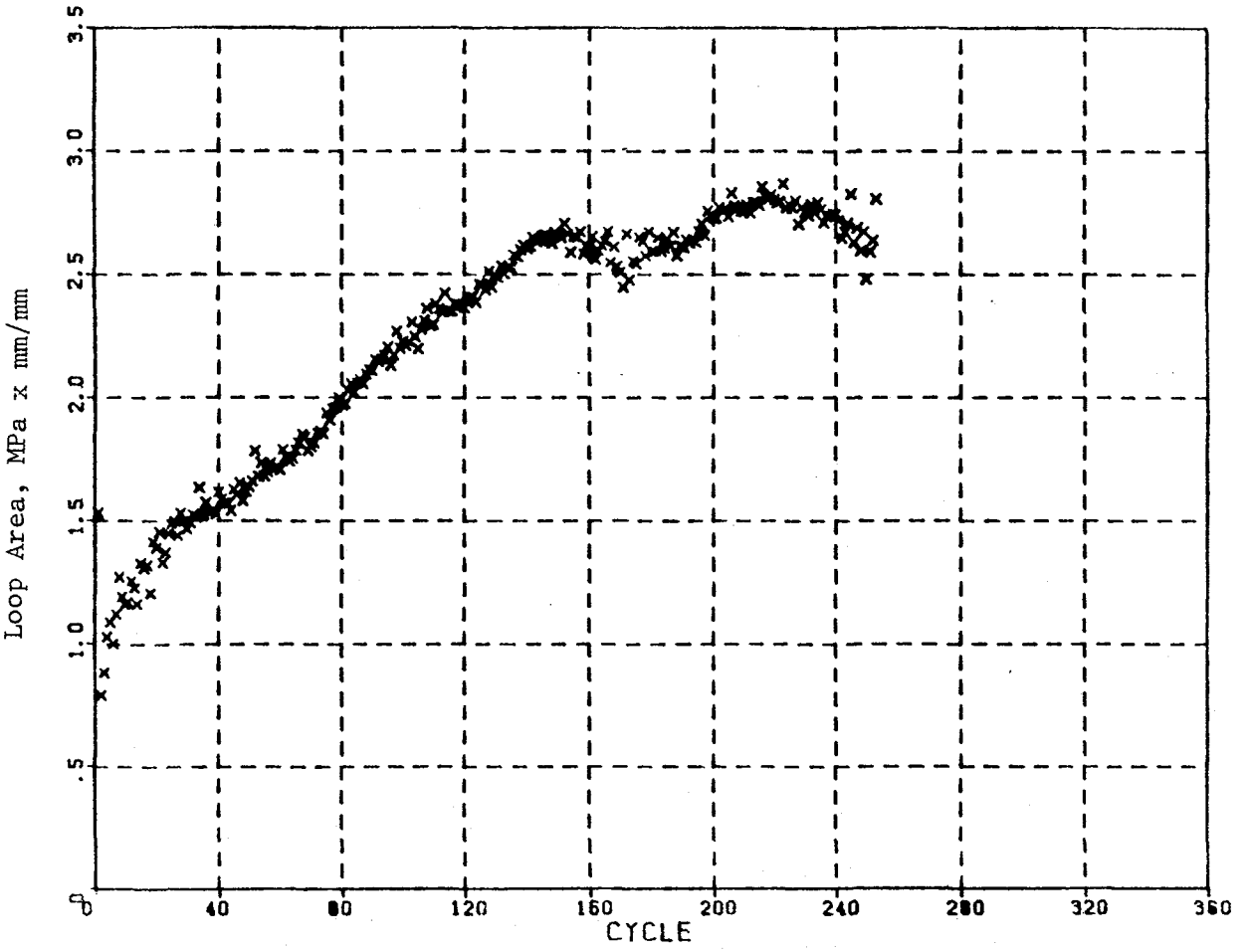

Figure 61. Loop Area Versus Cycles for Test 9.

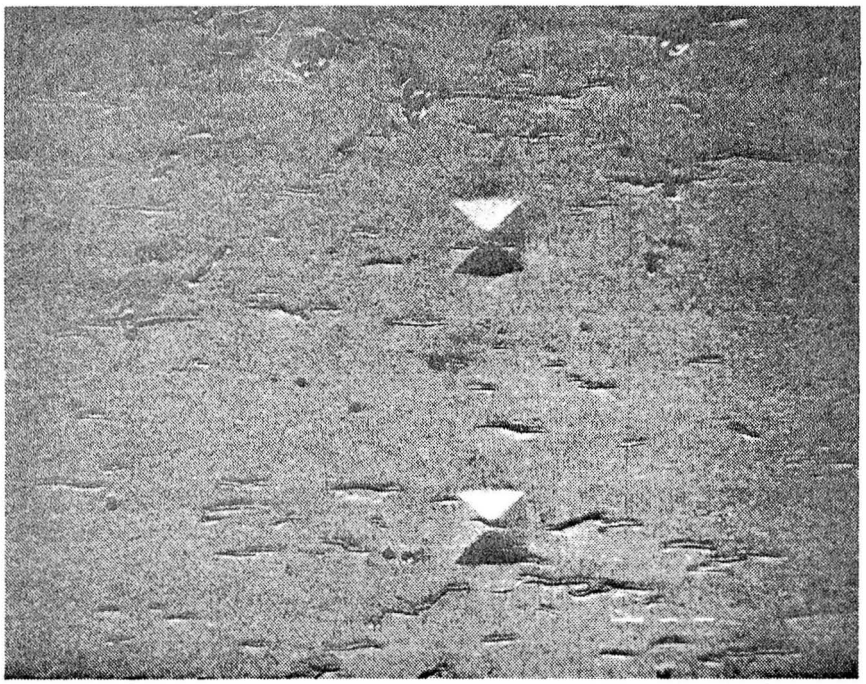

Figure 62. SEM Photo of Specimen No. 12 After Test 9.

5.2.6 Load Pattern VI

Specimen No. 13 was subjected to this load pattern. The test log is presented below.

Spec. No.	Test No.	Load Range (N)	Load Range (lb)	No. of Cycles
13	11A	25,187, -15,103	5660, -3394	1000
	11B	29,886, -17,933	6716, -4030	185

Load Pattern VI is a combination of Load Patterns I and V. For comparison sake, it was decided to use the identical load ranges employed in Test Nos. 6 and 9 for Test Nos. 11A and 11B. Figures 63 through 66 depict the test history of Specimen No. 13. The 1000 cycles of continuous cycle loading imposed on the specimen in Test No. 11A seemed to shorten the test life of the specimen considerably. The strain growth rate observed in Test No. 11B was almost twice as great as that detected in Test No. 9. It should be noted here that the slight offset evident at the completion of Test No. 11A is not contained in the data for Test No. 11B. The computer program controlling the measuring system automatically zeroes the measured strain values in reference to zero load on the initial cycle of a new load pattern. Plots of the loop area versus cycle for Test Nos. 11A and 11B are smooth, Figures 67 and 68. A SEM photomicrograph of the notch region at the completion of the tests displays small surface cracks beginning to form, Figure 69.

5.3 TEST DATA DOCUMENTATION

The data collected in this program are available on a DEC RL01 hard disk. Table IX lists the order of appearance of these data on the disk, as well as pertinent information needed to recover it from the disk. The data were stored by cycle or sample number in section sizes defined by the record size. A FORTRAN program which will print the data is presented below:

```
      DIMENSION LOAD(Recordsize), ISTRAIN(Recordsize)
      OPEN(UNIT=1,NAME='DL:filename',TYPE='OLD',ACCESS='DIRECT',
     *RECORDSIZE=?)
      READ(1'cycle number)NCYCLE,(LOAD(J),ISTRAIN(J),J=1,recordsize)
      WRITE(7,10) NCYCLE
10    FORMAT(1X,'CYCLE NUMBER=',I3)
      DO 20 J=1,recordsize
      WRITE(7,20) LOAD(J),ISTRAIN(J)
```

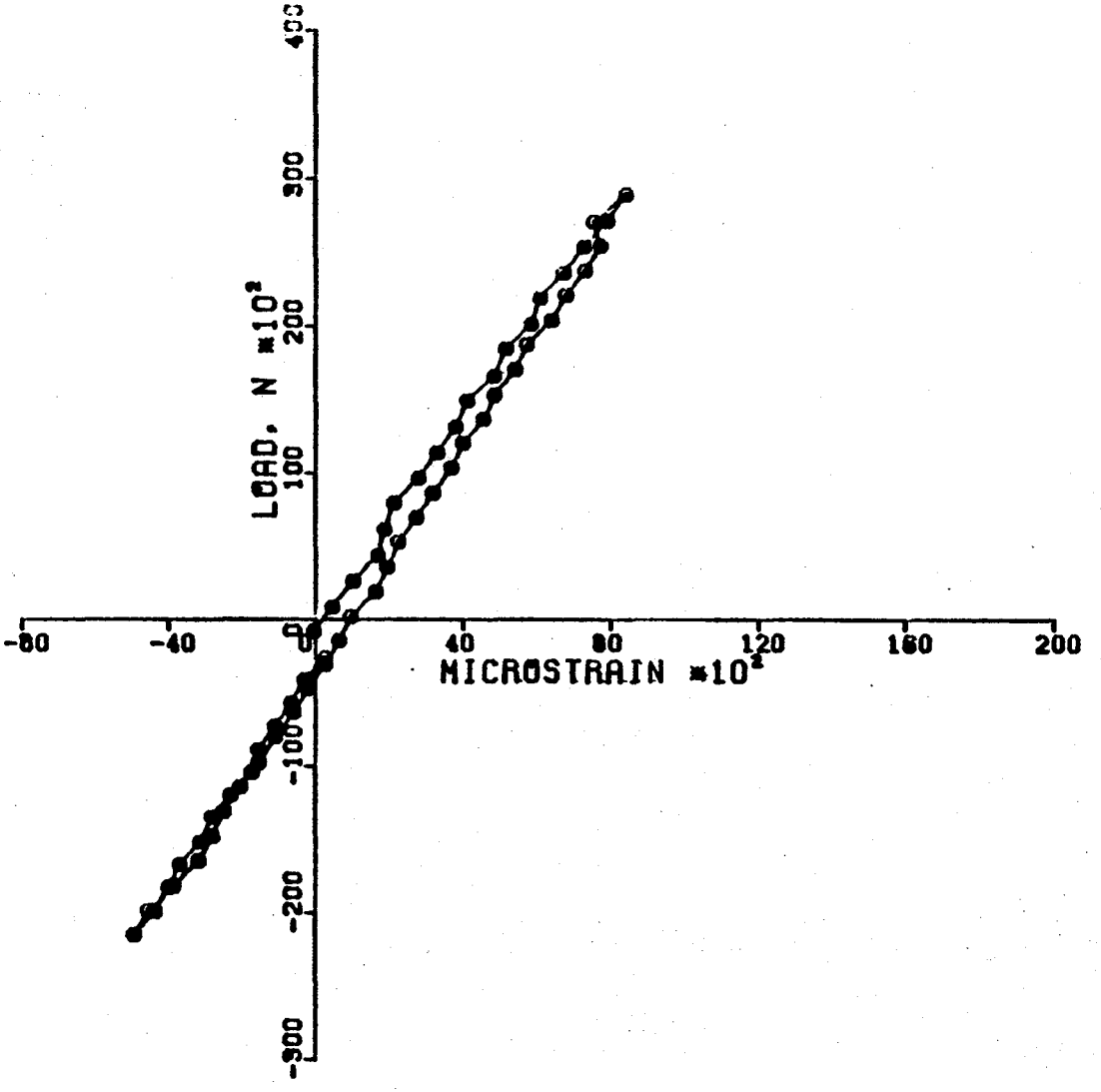

Figure 63. Cycle 1, Test 11A, Continuous Fatigue.

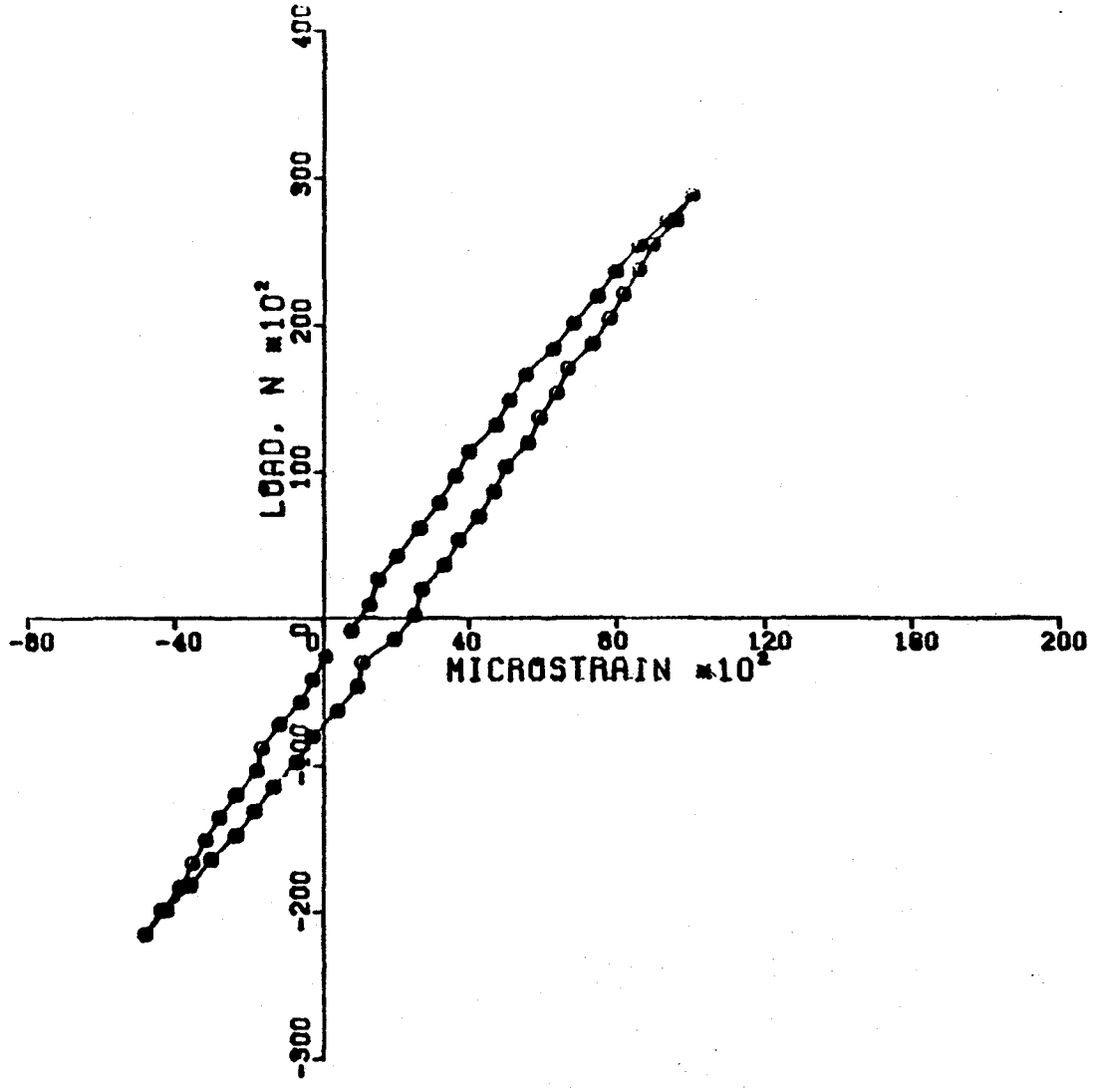

Figure 64. Cycle 1000, Test 11A, Continuous Fatigue.

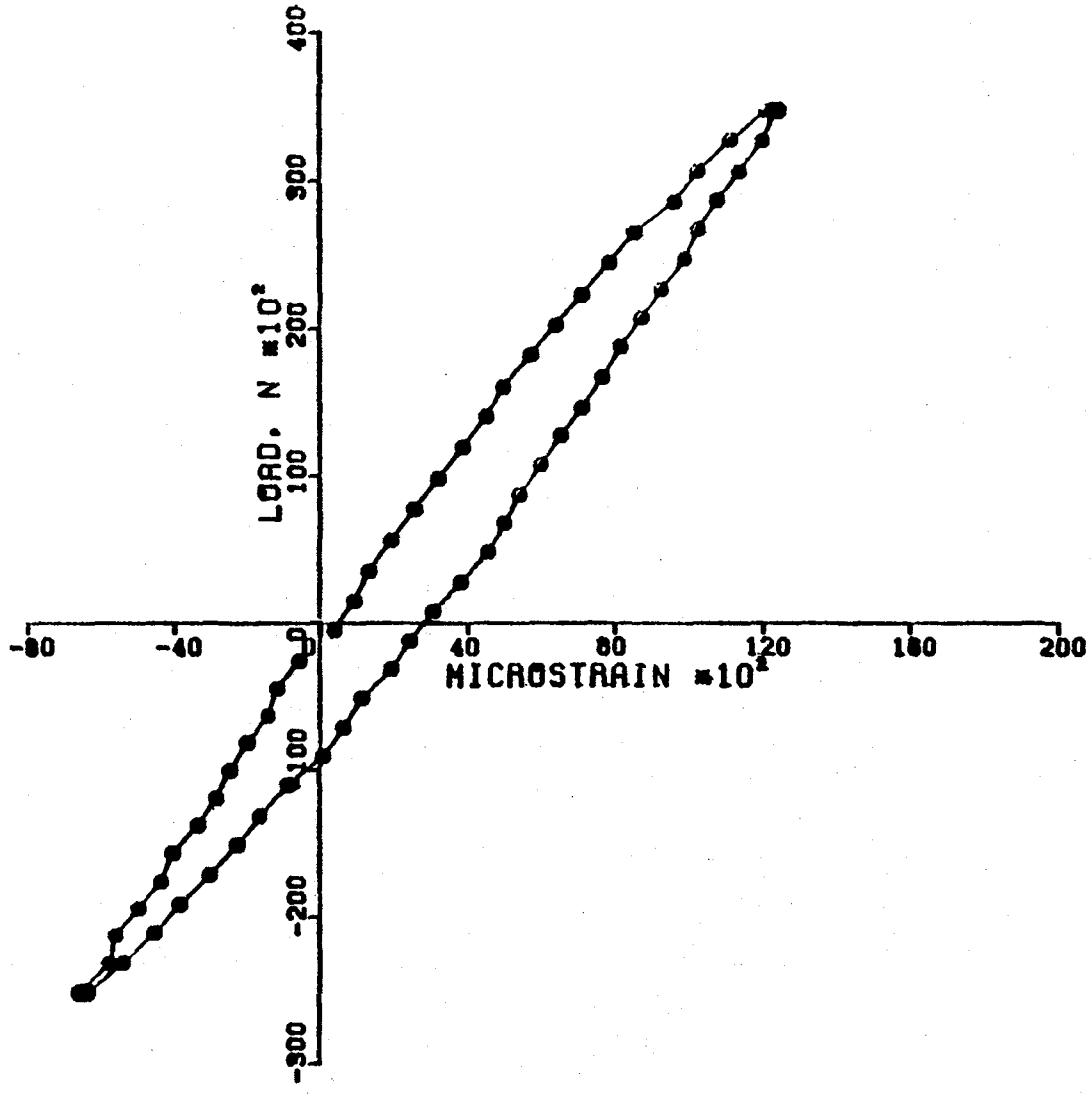

Figure 65. Cycle 1, Test 11B, Tension/Compression Hold.

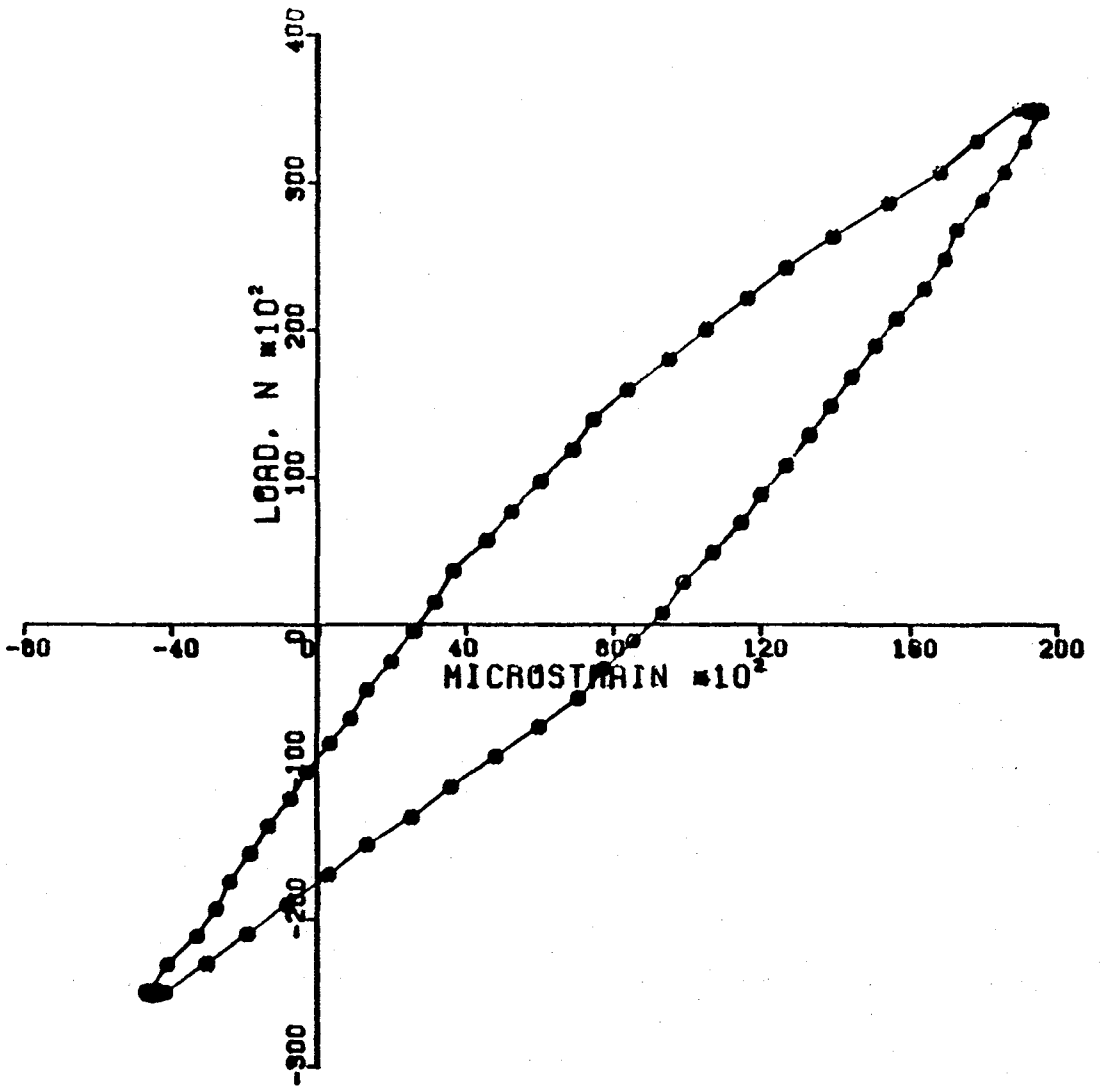

Figure 66. Cycle 185, Test 11B, Tension/Compression Hold.

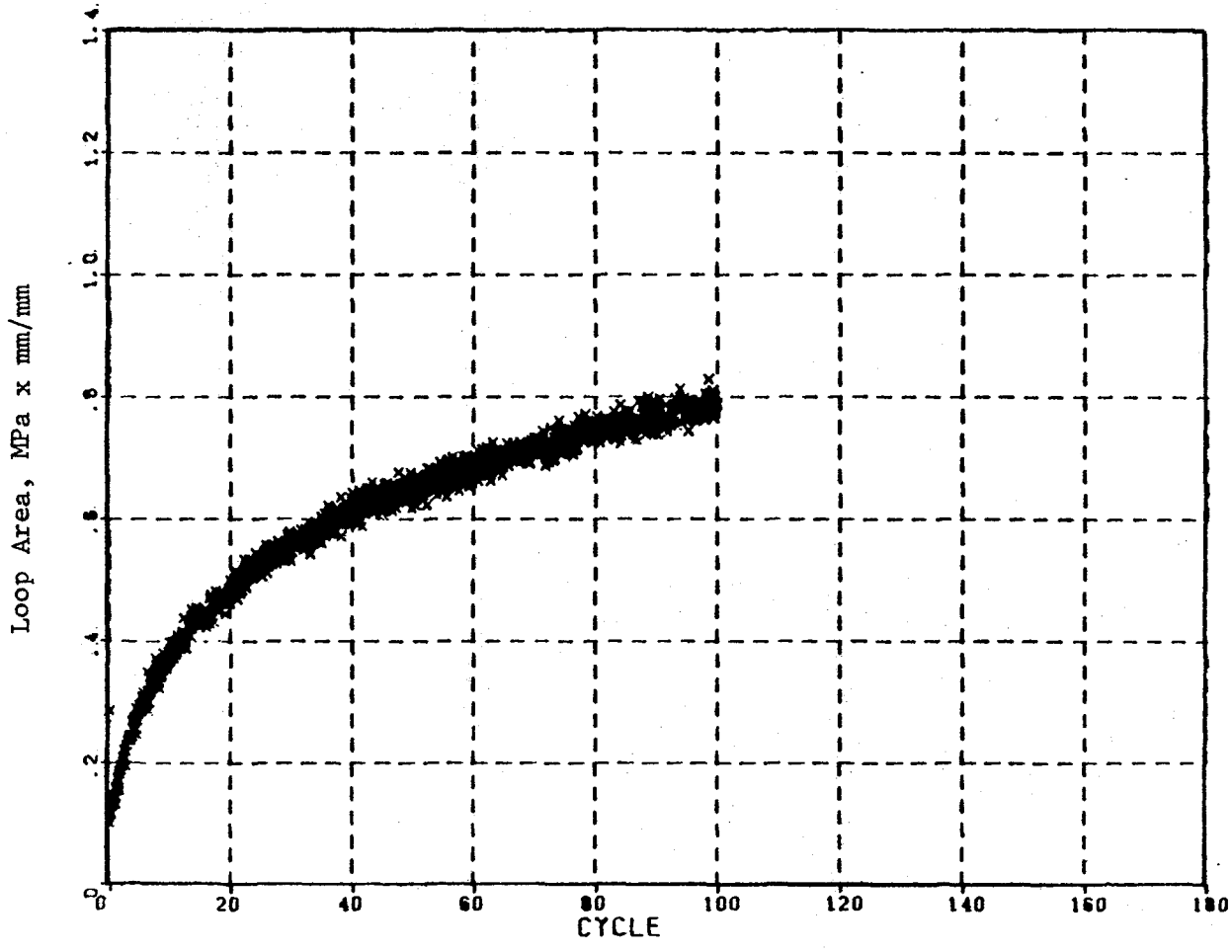

Figure 67. Loop Area Versus Cycles for Test 11A.

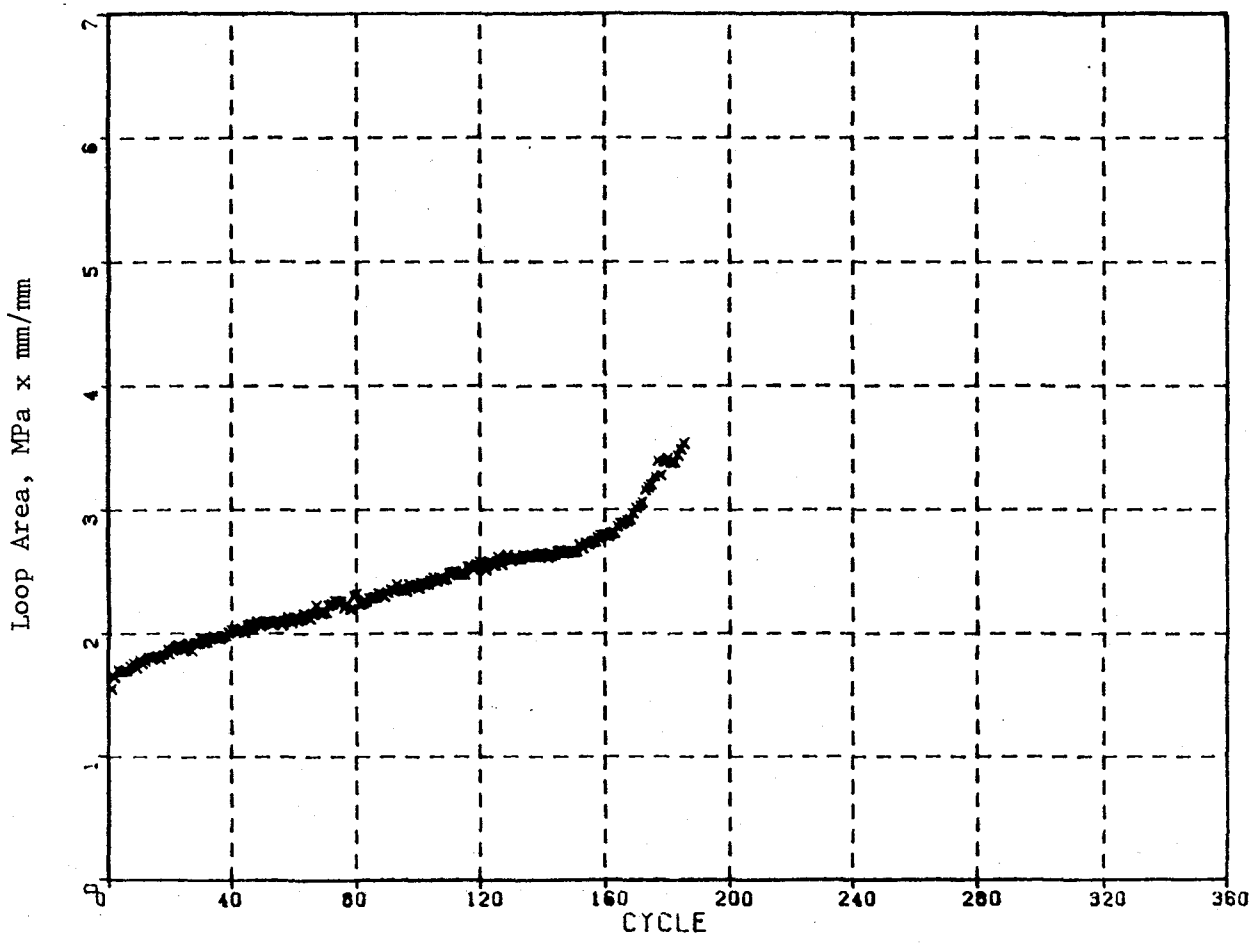

Figure 68. Loop Area Versus Cycles for Test 11B.

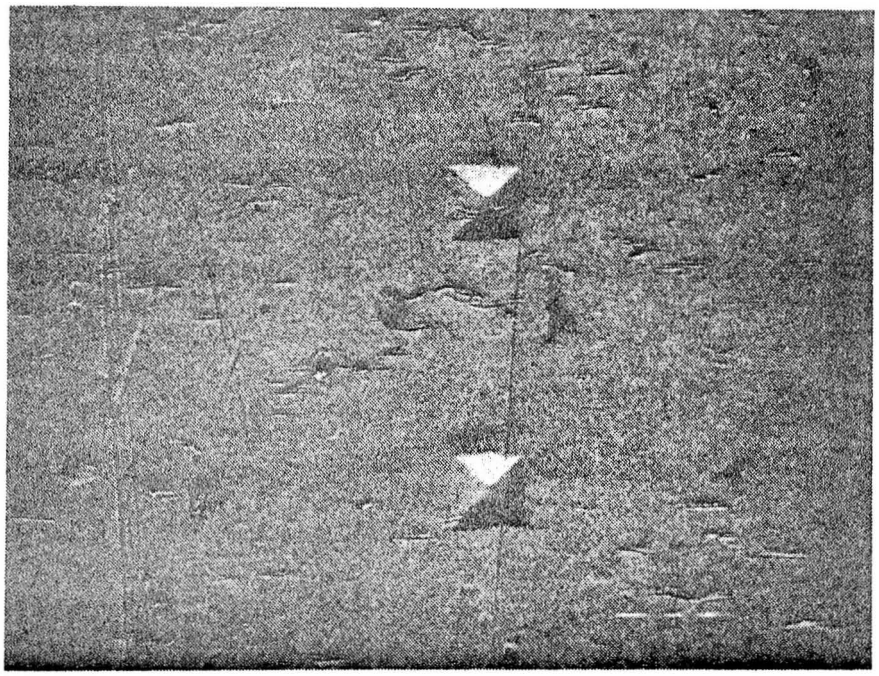

Figure 69. SEM Photo of Specimen No. 13 After Tests 11A and 11B.

Table IX. Test Data - DEC RL01 Disk.

Files Listed in Order of Appearance on Disk

File Name	Description of Test	No. Cycles	Record Size
CAL6.DAT	Rm. Temp. CALBN for Tests 6&7, Spec. No. 1	20	64
TEST6.DAT	Fatigue, Test No. 6, LD Range 5660, 3390 Spec. No. 1	1000	64
TEST7.DAT	Continuation of Fatigue Test No. 6 Spec. No. 1, LD Range 6716, - 4030	884	64
CAL8.DAT	Rm Temp CALBN for Test No. 8 Specimen No. 8	5	94
TEST8.DAT	Fatigue - Comp. Hold, Test No. 8 Spec. No. 8 LD Range + 6716#, -4030#, 2-Min Hold in Comp. approximately 12-Hour Test Duration	345	94
CAL9.DAT	Rm. Temp. CALBN for Test No. 9 Spec. No. 12	5	124
TEST9.DAT	Hold-Hold Pattern, Test No. 9, Spec. No. 12 LD Range + 6716#, -4030# 2-Min. Hold Times in Tension and Compression, approximately 17-Hour Test Duration	253	124
CAL10.DAT	Rm. Temp. CALBN for Test No. 10 Spec. No. 11	10	94
TEST10.DAT	Tension Hold Fatigue, Test No. 10, Spec. No. 11 LD Range + 6716#, -4030#, 2-Min Hold Time approximate Test Duration 13.5 Hours	384	94
CAL11.DAT	Rm Temp. CALBN for Test No. 11A & 11B Specimen No. 13	20	64
TES11A.DAT	Fatigue Section of Combined Fatigue, Hold-Hold Test No. 11a, Spec. No. 13 LD Range + 5660,#, -3394#	1000	64
TES11B. DAT	Hold-Hold Section of Combined Test, LD Range +6716#, -4030# Spec. No. 13, Test No. 11b	185	124
CAL12.DAT	Rm. Temp. CALBN for Test No. 12 Spec. No. 9	20	64

Table IX. Test Data - DEC RL01 Disk (Concluded).

Files Listed in Order of Appearance on Disk

File Name	Description of Test	No. Cycles / No. of Samples	Record Size
TES12A.DAT	Creep Test, 1st Part Test Duration approximately 5.5 Hours Sample Rate @ Peak Load approximately 1/2.1 Secs. LD Initially @ + 6716# Incremented Periodically. Spec. No. 9	8700	2
TES12B.DAT	Creep Test, 2nd Part Spec. No. 9 LD. Initially @ +7660# 2.1 Secs/Sample @ Load	3435	2

```
20    FORMAT(1X,'LOAD=',I5,1X,'LBS.',5X,'MICROSTRAIN=',7X)
      STOP
      END
```

Sample data of the first five initial cycles and one stabilized cycle of each test are listed in the appendix. The complete data set may be obtained at no cost by mailing a blank DEC RL01 hard disk to:

Fatigue Research Section, M.S. 49-6
Structures and Mechanical Technologies Division
NASA-Lewis Research Center
21000 Brookpark Road
Cleveland, Ohio 44135

Attn: Dr. G.R. Halford

5.4 ASSESSMENT OF VALIDITY OF MEASUREMENTS

In order to ensure the validity of the results obtained from the benchmark tests, a room temperature calibration for each notched specimen was conducted prior to the actual testing of the specimen. The calibration tests were made using the ISDG to measure strain at the notch root of a specimen corresponding to loads well within the elastic limit of Inconel 718. Typically, 20 cycles of data were collected. The slope of a linear regression of the average of these cycles, multiplied by the stress concentration factor for the notch geometry, $K_t = 1.9$, was used to determine a room temperature elastic modulus, E, for the specimen.

The initial elastic modulus of each specimen at 649° C (1200° F) was also established. This value was determined from the linear portion of the initial test cycle. The elastic moduli of elasticity as measured at both temperatures for each specimen are presented in Table X.

Table X. Calibration Results.

		21° C (70° F)	649° C (1200° F)
Test No. 6		208.9	167.5 x 10^9 Pa
Test No. 7	(E)	(30.3)	(24.3 x 10^6 psi)
Spec. No. 1	(R^2)	0.9995	0.9970
		217.2	165.5
Test No. 8	(E)	(31.5)	(24.0)
Spec. No. 8	(R^2)	0.9983	0.9927
		199.3	157.9
Test No. 9	(E)	(28.9)	(22.9)
Spec. No. 12	(R^2)	0.9981	0.9974
		200.6	157.9
Test No. 10	(E)	(29.1)	(22.9)
Spec. No. 11	(R^2)	0.9983	0.9964
		207.5	166.9
Test No. 11	(E)	(30.1)	(24.2)
Spec. No. 13	(R^2)	0.9987	0.9950
		203.4	163.4
Test No. 12	(E)	(29.5)	(23.7)
Spec. No. 9	(R^2)	0.9990	0.9956

R^2 = Regression Coefficient

The modulus of elasticity of Inconel 718 bar stock as measured in the pedigree testing was presented in Table VII. The moduli measured by the ISDG are within 1.7 standard deviations of the mean measured pedigree values at 649° C.

Since Test Nos. 6 and 11A are identical, a direct comparison of the measured data can be made. Figures 70 and 71 compare the 1st and 1000th cycles of each test. A very good correlation is noted, thus lending added confidence to the repeatability of the measurement program.

In conclusion, it is felt that the ISDG performed within the previously established relative uncertainty of ±3% with an additional uncertainty of ±150 microstrain during the benchmark test program.

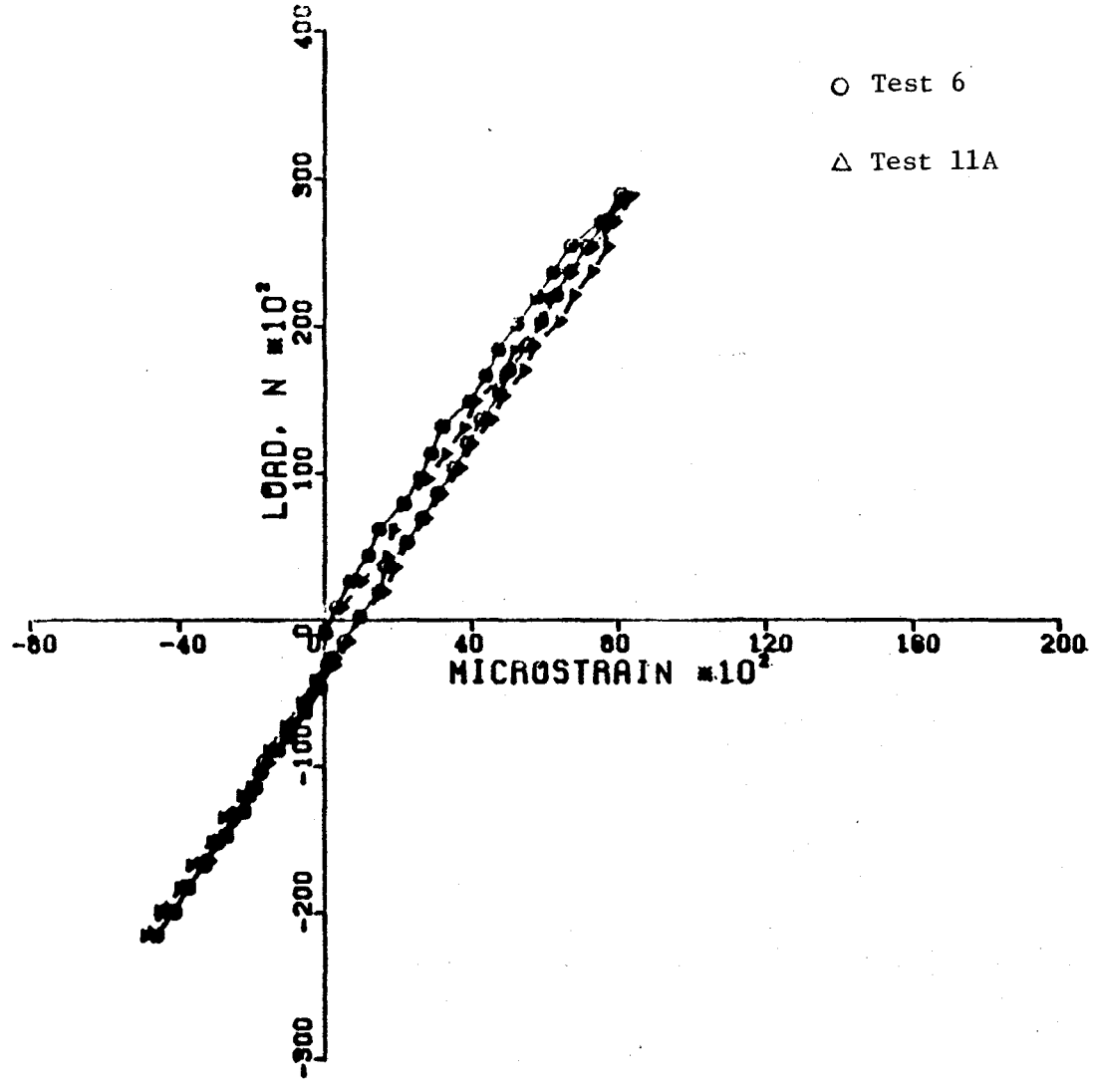

Figure 70. Cycle 1 of Tests 6 and 11A, Continuous Fatigue.

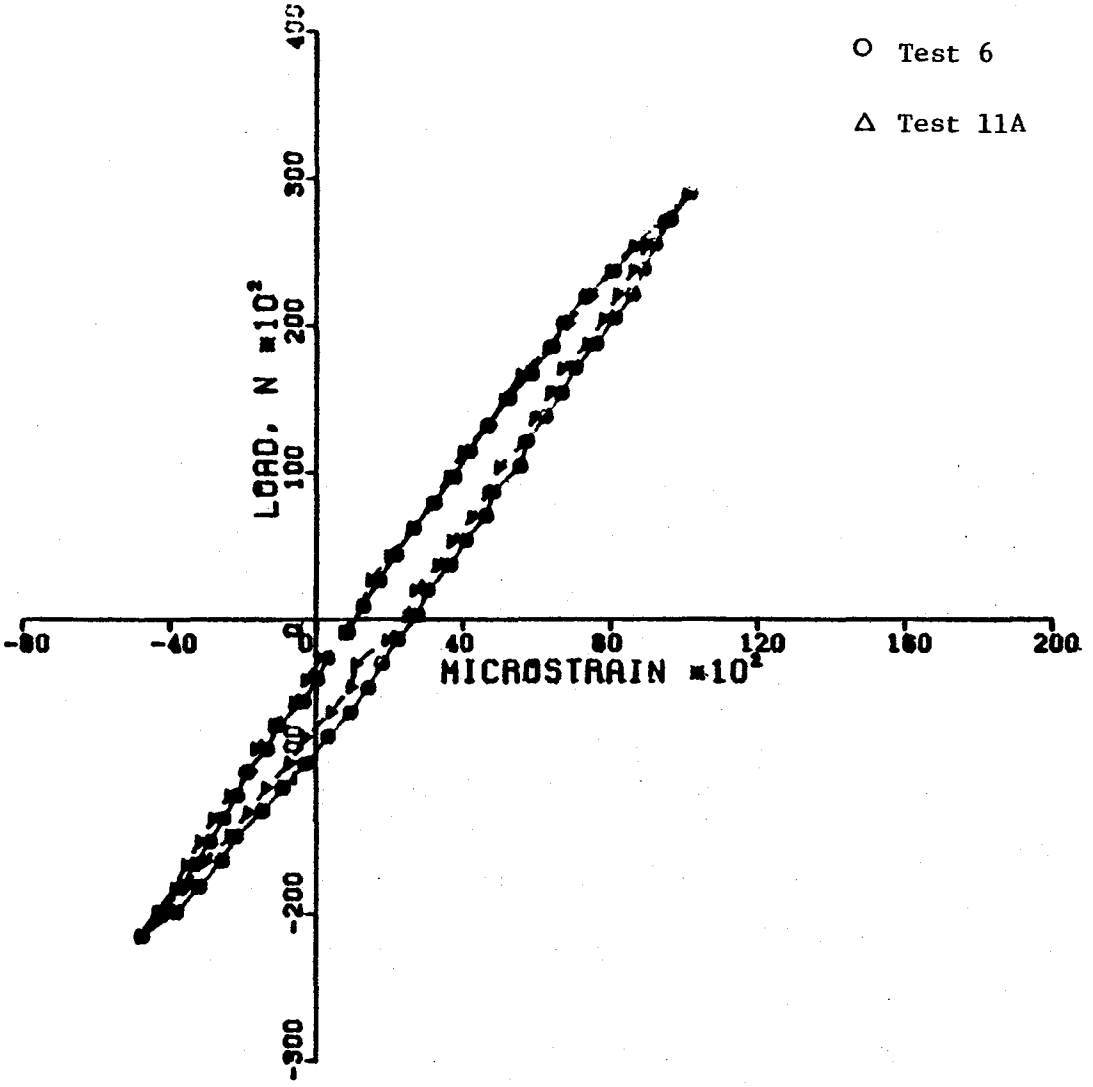

Figure 71. Cycle 1000 of Tests 6 and 11A, Continuous Fatigue.

6.0 TASK IV - STRAIN ANALYSIS

6.1 NEUBER NOTCH ANALYSIS

Neuber's rule which was derived by considering a notched prismatic body under antiplane shear can be written as (Reference 16).

$$K_\sigma K_\varepsilon = K_t^2 \tag{5}$$

where K_σ is the stress concentration factor, K_ε is the strain concentration factor, and K_t is the theoretical elastic stress concentration factor obtained from the theory of elasticity (or some appropriate numerical stress analysis). A more detailed definition of Equation 5 is shown in Figure 72.

In this figure, a plate with a hole is used to illustrate the notch root factors although in theory any specimen geometry could be likewise analyzed. Following the definition of a net section stress, S_{net}, the material's stress-strain curve is used to define the net section strain, e_{net}. The local notch root stress, σ, must also lie on the stress-strain curve which defines the local strain, ε. The stress and strain concentration factors can then be described as shown in Figure 72b. If these concentration factors are plotted as a function of load, P, results as shown in Figure 72c are obtained. K_σ and K_ε deviate as yielding occurs. In Equation 5, Neuber states that the theoretical stress-concentration factor is equal to the geometric mean of the actual stress- and strain-concentration factors.

Substituting net section and local stresses and strains for K_σ and K_ε in Equation 5 gives

$$K_\sigma K_\varepsilon = \frac{\sigma}{S_{net}} \frac{\varepsilon}{e_{net}} = K_t^2$$

which can be rearranged to give (Reference 16)

$$\sigma\varepsilon = K_t^2 S_{net} e_{net} \tag{6}$$

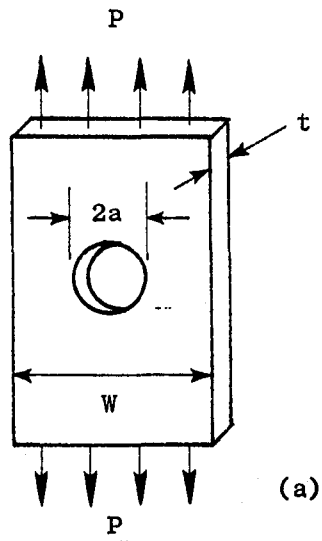

$$S_{net} = \frac{P}{(W-2a)t}$$

(a) A Typical Notch Geometry

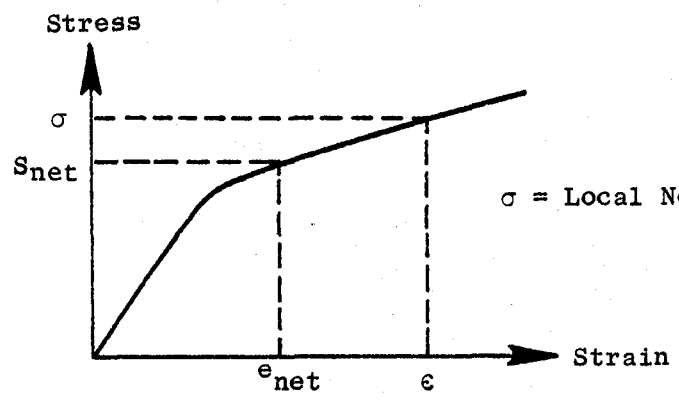

$$K_\sigma = \frac{\sigma}{S_{net}} \quad , \quad K_\varepsilon = \frac{\varepsilon}{e_{net}}$$

(b) Definition of Local and Net Section Quantities

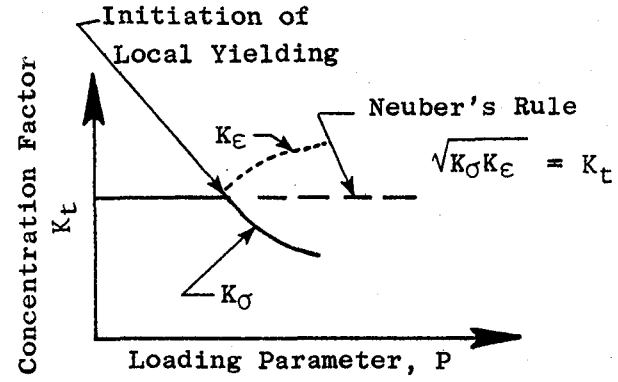

(c) Behavior of K_σ and K_ε with Loading

Figure 72. Definitions of K_σ and K_ε.

where, $\varepsilon = \sigma/E + \varepsilon^P$, $e_{net} = S_{net}/E + e^P$, E is the modulus of elasticity, ε^P and e^P are the local and net section plastic strains, respectively. Equation 6 can be further expressed as (Reference 21)

$$\sigma \left(\frac{\sigma}{E} + \varepsilon P\right) = K_t^2 \, S_{net} \left(\frac{S_{net}}{E} + e^P\right) \tag{7}$$

The right-hand side of this equation is known from the external loading so that the left-hand side can be iteratively determined. Such an iteration scheme is simplified for computer application by using an analytic function for the stress strain curve (in this study, the Ramberg-Osgood Equation was used although any suitable form could be readily adopted). Upon reversal, one introduces ranges in stress and strain into Equation 7 (Reference 30),

$$\Delta\sigma \left(\frac{\Delta\sigma}{E} + \Delta\varepsilon^P\right) = K_t^2 \, \Delta S_{net} \left(\frac{\Delta S_{net}}{E} + \Delta\varepsilon^P\right) \tag{8}$$

Figure 73 schematically illustrates this equation. In addition, in order to introduce realistic cyclic material behavior, it is necessary to introduce the Massing (or kinematic hardening) hypothesis which essentially scales the original stress strain curve by a factor of 2. The above-mentioned methodology is well suited for cyclically stable materials (i.e., materials which do not harden or soften or relax mean stress as a function of cycles). For applications involving unstable materials, a method is needed to describe these effects. Material models which purport to be able to model generally transient effects are given in References 31 and 32.

It should be noted that the previous equations were written in a uniaxial form which assumes that the local notch root stress is uniaxial. For multiaxial states of stress and strain, Neuber approaches can be used by defining K_σ and K_ε in terms of effective stress and strain. However, the complexity at the notch root in terms of the degree of multiaxiality and the point-to-point variation of the principal stresses and strains, certainly cannot be treated precisely by a simple concept. Another recognized difficulty of the Neuber analysis is the stress redistribution due to local and net section plasticity. It will predict excessively high notch root strains if there is extensive local plasticity.

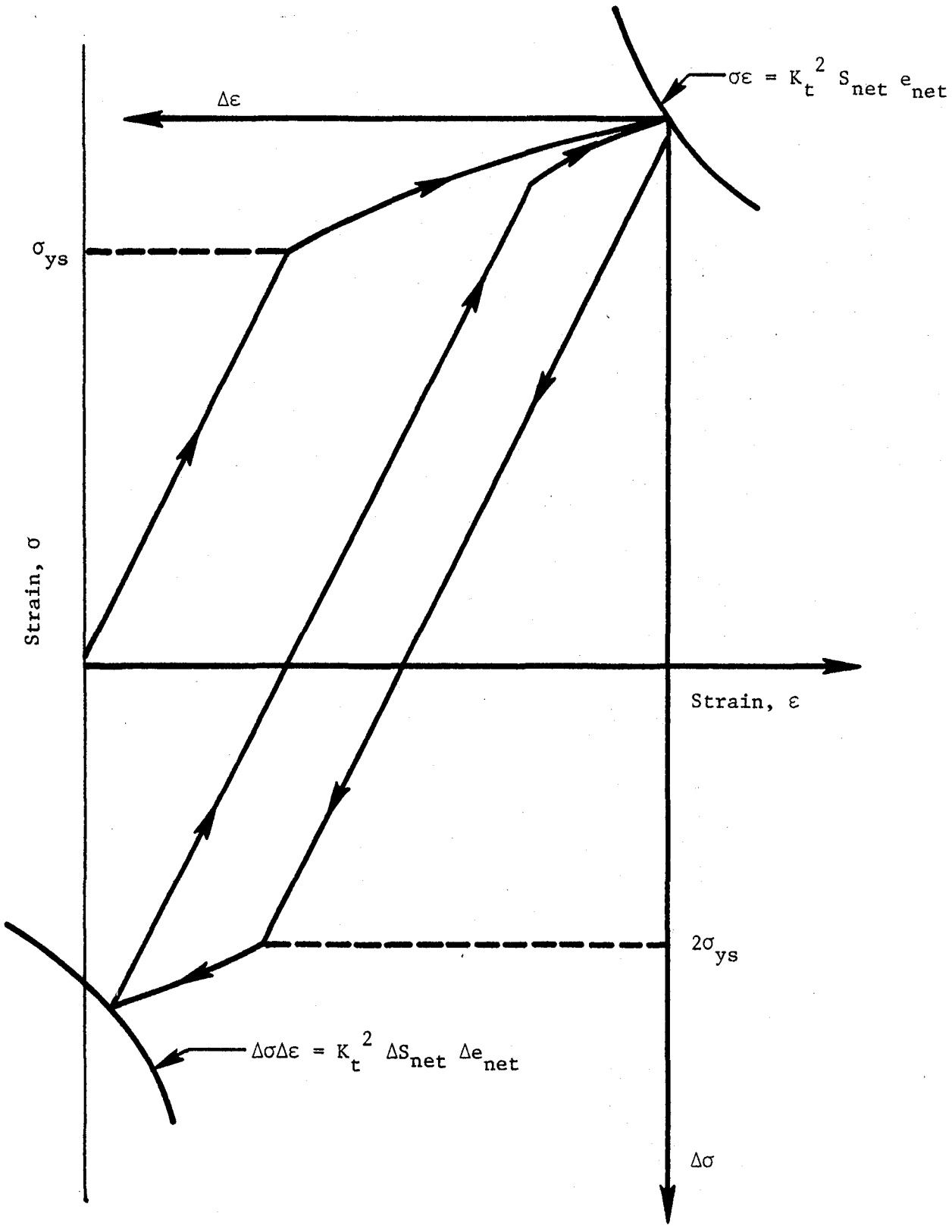

Figure 73. Schematic Illustration of the Application of Neuber's Rule to Cyclic Loading.

A procedure of simulating the plastic stress redistribution is to modify the nominal stress in the standard formulation. First, the elastic stress distribution is represented by a third order equation (Figure 74). Then, an approximate representation of the plastically redistributed stress is established by a linear equation which connects the initial Neuber estimation of local surface stress and the pivot point (at Y = net section nominal stress). It may be considered that the elastic stress y represents the imposed load, while the plastic stress y' is the load carrying capability of the notch area. The area "A" represents the unbalanced load which has to be redistributed to other portions of the structure. It, in turn, reduces the amount of nominal stress imposed on the notch area. The amount of reduction is assumed to be:

$$\Delta\sigma_n = \frac{\text{Area "A"}}{\text{Net Section Width "w"}} \tag{9}$$

This modification has been shown to be in closer agreement with other prediction methods such as the finite-element technique.

In the case of creep, the Neuber equation may be extended to

$$\sigma \left(\frac{\sigma}{E} + \varepsilon^P + \varepsilon^c\right) = K_t^2 S_{net} \left(\frac{S_{net}}{E} + e^P + e^c\right) \tag{10}$$

where ε^c and e^c are the notch root and net section creep strains, respectively. For such analyses, it is convenient to represent the creep strain-stress-time relationship in an analytical form. The form used in this study was:

$$\varepsilon^c = K \left(\frac{\sigma}{100}\right)^n t^m + Q \left(\frac{\sigma}{100}\right)^r t \tag{11}$$

where K, n, m, Q, and r are constants and t is time.

In this case, Equation 7 would be used to predict the initial loading, followed by Equation 10 to predict the influence of creep. Equation 8 (suitably modified to account for the prior creep) would then be used to predict the response due to unloading. This combined cyclic elastic-plastic-creep effect is schematically shown in Figure 75.

A computer code based on the above methodology was used for the Neuber predictions in this program.

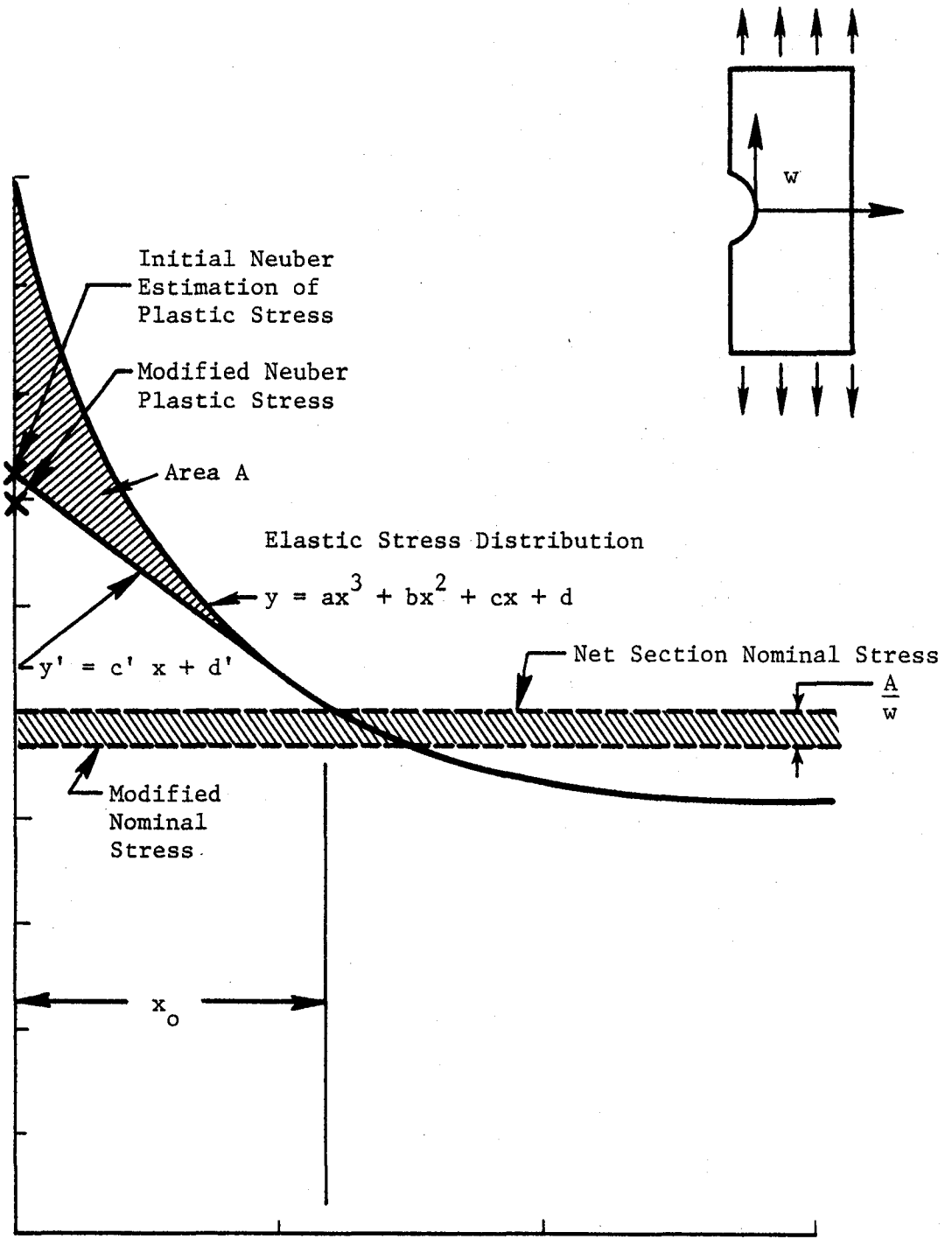

Figure 74. Modified Neuber Notch Analysis.

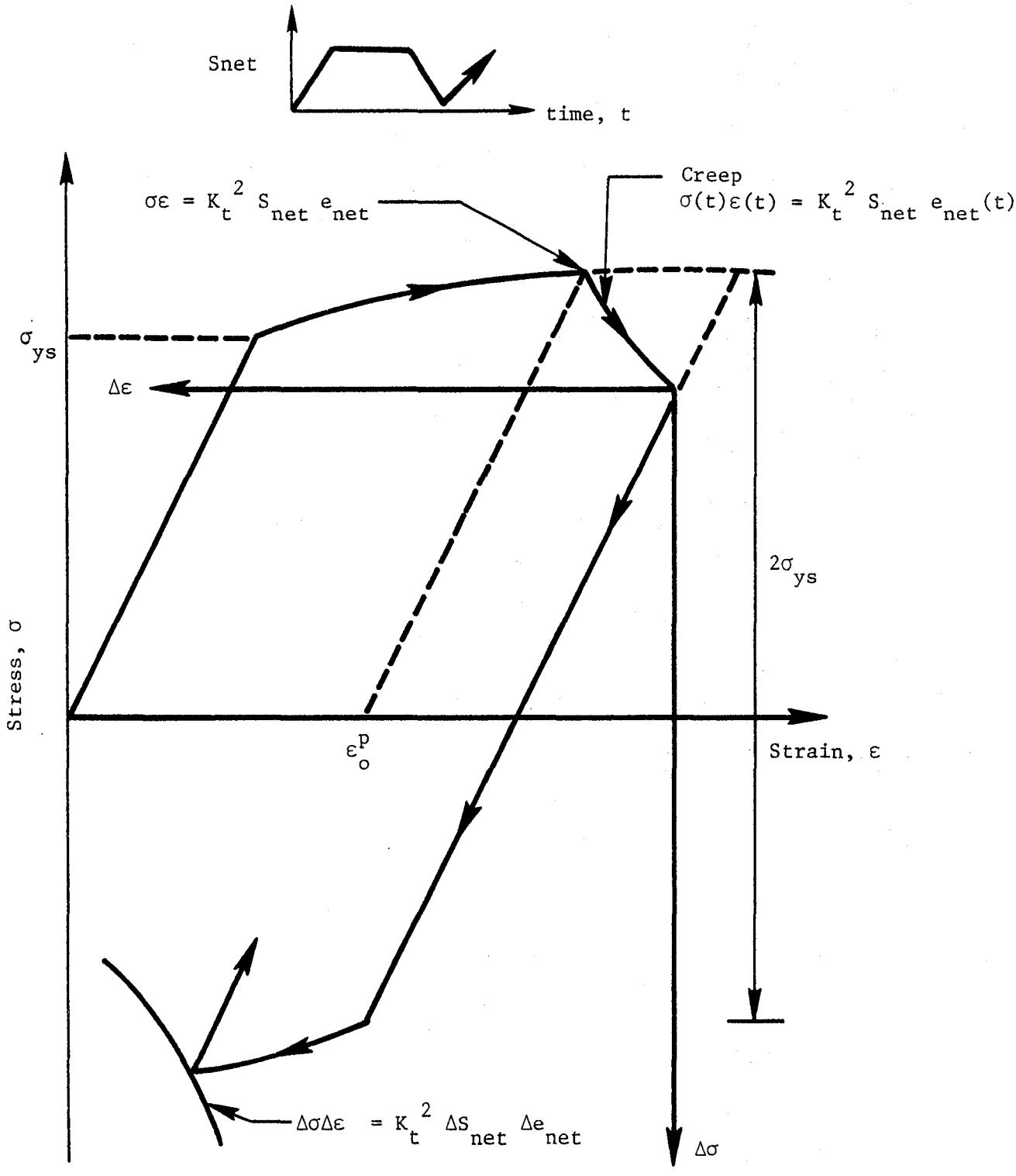

Figure 75. Schematic Illustration of the Combined Effect of Cyclic Plasticity and Creep.

6.2 FINITE-ELEMENT ANALYSIS

The finite-element method (FEM) is currently the most widely used method in the industry for solution of complex stress analysis problems. Although detailed FEM analyses were not conducted for this program, FEM studies were done in several cases for comparison purposes.

The computer program employed is the plane stress version of the elastic-plastic-creep finite-element program CYANIDE. The program utilizes the method of subvolumes as described in detail in References 26 and 33. Briefly, the program employs constant strain axisymmetric triangular elements and the method of subvolumes to introduce plastic flow and hardening characteristics. This nonlinear FEM solves the system of equations:

$$[K] \quad (q) \quad = \quad (P) \qquad (12)$$

where:

[K] is the stiffness matrix
(q) is the nodal point displacement vector
(P) is the nodal point force vector.

The solution is obtained by iterative perturbations of the right-hand side of Equation 12 through the addition of a plastic pseudoforce vector (P_p):

$$[K] \quad (q) \quad = \quad (P) \quad + \quad (P_p) \qquad (13)$$

This procedure is more economical than the more conventional iterative revision of the stiffness matrix K. The plasticity theory which is used to depict the nonlinear cyclic behavior is an extension of the one proposed by Besseling (Reference 34).

The model is capable of simulating the Bauschinger effect of reduced cyclic yield stress and cross-hardening, two effects considered to be important in cyclically loaded structures.

The computer code solutions have been verified elastically through correlations with known closed-form solutions and photoelastic tests. Stress and strain solutions involving plasticity and creep have been indirectly verified through correlations obtained between predictions and observations of low cycle fatigue and crack propagation test results (References 26 and 33).

6.3 NEUBER PREDICTION OF NOTCH ROOT STRESS AND STRAIN

Using Equation 10, predictions of the notch root behavior for each test condition were conducted and are graphically presented in Figures 76 to 83. In the computation, the notch root stress concentration factor of 1.90 was used. The monotonic and the cyclic elastic-plastic stress-strain and creep relationships were derived from the axially loaded smooth bar test data discussed in Section 3.2. The elastic-plastic stress-strain relationships used in the Neuber prediction were:

$$\varepsilon = \frac{\sigma}{23800} + \left(\frac{\sigma}{210.0}\right)^{\frac{1}{0.063}} \qquad \text{for monotonic behavior } (\dot{\varepsilon} = 20\%/\text{minute}) \qquad (14)$$

and

$$\varepsilon = \frac{\sigma}{23900} + \left(\frac{\sigma}{188.7}\right)^{\frac{1}{0.110}} \qquad \text{for cyclic behavior } (\dot{\varepsilon} = 20\%/\text{minute}) \qquad (15)$$

where σ has the units ksi and ε has units of in./in. The creep strain relationship was

$$\varepsilon_c = 4.416 \times 10^{-4} \left(\frac{\sigma}{100}\right)^{6.6507} t^{0.42995} + 1.6894 \times 10^{-5} \left(\frac{\sigma}{100}\right)^{8.9591} t \qquad (16)$$

where t has the units of hours.

Results of a complete cycle are presented in the form of

- Load pattern (load versus time)
- Load versus predicted local strain
- Predicted local stress versus predicted local strain
- Predicted local strain versus time

Test Nos. 6 and 11A (shown in Figures 76 and 81) and Test Nos. 9 and 11B (shown in Figures 79 and 82) are essentially the same types of test. No differentiation exists in prediction. In the test involving hold time (shown in Figures 78, 79, 80, and 82), the amount of creep strain response in 2 minutes

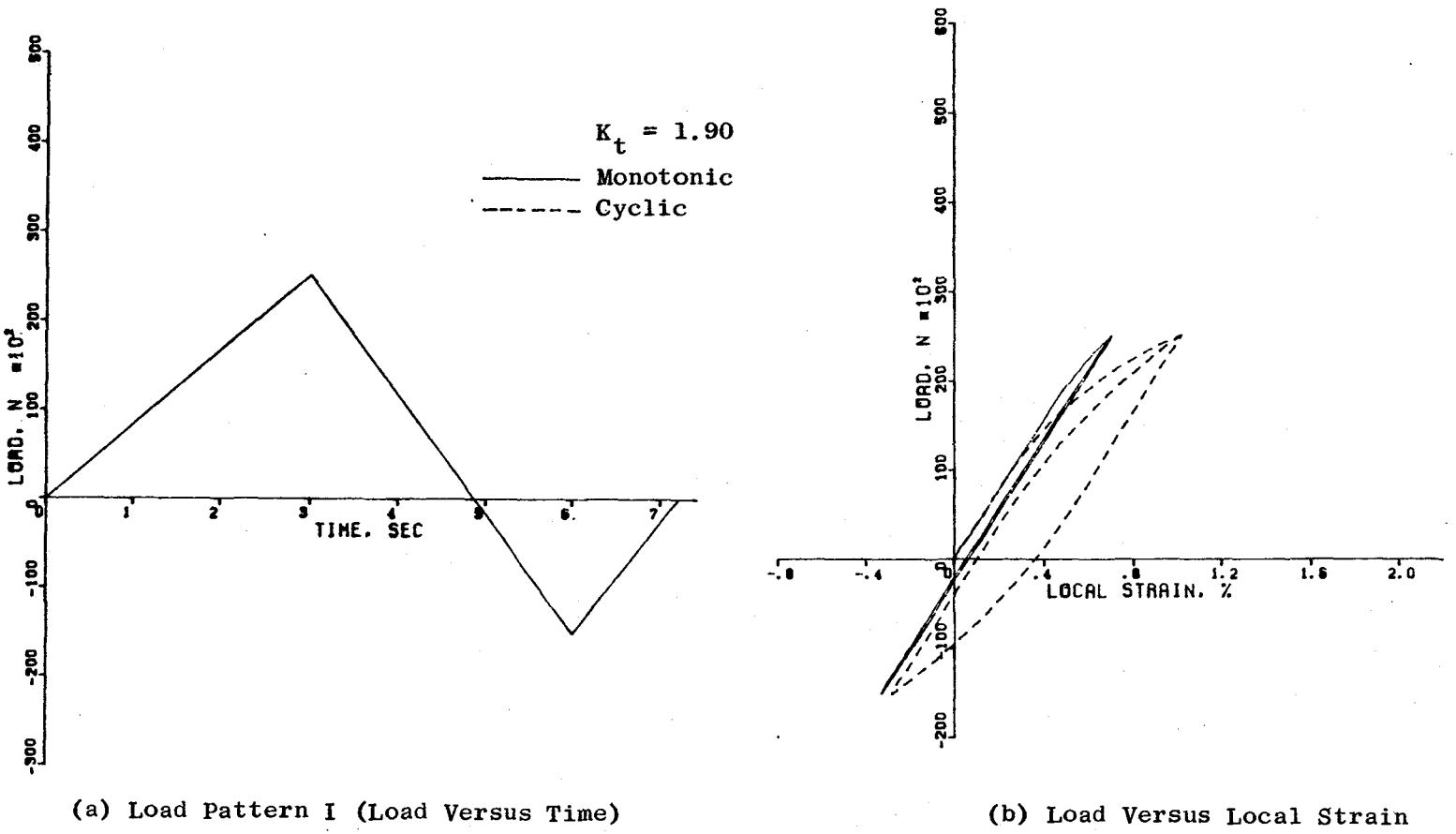

(a) Load Pattern I (Load Versus Time)

(b) Load Versus Local Strain

Figure 76. Neuber Predicted Stress-Strain Behavior for Inconel 718 Notched Bar at 649° C for Load Pattern I (Continuous Cycle), Test 6.

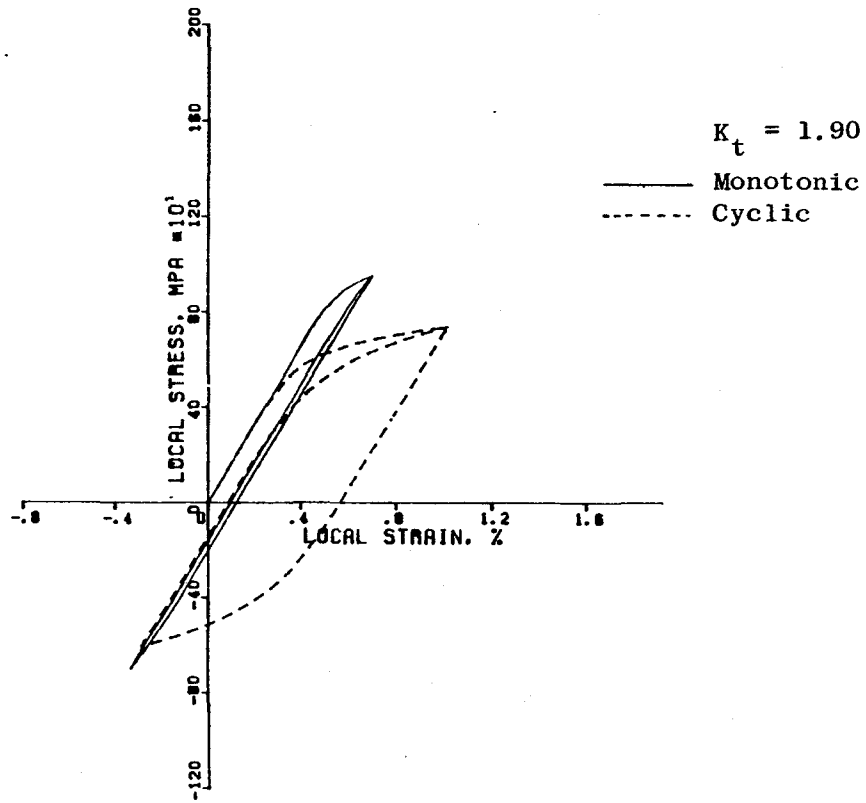

(c) Local Stress Versus Local Strain

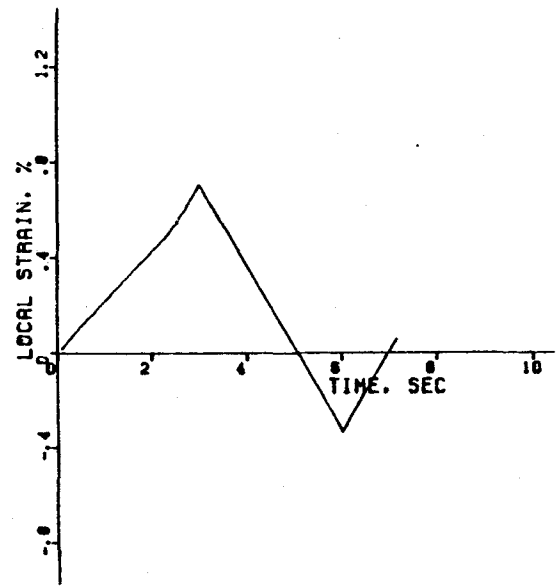

(d) Local Strain Versus Time

Figure 76. Neuber Predicted Stress-Strain Behavior for Inconel 718 Notched Bar at 649° C for Load Pattern I (Continuous Cycle), Test 6 (Concluded).

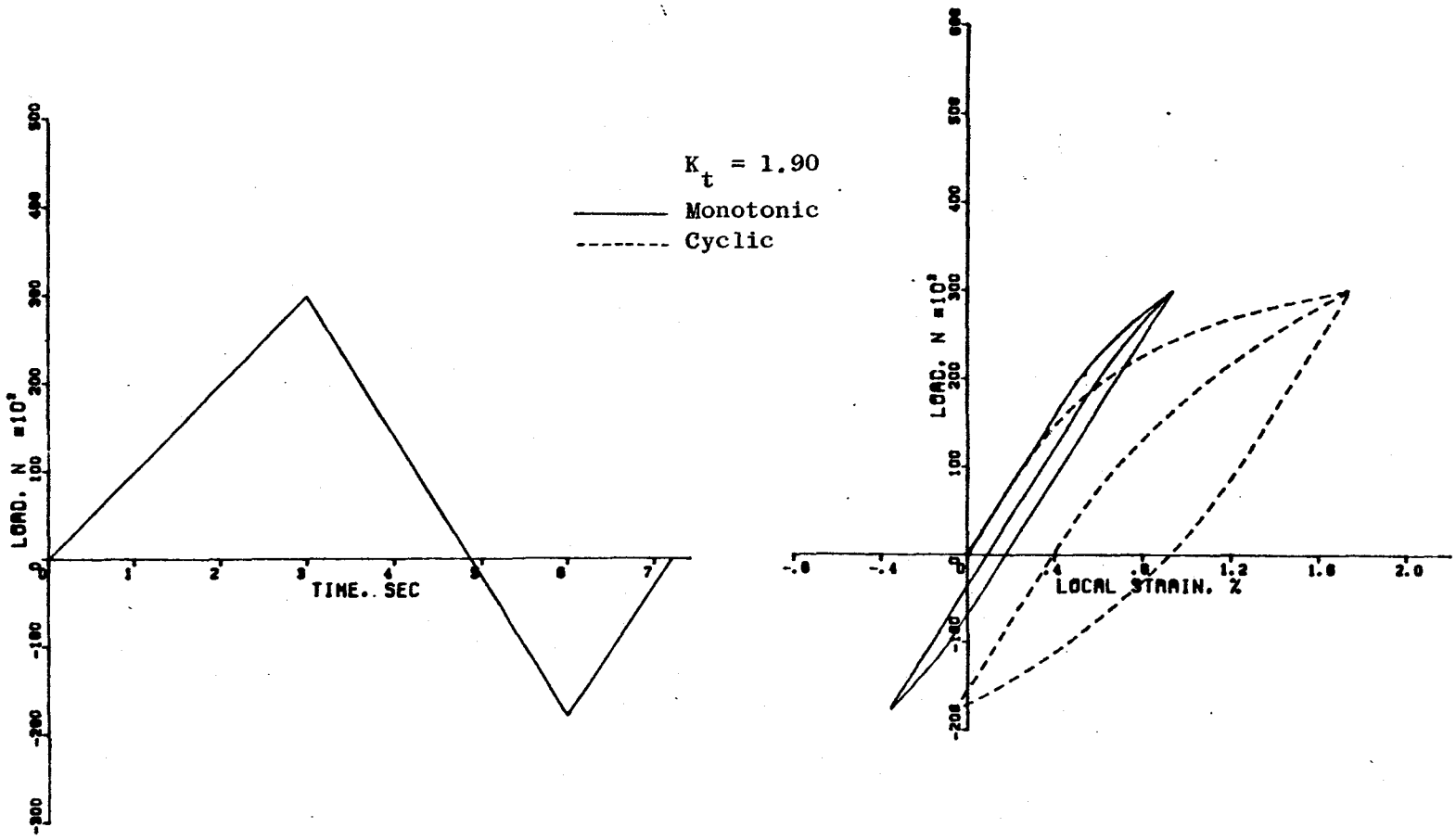

(a) Load Pattern I (Load Versus Time)

(b) Load Versus Local Strain

Figure 77. Neuber Predicted Stress-Strain Behavior for Inconel 718 Notched Bar at 649° C for Load Pattern I (Continuous Cycle), Test 7.

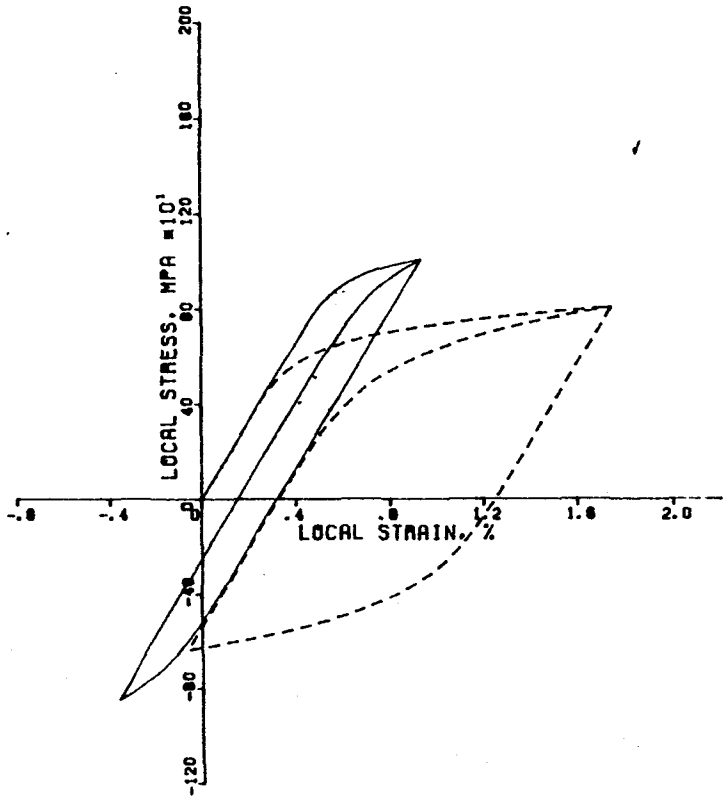

(c) Local Stress Versus Local Strain

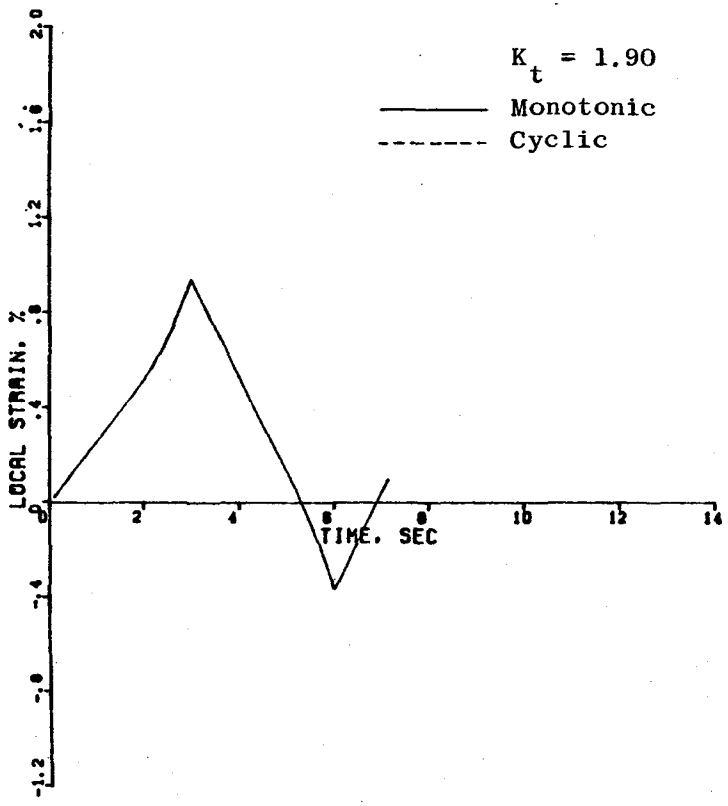

(d) Local Strain Versus Time

Figure 77. Neuber Predicted Stress-Strain Behavior for Inconel 718 Notched Bar at 649° C for Load Pattern I (Continuous Cycle), Test 7 (Concluded).

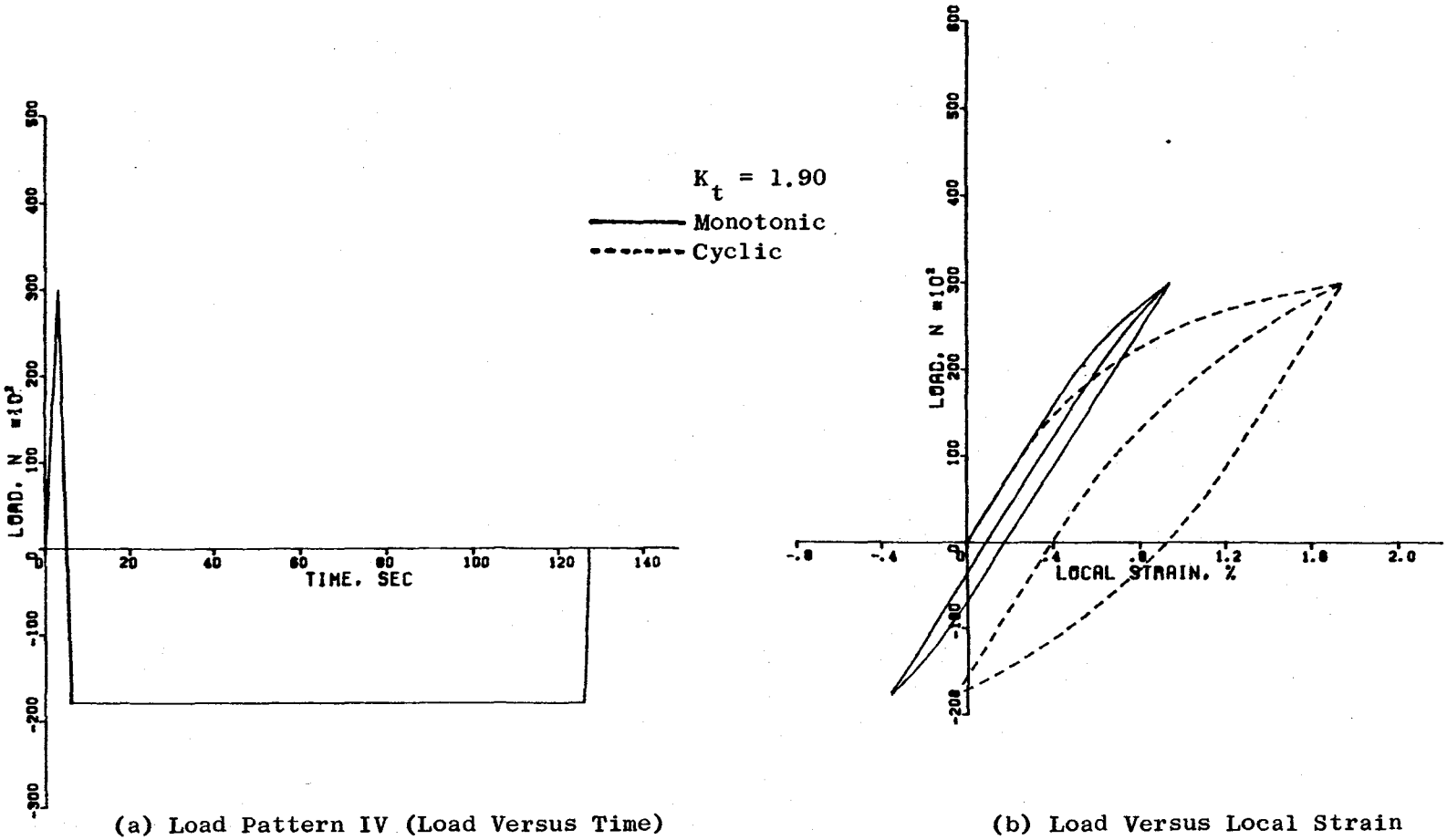

(a) Load Pattern IV (Load Versus Time)

(b) Load Versus Local Strain

Figure 78. Neuber Predicted Stress-Strain Behavior for Inconel 718 Notched Bar at 649° C for Load Pattern IV (Compression Hold), Test 8.

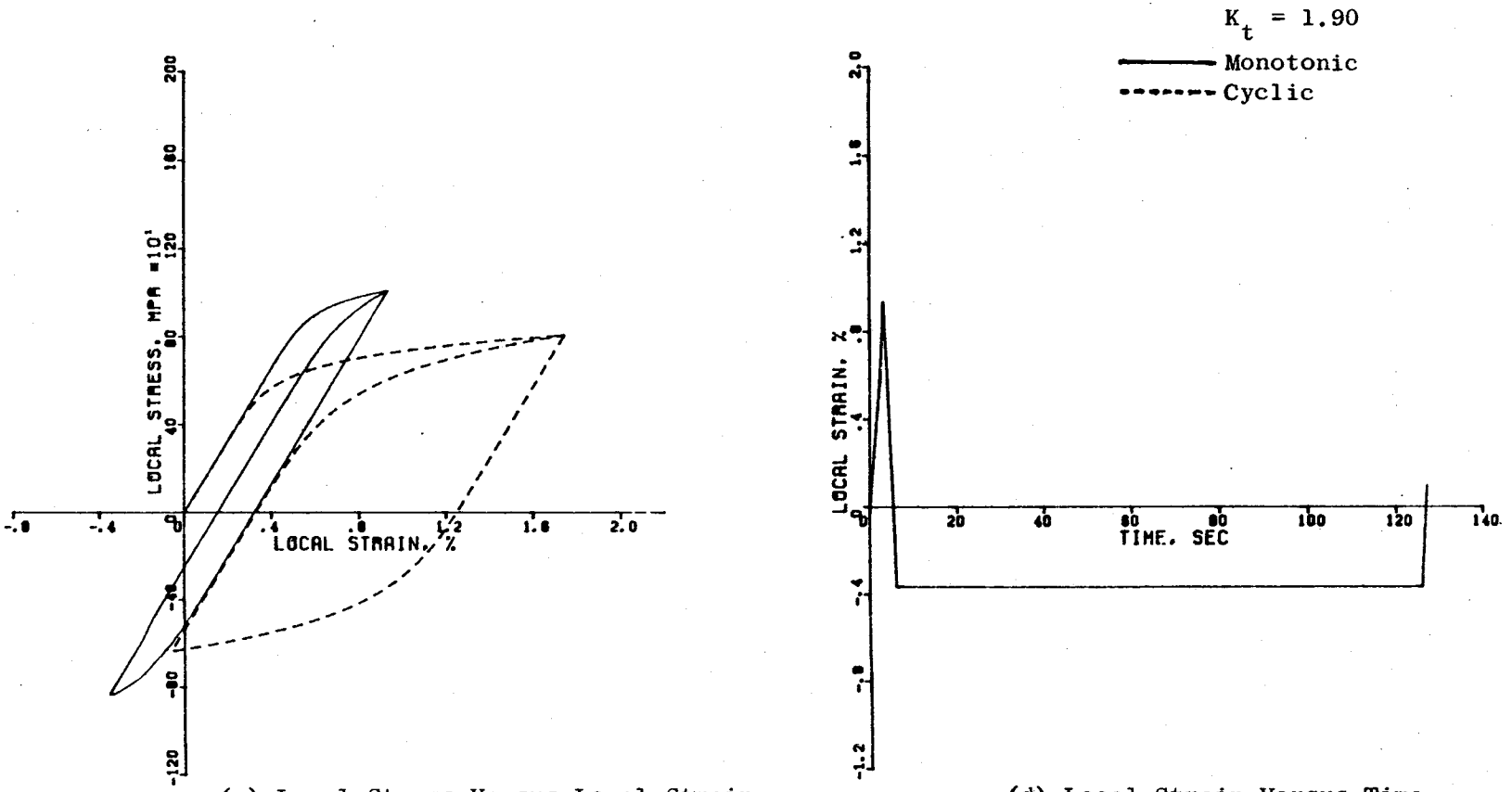

(c) Local Stress Versus Local Strain

(d) Local Strain Versus Time

Figure 78. Neuber Predicted Stress-Strain Behavior for Inconel 718 Notched Bar at 649° C for Load Pattern IV (Compression Hold), Test 8 (Concluded).

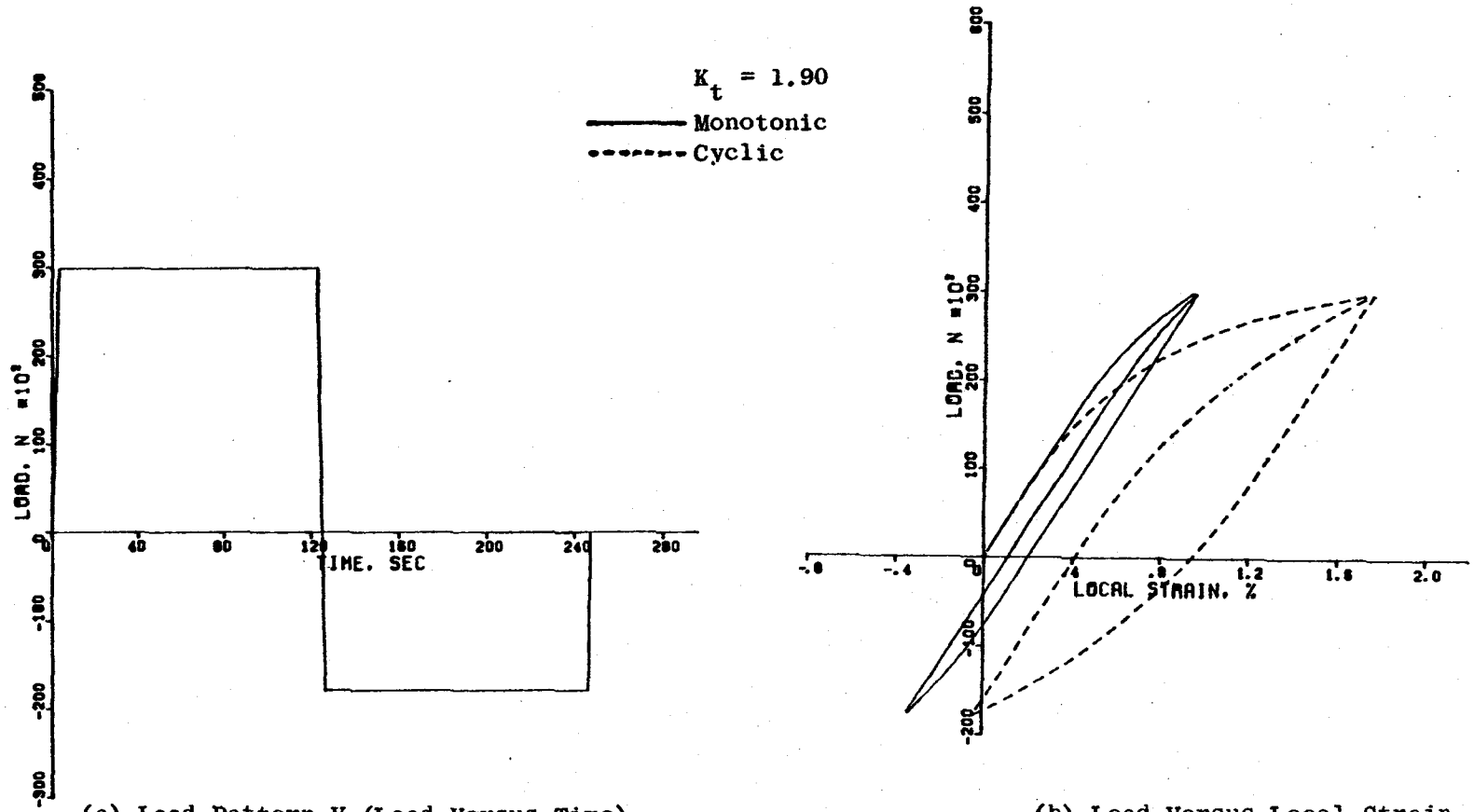

(a) Load Pattern V (Load Versus Time)

(b) Load Versus Local Strain

Figure 79. Neuber Predicted Stress-Strain Behavior for Inconel 718 Notched Bar at 649° C for Load Pattern V (Tension/Compression Hold), Test 9.

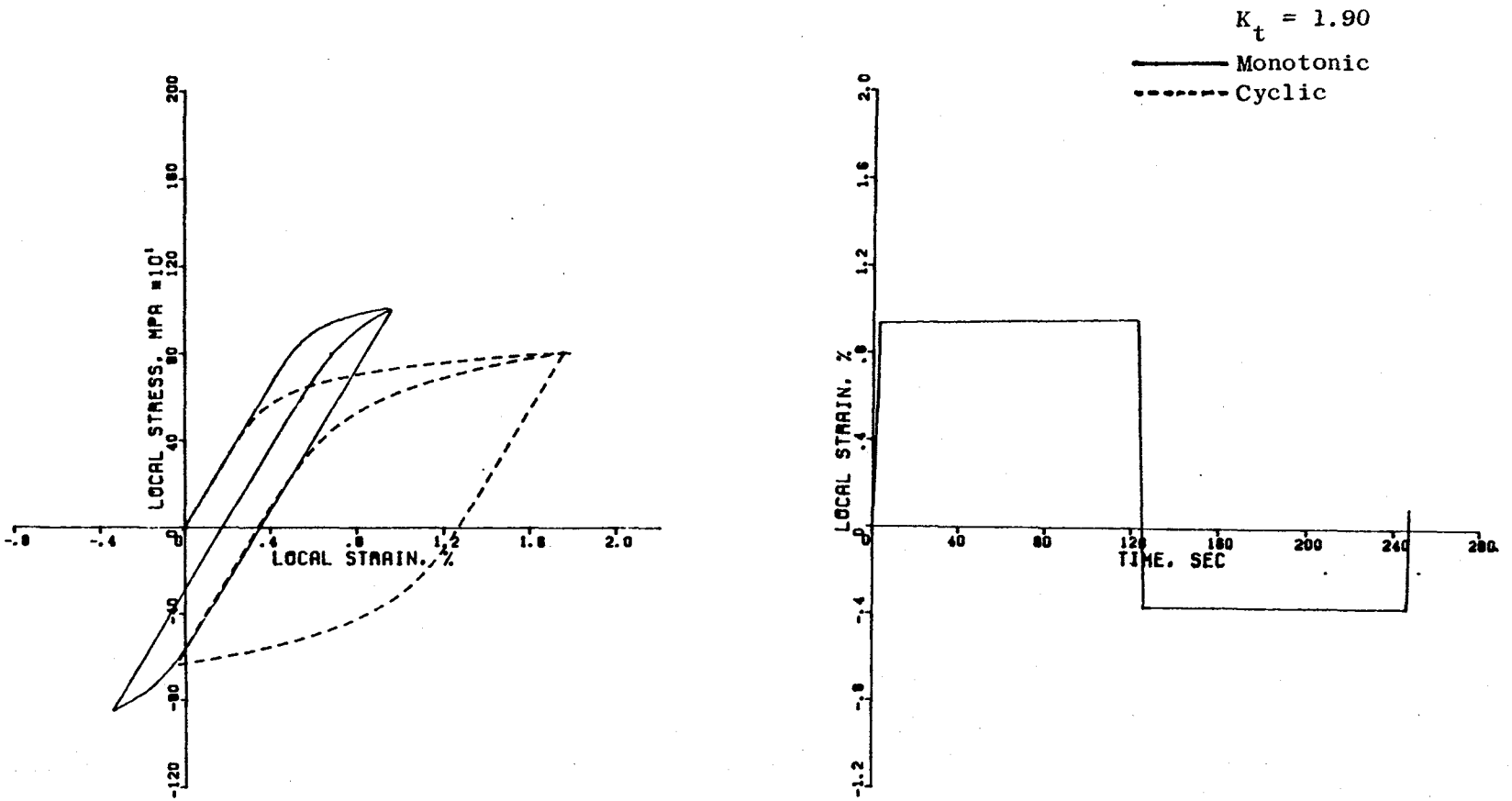

(c) Local Stress Versus Local Strain

(d) Local Strain Versus Time

Figure 79. Neuber Predicted Stress-Strain Behavior for Inconel 718 Notched Bar at 649° C for Load Pattern V (Tension/Compression Hold), Test 9 (Concluded).

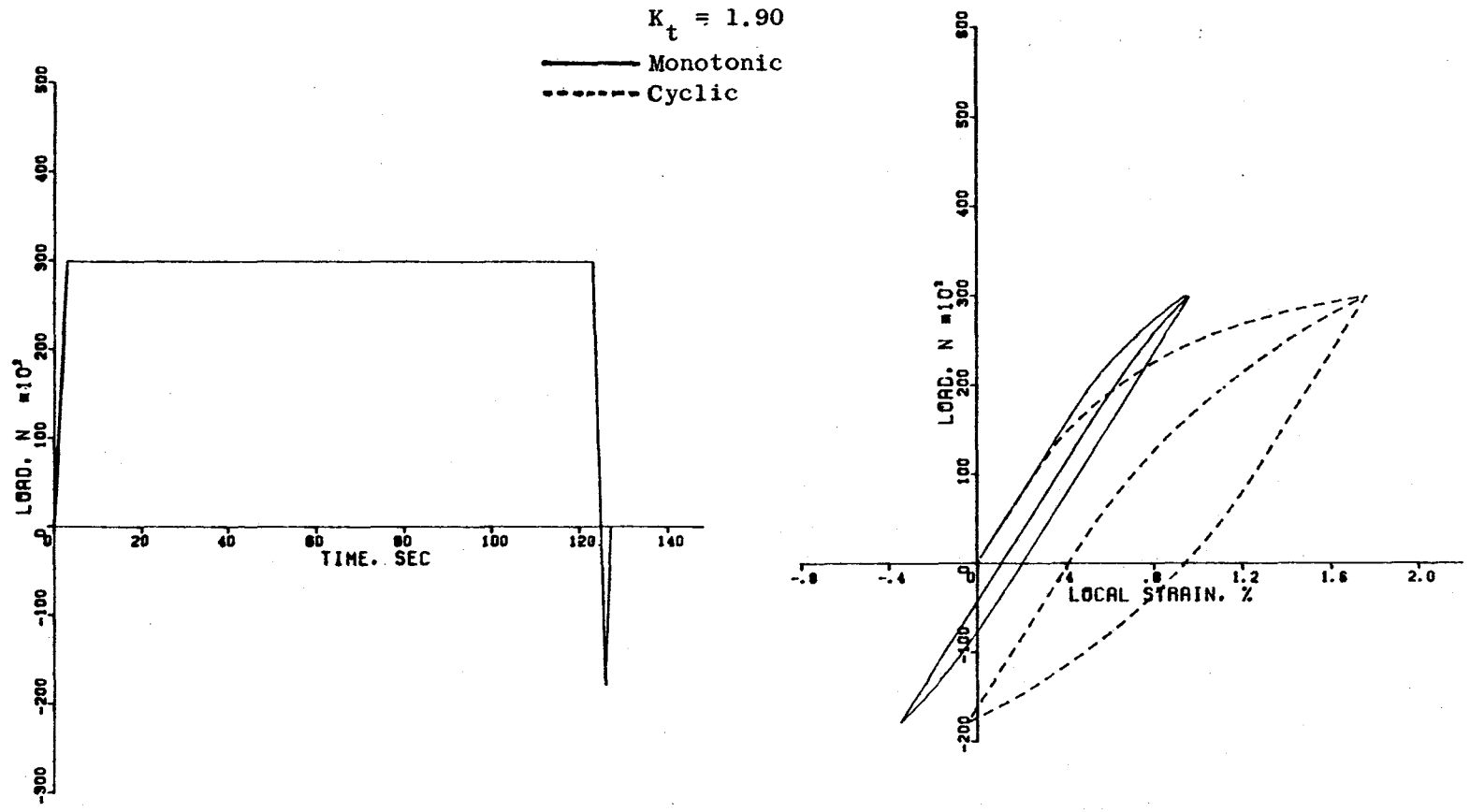

(a) Load Pattern III (Load Versus Time)

(b) Load Versus Local Strain

Figure 80. Neuber Predicted Stress-Strain Behavior for Inconel 718 Notched Bar at 649° C for Load Pattern III (Tension Hold), Test 10.

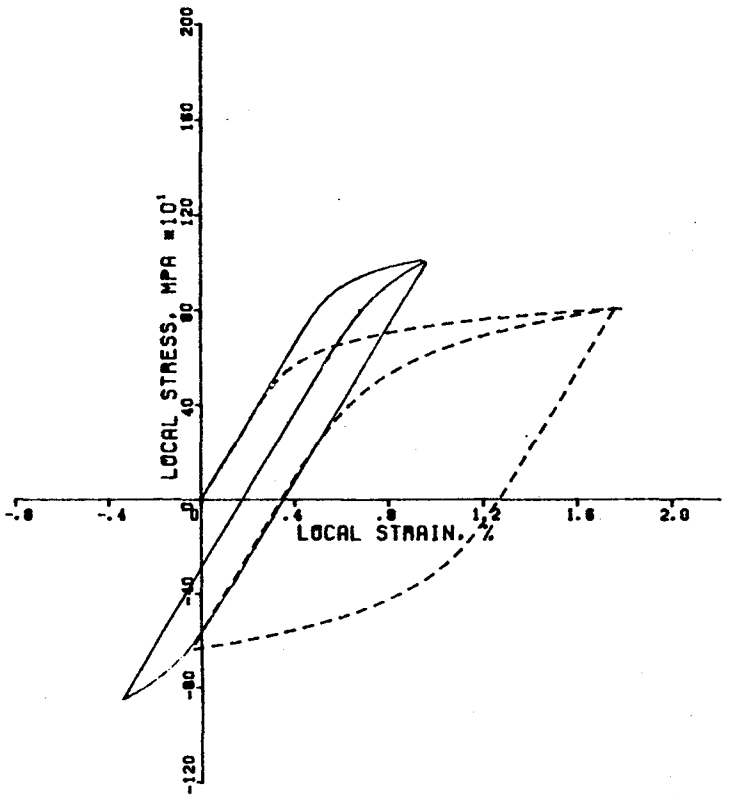

(c) Local Stress Versus Local Strain

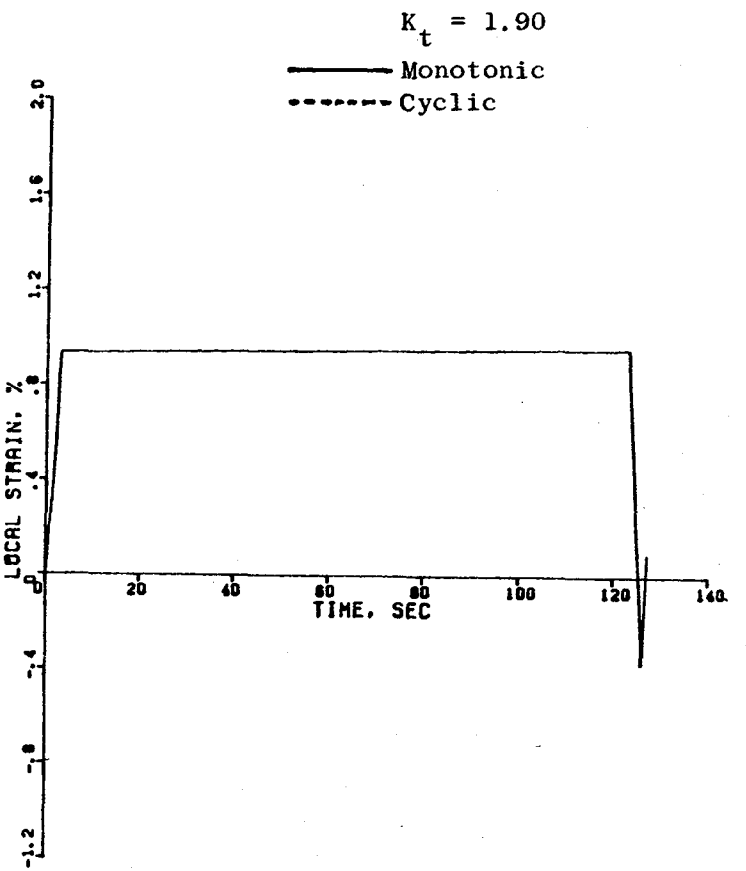

(d) Local Strain Versus Time

Figure 80. Neuber Predicted Stress-Strain Behavior for Inconel 718 Notched Bar at 649° C for Load Pattern III (Tension Hold), Test 10 (Concluded).

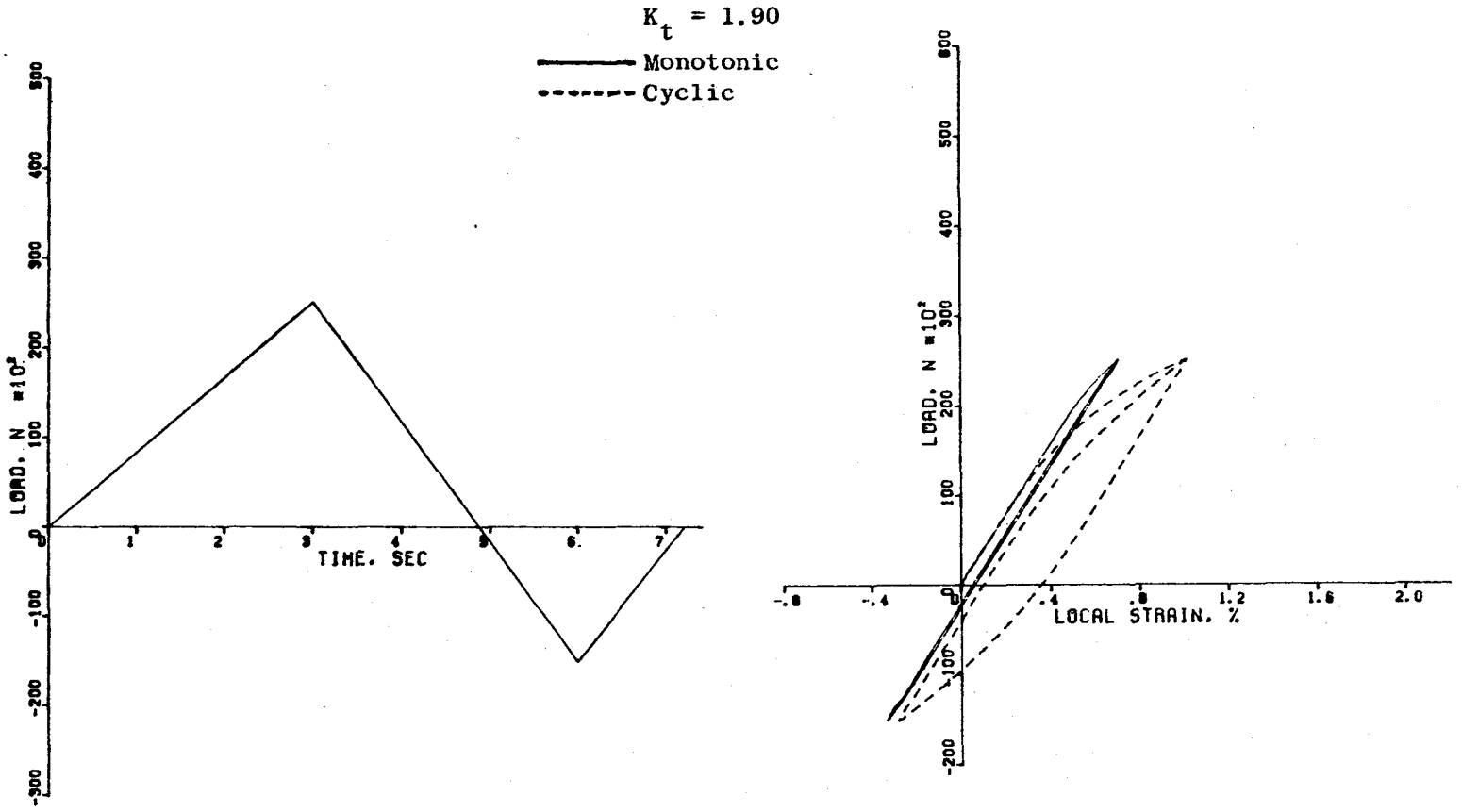

(a) Load Pattern I (Load Versus Time)

(b) Load Versus Local Strain

Figure 81. Neuber Predicted Stress-Strain Behavior for Inconel 718 Notched Bar at 649° C for Load Pattern I (Continuous Cycle), Test 11A.

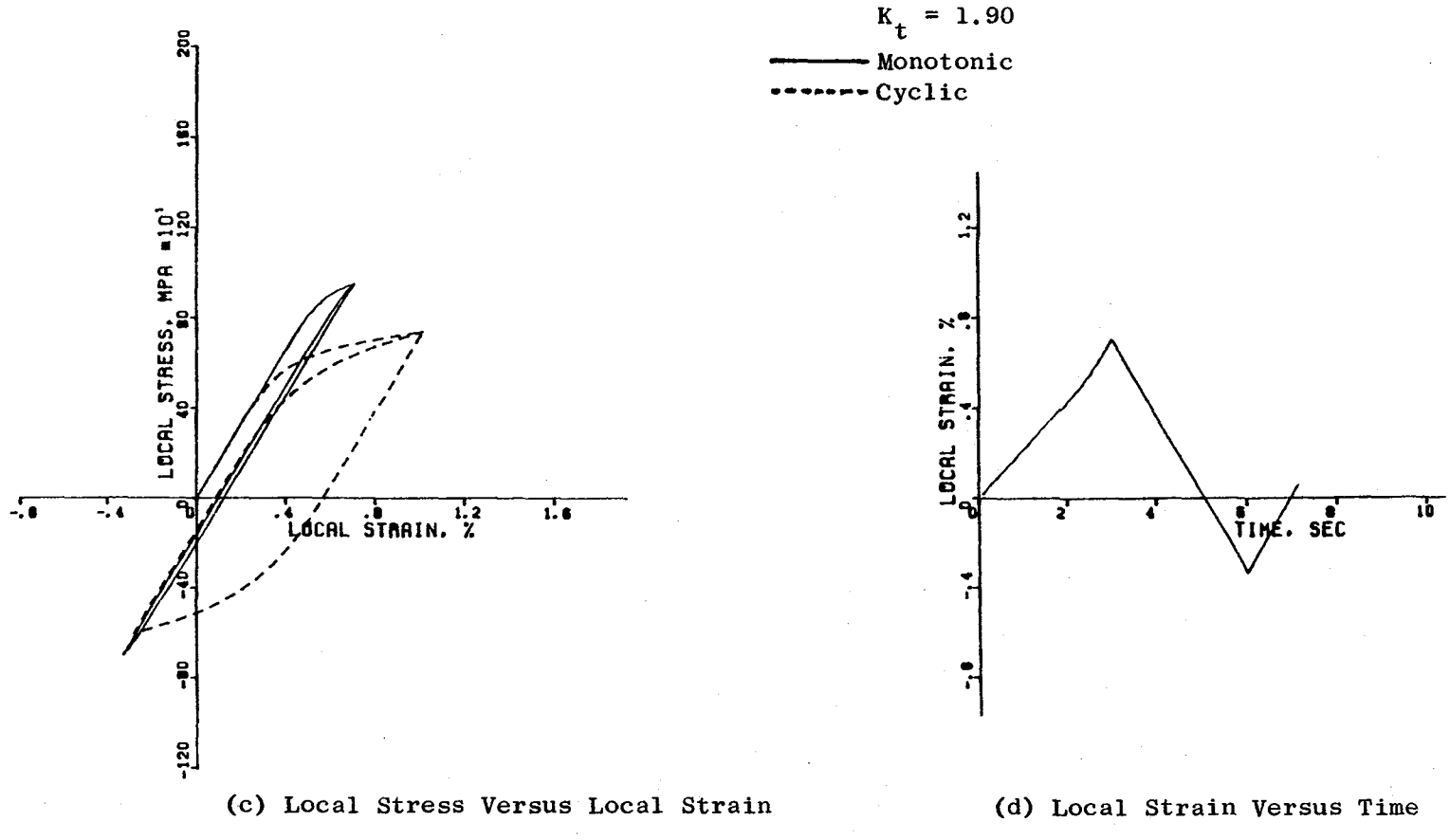

(c) Local Stress Versus Local Strain

(d) Local Strain Versus Time

Figure 81. Neuber Predicted Stress-Strain Behavior for Inconel 718 Notched Bar at 649° C for Load Pattern I (Continuous Cycle), Test 11A (Concluded).

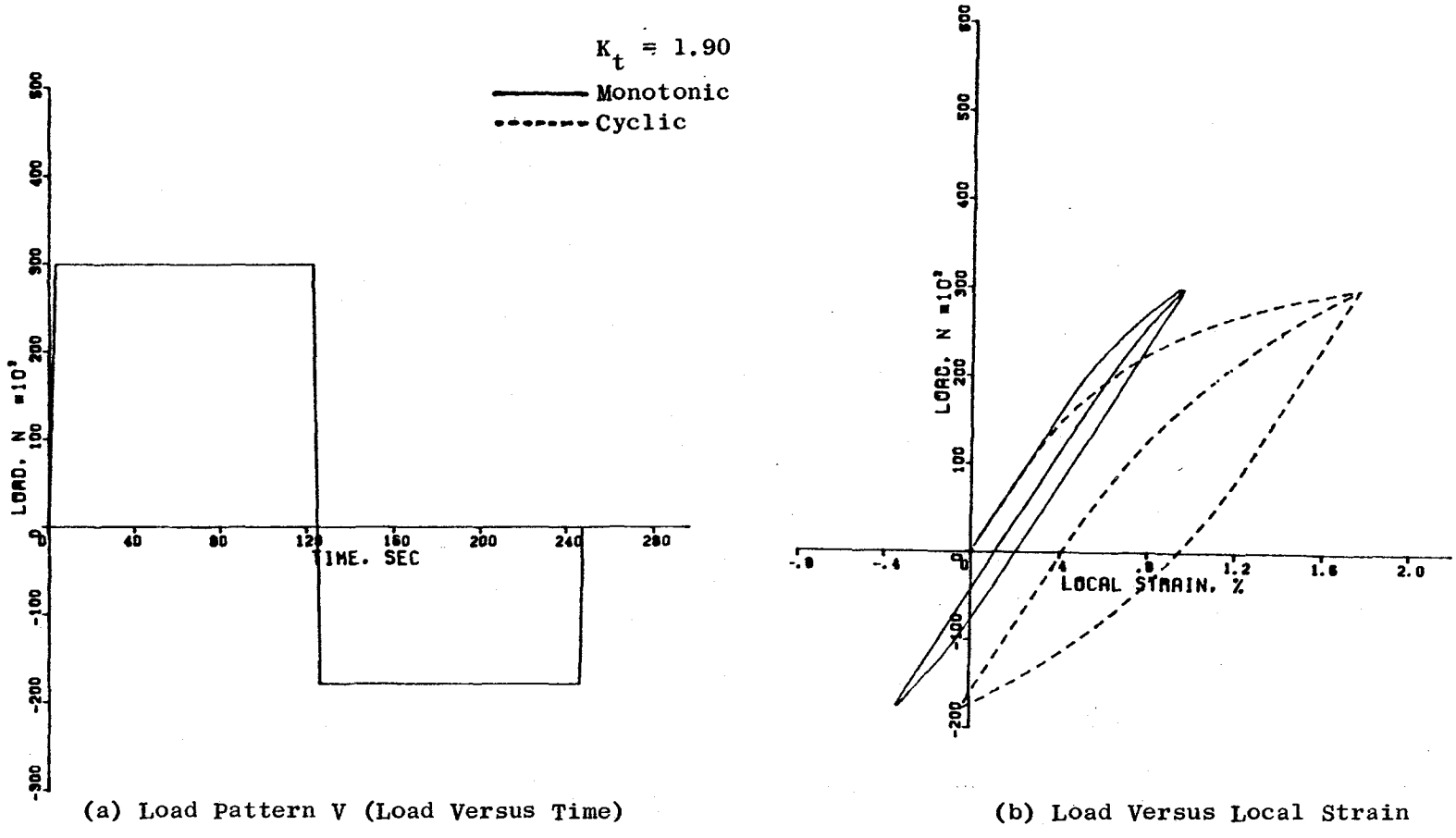

(a) Load Pattern V (Load Versus Time)

(b) Load Versus Local Strain

Figure 82. Neuber Predicted Stress-Strain Behavior for Inconel 718 Notched Bar at 649° C for Load Pattern V (Tension/Compression Hold), Test 11B.

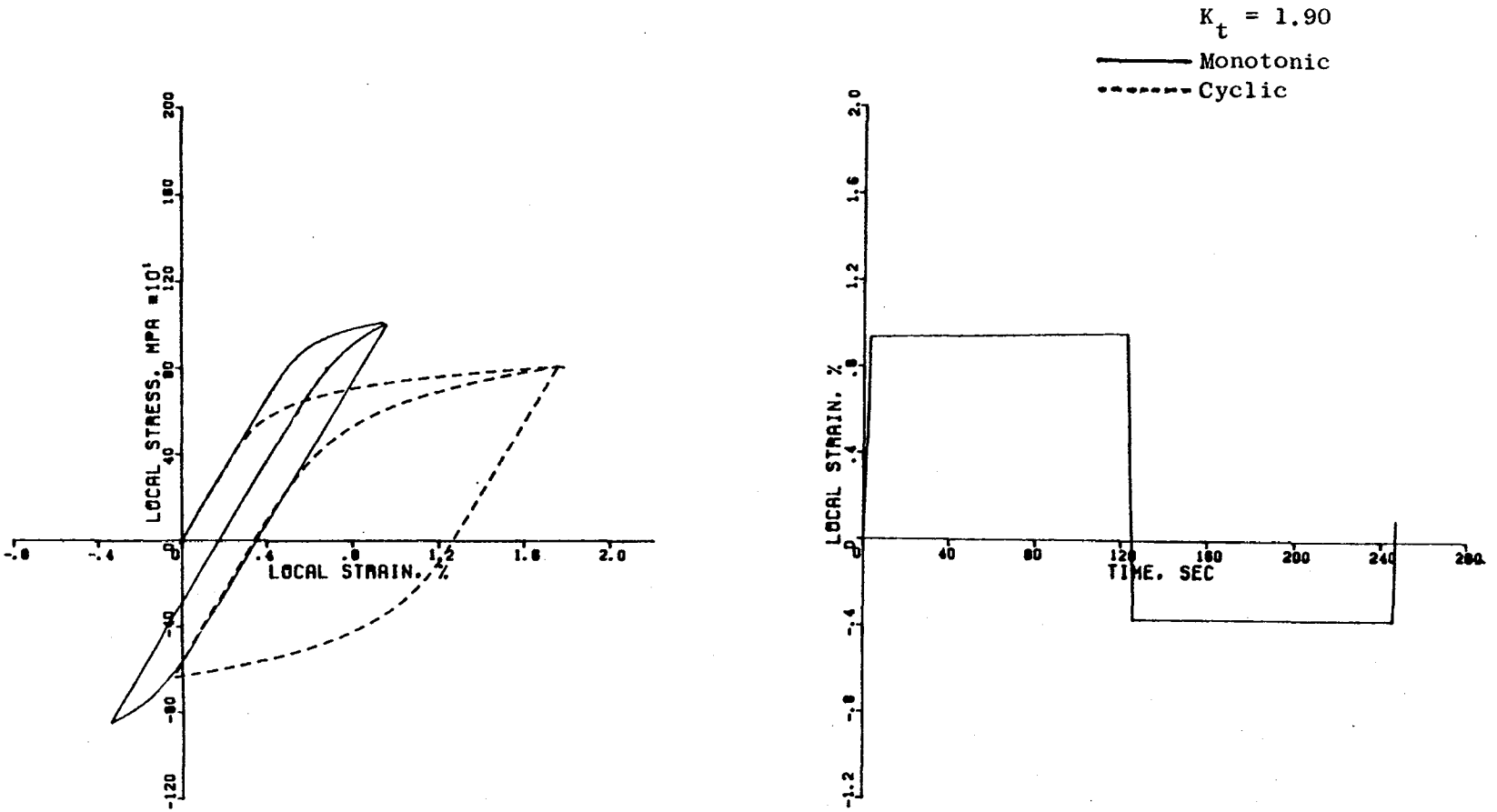

(c) Local Stress Versus Local Strain

(d) Local Strain Versus Time

Figure 82. Neuber Predicted Stress-Strain Behavior for Inconel 718 Notched Bar at 649° C for Load Pattern V (Tension/Compression Hold), Test 11B (Concluded).

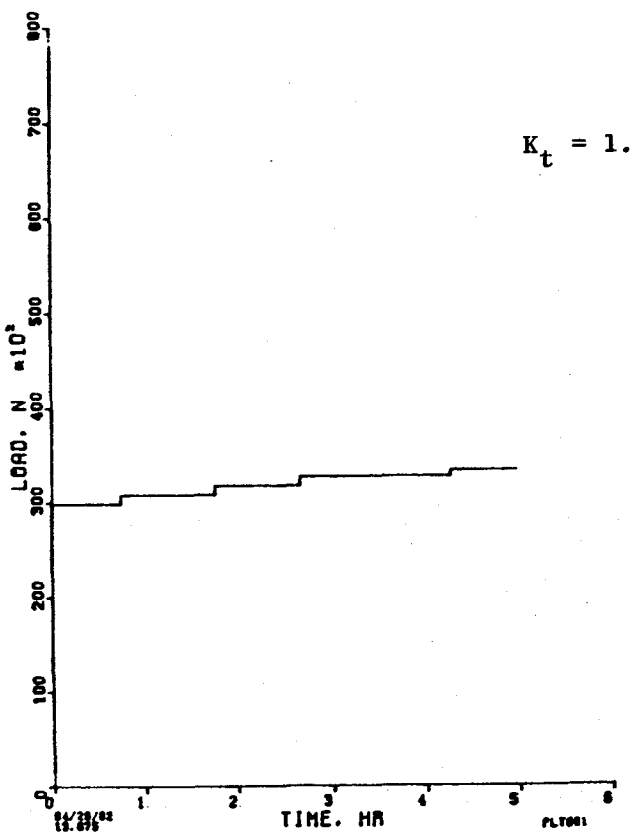

(a) Load Pattern II (Load Versus Time)

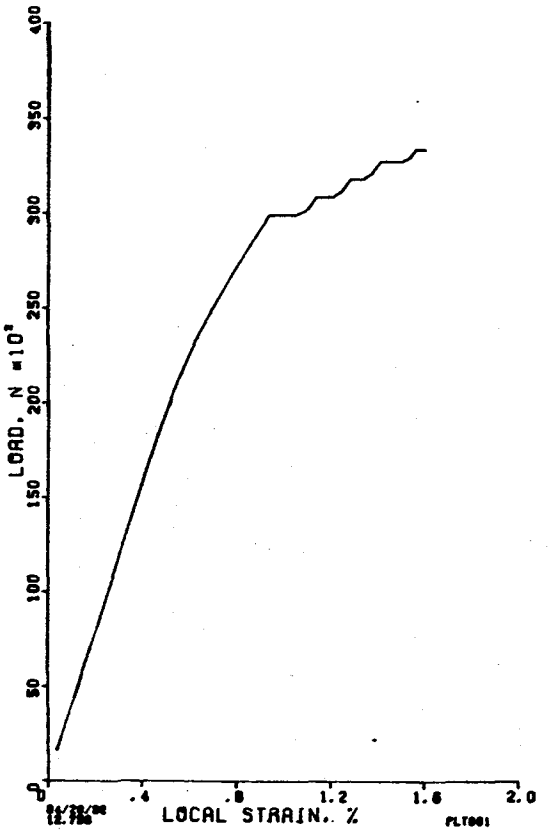

(b) Load Versus Local Strain

Figure 83. Neuber Predicted Stress-Strain Behavior for Inconel 718 Notched Bar at 649° C for Load Pattern II (Creep Test) Test 12.

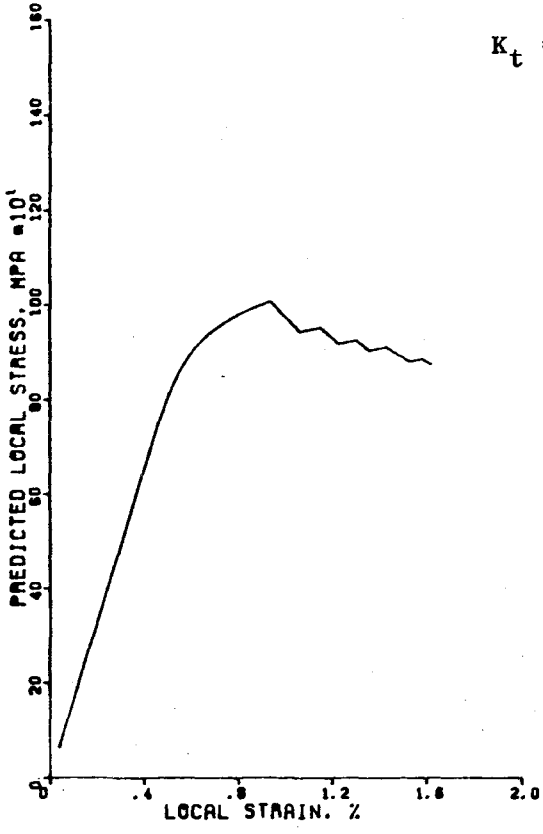

(c) Local Stress Versus Local Strain

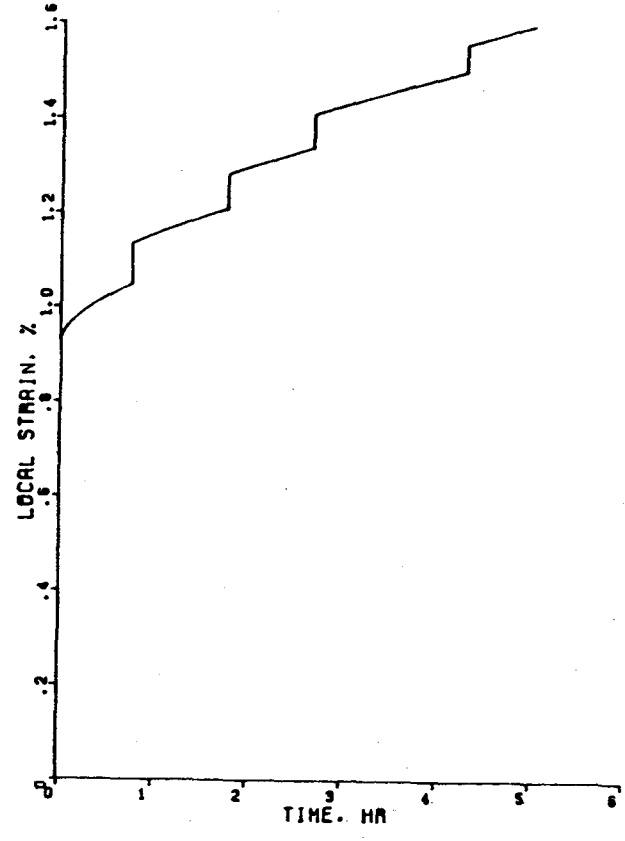

(d) Local Strain Versus Time

Figure 83. Neuber Predicted Stress-Strain Behavior for Inconel 718 Notched Bar at 649° C for Load Pattern II (Creep Test), Test 12 (Concluded).

hold was predicted to be very small (0.02% local creep strain in the tension hold case). Significant creep strain and some load relaxation at the notch root are predicted in the multistep creep test (Test No. 12) as shown in Figure 83. It was assumed in the analysis that the basic behavior of the creep response was not affected by the load step changes.

7.0 TASK V - COMPARISON OF EXPERIMENTAL VERSUS ANALYTICAL RESULTS

7.1 NEUBER ANALYSIS VERSUS EXPERIMENTAL RESULTS

Comparisons between the measured notch root strain responses and the Neuber predictions (based on the monotonic stress-strain relationship only) are made schematically in Figures 84 through 89 for the first complete cycle of each load pattern. In all cases, since there is relatively little initial plasticity, the Neuber method has predicted local strain very well. One question addressed in Section 6.1 is the Neuber model's inability to handle stress redistribution when the plasticity at the notch root becomes large. Using the modified Neuber analysis described in that section, the prediction is shown in Figure 90. It is unclear from these data if this represents an improved prediction.

Significant scatter in the strain measurement was observed during the 2-minute hold time, which precludes an accurate measurement of the creep strain. (This is consistent with the predicted low creep strain during this hold.) However, the creep deformation could be observed clearly in the multi-step creep test (Test No. 12) which had longer hold time in each load step. The initial plastic strain is well predicted. However, during the first hold period the measured strain decreases while the predicted strain increases. This phenomenon occurred at several of the load increments. Although the explanation for this is unclear, the overall trend of the predicted creep strain agrees fairly well with the test data.

Several intermediate cycles which gradually approach the steady-state cyclic response of each load pattern were examined and compared with analytical predictions on the basis of null initial strain (Figures 91 through 97). The trend of increasing hysteresis loop size as cycling proceeds indicates the softening behavior of the material. These figures also illustrate monotonic/cyclic transition of material behavior. In Test Nos. 7 and 11B (shown in Figures 92 and 97), decreases of the elastic loading slope, which is indicative of the stiffness of the specimen, were observed in the final cycles. This is indicative of the formation and propagation of cracks at the notch root.

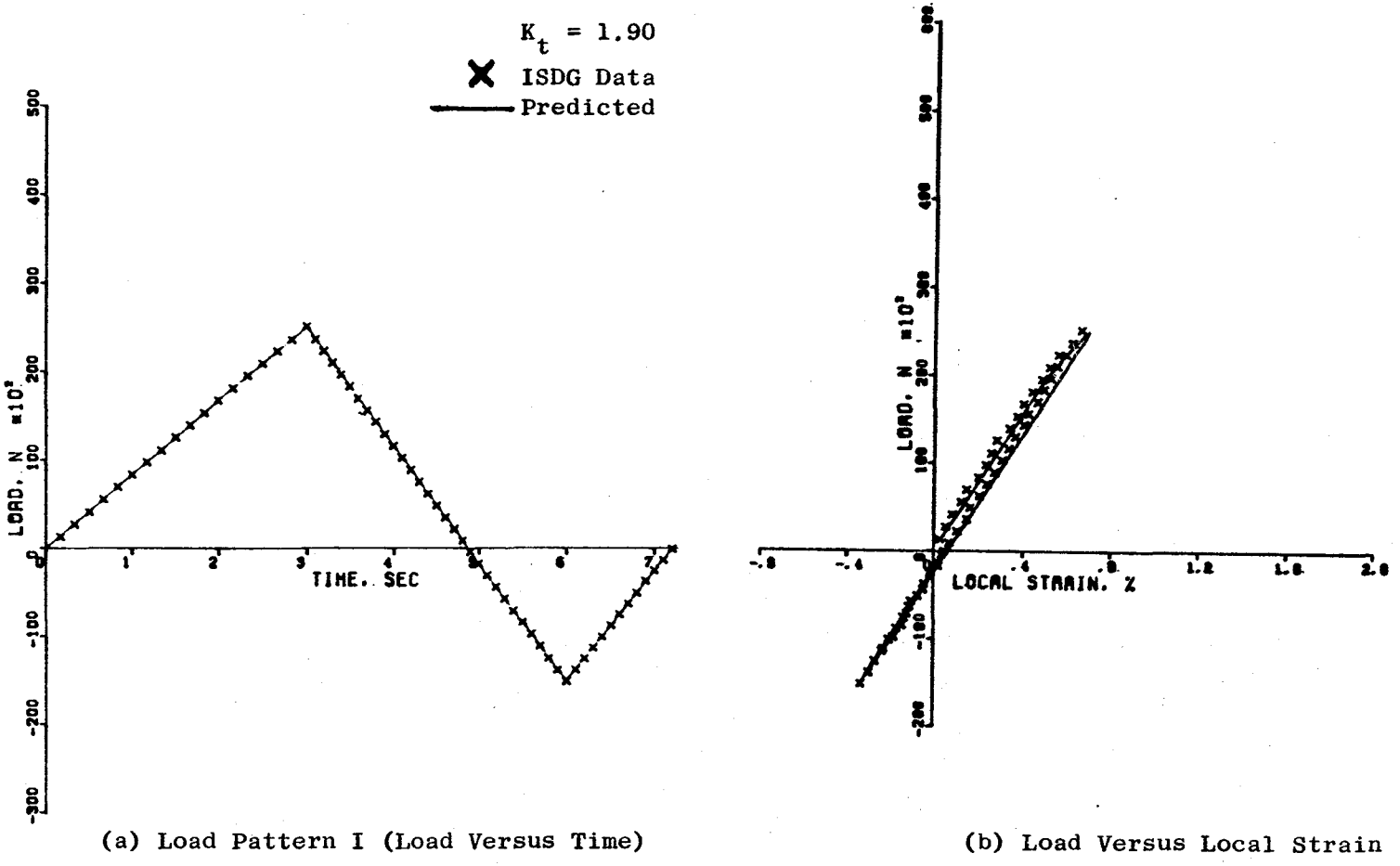

(a) Load Pattern I (Load Versus Time)

(b) Load Versus Local Strain

Figure 84. Comparison of Neuber Predicted and ISDG Measured First Cycle Stress-Strain Behavior for Inconel 718 Notched Bar at 649° C for Load Pattern I (Continuous Cycle), Test 6.

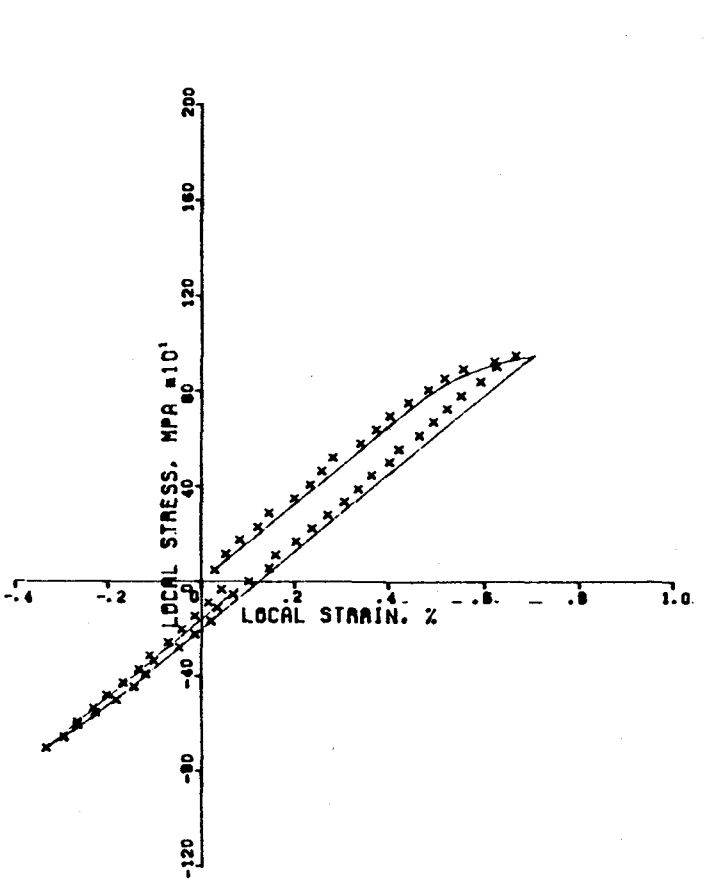

(c) Local Stress Versus Local Strain

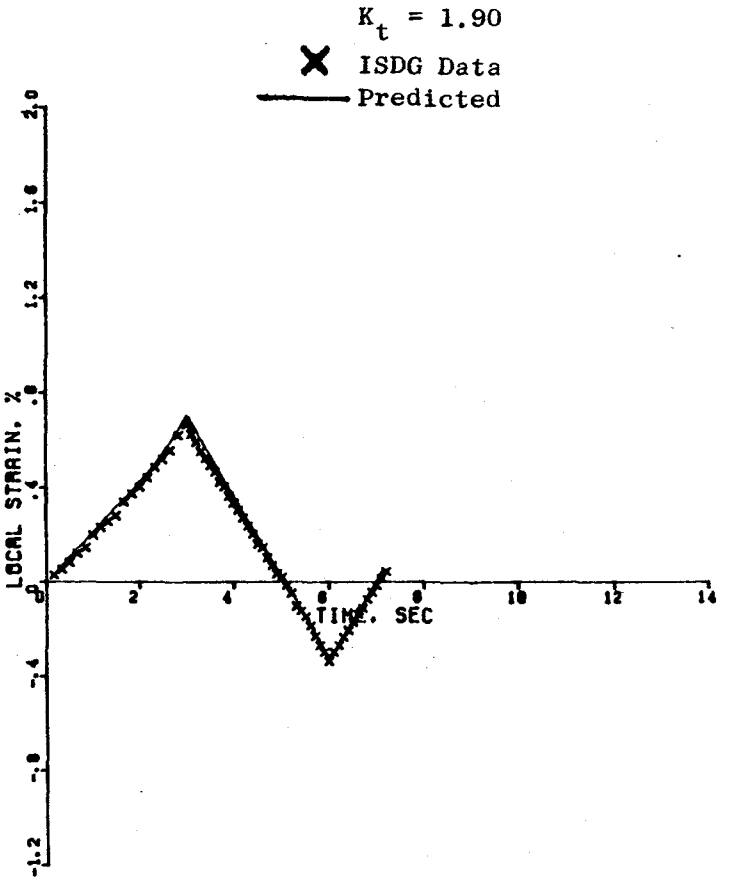

(d) Local Strain Versus Time

Figure 84. Comparison of Neuber Predicted and ISDG Measured First Cycle Stress-Strain Behavior for Inconel 718 Notched Bar at 649° C for Load Pattern I (Continuous Cycle), Test 6 (Concluded).

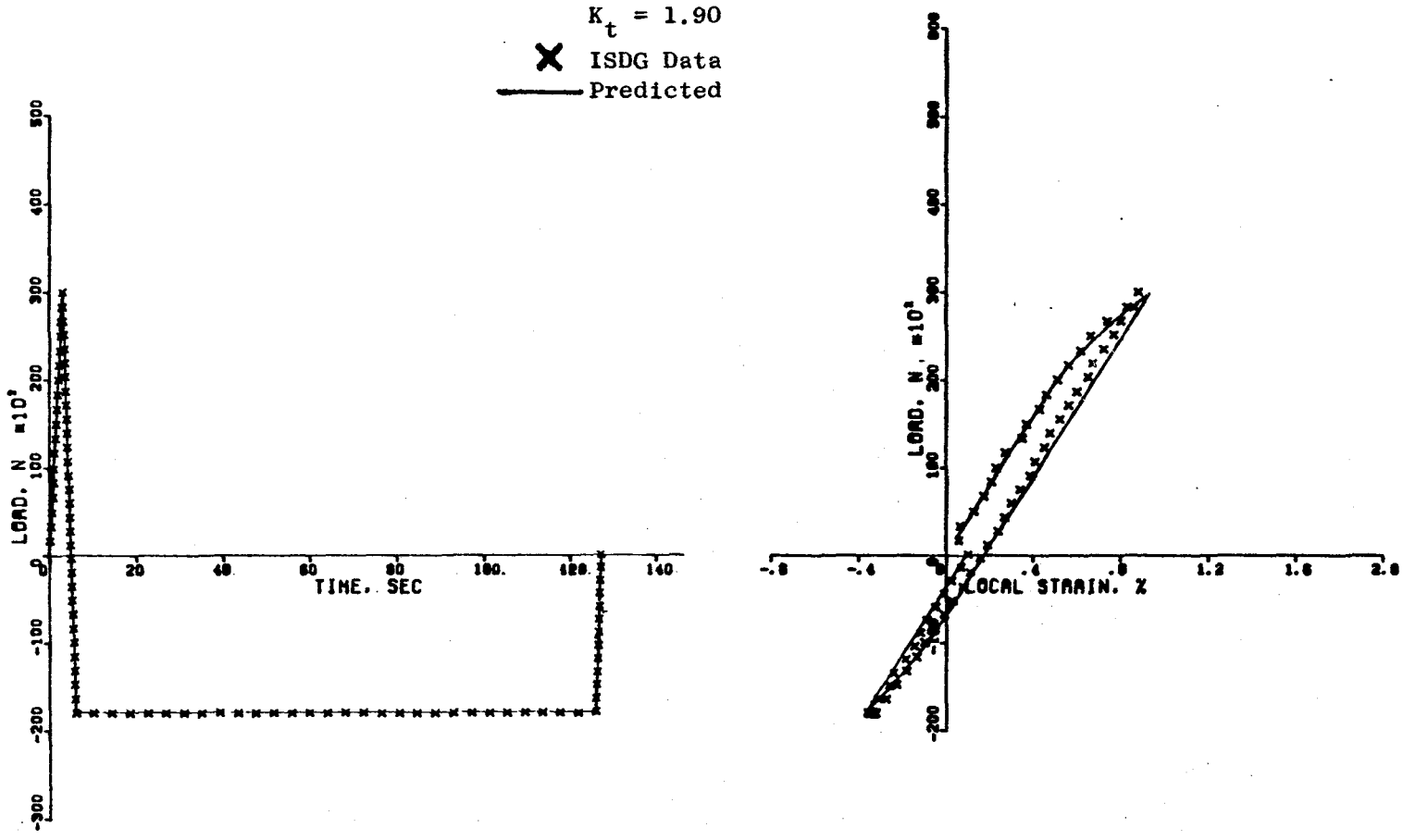

(a) Load Pattern IV (Load Versus Time)

(b) Load Versus Local Strain

Figure 85. Comparison of Neuber Predicted and ISDG Measured First Cycle Stress-Strain Behavior for Inconel 718 Notched Bar at 649° C for Load Pattern IV (Compression Hold), Test 8.

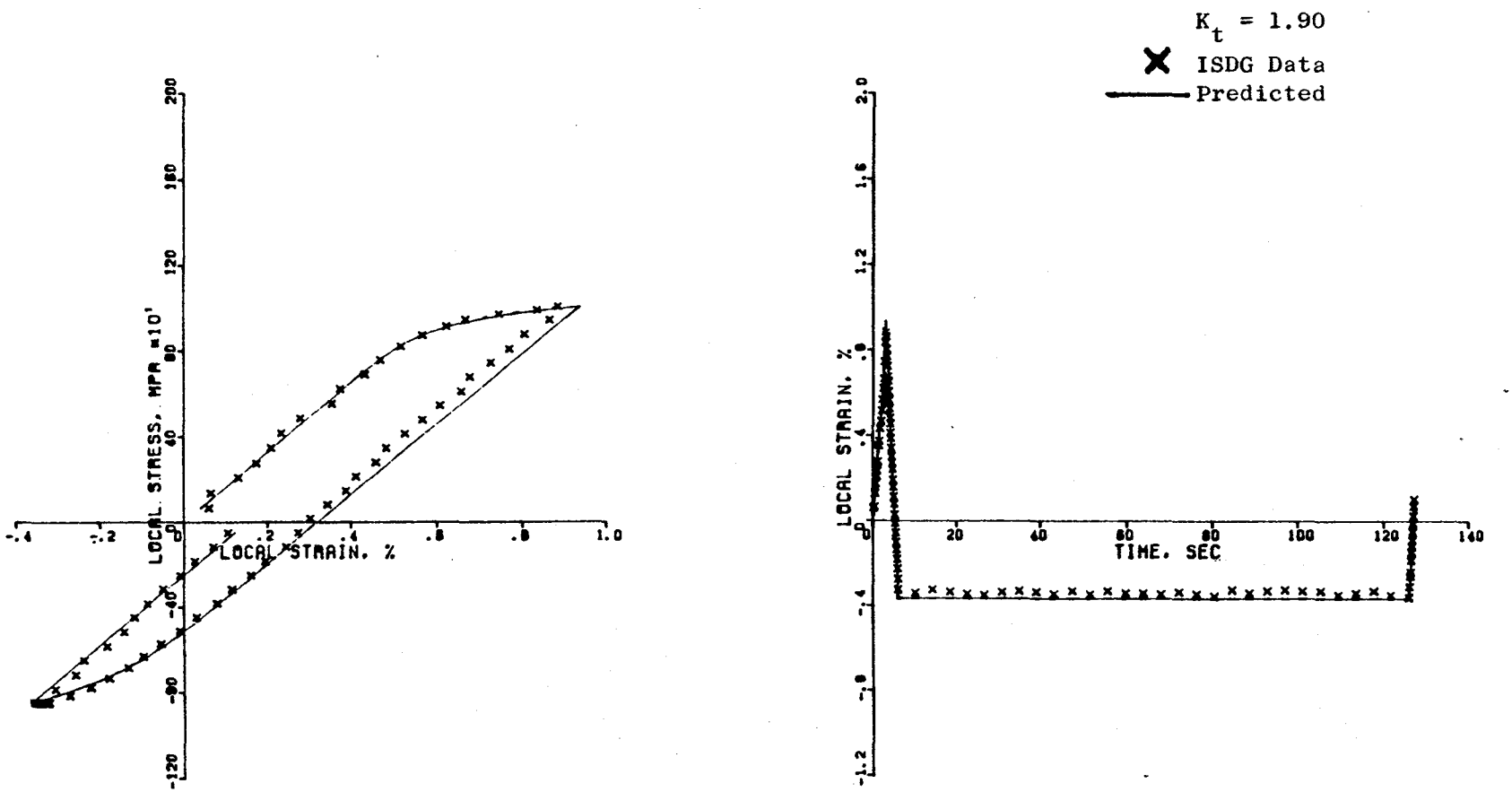

(c) Local Stress Versus Local Strain

(d) Local Strain Versus Time

Figure 85. Comparison of Neuber Predicted and ISDG Measured First Cycle Stress-Strain Behavior for Inconel 718 Notched Bar at 649° C for Load Pattern IV (Compression Hold), Test 8 (Concluded).

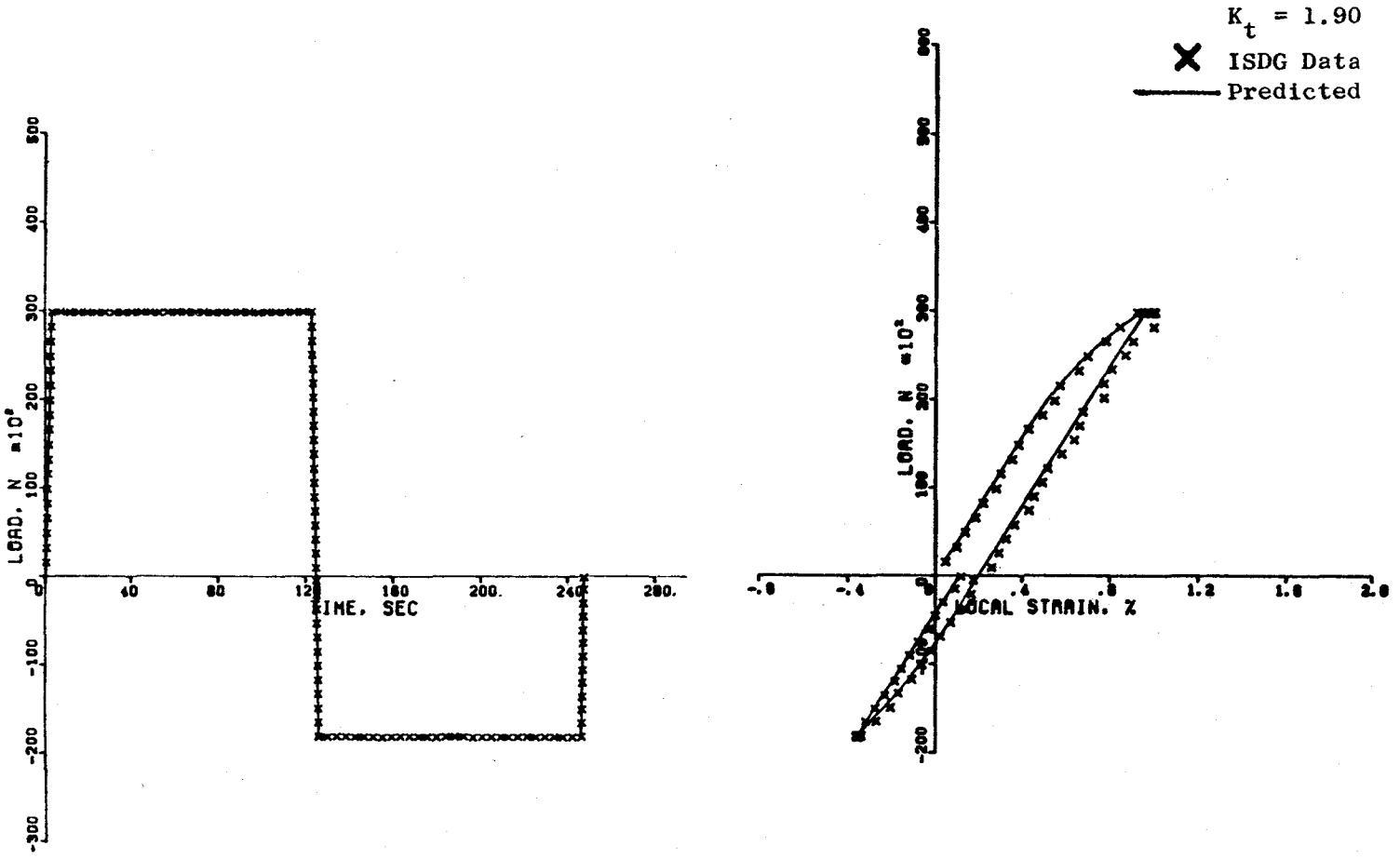

(a) Load Pattern V (Load Versus Time)

(b) Load Versus Local Strain

Figure 86. Comparison of Neuber Predicted and ISDG Measured First Cycle Stress-Strain Behavior for Inconel 718 Notched Bar at 649° C for Load Pattern V (Tension/Compression Hold), Test 9.

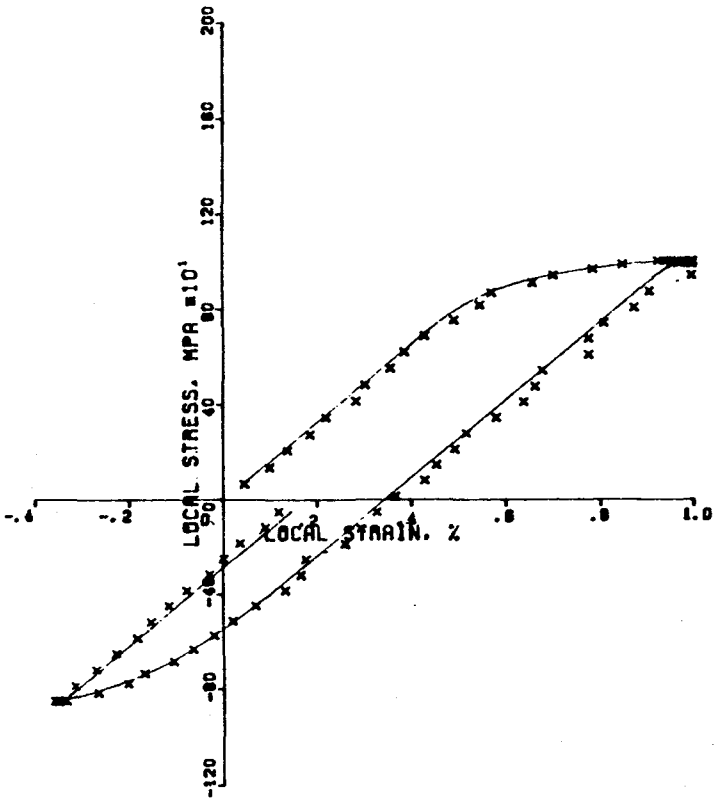

(c) Local Stress Versus Local Strain

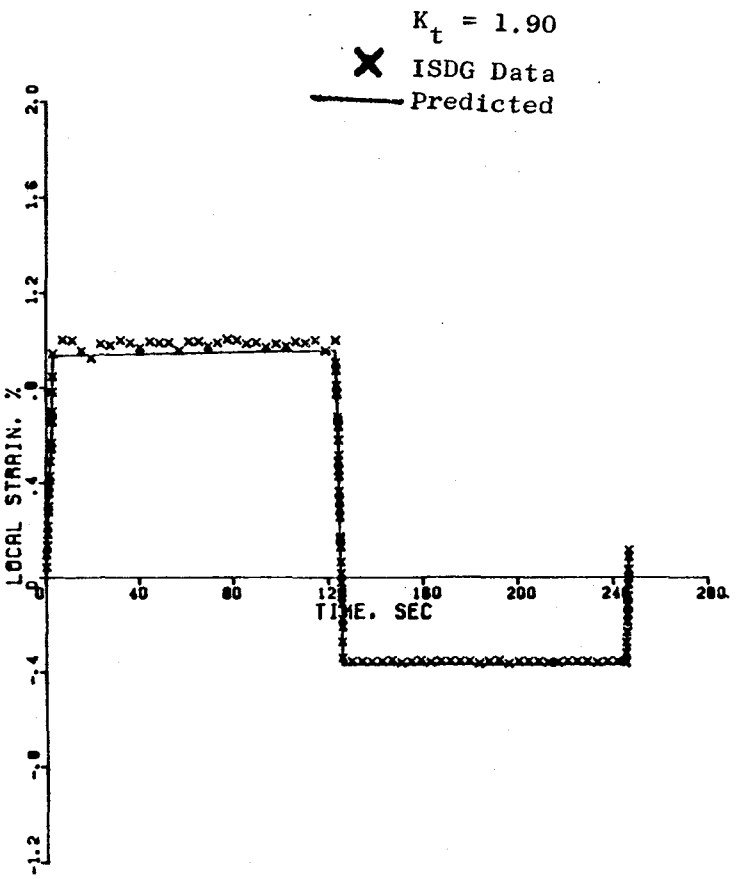

(d) Local Strain Versus Time

Figure 86. Comparison of Neuber Predicted and ISDG Measured First Cycle Stress-Strain Behavior for Inconel 718 Notched Bar at 649° C for Load Pattern V (Tension/Compression Hold), Test 9 (Concluded).

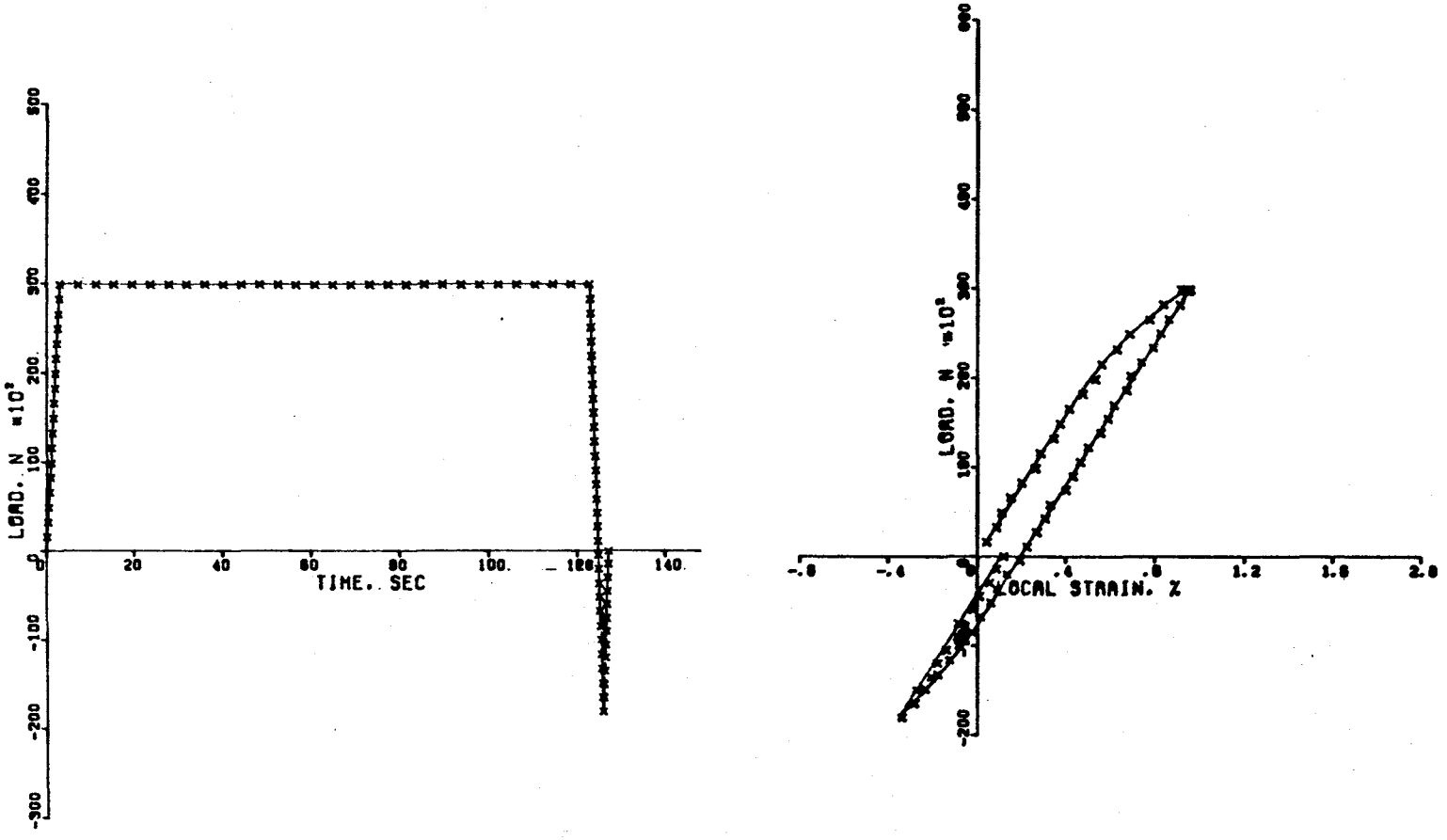

(a) Load Pattern III (Load Versus Time)

(b) Load Versus Local Strain

Figure 87. Comparison of Neuber Predicted and ISDG Measured First Cycle Stress-Strain Behavior for Inconel 718 Notched Bar at 649° C for Load Pattern III (Tension Hold), Test 10.

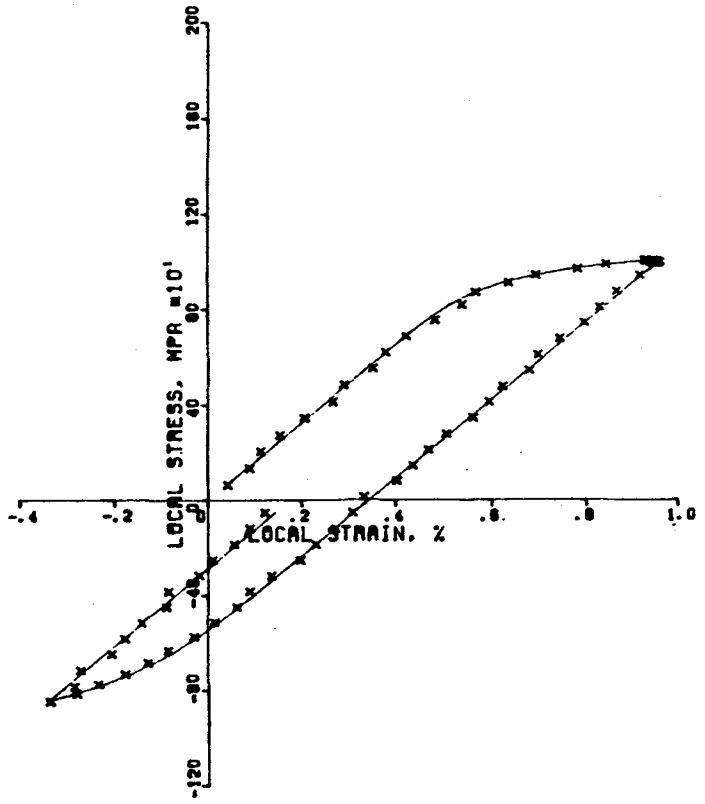

(c) Local Stress Versus Local Strain

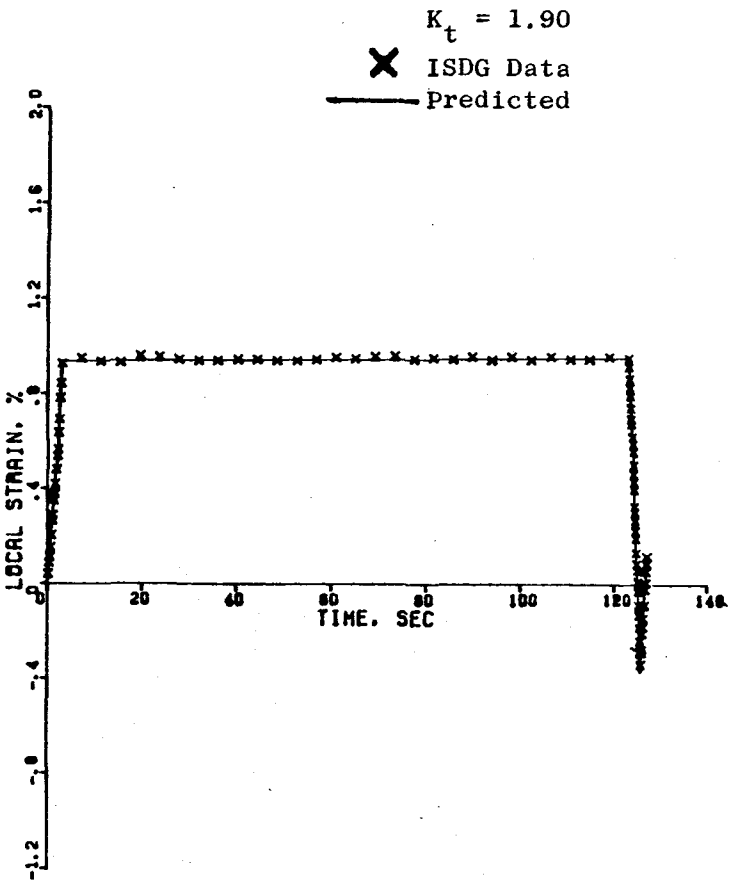

(d) Local Strain Versus Time

Figure 87. Comparison of Neuber Predicted and ISDG Measured First Cycle Stress-Strain Behavior for Inconel 718 Notched Bar at 649° C for Load Pattern III (Tension Hold), Test 10 (Concluded).

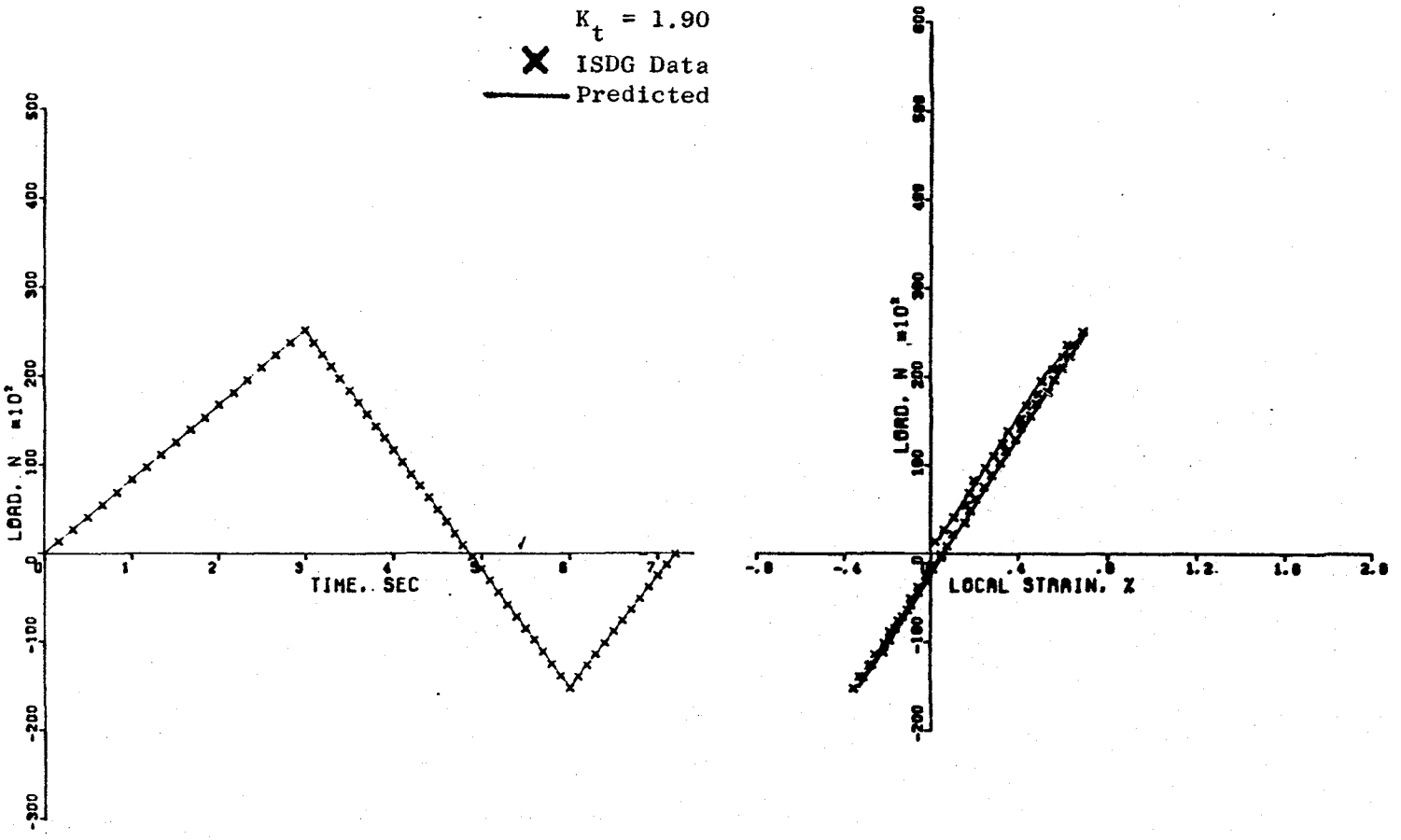

(a) Load Pattern VI (Load Versus Time)

(b) Load Versus Local Strain

Figure 88. Comparison of Neuber Predicted and ISDG Measured First Cycle Stress-Strain Behavior for Inconel 718 Notched Bar at 649° C for Load Pattern VI (Continuous Cycle), Test 11A.

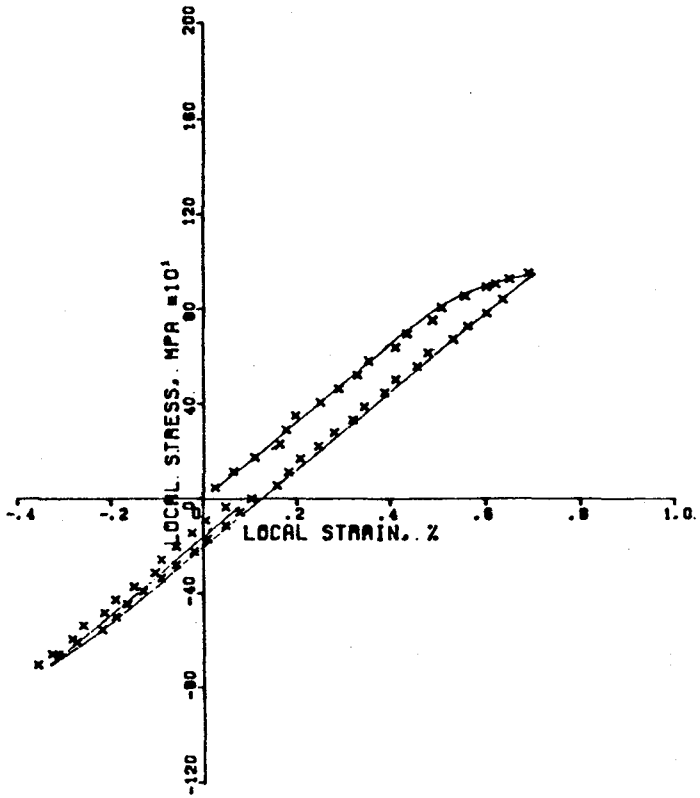

(c) Local Stress Versus Local Strain

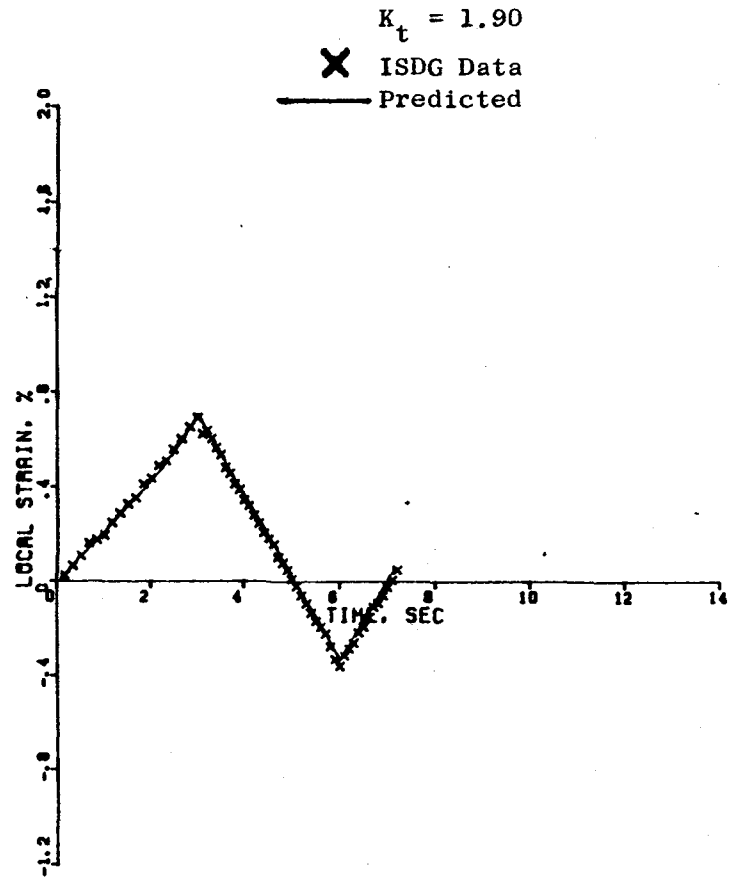

(d) Local Strain Versus Time

Figure 88. Comparison of Neuber Predicted and ISDG Measured First Cycle Stress-Strain Behavior for Inconel 718 Notched Bar at 649° C for Load Pattern VI (Continuous Cycle), Test 11A (Concluded).

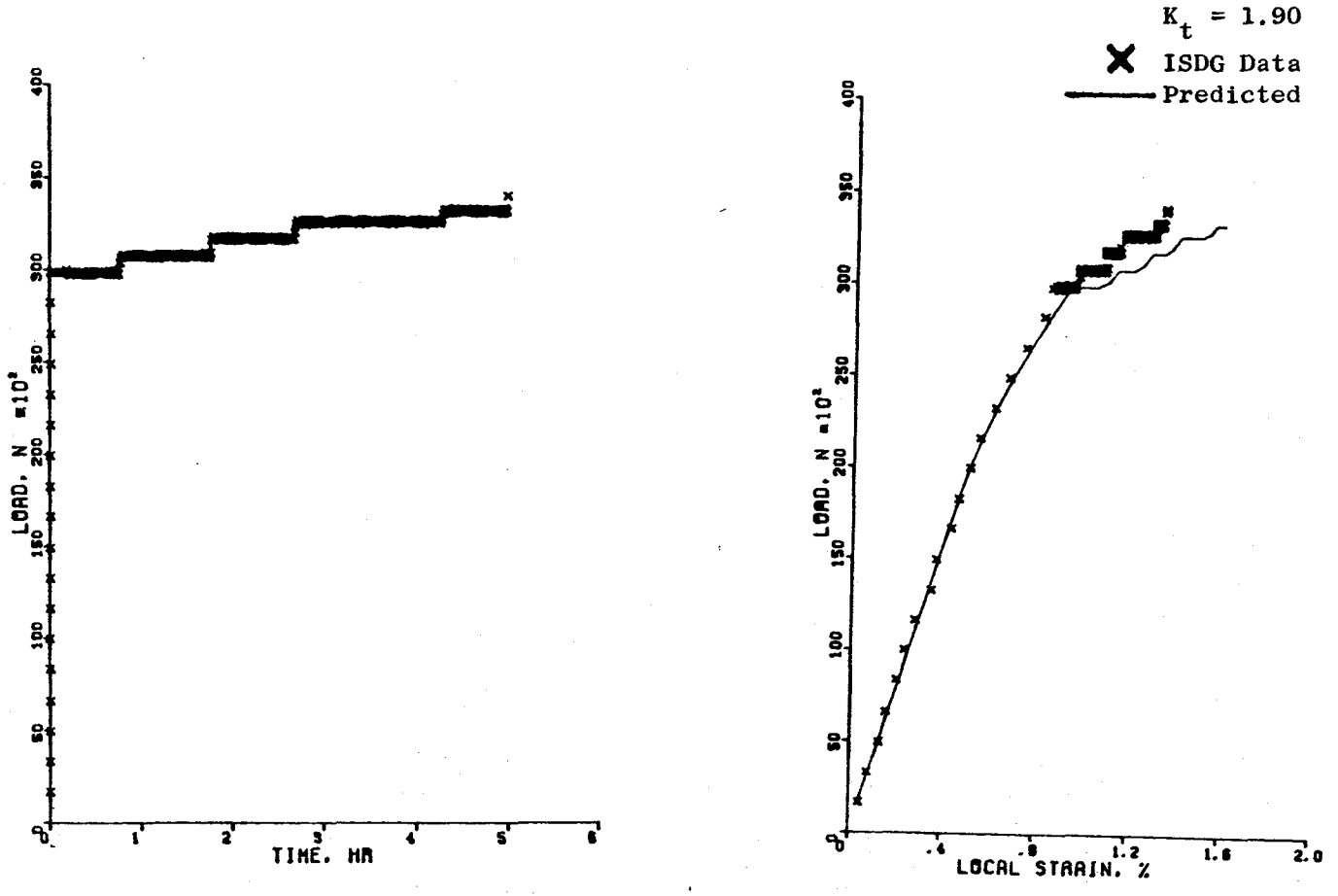

(a) Load Pattern II (Load Versus Time)

(b) Load Versus Local Strain

Figure 89. Comparison Of Neuber Predicted and ISDG Measured First Cycle Stress-Strain Behavior for Inconel 718 Notched Bar at 649° C for Load Pattern II (Creep Test), Test 12.

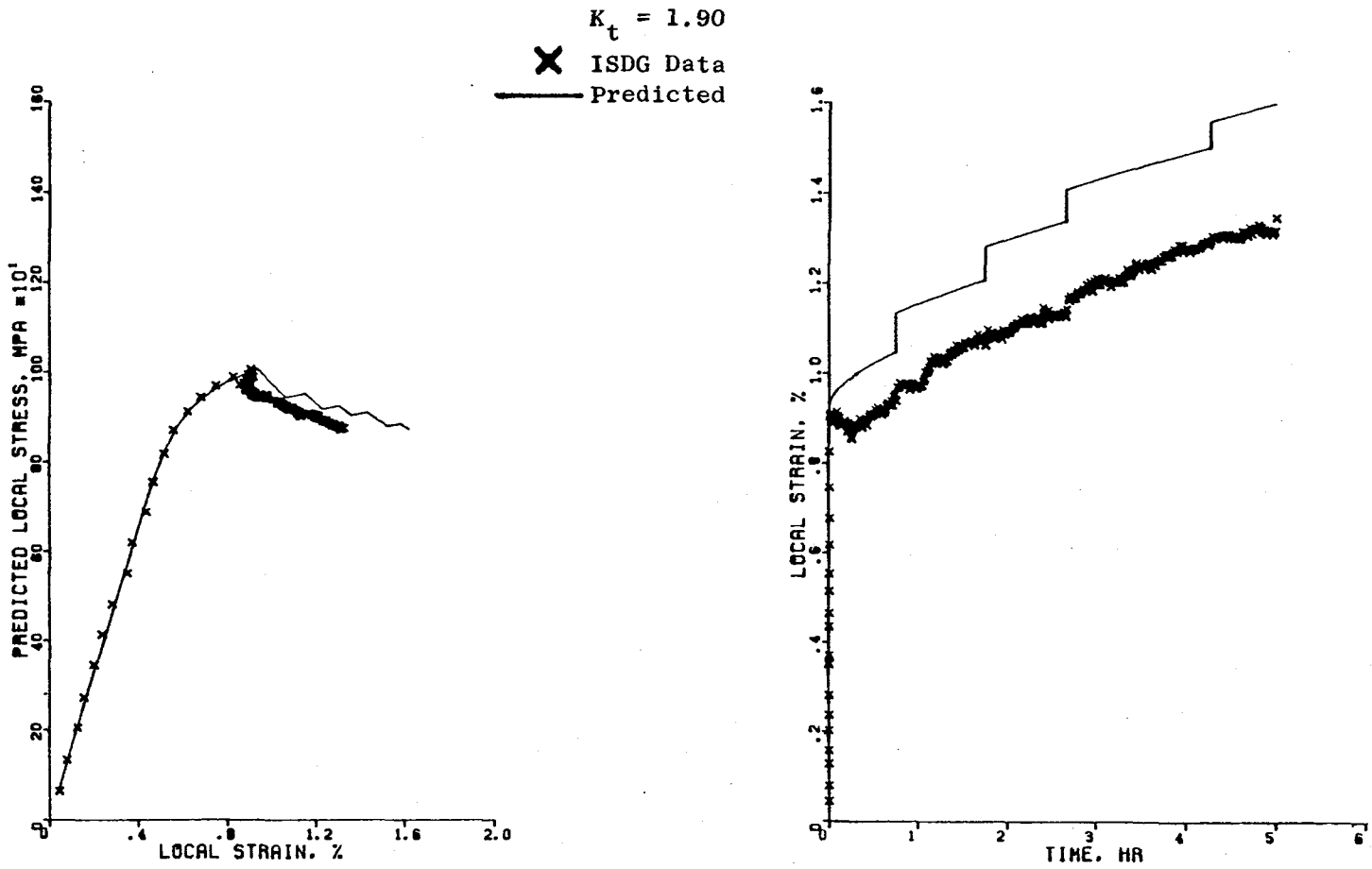

(c) Local Stress Versus Local Strain

(d) Local Strain Versus Time

Figure 89. Comparison of Neuber Predicted and ISDG Measured First Cycle Stress-Strain Behavior for Inconel 718 Notched Bar at 649° C for Load Pattern II (Creep Test), Test 12 (Concluded).

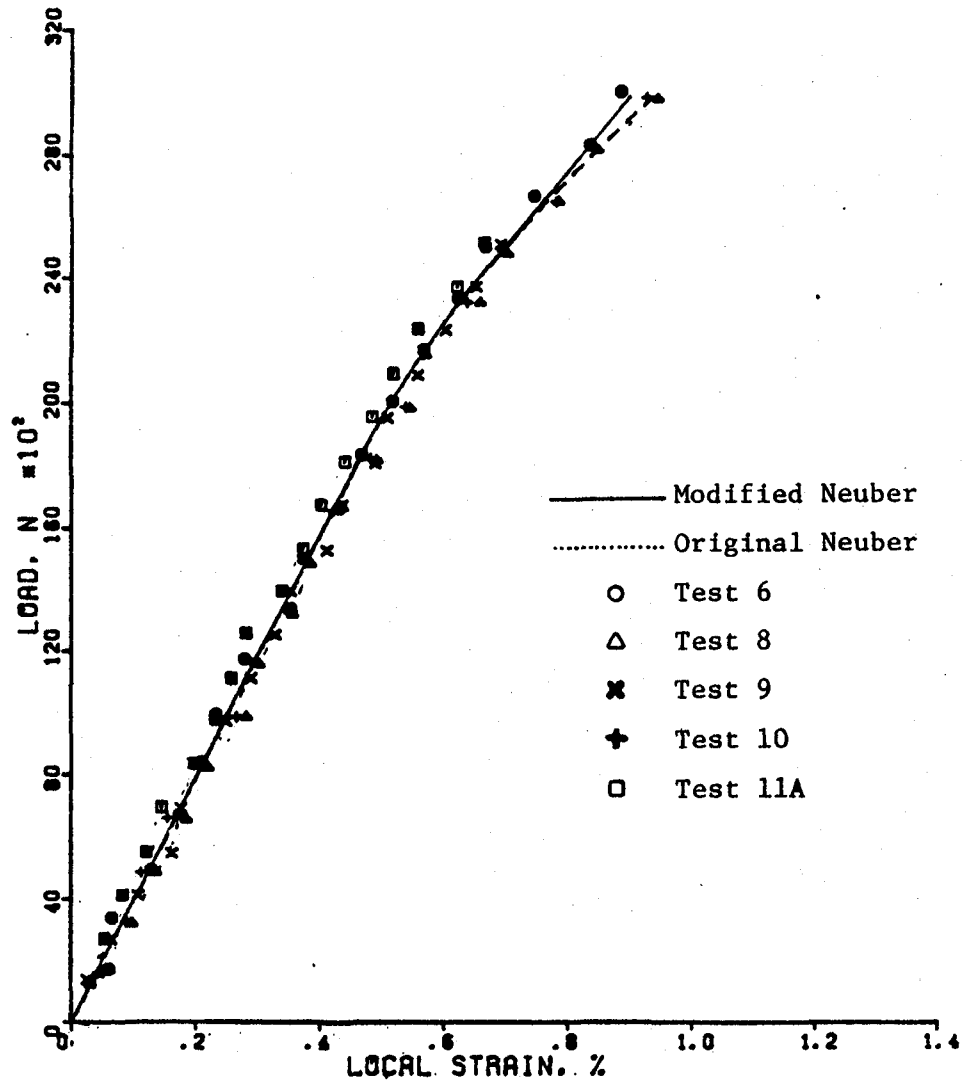

Figure 90. Comparison of Modified and Original Neuber Predictions (Based on 20%/Minute Strain Rate Stress-Strain Relationship) and ISDG Measured Notch Root Strain Behavior.

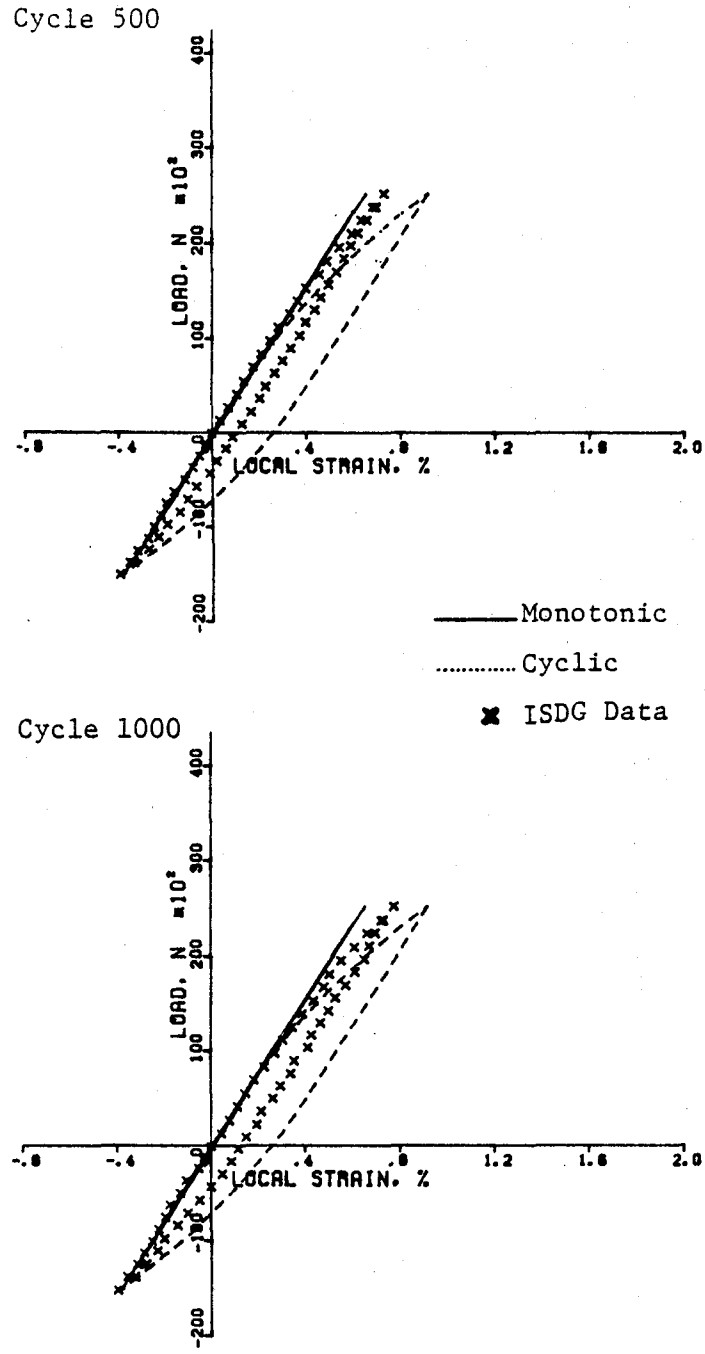

Figure 91. Comparison of Neuber Predictions and ISDG Measured Intermediate Cycle Notch Root Strain Behavior of Test 6 (Continuous Cycle).

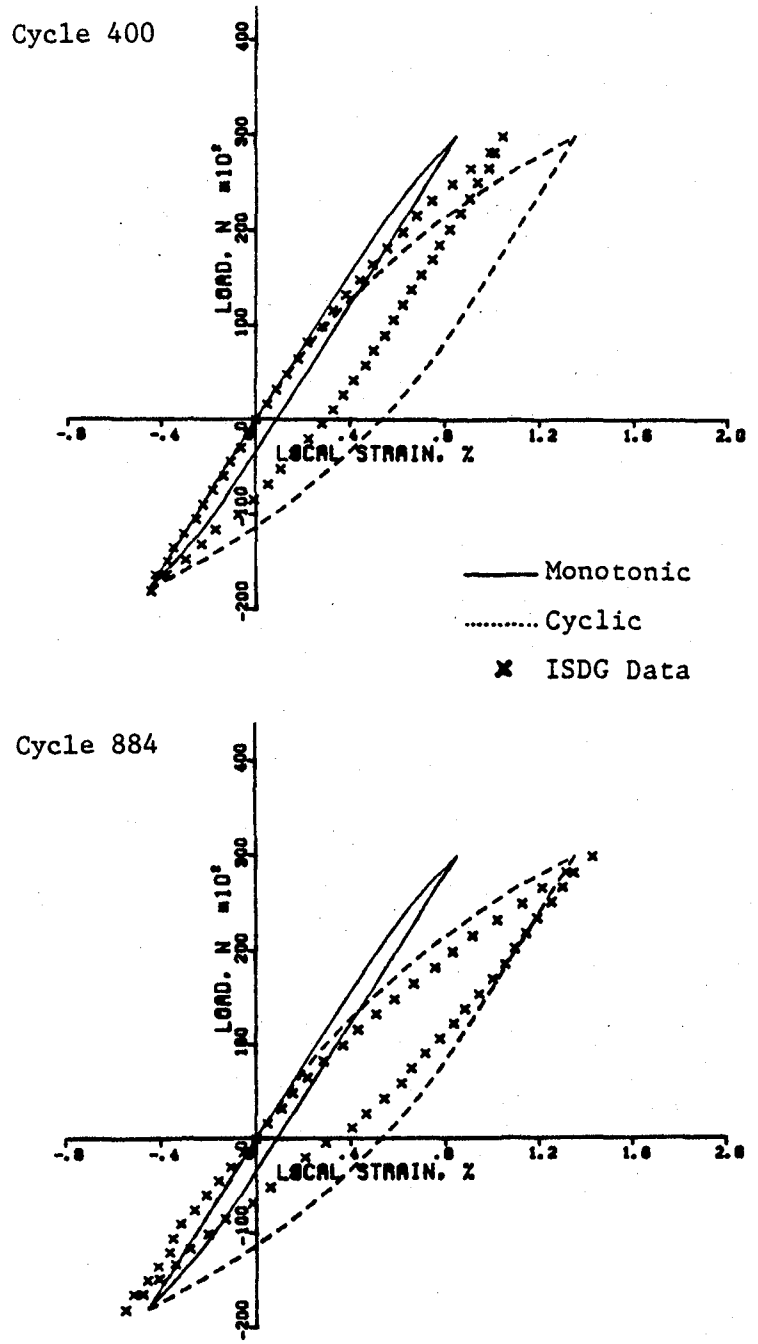

Figure 92. Comparison of Neuber Predictions and ISDG Measured Intermediate Cycle Notch Root Strain Behavior of Test 7 (Continuous Cycle).

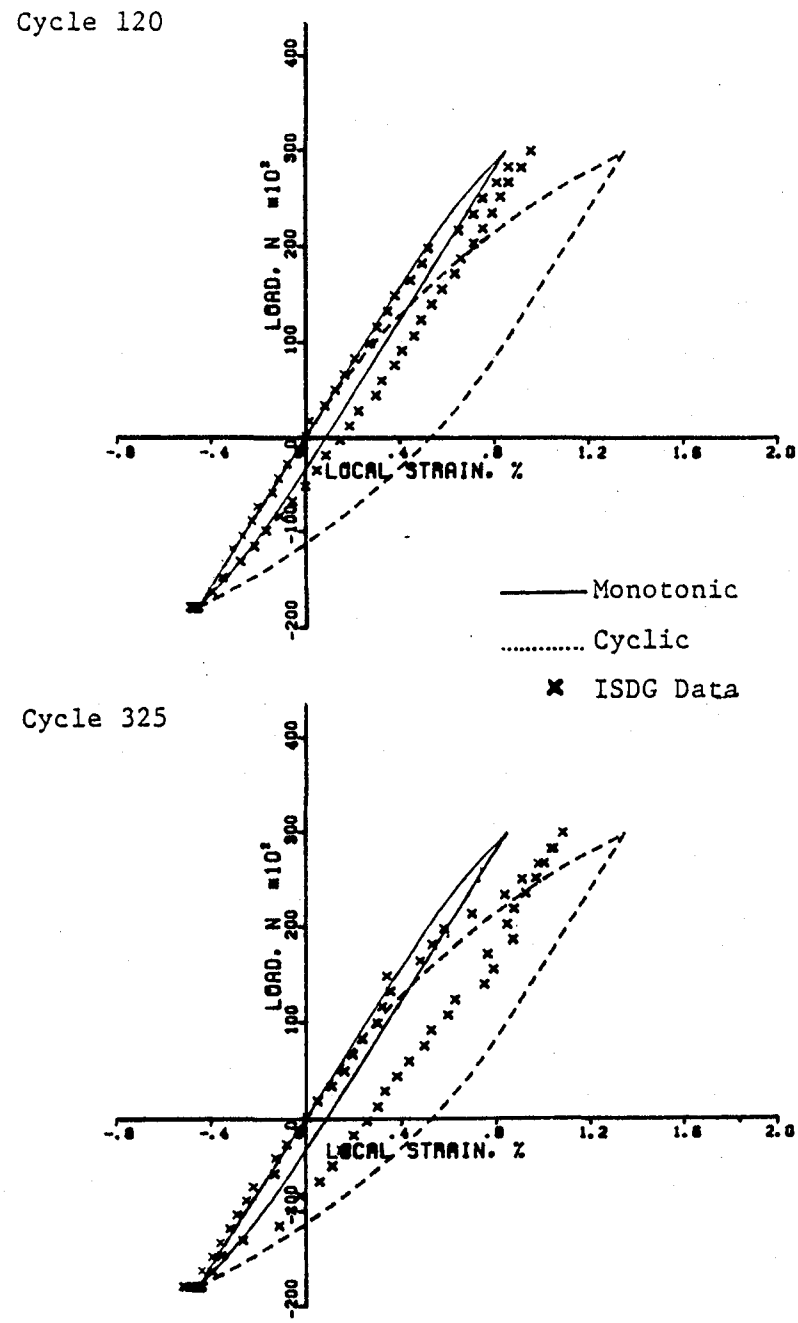

Figure 93. Comparison of Neuber Predictions and ISDG Measured Intermediate Cycle Notch Root Strain Behavior of Test 8 (Compression Hold).

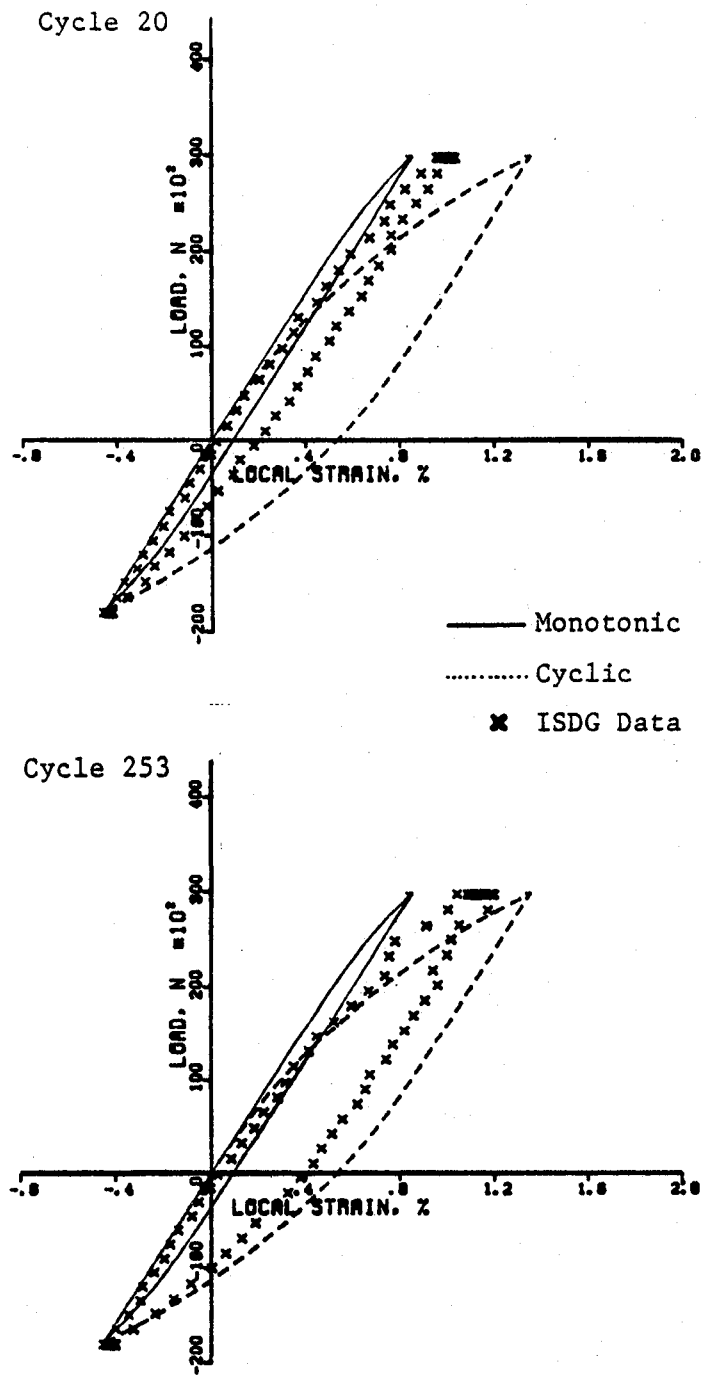

Figure 94. Comparison of Neuber Predictions and ISDG Measured Intermediate Cycle Notch Root Strain Behavior of Test 9 (Tension/Compression Hold).

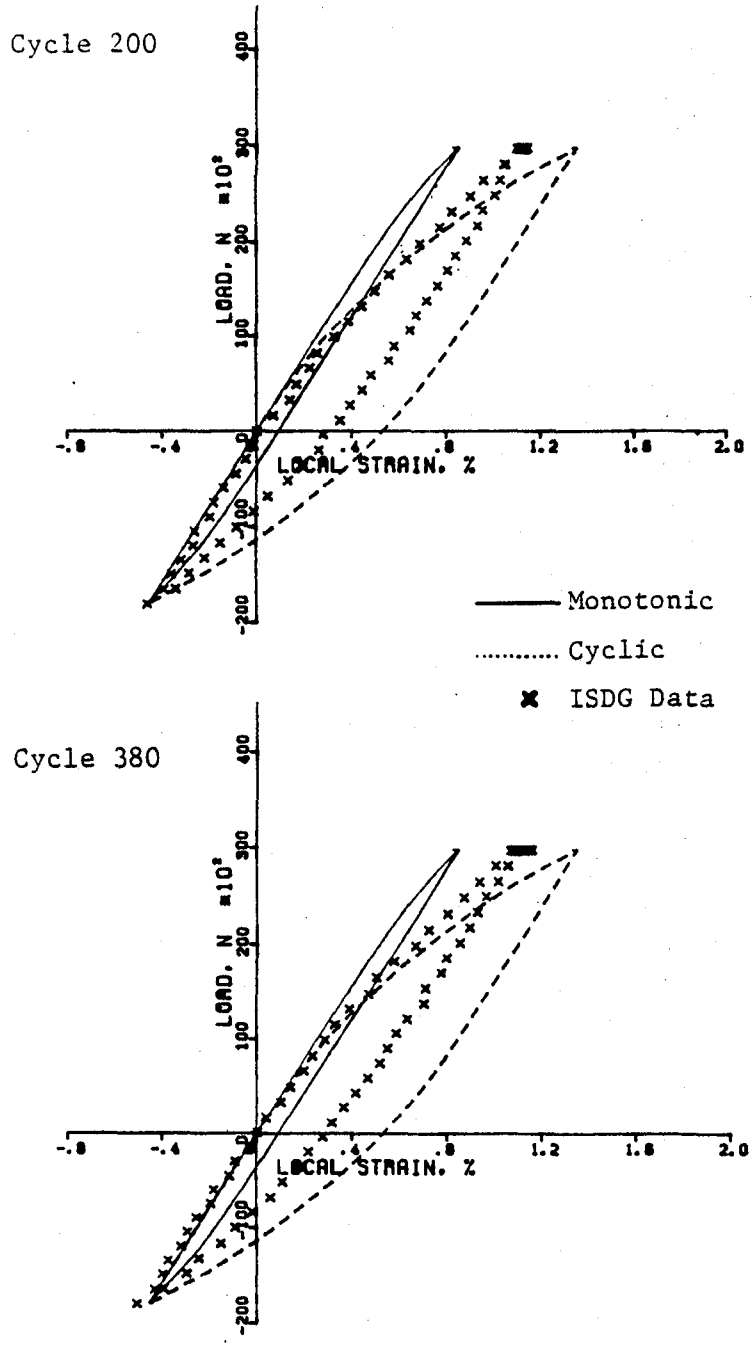

Figure 95. Comparison of Neuber Predictions and ISDG Measured Intermediate Cycle Notch Root Strain Behavior of Test 10 (Tension Hold).

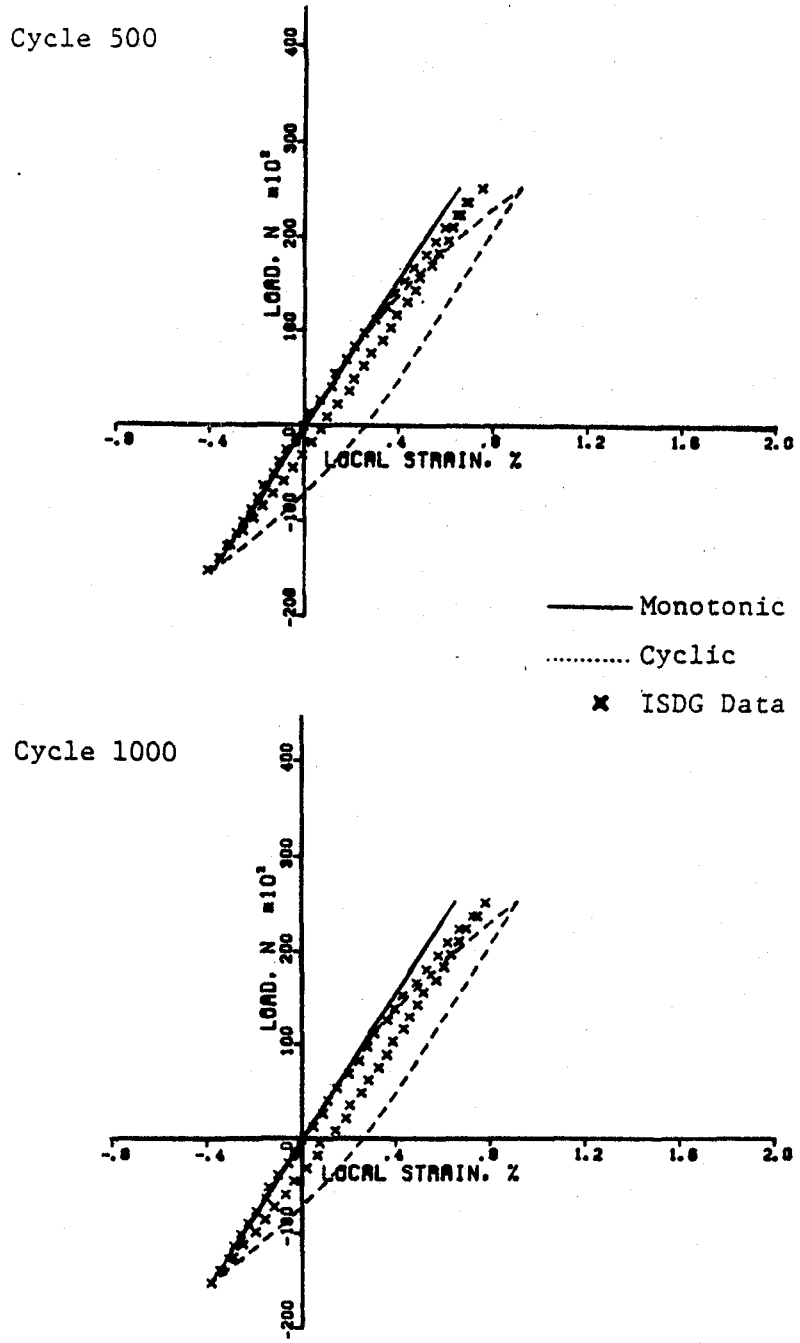

Figure 96. Comparison of Neuber Predictions and ISDG Measured Intermediate Cycle Notch Root Strain Behavior of Test 11a (Continuous Cycle).

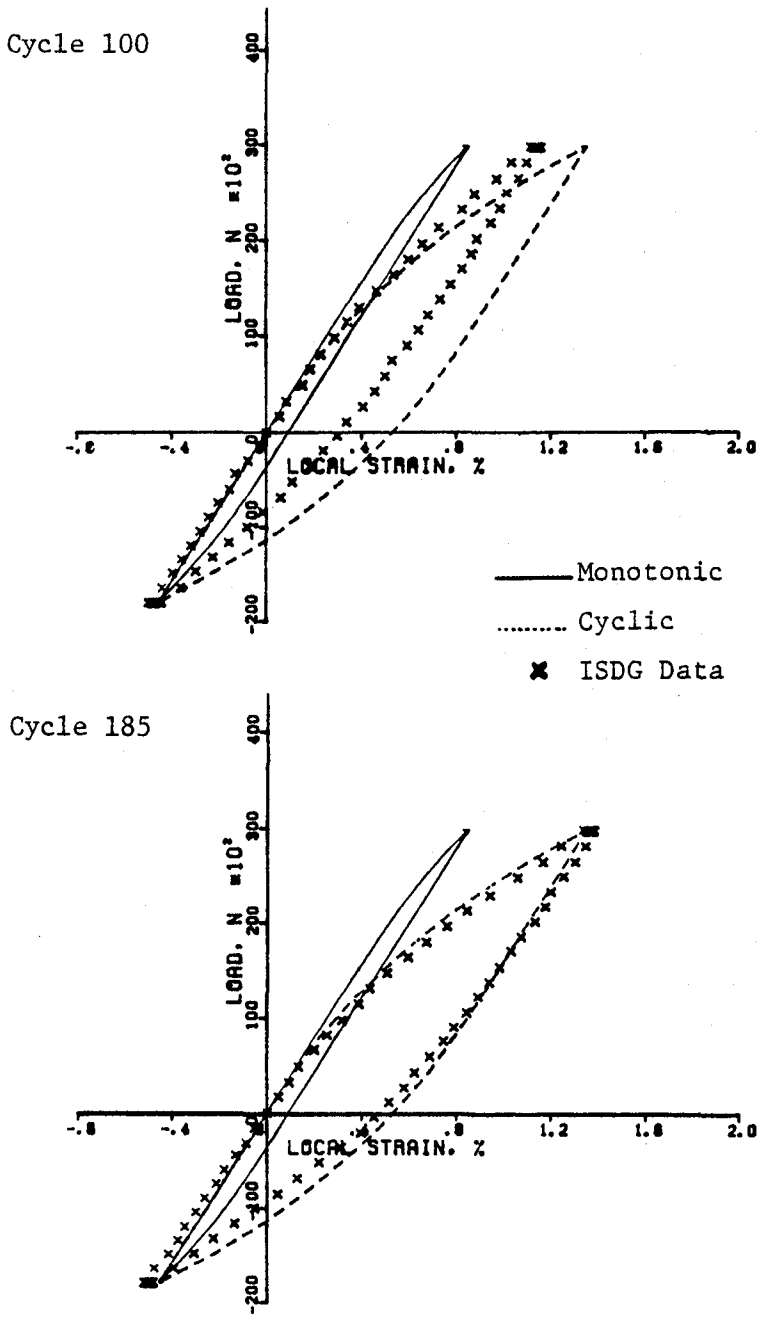

Figure 97. Comparison of Neuber Predictions and ISDG Measured Intermediate Cycle Notch Root Strain Behavior of Test 11b (Tension Hold).

Since stress cannot be measured, an indirect method was used to obtain an experimental value for notch root stress. By applying a known strain history to a strain-controlled, smooth fatigue test bar, and by monitoring the load required to produce the given strain, the stress associated with that strain can be determined. The notch root stress is obtained by using the notch root strain history. The notch root stress of Test No. 6 was evaluated through a strain control smooth bar test at 649° C using the notch root strain pattern recorded by the ISDG during the notch specimen test. (A programmable mini-computer-controlled test system was used.) Only the first 52 strain cycles were imposed on the test. Figure 98 shows the comparison of the test results with Neuber predictions. At maximum loads, the transitional changes of the measured stress from the monotonic to cyclic predictions were successfully predicted. However, at unloaded points the Neuber analysis, based on the monotonic stress-strain relationship, predicts higher compressive stress than that measured in initial cycles. In both cases, the Neuber notch root stress prediction using the cyclic stress-strain relationship is in excellent agreement with the stabilized stresses measured in the smooth bar test. For comparison purposes, the finite-element solution (based on stress-strain relationships in Equations 14 and 15) is also shown in the figure. It is important to note that stabilization of the cyclic softening would not have been complete in this test (refer to Figure 42). The finite-element solution would be approached as softening continued. These results may imply that the Massing (or kinematic hardening) hypothesis, addressed in Section 6.1, is suited for cyclically stable material behavior only.

7.2 FINITE-ELEMENT ANALYSIS VERSUS EXPERIMENTAL RESULTS

Strain analysis using the finite-element method was conducted for two continuous cycle load patterns (Tests No. 6 and 7) to ascertain the degree of correlation between the Neuber predictions, finite-element predictions, and the experimental measurements (Figures 99 and 100). The stress-strain relationships used in the analysis were given in Equations 14 and 15 for the monotonic and the cyclic cases, respectively. Better correlation with respect to the experimentally measured results was obtained for the finite-element method as compared to the previous Neuber solution. Significantly, the measured

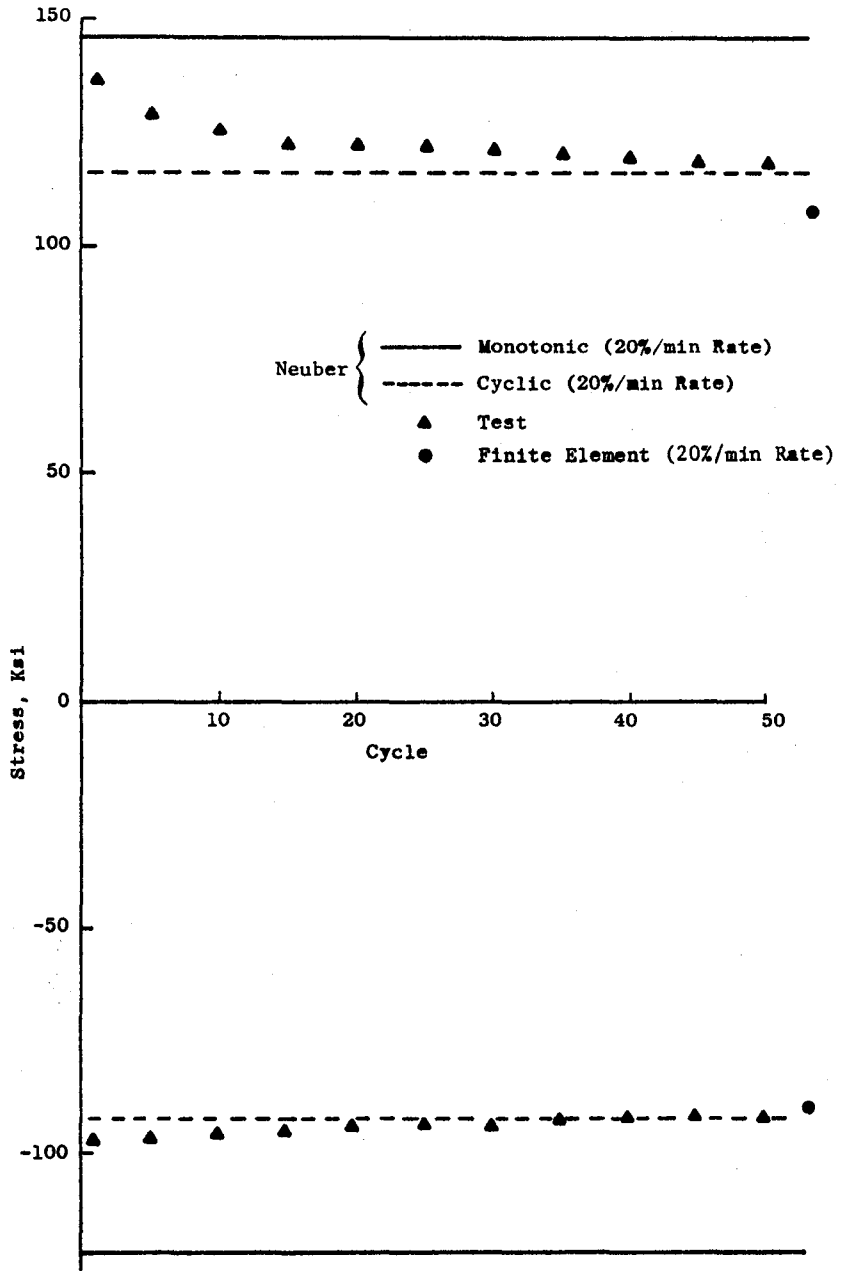

Figure 98. Comparison of Analytical Predictions of Notch Root Stress and the Result of a Strain-Controlled Smooth Bar Test Using the Strain Pattern Recorded in Test No. 6.

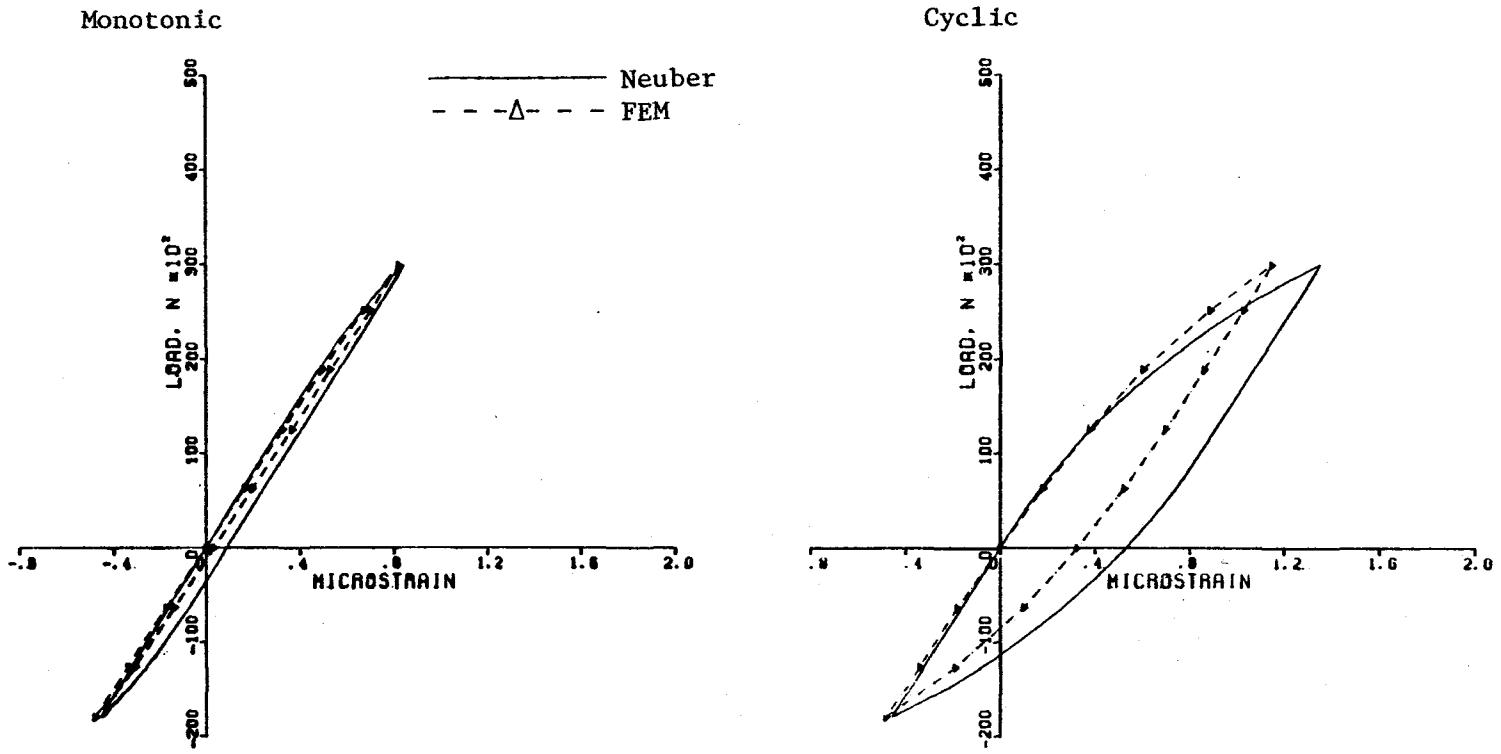

Figure 99. Comparison of Neuber and Finite-Element Predictions of Notch Root Strain Behavior for Test 7.

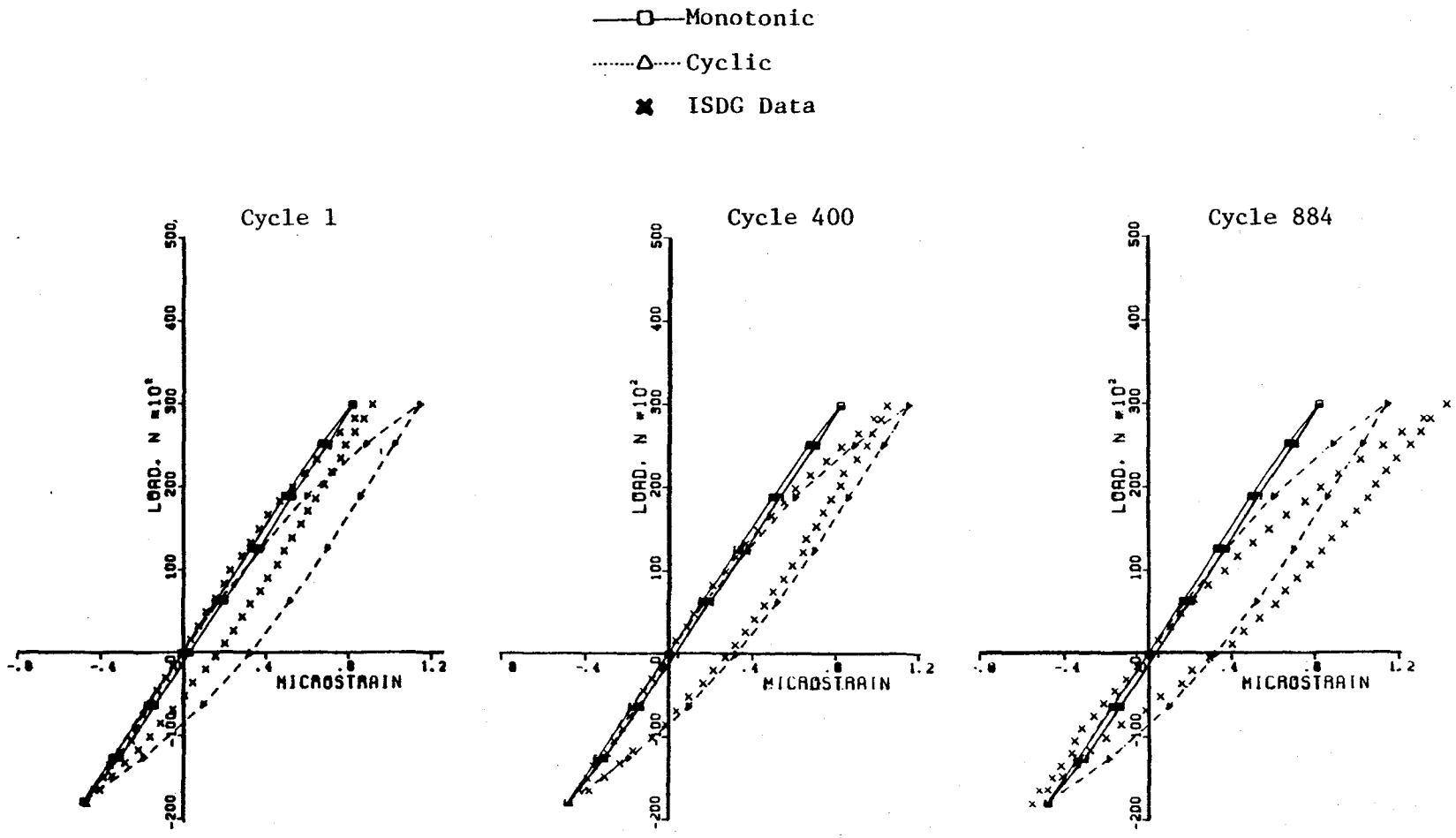

Figure 100. Comparison of Finite-Element Predicted and ISDG Measured Stress-Strain Behavior for Inconel 718 Notched Bar at 649° C for Load Pattern I, Test 7 (Continuous Cycle).

results never reached the cyclic stress-strain curve predictions despite the fact that stabilization had been essentially achieved.

7.3 ADDITIONAL OBSERVATIONS FROM DETAILED DATA ASSESSMENT

One of the important features realized in this program is the utilization of a computer-based data acquisition system which is capable of gathering and processing large amounts of experimental data and provides efficient and flexible ways for data retrieval and manipulation. Several data processing algorithms have been developed in this program to examine some important parameters through the entire test history. The elastic slopes, in terms of net section stress over local strain in the linear portion of loading and unloading cycles, were evaluated on a cycle-by-cycle basis by a least squares method. The slope, which corresponds to the modulus of the material and the stiffness of the specimen, could be scrutinized against the elapsed cycles to oversee the transient changes of material or structural parameters. As an example, Figure 101 represents the loading and unloading slopes versus cycles of a continuous cycle test (Test No. 7)*. It appears that the slope decreases slightly at the start of a cyclic test. This phenomenon was observed in several other load patterns. The slope decreases drastically toward the end of cyclic test indicating occurrence of crack formation or propagation in the specimen.

Another parameter of interest is the local plastic strain, ε_p, which can be expressed mathematically as a power function of local stress, σ, as:

$$\varepsilon_p = \left(\frac{\sigma}{A}\right)^{\frac{1}{\eta}}$$

*Loading slopes were determined with an origin at the minimum load-strain point. Unloading slopes were determined with an origin at the maximum load-strain point.

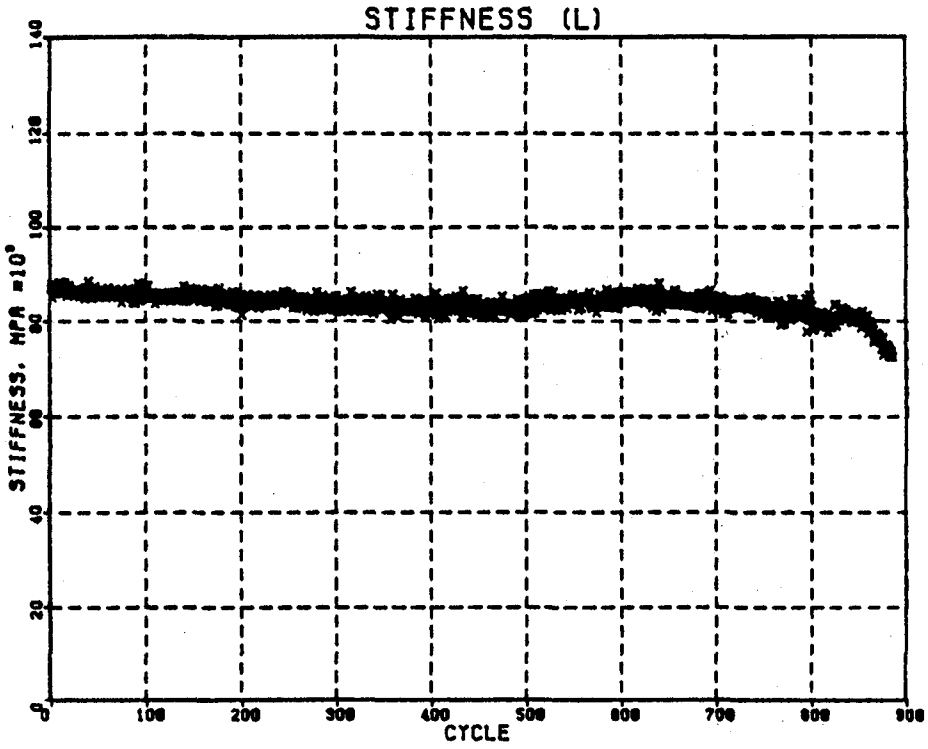

(a) Loading

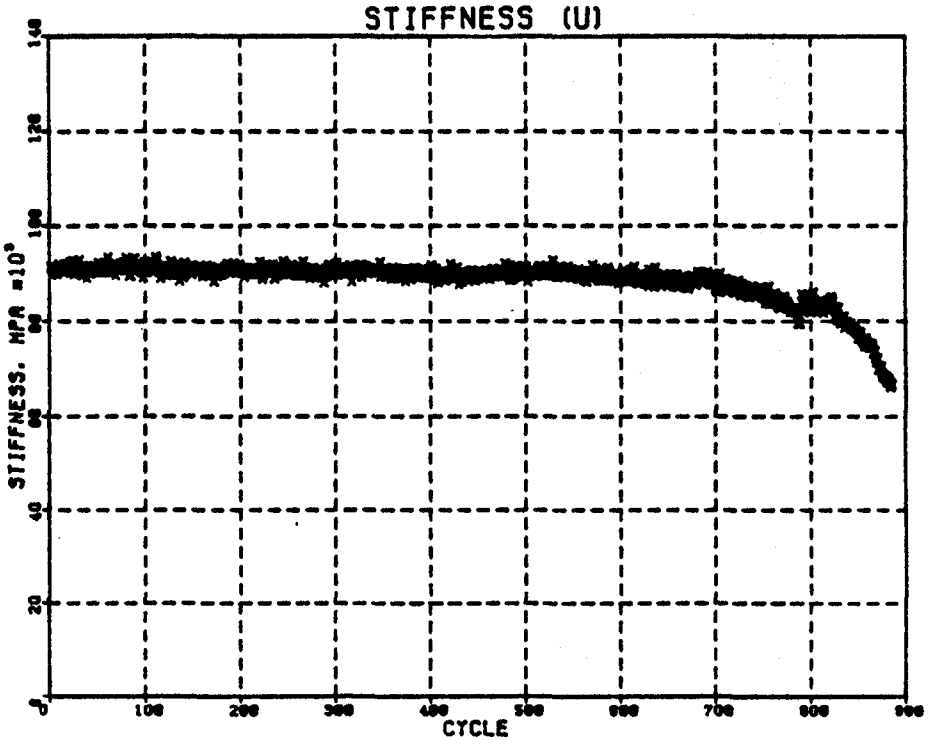

(b) Unloading

Figure 101. Variation of Elastic Slopes in the Cycle History of Test 7.

where n is defined as the strain-hardening exponent and A is the strength coefficient. Both n and A are regarded as material properties. If we define the relationship of plastic strain to the net section stress in a similar fashion as:

$$\epsilon_p = \left(\frac{S}{A'}\right)^{\frac{1}{n'}}$$

where n' and A' are material- and geometric-dependent, we can investigate the cyclic changes of these material properties*. Figures 102 and 103 are examples for n' and A' from Test No. 8. Both cyclic-hardening exponent, n', and strength coefficient, A', are close to being constant with values 0.22 and 4000 MPa, respectively, through most of cyclic history. Both parameters increase in the final cycles indicating cyclic-softening material behavior, or, more probably, crack initiation.

The strain hysteresis loop area has been regarded as a measurement of inelastic behavior and energy dissipation. The latter has been used for prediction of fatigue initiation life. The loop area (from net section stress versus local strain plots) of the tension hold test (Test No. 10) is shown in Figure 104. It clearly shows that the cyclic stress-strain behavior stabilizes around 200 cycles. Note the exceptionally well-behaved trends of this parameter.

The width of the strain hysteresis loop defines the size of the loop; therefore, it is also an indication of inelastic behavior. Figure 105 (Test No.10) presents a typical trend of this variable with respect to the elapsed cycles.

The initial strain locates the hysteresis loop in stress-strain space. Figure 106, the initial strain plot for the tension hold test (Test No. 10), illustrates the interesting phenomenon of ratchetting.

The last item examined is the creep strain in the hold-time test. As was concluded in Section 7.1, the creep strain during the 2-minute periods could

*The curve fit employed the nonlinear data points, defined for convenience as the last 12 points in the loading cycle.

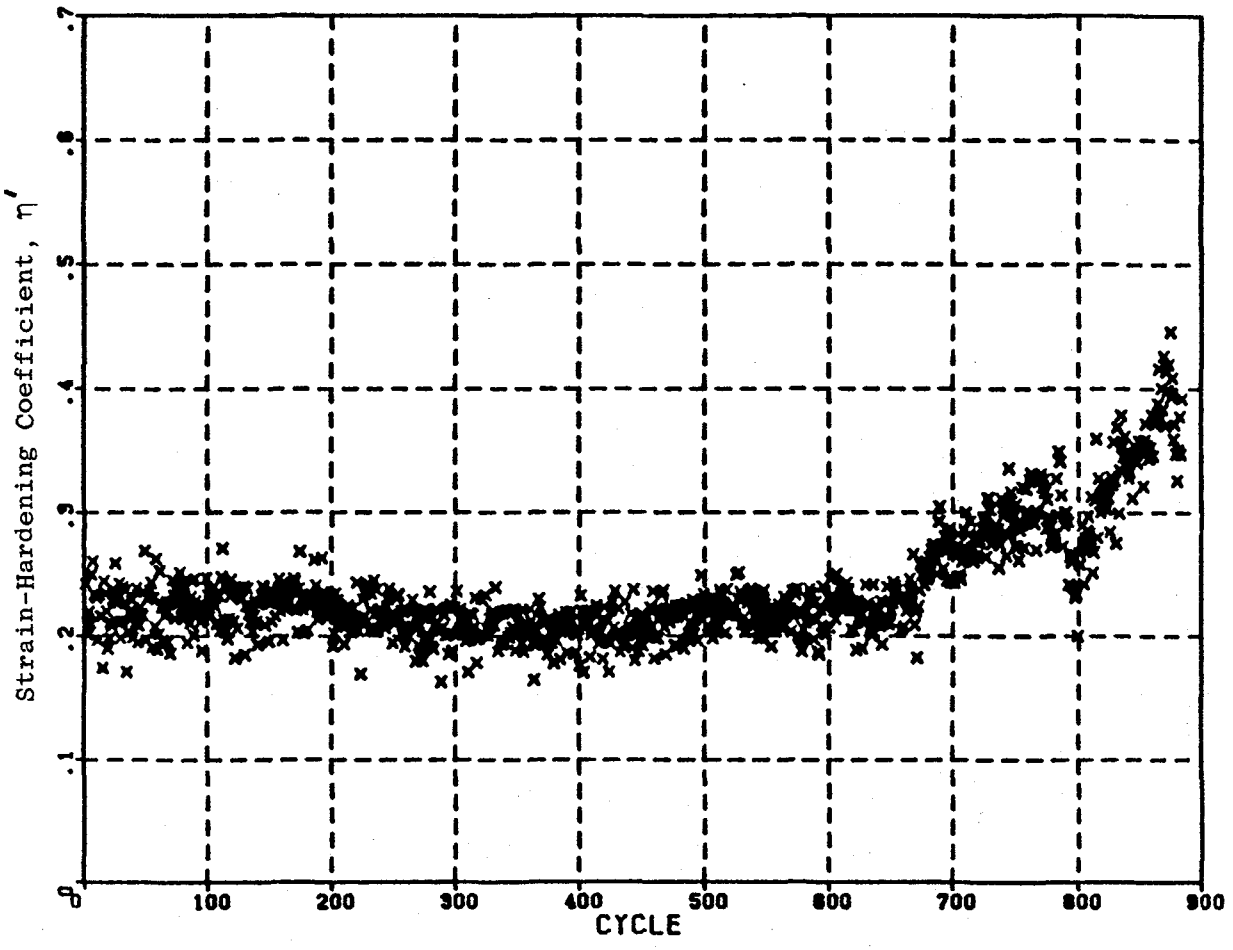

Figure 102. Variation of Strain-Hardening Coefficient in the Cycle History of Test 7.

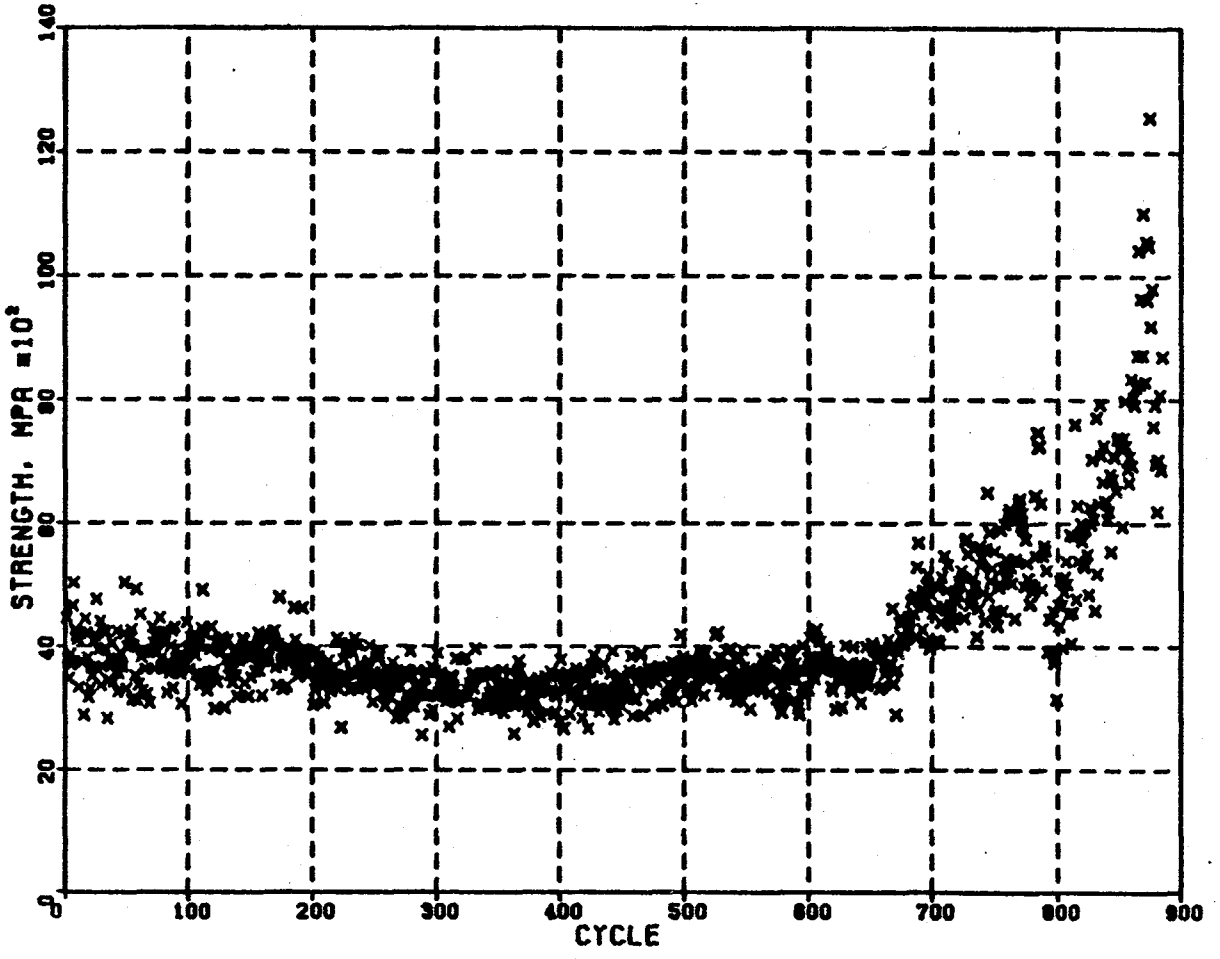

Figure 103. Variation of Strength Coefficient in the Cycle History of Test 7.

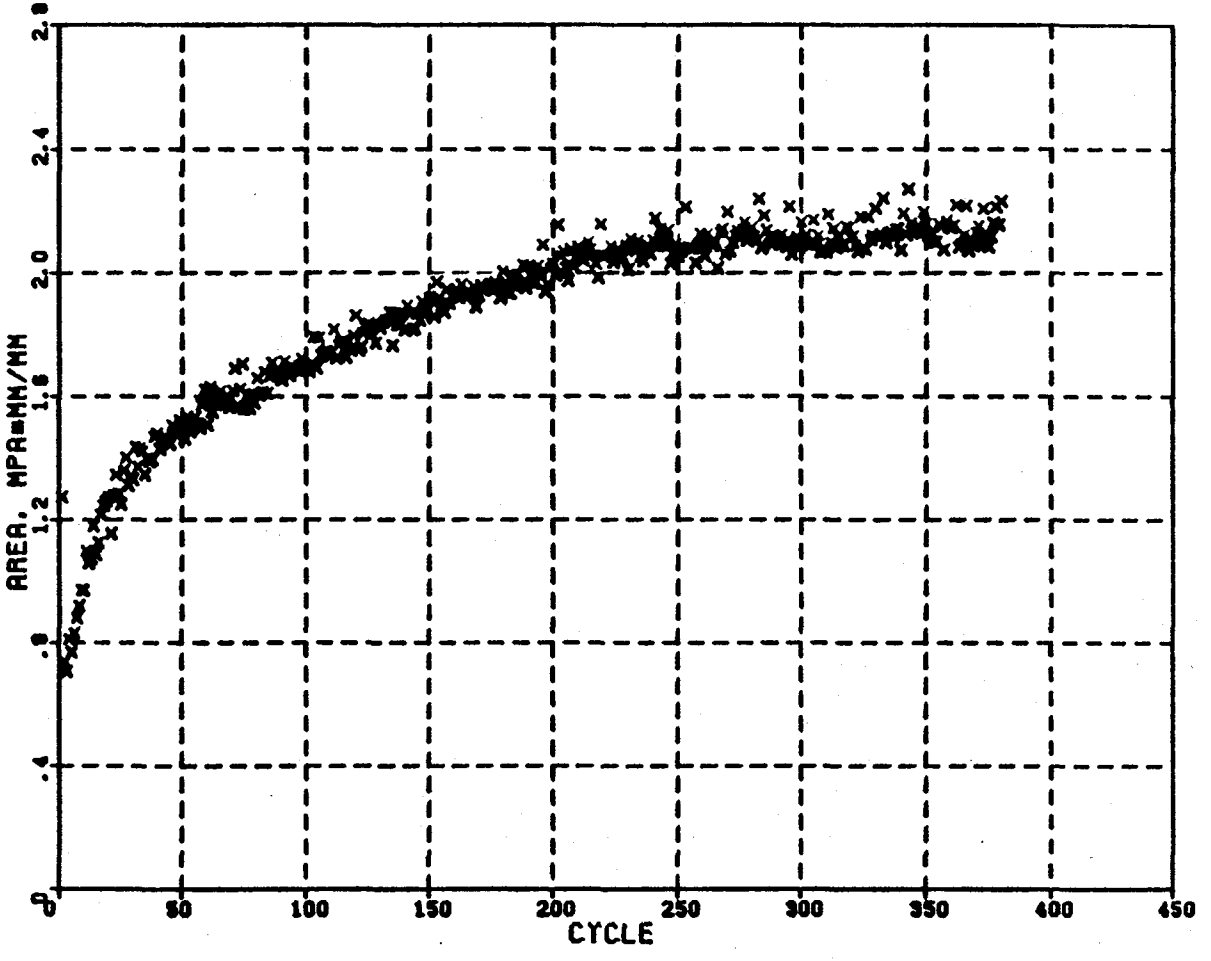

Figure 104. Variation of Hysteresis Loop Area in the Cycle History of Test 10.

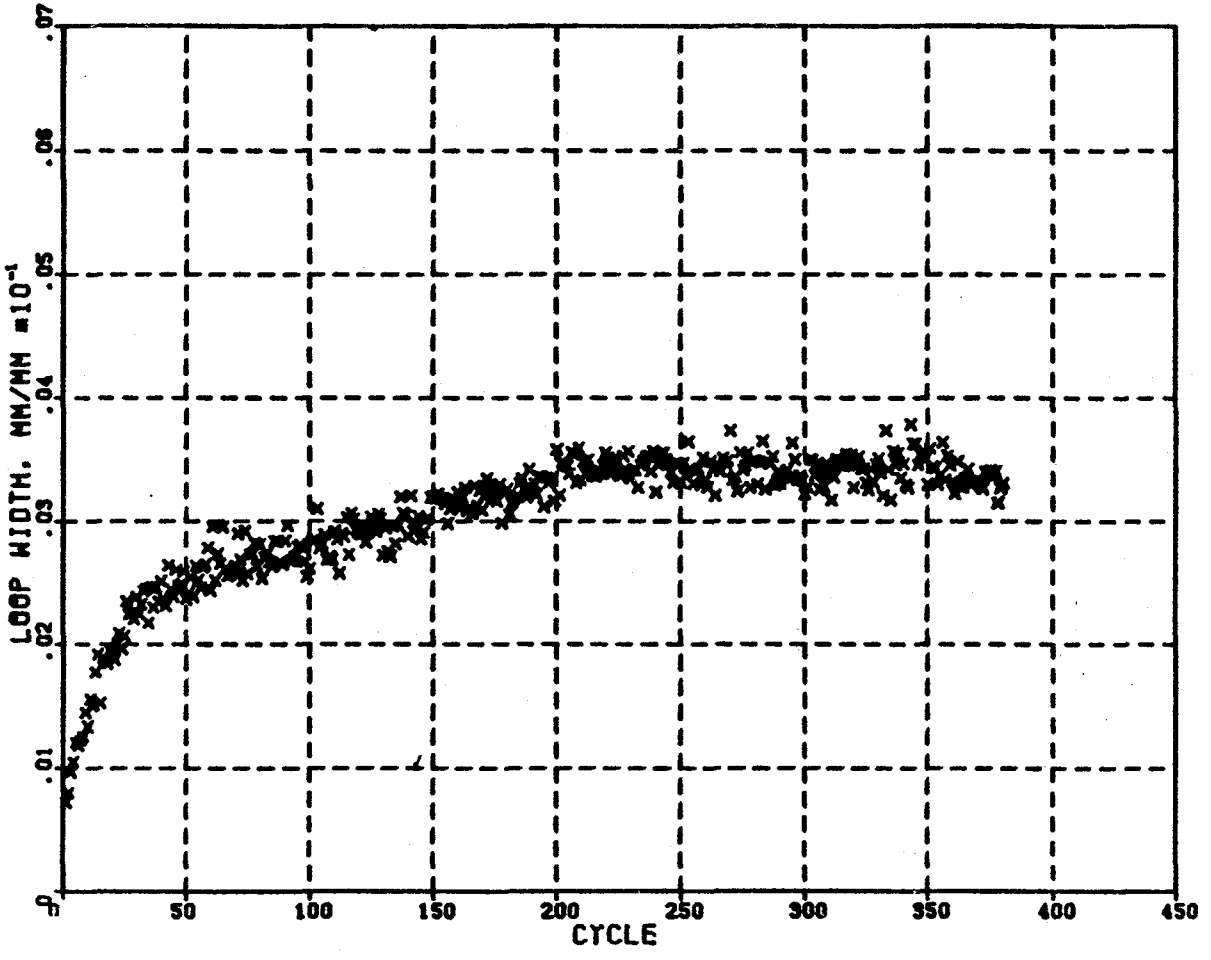

Figure 105. Varation of Hysteresis Loop Width in the Cycle History of Test 10.

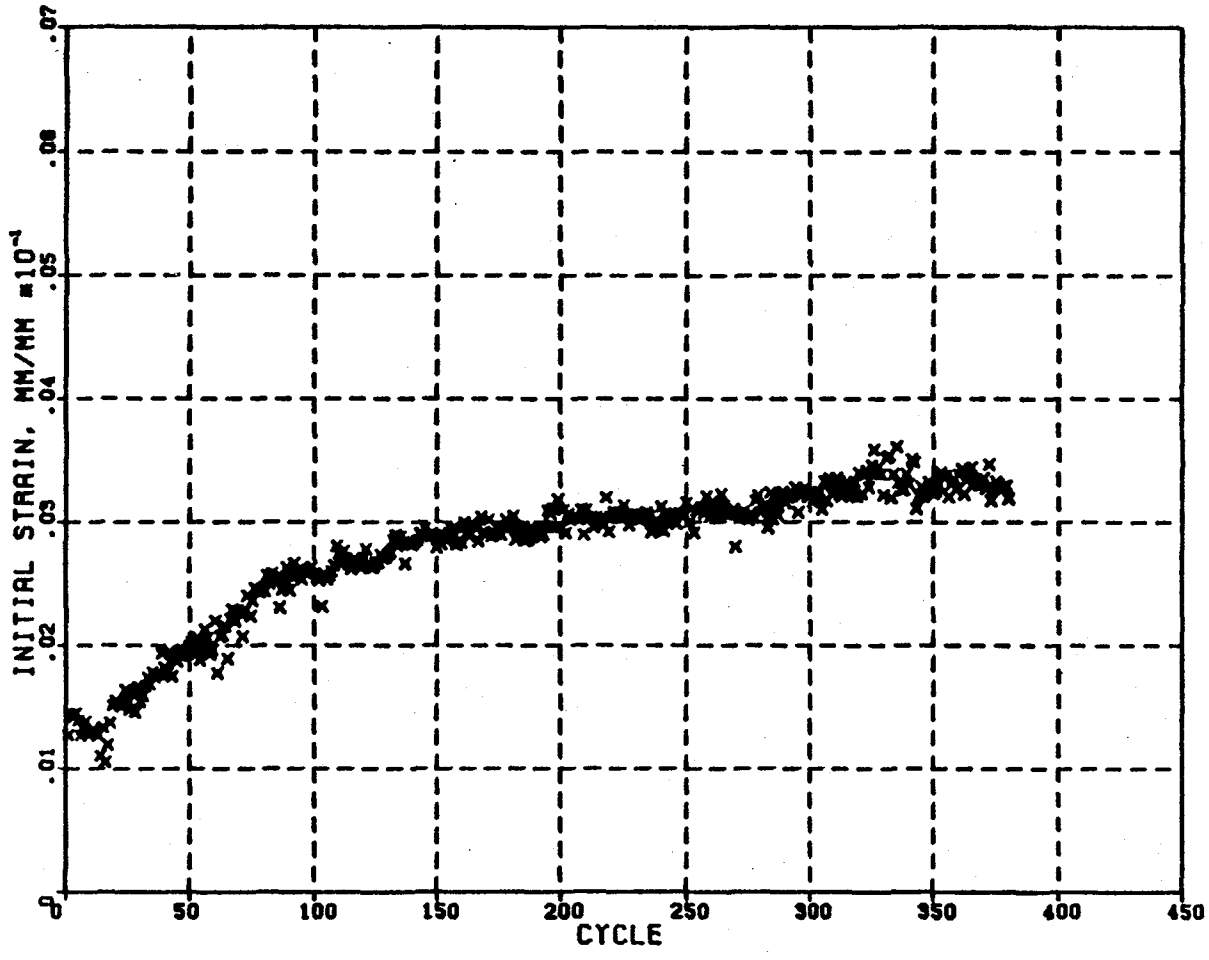

Figure 106. Varation of Initial Strain in the Cycle History of Test 10.

not be accurately measured for each individual cycle due to the large scatter of the experimental data for the small strains. However, if the difference between the first and last measurements during the hold-time period is accumulated cycle-by-cycle, the result (shown in Figure 107 for the tensile hold test) appears to show the general trend of total creep strain throughout the entire test.

These varied parameters have not been extensively investigated but are illustrative of the wealth of information contained in the measured results. Evaluation of these parameters should be continued to assess their applicability to life prediction.

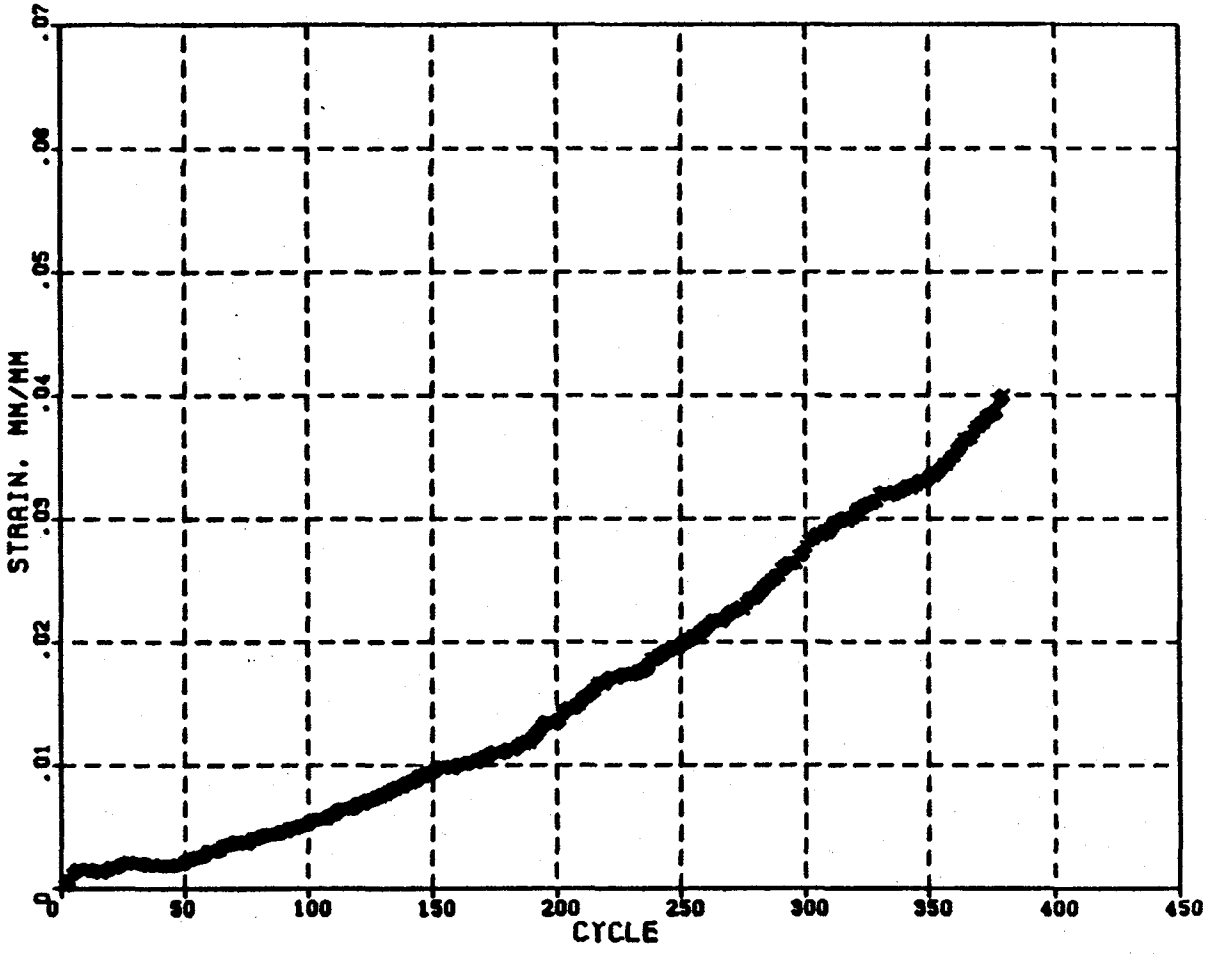

Figure 107. Cumclative Creep Strain in the Cycle History of Test 10.

8.0 DISCUSSION OF RESULTS

The Benchmark Notch Program was successfully completed with the generation of substantial quantities of strain measurement data for a notched geometry, Ni-base superalloy specimen at elevated temperature. A standard Neuber analysis can be used for the notch root stress-strain determination with reasonable engineering accuracy for initial cycles. However, if the specimen has a high degree of plasticity, some adjustment for stress redistribution may be required to improve the solution.

For later cycles, the local notch root stress and strain did not approach that predicted using the cyclic stress-strain curve. This is probably due to the distribution of plasticity near the notch. The notch surface would tend to approach the stable cyclic curve; however, the surrounding material is not as highly strained and converges to a different stable condition and so on as one moves away from the notch. This constraint behavior must be more closely modelled in order to achieve correlation with the measured results.

The 2-minute hold period adopted in the hold-time tests was found to be insufficient for detailed creep strain measurement. Longer hold time should be used to enhance the measurement of creep strain and verify the effect of cyclic load on the creep behavior. However, a modified Neuber prediction that includes creep strain and stress relaxation in the analysis was shown to be in good agreement with the general trends of the measured results from the multi-step creep test. Initial strain decreases following load-step changes remain unexplained.

The finite-element method resulted in a better notch root solution due to the improved treatment of stress redistribution, but the finite-element solution using the cyclic stress-strain curve also failed to correlate the higher cycle results. For a better simulation, the material properties of the finite-element model should be properly chosen for selected areas.

The computer-based data acquisition system facilitated the process of experimental data collection and documentation. This strongly suggests computerized testing procedures should be adopted in more laboratories. The

additional observations of certain parameters highlight the insight to be gained by scanning the entire test history. These same parameters may also provide information for fatigue life prediction, although further exploration in this area is needed.

9.0 CONCLUSIONS

The following summary conclusions are drawn from this study.

Benchmark notch root strain measurements were made and documented for six load patterns representative of typical aircraft engine cycles on a nickel-base superalloy at elevated temperature.

The laser interferometric strain displacement gage (ISDG) measuring system was demonstrated to be adaptable to continuous notch strain measurement at 649° C (1200° F) on Inconel 718.

The ISDG performed within the relative uncertainty of ± 3% with an additional uncertainty of ± 150 microstrain for continuous and hold-time tests.

The computer-based data acquisition system is a versatile tool for laboratory experimental programs. It facilitates the process of data gathering, retrieval, and manipulation.

The double-notched, plane stress, K_t = 1.9, buttonhead test specimen is well suited to this type of experimental strain measurement system. No major experimental problems were encountered in its use.

Neuber-based analysis can be used to determine notch root stress and strain within engineering accuracy for monotonic loading. Modifications of the Neuber analysis to account for creep behavior successfully predicted measured local creep strain trends.

In the Neuber analysis, the importance of using strain rate dependent material properties was demonstrated.

The Neuber predictions of stable local notch root stress-strain hysteresis loops, based on appropriate strain rate cyclic stress-strain curves, did not, in general, agree with test results. In some tests, complete stabilization may not have been achieved; however, this lack of correlation was also observed in tests where essentially complete softening had occurred.

A limited elastic-plastic finite-element analysis improved the calculations, but did not totally alleviate the observed differences.

The monotonic and cyclic maximum stresses and the cyclic minimum stresses were, however, well predicted by the Neuber approach while early cyclic minimum stresses were not. This suggests that the kinematic-hardening assumptions may be inappropriate for the early transitional behavior.

The 2-minute period used in the hold-time test was found to be inadequate for measurement of creep strain and verification of the basic behavior of the fatigue-creep interaction. Persistent creep did occur, however, and could be assessed by calculating cumulative creep strain from the ISDG measurements.

Scrutinizing various testing and material parameters, such as hysteresis loop width, loop area, etc., has provided understanding of the transitional changes in material behavior and response throughout the entire testing history.

The loading modulus parameter provides a convenient means of determining notch root crack formation while the hysteresis loop area parameter clearly defines stabilization.

REFERENCES

1. Merrill, P.S., "Photodot Investigation of Plastic-Strain Pattern in Flat Sheet with a Hole," Experimental Mechanics, August 1961, pp. 73-80.

2. Dixon, J.R., "Elastic-Plastic Strain Distribution in Flat Bars Containing Holes or Notches," Journal of Mechanics, Physics and Solids, Vol. 10, 1962, pp. 253-263.

3. Durelli, A.J., and Sciammarella, C.A., "Elastoplastic Stress and Strain Distribution in a Finite Plate with a Circular Hole Subjected to Unidimensional Load," Journal of Applied Mechanics, March 1963, pp. 115-121.

4. Griffith, G.E., "Experimental Investigation of the Effects of Plastic Flow in a Tension Panel with a Circular Hole," NACA Technical Note 1705, National Advisory Committee for Aeronautics, 1949.

5. Carroll, J.R., et al., "Investigation of Stress-Strain History Modeling at Stress Risers, Phase I," AFFDL-TR-76-150, June 1977.

6. Carroll, J.R., et al., "Investigation of Stress-Strain History Modeling at Stress Risers, Phase II," AFFDL-TR-78-167, December 1978.

7. Carroll, J.R., "Time Dependent Changes in Notch Stress-Notch Strain and Their Effects on Crack Initiation," ASTM STP 714, 1980, pp. 24-40.

8. Crews, J.H., Jr., and Hardrath, H.F., "A Study of Cyclic Plastic Stresses at a Notch Root," Experimental Mechanics, Vol. 6, No. 6, June 1966, pp. 99-110.

9. Leis, B.H., Gowda, C.V.B., and Topper, T.H., "Some Studies of the Influence of Localized and Gross Plasticity on the Monotonic and Cyclic Concentration Factors," Journal of Testing and Evaluation, Vol. 1, No. 4, July 1973, pp. 341-343.

10. Bofferding, C.H., III, "A Study of Cyclic Stress and Strain Concentration Factors at Notch Roots Throughout Fatigue Life," M.S. Thesis, Michigan State University, 1980.

11. Guillot, M., "An Experimental Evaluation of Neuber's Cyclic Relation at Room and Elevated Temperature," Ph.D. Dissertation, Louisiana State University, 1981.

12. Neuber, H., Theory of Notch Stresses, J.W. Edwards, Ann Arbor, Michigan, 1960.

13. Savin, G.N., Stress Concentration Around Holes, Pergamon, 1961.

14. Savin, G.N., "Stress Distribution Around Holes," NASA TT-F-607, Naukova Dumka Press, Kiev, 1968.

15. Peterson, R.E., Stress Concentration Factors, Wiley, 1974.

16. Neuber, H., "Theory of Stress Concentration for Shear-Strained Prismatical Bodies with Arbitrary Nonlinear Stress-Strain Law," Appl. Mech., Vol. 28, 1961, pp. 554-560.

17. Potter, J.M., "A Simple Graphical Procedure for Determining Cyclic Elastic-Plastic Notch Stresses," AIAA Journal, Vol. 10, No. 10, October 1972.

18. Weiss, V., "Notch Analysis of Fracture," Fracture Vol. III, Academic Press, 1971.

19. Topper, T.H., et. al, "Neuber's Rule Applied to Fatigue of Notched Specimens," Jour. of Mat'ls, JMLSA Vol. 4, No. 1, March 1969.

20. Leis, B.N., Gowda, C.V.B., and Topper, T.H., "Cyclic Inelastic Deformation and the Fatigue Notch Factor," ASTM STP 519, ASTM, 1973, pp. 133-150.

21. Hardrath, H.F. and Ohman, L., "A Study of Elastic and Plastic Stress Concentration Factors Due to Notches and Fillets in Flat Plates," NASA TR-1117, 1953.

22. Crews, J.H., Jr., "Elastoplastic Stress-Strain Behavior at Notch Roots in Sheet Specimens Under Constant-Amplitude Loading," NASA TN D-5253, June 1969.

23. Taira, S. and Ohtani, R., "Creep Crack Propagation and Creep Rupture of Notched Specimens," Instn. Mech. Engrgs., Conf. Publication 13, 1973.

24. Mowbray, D.F. and Slot, T., "Note on Stress and Strain Redistribution in a Notched Plate Specimen During Cyclic Loading," Jour. of Basic Eng., ASME Paper No. 69-Met-C, December 22, 1969.

25. Socie, D.F., "Estimating Fatigue Crack Initiation and Propagation Lives in Notched Plate Under Variable Loading Histories," Univ. of Illinois at Urbana-Champaign, Ph.D. Dissertation, 1977.

26. McKnight, R.L., "Finite-Element Cyclic Thermoplasticity Analysis by the Method of Subvolumes," Ph.D. Dissertation, University of Cincinnati, 1975.

27. Landgraf, R.W., Morrow, J., and Ende, T., "Determination of the Cyclic Stress-Strain Curve," Journal of Materials, March 1-4, 1962, pp. 176-188.

28. Cook, T.S., "Cyclic Stress-Strain Behavior of Inconel 718," presented at ASTM Meeting at Bal Harbor, November 1980, to appear in an ASTM STP.

29. Stowell, E.Z., "Stress and Strain Concentration at a Circular Hole in an Infinite Plate," NACA TN 2073, 1950.

30. Wetzel, R.M., "Smooth Specimen Simulation of the Fatigue Simulation of Notches," Journal of Materials, Vol. 3, September 1968, pp. 646-657.

31. Martin, J.F., Topper, T.H., and Sinclair, G.M., "Computer-Based Simulation of Cyclic Stress-Strain Behavior with Application to Fatigue," Materials Research and Standards, Volume 11, No. 2, February 1971, pp. 23-28, 50.

32. Eisenberg, M.A., "A Generalization of Plastic Flow Theory with Application to Cyclic Hardening and Softening Phenomena," Journal of Engineering Materials and Technology, Paper No. 75-WA/Mat-3, 1975.

33. McKnight, R.L. and Sobel, L.H., "Finite-Element Cyclic Thermoplasticity Analysis by the Method of Subvolumes," Computers and Structures, Vol. 7, No. 2, April 1977, pp. 189-196.

34. Besseling, J.R., "A Theory of Elastic, Plastic, and Creep Deformations of an Initially Isotropic Material Showing Anisotropic Strain Hardening, Creep Recovery, and Secondary Creep," J. of Appl. Mechs., December 1958. pp. 529-536.

APPENDIX

DATA SUMMARIES

In this appendix, samples of the notch root strain data obtained are given*. For each cyclic test, data points consisting of applied load-measured notch root strain pairs are given for the first five cycles and for one stabilized cycle. For the creep tests, typical points at selected time increments are listed. Complete data summaries are available from NASA. (See Section 5.3 for details.)

---

*NOTE: Sequential entries are listed across the page.

CONTINUOUS CYCLE, TEST 6 - CYCLE 1 -

LOAD (N)	LOAD (LB)	STRAIN (με)	LOAD (N)	LOAD (LB)	STRAIN (με)	LOAD (N)	LOAD (LB)	STRAIN (με)	LOAD (N)	LOAD (LB)	STRAIN (με)	LOAD (N)	LOAD (LB)	STRAIN (με)
1289	290	290	2713	610	533	4136	930	823	5560	1250	1211	6983	1570	1454
8362	1880	1987	9786	2200	2326	11120	2500	2668	12588	2830	2811	13967	3140	3392
15346	3450	3732	16769	3770	4022	18148	4080	4410	19572	4400	4846	20951	4710	5186
22374	5030	5574	23708	5330	6204	25176	5660	6640	23708	5330	6252	22374	5030	5913
21039	4730	5525	19705	4430	5234	18371	4130	4943	16992	3820	4653	15657	3520	4216
14367	3230	4022	12988	2920	3635	11654	2620	3344	10319	2320	3053	8940	2010	2714
7606	1710	2375	6271	1410	2035	4937	1110	1599	3603	810	1454	2224	500	1017
889	200	678	-400	-90	339	-1690	-380	193	-3024	-680	-145	-4359	-980	-484
-5693	-1280	-1017	-7117	-1600	-1211	-8451	-1900	-1454	-9786	-2200	-1841	-11120	-2500	-2278
-12543	-2820	-2665	-13878	-3120	-2956	-15168	-3410	-3344	-13878	-3120	-2956	-12588	-2830	-2665
-11387	-2560	-2326	-10097	-2270	-2035	-8807	-1980	-1696	-7561	-1700	-1357	-6316	-1420	-1114
-5070	-1140	-727	-3736	-840	-436	-2535	-570	-145	-1289	-290	145	-44	-10	436

CONTINUOUS CYCLE, TEST 6 - CYCLE 2 -

LOAD (N)	LOAD (LB)	STRAIN (με)	LOAD (N)	LOAD (LB)	STRAIN (με)	LOAD (N)	LOAD (LB)	STRAIN (με)	LOAD (N)	LOAD (LB)	STRAIN (με)	LOAD (N)	LOAD (LB)	STRAIN (με)
1334	300	678	2668	600	1114	4136	930	1357	5471	1230	1551	6983	1570	2132
8273	1860	2278	9741	2190	2762	11120	2500	3150	12588	2830	3538	13967	3140	3780
15346	3450	4119	16769	3770	4507	18148	4080	4750	19572	4400	5040	20951	4710	5525
22374	5030	5913	23753	5340	6204	25176	5660	6640	23664	5320	6397	22374	5030	5864
21039	4730	5477	19705	4430	5234	18371	4130	4943	16992	3820	4701	15657	3520	4410
14323	3220	4022	13033	2930	3732	11698	2630	3392	10319	2320	3102	8940	2010	2617
7606	1710	2423	6271	1410	1987	4893	1100	1744	3603	810	1502	2224	500	1017
889	200	727	-355	-80	484	-1734	-390	193	-3024	-680	-242	-4359	-980	-436
-5693	-1280	-920	-7161	-1610	-1260	-8451	-1900	-1502	-9786	-2200	-1793	-11120	-2500	-2132
-12499	-2810	-2617	-13833	-3110	-3005	-15212	-3420	-3392	-13878	-3120	-2956	-12543	-2820	-2665
-11342	-2550	-2278	-10097	-2270	-1987	-8762	-1970	-1599	-7561	-1700	-1454	-6316	-1420	-1163
-5026	-1130	-775	-3736	-840	-436	-2535	-570	-242	-1245	-280	96	0	0	484

CONTINUOUS CYCLE, TEST 6 - CYCLE 3 -

LOAD (N)	LOAD (LB)	STRAIN (με)	LOAD (N)	LOAD (LB)	STRAIN (με)	LOAD (N)	LOAD (LB)	STRAIN (με)	LOAD (N)	LOAD (LB)	STRAIN (με)	LOAD (N)	LOAD (LB)	STRAIN (με)
1378	310	678	2668	600	1066	4092	920	1454	5471	1230	1696	6894	1550	2035
8318	1870	2471	9741	2190	2811	11164	2510	3102	12588	2830	3489	13967	3140	3629
15346	3450	4168	16769	3770	4604	18193	4090	4846	19572	4400	5186	20951	4710	5574
22374	5030	5913	23753	5340	6252	25176	5660	6737	23708	5330	6349	22374	5030	5913
21084	4740	5719	19705	4430	5283	18415	4140	5089	16992	3820	4798	15702	3530	4410
14278	3210	4071	12988	2920	3829	11654	2620	3441	10364	2330	3053	8940	2010	2714
7606	1710	2423	6271	1410	2181	4937	1110	1744	3558	800	1454	2224	500	1163
889	200	823	-400	-90	533	-1734	-390	242	-3024	-680	-145	-4359	-980	-484
-5738	-1290	-872	-7206	-1620	-1260	-8451	-1900	-1405	-9786	-2200	-1793	-11120	-2500	-2132
-12499	-2810	-2665	-13833	-3110	-3005	-15168	-3410	-3295	-13833	-3110	-2908	-12588	-2830	-2714
-11342	-2550	-2326	-10097	-2270	-1987	-8762	-1970	-1647	-7517	-1690	-1308	-6316	-1420	-1114
-5070	-1140	-823	-3780	-850	-484	-2490	-560	-193	-1245	-280	193	0	0	436

CONTINUOUS CYCLE, TEST 6 - CYCLE 4 -

LOAD (N)	LOAD (LB)	STRAIN (με)	LOAD (N)	LOAD (LB)	STRAIN (με)	LOAD (N)	LOAD (LB)	STRAIN (με)	LOAD (N)	LOAD (LB)	STRAIN (με)	LOAD (N)	LOAD (LB)	STRAIN (με)
1378	310	775	2713	610	1017	4136	930	1357	5471	1230	1696	6939	1560	2181
8318	1870	2471	9786	2200	2859	11164	2510	3247	12588	2830	3538	13967	3140	3732
15346	3450	4216	16769	3770	4507	18148	4080	4846	19527	4390	5234	20906	4700	5670
22329	5020	5913	23753	5340	6349	25176	5660	6834	23708	5330	6301	22374	5030	6010
21039	4730	5670	19750	4440	5380	18415	4140	5089	16992	3820	4750	15702	3530	4362
14367	3230	4071	12988	2920	3732	11654	2620	3586	10275	2310	3247	8940	2010	2762
7606	1710	2423	6271	1410	2084	4937	1110	1793	3603	810	1502	2224	500	1260
889	200	727	-400	-90	581	-1690	-380	145	-3024	-680	-48	-4314	-970	-533
-5738	-1290	-823	-7117	-1600	-1163	-8451	-1900	-1454	-9786	-2200	-1841	-11076	-2490	-2181
-12499	-2810	-2617	-13833	-3110	-3005	-15168	-3410	-3247	-13922	-3130	-2956	-12588	-2830	-2665
-11298	-2540	-2326	-10097	-2270	-1987	-8762	-1970	-1647	-7561	-1700	-1454	-6316	-1420	-1163
-5026	-1130	-775	-3736	-840	-436	-2490	-560	-242	-1245	-280	96	-44	-10	387

CONTINUOUS CYCLE, TEST 6 - CYCLE 5 -

LOAD (N)	LOAD (LB)	STRAIN (με)	LOAD (N)	LOAD (LB)	STRAIN (με)	LOAD (N)	LOAD (LB)	STRAIN (με)	LOAD (N)	LOAD (LB)	STRAIN (με)	LOAD (N)	LOAD (LB)	STRAIN (με)
1334	300	727	2713	610	1017	4092	920	1405	5471	1230	1696	6894	1550	2084
8318	1870	2471	9786	2200	2811	11120	2500	3198	12543	2820	3538	13967	3140	3829
15346	3450	4265	16769	3770	4604	18104	4070	4943	19572	4400	5137	20951	4710	5574
22329	5020	5961	23753	5340	6446	25176	5660	6785	23753	5340	6446	22374	5030	6010
21039	4730	5719	19705	4430	5428	18371	4130	5186	17036	3830	4750	15657	3520	4410
14323	3220	4168	13033	2930	3829	11698	2630	3586	10319	2320	3053	8940	2010	2811
7606	1710	2520	6227	1400	2181	4937	1110	1890	3603	810	1502	2179	490	1211
889	200	872	-400	-90	533	-1734	-390	290	-2980	-670	-145	-4359	-980	-484
-5738	-1290	-823	-7161	-1610	-1211	-8451	-1900	-1454	-9786	-2200	-1890	-11120	-2500	-2229
-12499	-2810	-2665	-13833	-3110	-2956	-15212	-3420	-3392	-13878	-3120	-3005	-12588	-2830	-2665
-11342	-2550	-2326	-10097	-2270	-1987	-8807	-1980	-1647	-7561	-1700	-1405	-6271	-1410	-1066
-5070	-1140	-823	-3736	-840	-484	-2535	-570	-242	-1289	-290	193	-44	-10	436

CONTINUOUS CYCLE, TEST 6 - CYCLE 1000 -

LOAD (N)	LOAD (LB)	STRAIN (με)	LOAD (N)	LOAD (LB)	STRAIN (με)	LOAD (N)	LOAD (LB)	STRAIN (με)	LOAD (N)	LOAD (LB)	STRAIN (με)	LOAD (N)	LOAD (LB)	STRAIN (με)
1334	300	969	2713	610	1308	4136	930	1647	5515	1240	1987	6983	1570	2375
8362	1880	2811	9786	2200	3247	11164	2510	3586	12543	2820	3974	14011	3150	4410
15346	3450	4895	16814	3780	5331	18148	4080	5574	19572	4400	6058	20951	4710	6640
22374	5030	7173	23708	5330	7755	25176	5660	8288	23753	5340	7852	22418	5040	7512
21084	4740	7270	19705	4430	7028	18415	4140	6640	16992	3820	6252	15702	3530	5816
14323	3220	5525	13033	2930	5186	11698	2630	4798	10364	2330	4653	8985	2020	4071
7650	1720	3926	6316	1420	3489	4981	1120	3150	3603	810	2665	2268	510	2471
934	210	2035	-355	-80	1696	-1690	-380	1405	-3024	-680	1017	-4314	-970	533
-5782	-1300	48	-7117	-1600	-436	-8407	-1890	-872	-9786	-2200	-1454	-11076	-2490	-1744
-12499	-2810	-2229	-13833	-3110	-2714	-15168	-3410	-3441	-13833	-3110	-3053	-12543	-2820	-2617
-11298	-2540	-2326	-10052	-2260	-1987	-8807	-1980	-1696	-7561	-1700	-1405	-6271	-1410	-1211
-5026	-1130	-775	-3736	-840	-533	-2446	-550	0	-1201	-270	290	-44	-10	533

CONTINUOUS CYCLE, TEST 7 - CYCLE 1 -

LOAD (N)	LOAD (LB)	STRAIN (με)	LOAD (N)	LOAD (LB)	STRAIN (με)	LOAD (N)	LOAD (LB)	STRAIN (με)	LOAD (N)	LOAD (LB)	STRAIN (με)	LOAD (N)	LOAD (LB)	STRAIN (με)
1645	370	385	3247	730	771	4937	1110	1157	6583	1480	1591	8273	1860	1977
9919	2230	2266	11654	2620	2845	13255	2980	3279	14901	3350	3713	16636	3740	4147
18282	4110	4726	19927	4480	5353	21618	4860	5931	23264	5230	6510	24954	5610	7041
26555	5970	7619	28246	6350	8343	29936	6730	9211	28201	6340	8777	26600	5980	8343
25043	5630	7909	23442	5270	7668	21840	4910	7234	20239	4550	6848	18593	4180	6462
17081	3840	6076	15479	3480	5739	13833	3110	5305	12277	2760	4919	10631	2390	4581
9029	2030	4099	7472	1680	3761	5916	1330	3279	4314	970	2893	2668	600	2459
1112	250	2025	-444	-100	1591	-2001	-450	1109	-3603	-810	482	-5204	-1170	96
-6850	-1540	-482	-8451	-1900	-1061	-10052	-2260	-1591	-11654	-2620	-2170	-13255	-2980	-2797
-14812	-3330	-3424	-16458	-3700	-4002	-18015	-4050	-4629	-16458	-3700	-4243	-14945	-3360	-3809
-13478	-3030	-3520	-11921	-2680	-3038	-10497	-2360	-2507	-8985	-2020	-2266	-7428	-1670	-1929
-6005	-1350	-1543	-4492	-1010	-1205	-2980	-670	-819	-1467	-330	-482	-44	-10	-96

CONTINUOUS CYCLE, TEST 7 - CYCLE 2 -

LOAD (N)	LOAD (LB)	STRAIN (με)	LOAD (N)	LOAD (LB)	STRAIN (με)	LOAD (N)	LOAD (LB)	STRAIN (με)	LOAD (N)	LOAD (LB)	STRAIN (με)	LOAD (N)	LOAD (LB)	STRAIN (με)
1601	360	289	3247	730	626	4893	1100	1061	6583	1480	1591	8273	1860	1929
9919	2230	2411	11609	2610	3038	13255	2980	3375	14901	3350	3954	16636	3740	4436
18237	4100	5015	19927	4480	5546	21618	4860	6124	23264	5230	6703	24909	5600	7427
26555	5970	7861	28201	6340	8729	29891	6720	9259	28246	6350	8729	26600	5980	8343
25043	5630	8005	23442	5270	7668	21796	4900	7282	20239	4550	6848	18637	4190	6414
17081	3840	6124	15479	3480	5739	13833	3110	5353	12277	2760	4870	10631	2390	4581
9074	2040	4195	7472	1680	3761	5916	1330	3279	4270	960	2893	2668	600	2507
1067	240	1977	-444	-100	1687	-2046	-460	1157	-3603	-810	578	-5159	-1160	48
-6805	-1530	-434	-8451	-1900	-1061	-10008	-2250	-1639	-11654	-2620	-2218	-13255	-2980	-2797
-14812	-3330	-3327	-16458	-3700	-4051	-18059	-4060	-4533	-16458	-3700	-4147	-14945	-3360	-3665
-13478	-3030	-3375	-11965	-2690	-3038	-10453	-2350	-2604	-9029	-2030	-2218	-7472	-1680	-1784
-5960	-1340	-1495	-4492	-1010	-1109	-2980	-670	-675	-1467	-330	-434	0	0	-48

CONTINUOUS CYCLE, TEST 7 - CYCLE 3 -

LOAD (N)	LOAD (LB)	STRAIN (με)	LOAD (N)	LOAD (LB)	STRAIN (με)	LOAD (N)	LOAD (LB)	STRAIN (με)	LOAD (N)	LOAD (LB)	STRAIN (με)	LOAD (N)	LOAD (LB)	STRAIN (με)
1645	370	337	3247	730	626	4893	1100	1157	6583	1480	1543	8184	1840	2073
9963	2240	2459	11609	2610	2990	13255	2980	3424	14901	3350	3954	16591	3730	4533
18237	4100	5063	19927	4480	5642	21618	4860	6173	23219	5220	6848	24865	5590	7475
26555	5970	8005	28246	6350	8680	29891	6720	9356	28201	6340	8922	26644	5990	8488
25043	5630	8102	23442	5270	7716	21840	4910	7330	20194	4540	6944	18637	4190	6607
17081	3840	6173	15435	3470	5739	13878	3120	5353	12277	2760	5063	10631	2390	4629
9074	2040	4195	7472	1680	3809	5871	1320	3424	4270	960	2990	2668	600	2604
1067	240	2170	-400	-90	1736	-2046	-460	1205	-3603	-810	626	-5204	-1170	192
-6850	-1540	-337	-8496	-1910	-868	-10008	-2250	-1591	-11654	-2620	-2170	-13211	-2970	-2748
-14856	-3340	-3375	-16458	-3700	-3954	-18059	-4060	-4629	-16458	-3700	-4147	-14990	-3370	-3713
-13478	-3030	-3375	-11965	-2690	-3038	-10453	-2350	-2556	-8985	-2020	-2218	-7428	-1670	-1736
-5960	-1340	-1398	-4448	-1000	-1109	-2980	-670	-626	-1423	-320	-337	-44	-10	48

CONTINUOUS CYCLE, TEST 7 - CYCLE 4 -

LOAD (N)	LOAD (LB)	STRAIN (με)	LOAD (N)	LOAD (LB)	STRAIN (με)	LOAD (N)	LOAD (LB)	STRAIN (με)	LOAD (N)	LOAD (LB)	STRAIN (με)	LOAD (N)	LOAD (LB)	STRAIN (με)
1601	360	385	3247	730	675	4893	1100	1205	6583	1480	1639	8184	1840	2122
9919	2230	2507	11609	2610	3038	13255	2980	3472	14901	3350	3954	16591	3730	4533
18237	4100	5208	19927	4480	5642	21573	4850	6221	23264	5230	6848	24865	5590	7475
26555	5970	8102	28246	6350	8536	29891	6720	9259	28201	6340	8922	26600	5980	8439
25043	5630	8102	23442	5270	7812	21796	4900	7427	20239	4550	6896	18637	4190	6655
17081	3840	6269	15479	3480	5883	13878	3120	5353	12232	2750	5063	10675	2400	4678
9074	2040	4244	7472	1680	3906	5871	1320	3424	4270	960	2990	2668	600	2556
1023	230	2122	-444	-100	1639	-2046	-460	1157	-3647	-820	771	-5204	-1170	241
-6805	-1530	-434	-8451	-1900	-819	-10008	-2250	-1639	-11609	-2610	-2170	-13211	-2970	-2797
-14856	-3340	-3279	-16413	-3690	-4002	-18059	-4060	-4581	-16458	-3700	-4099	-14990	-3370	-3665
-13478	-3030	-3375	-11965	-2690	-2990	-10497	-2360	-2604	-8985	-2020	-2170	-7472	-1680	-1736
-6005	-1350	-1398	-4492	-1010	-1061	-3024	-680	-675	-1467	-330	-337	0	0	0

CONTINUOUS CYCLE, TEST 7 - CYCLE 5 -

LOAD (N)	LOAD (LB)	STRAIN (με)	LOAD (N)	LOAD (LB)	STRAIN (με)	LOAD (N)	LOAD (LB)	STRAIN (με)	LOAD (N)	LOAD (LB)	STRAIN (με)	LOAD (N)	LOAD (LB)	STRAIN (με)
1645	370	385	3247	730	819	4893	1100	1157	6583	1480	1639	8184	1840	2073
9875	2220	2556	11654	2620	2990	13255	2980	3520	14901	3350	4051	16636	3740	4629
18282	4110	5160	19927	4480	5739	21618	4860	6317	23264	5230	6944	24865	5590	7475
26555	5970	8053	28246	6350	8777	29847	6710	9307	28201	6340	8970	26600	5980	8536
25043	5630	8102	23486	5280	7716	21840	4910	7330	20239	4550	6944	18637	4190	6655
17081	3840	6317	15435	3470	5883	13878	3120	5401	12277	2760	5063	10675	2400	4629
9029	2030	4244	7472	1680	3906	5871	1320	3472	4270	960	3086	2668	600	2604
1067	240	2073	-444	-100	1687	-2046	-460	1253	-3647	-820	723	-5204	-1170	241
-6805	-1530	-289	-8451	-1900	-819	-10052	-2260	-1495	-11609	-2610	-2122	-13211	-2970	-2700
-14856	-3340	-3279	-16413	-3690	-3906	-18015	-4050	-4533	-16502	-3710	-4051	-14945	-3360	-3665
-13522	-3040	-3279	-11965	-2690	-2893	-10453	-2350	-2604	-8940	-2010	-2218	-7472	-1680	-1736
-6005	-1350	-1495	-4492	-1010	-1012	-2980	-670	-675	-1467	-330	-337	0	0	48

CONTINUOUS CYCLE, TEST 7 - CYCLE 450 -

LOAD (N)	LOAD (LB)	STRAIN (με)	LOAD (N)	LOAD (LB)	STRAIN (με)	LOAD (N)	LOAD (LB)	STRAIN (με)	LOAD (N)	LOAD (LB)	STRAIN (με)	LOAD (N)	LOAD (LB)	STRAIN (με)
1645	370	0	3247	730	530	4893	1100	868	6583	1480	1253	8273	1860	1784
9919	2230	2266	11609	2610	2700	13255	2980	3279	14901	3350	3809	16591	3730	4388
18237	4100	5063	19883	4470	5642	21573	4850	6366	23219	5220	7089	24865	5590	7812
26511	5960	8536	28157	6330	9259	29847	6710	10127	28201	6340	9693	26600	5980	9307
25043	5630	8873	23442	5270	8536	21840	4910	8150	20239	4550	7764	18637	4190	7330
17081	3840	6944	15479	3480	6558	13878	3120	6124	12277	2760	5787	10675	2400	5401
9029	2030	4919	7517	1690	4581	5871	1320	4051	4314	970	3665	2668	600	3231
1067	240	2748	-444	-100	2363	-2001	-450	1784	-3603	-810	1157	-5248	-1180	626
-6894	-1550	-96	-8451	-1900	-578	-10097	-2270	-1302	-11609	-2610	-2122	-13211	-2970	-2845
-14856	-3340	-3472	-16413	-3690	-4292	-18059	-4060	-5256	-16458	-3700	-4774	-14990	-3370	-4340
-13478	-3030	-4002	-11965	-2690	-3520	-10497	-2360	-3038	-8940	-2010	-2748	-7428	-1670	-2459
-5960	-1340	-1880	-4448	-1000	-1639	-3024	-680	-1205	-1467	-330	-868	0	0	-482

COMPRESSION HOLD CYCLE, TEST 8 - CYCLE 1 -

LOAD (N)	LOAD (LB)	STRAIN (με)	LOAD (N)	LOAD (LB)	STRAIN (με)	LOAD (N)	LOAD (LB)	STRAIN (με)	LOAD (N)	LOAD (LB)	STRAIN (με)	LOAD (N)	LOAD (LB)	STRAIN (με)
1734	390	596	3380	760	646	4981	1120	1292	6716	1510	1740	8407	1890	2089
9963	2240	2336	11743	2640	2784	13389	3010	3530	15034	3380	3728	16725	3760	4325
18371	4130	4673	20061	4510	5170	21707	4880	5567	23353	5250	6214	25043	5630	6662
26689	6000	7457	28335	6370	8352	30025	6750	8849	28290	6360	8651	26689	6000	8054
25176	5660	7706	23530	5290	7258	21929	4930	6761	20372	4580	6562	18726	4210	6065
17170	3860	5667	15568	3500	5270	13967	3140	4822	12365	2780	4574	10720	2410	4126
9118	2050	3878	7561	1700	3430	6005	1350	3032	4359	980	2734	2757	620	2436
1156	260	1939	-355	-80	1591	-1957	-440	1143	-3558	-800	795	-5115	-1150	298
-6716	-1510	-99	-8362	-1880	-546	-9919	-2230	-994	-11565	-2600	-1342	-13166	-2960	-1789
-14723	-3310	-2237	-16369	-3680	-2734	-17970	-4040	-3231	-17970	-4040	-3380	-17970	-4040	-3231
-17970	-4040	-3331	-17970	-4040	-3430	-17970	-4040	-3480	-17970	-4040	-3331	-18015	-4050	-3281
-17926	-4030	-3331	-17970	-4040	-3430	-17970	-4040	-3281	-17926	-4030	-3430	-17970	-4040	-3281
-17926	-4030	-3380	-17970	-4040	-3380	-17926	-4030	-3430	-17926	-4030	-3331	-18015	-4050	-3430
-17970	-4040	-3530	-17970	-4040	-3231	-17970	-4040	-3380	-17970	-4040	-3281	-17970	-4040	-3231
-17970	-4040	-3281	-17970	-4040	-3281	-17970	-4040	-3480	-17970	-4040	-3380	-17970	-4040	-3281
-17970	-4040	-3480	-17926	-4030	-3579	-16369	-3680	-3082	-14856	-3340	-2585	-13389	-3010	-2386
-11876	-2670	-1839	-10364	-2330	-1441	-8851	-1990	-1193	-7384	-1660	-894	-5871	-1320	-497
-4359	-980	-99	-2891	-650	248	-1378	-310	696	88	20	1044			

COMPRESSION HOLD CYCLE, TEST 8 - CYCLE 2 -

LOAD (N)	LOAD (LB)	STRAIN (με)	LOAD (N)	LOAD (LB)	STRAIN (με)	LOAD (N)	LOAD (LB)	STRAIN (με)	LOAD (N)	LOAD (LB)	STRAIN (με)	LOAD (N)	LOAD (LB)	STRAIN (με)
1734	390	1441	3380	760	1889	5026	1130	2336	6672	1500	2635	8318	1870	3182
10052	2260	3430	11698	2630	3878	13389	3010	4375	15034	3380	4574	16725	3760	5220
18371	4130	5518	20061	4510	5966	21707	4880	6463	23397	5260	6761	24954	5610	7209
26644	5990	7756	28335	6370	8452	29980	6740	8949	28335	6370	8601	26689	6000	8004
25132	5650	7706	23530	5290	7159	21974	4940	6910	20372	4580	6562	18726	4210	6115
17214	3870	5767	15568	3500	5419	13967	3140	5071	12365	2780	4723	10720	2410	4226
9163	2060	3778	7606	1710	3530	6005	1350	3082	4403	990	2734	2602	630	2336
1112	250	2088	-311	-70	1640	-1912	-430	1143	-3558	-800	745	-5115	-1150	298
-6716	-1510	-49	-8362	-1880	-596	-9919	-2230	-1044	-11565	-2600	-1441	-13122	-2950	-1789
-14723	-3310	-2237	-16324	-3670	-2784	-17926	-4030	-3380	-17926	-4030	-3380	-17970	-4040	-3430
-17926	-4030	-3331	-17970	-4040	-3331	-17970	-4040	-3281	-17970	-4040	-3430	-17970	-4040	-3281
-17970	-4040	-3281	-17926	-4030	-3231	-17970	-4040	-3331	-17970	-4040	-3480	-17970	-4040	-3331
-17926	-4030	-3281	-17970	-4040	-3281	-17970	-4040	-3331	-17970	-4040	-3281	-17970	-4040	-3430
-17970	-4040	-3231	-17970	-4040	-3430	-17970	-4040	-3231	-17970	-4040	-3430	-17970	-4040	-3380
-17970	-4040	-3430	-17970	-4040	-3530	-17970	-4040	-3480	-17926	-4030	-3530	-17970	-4040	-3530
-17970	-4040	-3430	-17926	-4030	-3480	-16369	-3680	-3132	-14856	-3340	-2635	-13389	-3010	-2287
-11832	-2660	-2137	-10408	-2340	-1591	-8851	-1990	-1193	-7339	-1650	-894	-5871	-1320	-596
-4359	-980	-99	-2891	-650	149	-1334	-300	546	88	20	994			

COMPRESSION HOLD CYCLE, TEST 8 - CYCLE 3 -

LOAD (N)	LOAD (LB)	STRAIN (με)	LOAD (N)	LOAD (LB)	STRAIN (με)	LOAD (N)	LOAD (LB)	STRAIN (με)	LOAD (N)	LOAD (LB)	STRAIN (με)	LOAD (N)	LOAD (LB)	STRAIN (με)
1734	390	1441	3380	760	1690	5026	1130	2237	6716	1510	2535	8362	1880	2983
9963	2240	3380	11654	2620	3828	13300	2990	4226	14945	3360	4574	16636	3740	5121
18237	4100	5469	19883	4470	5866	21573	4850	6463	23219	5220	6761	24865	5590	6960
26511	5960	7706	28112	6320	8203	29980	6740	8700	28335	6370	8352	26689	6000	8153
25176	5660	7507	23530	5290	7308	21974	4940	6811	20328	4570	6413	18726	4210	6115
17214	3870	5667	15524	3490	5419	13922	3130	4872	12365	2780	4623	10764	2420	4176
9163	2060	3828	7606	1710	3430	6005	1350	2983	4403	990	2635	2802	630	2137
1156	260	1839	-355	-80	1491	-1912	-430	944	-3514	-790	298	-5115	-1150	198
-6761	-1520	-248	-8318	-1870	-596	-9919	-2230	-1044	-11520	-2590	-1640	-13122	-2950	-1988
-14768	-3320	-2436	-16324	-3670	-2833	-17970	-4040	-3480	-17970	-4040	-3530	-17970	-4040	-3579
-17926	-4030	-3530	-17926	-4030	-3579	-17970	-4040	-3579	-17970	-4040	-3530	-17970	-4040	-3579
-17970	-4040	-3629	-17970	-4040	-3579	-17926	-4030	-3629	-17926	-4030	-3579	-17970	-4040	-3579
-17926	-4030	-3629	-17926	-4030	-3728	-18015	-4050	-3728	-17970	-4040	-3728	-17970	-4040	-3778
-17970	-4040	-3679	-17970	-4040	-3728	-17926	-4030	-3728	-17926	-4030	-3778	-17926	-4030	-3728
-17970	-4040	-3778	-17970	-4040	-3778	-17970	-4040	-3778	-17926	-4030	-3878	-17970	-4040	-3728
-17970	-4040	-3828	-17970	-4040	-3629	-16369	-3680	-3331	-14856	-3340	-2983	-13389	-3010	-2585
-11876	-2670	-2187	-10364	-2330	-1740	-8851	-1990	-1541	-7339	-1650	-1143	-5871	-1320	-696
-4359	-980	-298	-2935	-660	0	-1334	-300	198	88	20	845			

COMPRESSION HOLD CYCLE, TEST 8 - CYCLE 4 -

LOAD (N)	LOAD (LB)	STRAIN (με)	LOAD (N)	LOAD (LB)	STRAIN (με)	LOAD (N)	LOAD (LB)	STRAIN (με)	LOAD (N)	LOAD (LB)	STRAIN (με)	LOAD (N)	LOAD (LB)	STRAIN (με)
1734	390	1143	3380	760	1541	5026	1130	1939	6672	1500	2386	8318	1870	2635
10008	2250	2983	11654	2620	3579	13300	2990	4076	14945	3360	4325	16591	3730	4971
18237	4100	5419	19883	4470	5767	21573	4850	6314	23219	5220	6562	24865	5590	6910
26466	5950	7656	28157	6330	8203	29802	6700	8352	28157	6330	8203	26511	5960	7706
25221	5670	7408	23575	5300	6910	21929	4930	6513	20372	4580	6165	18726	4210	5817
17170	3860	5469	15568	3500	5121	13967	3140	4723	12321	2770	4325	10764	2420	4027
9163	2060	3579	7606	1710	3132	6005	1350	2784	4359	980	2386	2757	620	2038
1201	270	1541	-311	-70	1292	-1957	-440	845	-3514	-790	298	-5070	-1140	49
-6716	-1510	-546	-8362	-1880	-795	-9875	-2220	-1292	-11565	-2600	-1740	-13166	-2960	-2237
-14723	-3310	-2684	-16324	-3670	-3082	-17970	-4040	-3728	-17926	-4030	-3828	-17926	-4030	-3778
-17970	-4040	-3728	-17970	-4040	-3878	-17970	-4040	-3778	-17926	-4030	-3828	-18015	-4050	-3679
-17970	-4040	-3679	-17970	-4040	-3629	-17970	-4040	-3579	-17926	-4030	-3530	-17926	-4030	-3530
-17970	-4040	-3530	-17970	-4040	-3579	-17970	-4040	-3480	-17926	-4030	-3480	-17926	-4030	-3579
-18015	-4050	-3530	-17926	-4030	-3579	-17926	-4030	-3480	-17970	-4040	-3530	-17926	-4030	-3430
-17926	-4030	-3480	-17926	-4030	-3579	-17926	-4030	-3480	-17970	-4040	-3530	-17926	-4030	-3430
-17970	-4040	-3679	-17970	-4040	-3480	-16369	-3680	-2983	-14856	-3340	-2784	-13389	-3010	-2336
-11876	-2670	-1889	-10408	-2340	-1591	-8851	-1990	-1292	-7384	-1660	-795	-5871	-1320	-497
-4359	-980	-49	-2891	-650	248	-1378	-310	397	88	20	994			

COMPRESSION HOLD CYCLE, TEST 8 - CYCLE 5 -

LOAD (N)	LOAD (LB)	STRAIN (με)	LOAD (N)	LOAD (LB)	STRAIN (με)	LOAD (N)	LOAD (LB)	STRAIN (με)	LOAD (N)	LOAD (LB)	STRAIN (με)	LOAD (N)	LOAD (LB)	STRAIN (με)
1734	390	1392	3380	760	1740	5026	1130	2287	6716	1510	2585	8362	1880	2933
9919	2230	3331	11698	2630	3679	13255	2980	4027	14901	3350	4574	16636	3740	5071
18282	4110	5518	19838	4460	5767	21573	4850	6413	23219	5220	6761	24865	5590	7258
26466	5950	7756	28157	6330	8153	29758	6690	8501	28112	6320	8452	26511	5960	7955
24998	5620	7606	23442	5270	6910	21796	4900	6712	20239	4550	6463	18637	4190	6065
17214	3870	5667	15568	3500	5270	13967	3140	4822	12365	2780	4574	10764	2420	4275
9163	2060	3778	7606	1710	3231	6005	1350	2933	4403	990	2734	2802	630	2237
1201	270	1690	-311	-70	1491	-1868	-420	994	-3469	-780	447	-5070	-1140	248
-6716	-1510	-248	-8407	-1890	-646	-9919	-2230	-1143	-11520	-2590	-1541	-13122	-2950	-2038
-14723	-3310	-2386	-16369	-3680	-2933	-17926	-4030	-3480	-17926	-4030	-3530	-17926	-4030	-3579
-17926	-4030	-3579	-17926	-4030	-3579	-17970	-4040	-3530	-17970	-4040	-3579	-17970	-4040	-3629
-17926	-4030	-3530	-17970	-4040	-3530	-17926	-4030	-3579	-17970	-4040	-3530	-17970	-4040	-3530
-17970	-4040	-3530	-17970	-4040	-3629	-17926	-4030	-3579	-17926	-4030	-3579	-17926	-4030	-3480
-17926	-4030	-3629	-17926	-4030	-3629	-17926	-4030	-3530	-18015	-4050	-3579	-17926	-4030	-3629
-17926	-4030	-3530	-18015	-4050	-3629	-17926	-4030	-3828	-17970	-4040	-3579	-17926	-4030	-3629
-18015	-4050	-3530	-17970	-4040	-3679	-16324	-3670	-3082	-14856	-3340	-2933	-13389	-3010	-2436
-11876	-2670	-2038	-10364	-2330	-1740	-8896	-2000	-1392	-7384	-1660	-994	-5871	-1320	-646
-4359	-980	-149	-2891	-650	149	-1423	-320	696	88	20	845			

COMPRESSION HOLD CYCLE, TEST 8 - CYCLE 210 -

LOAD (N)	LOAD (LB)	STRAIN (με)	LOAD (N)	LOAD (LB)	STRAIN (με)	LOAD (N)	LOAD (LB)	STRAIN (με)	LOAD (N)	LOAD (LB)	STRAIN (με)	LOAD (N)	LOAD (LB)	STRAIN (με)
1734	390	1839	3380	760	2287	5070	1140	2784	6716	1510	3231	8318	1870	3579
9919	2230	4126	11654	2620	4623	13255	2980	5071	14856	3340	5319	16547	3720	6065
18104	4070	6662	19794	4450	7209	21707	4880	7756	23308	5240	8949	24954	5610	9347
26644	5990	9894	28246	6350	10440	29980	6740	11634	28290	6360	11037	26733	6010	10590
25087	5640	10242	23530	5290	9794	21885	4920	9546	20328	4570	8999	18771	4220	8700
17170	3860	8303	15568	3500	7756	14011	3150	7358	12277	2760	6861	10764	2420	6562
9163	2060	6115	7606	1710	5717	6005	1350	5220	4403	990	4723	2802	630	4176
1201	270	3679	-311	-70	3231	-1868	-420	2734	-3469	-780	2137	-5115	-1150	1690
-6672	-1500	994	-8318	-1870	745	-9830	-2210	-49	-11520	-2590	-447	-13122	-2950	-1143
-14634	-3290	-1690	-16235	-3650	-2485	-17881	-4020	-3082	-17926	-4030	-3132	-17881	-4020	-3132
-17837	-4010	-3231	-17881	-4020	-3182	-17881	-4020	-3281	-17881	-4020	-3480	-17881	-4020	-3182
-17881	-4020	-3281	-17881	-4020	-3380	-17881	-4020	-3331	-17881	-4020	-3281	-17881	-4020	-3182
-17837	-4010	-3331	-17926	-4030	-3380	-17881	-4020	-3182	-17837	-4010	-3281	-17926	-4030	-3430
-17837	-4010	-3281	-17881	-4020	-3281	-17881	-4020	-3430	-17881	-4020	-3281	-17881	-4020	-3579
-17881	-4020	-3380	-17881	-4020	-3430	-17881	-4020	-3281	-17881	-4020	-3629	-17881	-4020	-3231
-17881	-4020	-3430	-17881	-4020	-3182	-16280	-3660	-2734	-14768	-3320	-2485	-13344	-3000	-2336
-11743	-2640	-1789	-10319	-2320	-1292	-8807	-1980	-894	-7295	-1640	-546	-5827	-1310	99
-4314	-970	248	-2802	-630	944	-1378	-310	1093	88	20	1342			

TENSION-COMPRESSION HOLD CYCLE, TEST 9 - CYCLE 1 -

LOAD (N)	LOAD (LB)	STRAIN (με)	LOAD (N)	LOAD (LB)	STRAIN (με)	LOAD (N)	LOAD (LB)	STRAIN (με)	LOAD (N)	LOAD (LB)	STRAIN (με)	LOAD (N)	LOAD (LB)	STRAIN (με)
1556	350	438	3202	720	974	4893	1100	1364	6583	1480	1851	8229	1850	2192
9875	2220	2825	11565	2600	3020	13211	2970	3556	14856	3340	3848	16591	3730	4286
18193	4090	4920	19838	4460	5456	21529	4840	5599	23219	5220	6576	24820	5580	7014
26511	5960	7843	28157	6330	8476	29802	6700	9450	29847	6710	10035	29802	6700	9986
29802	6700	9548	29802	6700	9255	29802	6700	9840	29802	6700	9791	29802	6700	9986
29802	6700	9889	29802	6700	9694	29802	6700	9937	29802	6700	9889	29758	6690	9889
29802	6700	9548	29802	6700	9937	29802	6700	9937	29802	6700	9742	29802	6700	9889
29758	6690	10035	29802	6700	9986	29802	6700	9840	29802	6700	9889	29802	6700	9694
29758	6690	9840	29802	6700	9742	29802	6700	9937	29802	6700	9889	29802	6700	9986
29802	6700	9548	29802	6700	9986	28112	6320	9986	26511	5960	9060	24954	5610	8719
23353	5250	8086	21751	4890	7745	20150	4530	7745	18548	4170	8771	16992	3820	6625
15390	3460	6381	13789	3100	5797	12143	2730	5163	10542	2370	4920	8940	2010	4530
7384	1660	4286	5782	1300	3653	4181	940	3263	2579	580	2922	934	210	2581
-533	-120	1753	-2135	-480	1656	-3736	-840	1315	-5293	-1190	682	-6894	-1550	194
-8540	-1920	-194	-10097	-2270	-633	-11743	-2640	-1071	-13300	-2990	-1705	-14945	-3360	-2046
-16502	-3710	-2679	-18104	-4070	-3361	-18148	-4080	-3507	-18104	-4070	-3507	-18104	-4070	-3507
-18148	-4080	-3507	-18148	-4080	-3458	-18148	-4080	-3556	-18193	-4090	-3507	-18148	-4080	-3458
-18104	-4070	-3556	-18104	-4070	-3507	-18104	-4070	-3507	-18104	-4070	-3507	-18193	-4090	-3507
-18104	-4070	-3604	-18104	-4070	-3507	-18104	-4070	-3458	-18193	-4090	-3604	-18148	-4080	-3507
-18148	-4080	-3507	-18148	-4080	-3507	-18148	-4080	-3556	-18104	-4070	-3556	-18104	-4070	-3507
-18148	-4080	-3507	-18104	-4070	-3507	-18104	-4070	-3556	-18148	-4080	-3507	-18104	-4070	-3507
-18104	-4070	-3556	-16502	-3710	-3166	-14990	-3370	-2728	-13567	-3050	-2289	-12010	-2700	-1851
-10586	-2380	-1558	-9029	-2030	-1169	-7517	-1690	-778	-6094	-1370	-292	-4537	-1020	0
-3024	-680	341	-1512	-340	876	-88	-20	1169						

TENSION-COMPRESSION HOLD CYCLE, TEST 9 - CYCLE 2 -

LOAD (N)	LOAD (LB)	STRAIN (με)	LOAD (N)	LOAD (LB)	STRAIN (με)	LOAD (N)	LOAD (LB)	STRAIN (με)	LOAD (N)	LOAD (LB)	STRAIN (με)	LOAD (N)	LOAD (LB)	STRAIN (με)
1556	350	1656	3158	710	2046	4848	1090	2581	6583	1480	3166	8140	1830	3458
9786	2200	3945	11520	2590	4384	13211	2970	4822	14812	3330	5407	16547	3720	5650
18193	4090	6089	19883	4470	6430	21529	4840	7063	23175	5210	7648	24820	5580	7940
26466	5950	8427	28157	6330	8817	29802	6700	9596	29802	6700	9791	29802	6700	9937
29802	6700	9791	29802	6700	10083	29802	6700	9645	29802	6700	9742	29802	6700	10132
29758	6690	9986	29802	6700	9596	29758	6690	10132	29758	6690	10230	29758	6690	10083
29758	6690	10181	29758	6690	9840	29758	6690	9986	29758	6690	10278	29758	6690	9986
29802	6700	9986	29802	6700	9694	29758	6690	10035	29758	6690	10376	29713	6680	10083
29713	6680	10181	29802	6700	9791	29758	6690	9742	29802	6700	9937	29802	6700	9889
29758	6690	9986	29802	6700	10083	28157	6330	9889	26511	5960	9012	24954	5610	8817
23353	5250	8476	21751	4890	7696	20150	4530	7453	18593	4180	7063	16992	3820	6722
15346	3450	6332	13789	3100	5748	12188	2740	5309	10586	2380	4920	8985	2020	4725
7428	1670	4092	5827	1310	3848	4181	940	3215	2624	590	2874	978	220	2289
-533	-120	1851	-2090	-470	1412	-3647	-820	1071	-5293	-1190	682	-6850	-1540	146
-8540	-1920	-292	-10097	-2270	-730	-11654	-2620	-1169	-13300	-2990	-1705	-14856	-3340	-2240
-16502	-3710	-2728	-18104	-4070	-3312	-18104	-4070	-3556	-18104	-4070	-3410	-18104	-4070	-3410
-18104	-4070	-3410	-18104	-4070	-3507	-18104	-4070	-3507	-18104	-4070	-3458	-18104	-4070	-3458
-18104	-4070	-3556	-18104	-4070	-3458	-18104	-4070	-3604	-18104	-4070	-3410	-18104	-4070	-3458
-18104	-4070	-3507	-18104	-4070	-3410	-18104	-4070	-3507	-18104	-4070	-3361	-18104	-4070	-3507
-18104	-4070	-3507	-18193	-4090	-3361	-18104	-4070	-3604	-18104	-4070	-3507	-18104	-4070	-3458
-18104	-4070	-3556	-18104	-4070	-3458	-18104	-4070	-3458	-18104	-4070	-3410	-18104	-4070	-3507
-18104	-4070	-3458	-16591	-3730	-3117	-14990	-3370	-2728	-13567	-3050	-2192	-12010	-2700	-1899
-10542	-2370	-1510	-9029	-2030	-1217	-7517	-1690	-682	-6049	-1360	-292	-4537	-1020	-48
-3024	-680	389	-1556	-350	779	-44	-10	1169						

TENSION-COMPRESSION HOLD CYCLE, TEST 9 - CYCLE 3 -

LOAD (N)	LOAD (LB)	STRAIN (με)	LOAD (N)	LOAD (LB)	STRAIN (με)	LOAD (N)	LOAD (LB)	STRAIN (με)	LOAD (N)	LOAD (LB)	STRAIN (με)	LOAD (N)	LOAD (LB)	STRAIN (με)
1556	350	1558	3202	720	1997	4804	1080	2435	6538	1470	3020	8140	1830	3312
9830	2210	3648	11476	2580	4286	13122	2950	4774	14768	3320	5017	16413	3690	5504
18059	4060	6040	19705	4430	6430	21351	4800	7014	23175	5210	7453	24865	5590	8066
26466	5950	8476	28157	6330	8963	29847	6710	9986	29758	6690	9889	29802	6700	10132
29802	6700	9742	29802	6700	10035	29802	6700	9596	29802	6700	10181	29802	6700	10376
29802	6700	10083	29802	6700	9645	29802	6700	9986	29802	6700	9791	29802	6700	10083
29802	6700	9742	29802	6700	10132	29802	6700	9986	29802	6700	9742	29802	6700	10035
29802	6700	10083	29758	6690	10181	29802	6700	9986	29802	6700	9791	29802	6700	10083
29802	6700	9596	29802	6700	10035	29802	6700	9937	29802	6700	10376	29802	6700	9742
29802	6700	9791	29758	6690	9937	28157	6330	9889	26511	5960	9401	24998	5620	9060
23397	5260	8427	21751	4890	7881	20150	4530	7599	18593	4180	7209	17036	3830	6868
15390	3460	6430	13789	3100	5991	12232	2750	5456	10586	2380	5163	8985	2020	4676
7428	1670	4286	5827	1310	3994	4225	950	3507	2668	600	3069	978	220	2728
-533	-120	2094	-2090	-470	1607	-3647	-820	1217	-5248	-1180	826	-6850	-1540	194
-8540	-1920	-194	-10052	-2260	-584	-11654	-2620	-1023	-13300	-2990	-1461	-14901	-3350	-2046
-16502	-3710	-2581	-18148	-4080	-3263	-18104	-4070	-3361	-18104	-4070	-3410	-18104	-4070	-3263
-18104	-4070	-3361	-18104	-4070	-3361	-18104	-4070	-3410	-18104	-4070	-3361	-18104	-4070	-3361
-18104	-4070	-3458	-18148	-4080	-3361	-18104	-4070	-3312	-18104	-4070	-3312	-18104	-4070	-3361
-18104	-4070	-3361	-18104	-4070	-3263	-18104	-4070	-3361	-18104	-4070	-3361	-18104	-4070	-3263
-18193	-4090	-3312	-18104	-4070	-3263	-18104	-4070	-3312	-18104	-4070	-3263	-18104	-4070	-3263
-18104	-4070	-3215	-18148	-4080	-3263	-18104	-4070	-3263	-18104	-4070	-3263	-18104	-4070	-3215
-18104	-4070	-3263	-16502	-3710	-2874	-15034	-3380	-2435	-13567	-3050	-1948	-12010	-2700	-1607
-10542	-2370	-1364	-9074	-2040	-876	-7472	-1680	-438	-6049	-1360	-48	-4537	-1020	243
-3069	-690	633	-1556	-350	1071	-44	-10	1461						

TENSION-COMPRESSION HOLD CYCLE, TEST 9 - CYCLE 4 -

LOAD (N)	LOAD (LB)	STRAIN (με)	LOAD (N)	LOAD (LB)	STRAIN (με)	LOAD (N)	LOAD (LB)	STRAIN (με)	LOAD (N)	LOAD (LB)	STRAIN (με)	LOAD (N)	LOAD (LB)	STRAIN (με)
1556	350	1899	3202	720	2289	4848	1090	2825	6538	1470	3263	8184	1840	3653
9786	2200	4238	11476	2580	4725	13122	2950	5066	14768	3320	5407	16413	3690	6040
18059	4060	6284	19705	4430	6917	21395	4810	7453	23130	5200	7794	24820	5580	8378
26466	5950	8719	28157	6330	9889	29802	6700	9840	29802	6700	9986	29802	6700	10230
29758	6690	10424	29802	6700	10376	29802	6700	10327	29802	6700	10278	29802	6700	10132
29802	6700	10473	29802	6700	10668	29802	6700	10473	29802	6700	10278	29802	6700	10424
29802	6700	10717	29802	6700	10717	29802	6700	10522	29802	6700	10863	29802	6700	10765
29802	6700	10619	29802	6700	10424	29802	6700	10912	29802	6700	10522	29802	6700	10522
29802	6700	10619	29802	6700	10522	29802	6700	10814	29802	6700	10912	29802	6700	10814
29802	6700	10863	29802	6700	10473	28112	6320	9986	26555	5970	9742	24998	5620	9012
23353	5250	8963	21796	4900	8476	20150	4530	7989	18548	4170	7599	17036	3830	7161
15390	3460	6381	13789	3100	6235	12232	2750	5845	10586	2380	5650	8985	2020	4968
7384	1660	4676	5827	1310	4433	4225	950	3848	2624	590	3458	1023	230	3069
-533	-120	2338	-2090	-470	1997	-3692	-830	1656	-5248	-1180	1217	-6850	-1540	682
-8496	-1910	243	-10097	-2270	-243	-11698	-2630	-828	-13300	-2990	-1217	-14901	-3350	-1753
-16502	-3710	-2289	-18104	-4070	-2825	-18104	-4070	-2971	-18104	-4070	-2971	-18104	-4070	-3069
-18104	-4070	-3020	-18104	-4070	-2922	-18104	-4070	-2971	-18104	-4070	-2874	-18104	-4070	-3020
-18059	-4060	-2922	-18104	-4070	-3020	-18104	-4070	-3020	-18104	-4070	-2971	-18104	-4070	-2971
-18104	-4070	-2922	-18104	-4070	-3020	-18148	-4080	-2922	-18104	-4070	-2971	-18059	-4060	-3020
-18104	-4070	-3020	-18104	-4070	-2971	-18104	-4070	-3020	-18104	-4070	-3020	-18104	-4070	-3020
-18104	-4070	-3117	-18104	-4070	-3166	-18104	-4070	-3166	-18104	-4070	-3166	-18104	-4070	-3215
-18104	-4070	-3215	-16502	-3710	-2874	-15079	-3390	-2338	-13567	-3050	-1948	-12010	-2700	-1607
-10542	-2370	-1364	-9029	-2030	-730	-7561	-1700	-438	-6049	-1360	-48	-4537	-1020	341
-3069	-690	730	-1556	-350	1023	-88	-20	1510						

TENSION-COMPRESSION HOLD CYCLE, TEST 9 - CYCLE 5 -

LOAD (N)	LOAD (LB)	STRAIN (με)	LOAD (N)	LOAD (LB)	STRAIN (με)	LOAD (N)	LOAD (LB)	STRAIN (με)	LOAD (N)	LOAD (LB)	STRAIN (με)	LOAD (N)	LOAD (LB)	STRAIN (με)
1556	350	1851	3202	720	2338	4848	1090	2874	6538	1470	3263	8184	1840	3653
9786	2200	4189	11520	2590	4676	13122	2950	5066	14768	3320	5504	16413	3690	5894
18104	4070	6381	19705	4430	6820	21351	4800	7502	23130	5200	7891	24820	5580	8427
26466	5950	8914	28157	6330	9548	29847	6710	10083	29802	6700	10424	29802	6700	10668
29802	6700	10083	29802	6700	10571	29758	6690	10083	29802	6700	10278	29802	6700	10619
29802	6700	10522	29802	6700	10619	29802	6700	10717	29802	6700	10765	29802	6700	10668
29802	6700	10814	29802	6700	10912	29802	6700	10717	29802	6700	10668	29802	6700	10814
29802	6700	10765	29847	6710	11155	29802	6700	10668	29847	6710	10619	29802	6700	10912
29802	6700	10814	29802	6700	10571	29802	6700	10473	29802	6700	10765	29802	6700	10473
29802	6700	10863	29802	6700	10668	28157	6330	10083	26511	5960	10035	24998	5620	9548
23397	5260	9012	21796	4900	8671	20194	4540	8281	18593	4180	7843	17036	3830	7502
15390	3460	6576	13789	3100	6527	12188	2740	5894	10586	2380	5748	8985	2020	5358
7428	1670	4920	5827	1310	4676	4225	950	4140	2624	590	3653	1023	230	3166
-489	-110	2581	-2135	-480	2094	-3692	-830	1656	-5248	-1180	1315	-6850	-1540	682
-8496	-1910	341	-10052	-2260	-97	-11654	-2620	-584	-13300	-2990	-1217	-14901	-3350	-1705
-16458	-3700	-2143	-18104	-4070	-2825	-18148	-4080	-2971	-18104	-4070	-2971	-18104	-4070	-2971
-18104	-4070	-2971	-18104	-4070	-3069	-18104	-4070	-3069	-18104	-4070	-2971	-18104	-4070	-2922
-18059	-4060	-3166	-18104	-4070	-3020	-18059	-4060	-2922	-18104	-4070	-2971	-18104	-4070	-3020
-18104	-4070	-3020	-18104	-4070	-3069	-18104	-4070	-2971	-18104	-4070	-3020	-18104	-4070	-3020
-18104	-4070	-3020	-18059	-4060	-3020	-18104	-4070	-3069	-18059	-4060	-3020	-18059	-4060	-3020
-18104	-4070	-3020	-18104	-4070	-3069	-18104	-4070	-3020	-18104	-4070	-3020	-18104	-4070	-3020
-18104	-4070	-3069	-16502	-3710	-2679	-15034	-3380	-2192	-13522	-3040	-1753	-12010	-2700	-1510
-10542	-2370	-974	-8985	-2020	-633	-7517	-1690	-194	-6049	-1360	48	-4537	-1020	535
-3069	-690	974	-1556	-350	1315	-44	-10	1607						

TENSION-COMPRESSION HOLD CYCLE, TEST 9 - CYCLE 140 -

LOAD (N)	LOAD (LB)	STRAIN (με)	LOAD (N)	LOAD (LB)	STRAIN (με)	LOAD (N)	LOAD (LB)	STRAIN (με)	LOAD (N)	LOAD (LB)	STRAIN (με)	LOAD (N)	LOAD (LB)	STRAIN (με)
1690	380	2338	3247	730	2825	4848	1090	3410	6583	1480	3751	8140	1830	4481
9786	2200	4871	11476	2580	5504	13122	2950	5943	14679	3300	6381	16369	3680	7209
18015	4050	7794	19572	4400	8427	21529	4840	9548	23175	5210	10035	24776	5570	11106
26422	5940	11788	28112	6320	12617	29802	6700	13006	29758	6690	13688	29758	6690	13493
29758	6690	13445	29758	6690	13493	29802	6700	13347	29758	6690	13493	29758	6690	13542
29713	6680	13445	29758	6690	13493	29758	6690	13640	29802	6700	13786	29802	6700	13493
29758	6690	13640	29802	6700	13445	29802	6700	13493	29758	6690	13640	29758	6690	13688
29758	6690	13445	29758	6690	13542	29758	6690	13396	29713	6680	13737	29802	6700	13591
29758	6690	13640	29802	6700	13786	29758	6690	13737	29758	6690	13834	29758	6690	13445
29758	6690	13542	29758	6690	13640	28112	6320	13347	26511	5960	13104	24998	5620	12470
23397	5260	12129	21796	4900	11886	20194	4540	11350	18593	4180	10912	16992	3820	10424
15435	3470	9640	13789	3100	9353	12232	2750	8914	10631	2390	8573	9029	2030	8281
7472	1680	7745	5827	1310	7112	4270	960	6673	2624	590	6381	1067	240	5699
-444	-100	5115	-1957	-440	4481	-3558	-800	3799	-5248	-1180	3020	-6805	-1530	2533
-8407	-1890	2094	-9919	-2230	1461	-11609	-2610	194	-13166	-2960	-292	-14768	-3320	-925
-16324	-3670	-1899	-17970	-4040	-2971	-17970	-4040	-2971	-17970	-4040	-2922	-17970	-4040	-2971
-17970	-4040	-2971	-18015	-4050	-3069	-17970	-4040	-3069	-17926	-4030	-3117	-17970	-4040	-3020
-18015	-4050	-3069	-17970	-4040	-3069	-18015	-4050	-3020	-18015	-4050	-3069	-18015	-4050	-3117
-17970	-4040	-3069	-17970	-4040	-3069	-17970	-4040	-3069	-18015	-4050	-3020	-18015	-4050	-3020
-18015	-4050	-3117	-17970	-4040	-3069	-17970	-4040	-3069	-17970	-4040	-3069	-18015	-4050	-3069
-18015	-4050	-3166	-17970	-4040	-3069	-17970	-4040	-3117	-17970	-4040	-3117	-17970	-4040	-3117
-17970	-4040	-3117	-16458	-3700	-2484	-14901	-3350	-2289	-13478	-3030	-1753	-11921	-2680	-1510
-10408	-2340	-1071	-8940	-2010	-682	-7428	-1670	-194	-5960	-1340	389	-4403	-990	682
-2980	-670	1217	-1467	-330	1510	44	10	1851						

TENSION HOLD CYCLE, TEST 10 - CYCLE 1 -

LOAD (N)	LOAD (LB)	STRAIN (με)	LOAD (N)	LOAD (LB)	STRAIN (με)	LOAD (N)	LOAD (LB)	STRAIN (με)	LOAD (N)	LOAD (LB)	STRAIN (με)	LOAD (N)	LOAD (LB)	STRAIN (με)
1601	360	421	3247	730	889	4893	1100	1123	6627	1490	1544	8273	1860	2059
9875	2220	2668	11609	2610	2902	13255	2980	3511	14901	3350	3791	16591	3730	4213
18237	4100	4821	19883	4470	5383	21573	4850	5664	23219	5220	6366	24909	5600	6928
26511	5960	7817	28201	6340	8426	29847	6710	9269	29802	6700	9503	29847	6710	9362
29847	6710	9315	29847	6710	9596	29847	6710	9549	29847	6710	9456	29847	6710	9409
29847	6710	9409	29847	6710	9456	29847	6710	9456	29847	6710	9409	29847	6710	9409
29802	6700	9456	29802	6700	9549	29802	6700	9503	29802	6700	9596	29847	6710	9643
29847	6710	9503	29802	6700	9549	29847	6710	9503	29847	6710	9596	29802	6700	9456
29802	6700	9596	29847	6710	9456	29847	6710	9596	29802	6700	9503	29847	6710	9503
29847	6710	9596	29847	6710	9549	28157	6330	9175	26555	5970	8660	24998	5620	8285
23397	5260	7958	21796	4900	7443	20239	4550	6975	18637	4190	6787	16992	3820	6226
15479	3480	5945	13878	3120	5617	12277	2760	5055	10631	2390	4681	9029	2030	4353
7472	1680	4025	5827	1310	3323	4270	960	3089	2713	610	2715	1067	240	2293
-444	-100	1966	-2001	-450	1357	-3647	-820	889	-5159	-1160	608	-6761	-1520	140
-8451	-1900	-280	-9963	-2240	-842	-11609	-2610	-1263	-13211	-2970	-1778	-14856	-3340	-2340
-16413	-3690	-2808	-18015	-4050	-3370	-16413	-3690	-2855	-14945	-3360	-2715	-13478	-3030	-2059
-11921	-2680	-1778	-10497	-2360	-1404	-8985	-2020	-889	-7517	-1690	-842	-5960	-1340	-187
-4492	-1010	93	-2980	-670	561	-1423	-320	889	0	0	1217			

TENSION HOLD CYCLE, TEST 10 - CYCLE 2 -

LOAD (N)	LOAD (LB)	STRAIN (με)	LOAD (N)	LOAD (LB)	STRAIN (με)	LOAD (N)	LOAD (LB)	STRAIN (με)	LOAD (N)	LOAD (LB)	STRAIN (με)	LOAD (N)	LOAD (LB)	STRAIN (με)
1601	360	1685	3247	730	2059	4893	1100	2387	6583	1480	2949	8273	1860	3417
9919	2230	3885	11609	2610	4353	13300	2990	4681	14945	3360	5149	16591	3730	5664
18193	4090	5992	19883	4470	6460	21573	4850	6834	23264	5230	7536	24865	5590	8051
26511	5960	8379	28201	6340	8988	29847	6710	9549	29847	6710	9737	29802	6700	9643
29847	6710	9549	29802	6700	9737	29847	6710	9690	29847	6710	9784	29802	6700	9643
29847	6710	9737	29802	6700	9690	29802	6700	9643	29847	6710	9737	29802	6700	9643
29802	6700	9971	29802	6700	9784	29802	6700	9690	29802	6700	9784	29847	6710	9830
29847	6710	9690	29847	6710	9737	29802	6700	9784	29847	6710	9737	29847	6710	9877
29802	6700	9690	29802	6700	9830	29847	6710	9690	29802	6700	9924	29847	6710	9737
29847	6710	9830	29847	6710	9784	28201	6340	9362	26555	5970	8988	25043	5630	8660
23442	5270	8285	21796	4900	7677	20194	4540	7396	18637	4190	6975	17081	3840	6460
15435	3470	6038	13878	3120	5851	12232	2750	5383	10586	2380	4962	9029	2030	4681
7472	1680	4072	5871	1320	3838	4314	970	3323	2668	600	2949	1112	250	2481
-444	-100	2340	-2046	-460	1685	-3692	-830	1170	-5204	-1170	655	-6805	-1530	280
-8451	-1900	-280	-10008	-2250	-749	-11609	-2610	-1170	-13211	-2970	-1591	-14901	-3350	-2059
-16413	-3690	-2621	-18015	-4050	-3323	-16413	-3690	-2715	-14901	-3350	-2527	-13478	-3030	-2059
-11965	-2690	-1685	-10453	-2350	-1357	-8985	-2020	-889	-7472	-1680	-608	-5960	-1340	-46
-4448	-1000	327	-3024	-680	561	-1467	-330	1029	0	0	1498			

TENSION HOLD CYCLE, TEST 10 - CYCLE 3 -

LOAD (N)	LOAD (LB)	STRAIN (με)	LOAD (N)	LOAD (LB)	STRAIN (με)	LOAD (N)	LOAD (LB)	STRAIN (με)	LOAD (N)	LOAD (LB)	STRAIN (με)	LOAD (N)	LOAD (LB)	STRAIN (με)
1601	360	2012	3247	730	2247	4848	1090	2855	6538	1470	2996	8273	1860	3604
9919	2230	3979	11654	2620	4447	13255	2980	4962	14901	3350	5383	16591	3730	5664
18237	4100	6179	19883	4470	6600	21573	4850	7256	23219	5220	7630	24820	5580	8332
26466	5950	8613	28201	6340	9222	29847	6710	9877	29847	6710	10018	29847	6710	9924
29847	6710	9971	29802	6700	9924	29847	6710	9924	29802	6700	9971	29802	6700	10018
29802	6700	10064	29802	6700	9830	29802	6700	9971	29802	6700	9971	29802	6700	10018
29847	6710	9784	29758	6690	9877	29802	6700	9971	29802	6700	10018	29802	6700	9971
29802	6700	9971	29802	6700	9830	29802	6700	9971	29847	6710	10064	29802	6700	10064
29802	6700	9924	29802	6700	10018	29802	6700	10018	29847	6710	9924	29802	6700	9877
29802	6700	9784	29802	6700	10064	28157	6330	9549	26600	5980	9081	24998	5620	8707
23442	5270	8285	21796	4900	7911	20194	4540	7630	18637	4190	7209	17081	3840	6741
15435	3470	6319	13833	3110	5945	12232	2750	5430	10631	2390	5102	9074	2040	4634
7428	1670	4306	5871	1320	3791	4270	960	3370	2713	610	3089	1067	240	2574
-444	-100	2387	-2046	-460	1685	-3603	-810	1170	-5159	-1160	842	-6805	-1530	421
-8407	-1890	-93	-10008	-2250	-468	-11609	-2610	-936	-13211	-2970	-1732	-14856	-3340	-2012
-16458	-3700	-2761	-18015	-4050	-3230	-16413	-3690	-2668	-14945	-3360	-2434	-13478	-3030	-2012
-11921	-2680	-1732	-10453	-2350	-1310	-8940	-2010	-889	-7428	-1670	-468	-5960	-1340	-93
-4448	-1000	327	-2980	-670	655	-1467	-330	983	0	0	1451			

TENSION HOLD CYCLE, TEST 10 - CYCLE 4 -

LOAD (N)	LOAD (LB)	STRAIN (με)	LOAD (N)	LOAD (LB)	STRAIN (με)	LOAD (N)	LOAD (LB)	STRAIN (με)	LOAD (N)	LOAD (LB)	STRAIN (με)	LOAD (N)	LOAD (LB)	STRAIN (με)
1645	370	1872	3247	730	2153	4893	1100	2761	6583	1480	2949	8318	1870	3698
9875	2220	3979	11609	2610	4540	13255	2980	4962	14901	3350	5289	16591	3730	5804
18282	4110	6319	19838	4460	6694	21573	4850	7396	23264	5230	7677	24865	5590	8285
26511	5960	8847	28157	6330	9362	29847	6710	9830	29847	6710	10018	29847	6710	10064
29802	6700	10018	29847	6710	10205	29802	6700	10298	29802	6700	9924	29802	6700	10111
29847	6710	9971	29847	6710	10111	29802	6700	10111	29802	6700	10205	29847	6710	10158
29847	6710	10205	29847	6710	10111	29847	6710	10158	29802	6700	10064	29802	6700	10064
29847	6710	10064	29847	6710	10205	29802	6700	9971	29802	6700	9971	29802	6700	10018
29802	6700	10018	29847	6710	10111	29802	6700	10252	29802	6700	10298	29802	6700	10205
29802	6700	10111	29802	6700	10298	28201	6340	9784	26511	5960	9222	24998	5620	8894
23397	5260	8473	21751	4890	8051	20239	4550	7677	18637	4190	7349	17081	3840	6834
15479	3480	6553	13878	3120	6085	12232	2750	5617	10631	2390	5289	9029	2030	4821
7472	1680	4587	5871	1320	4025	4270	960	3651	2668	600	3136	1067	240	2715
-444	-100	2293	-2046	-460	1872	-3603	-810	1404	-5159	-1160	983	-6761	-1520	468
-8451	-1900	-93	-10008	-2250	-421	-11654	-2620	-842	-13211	-2970	-1638	-14812	-3330	-2153
-16413	-3690	-2574	-18015	-4050	-3136	-16458	-3700	-2715	-14945	-3360	-2293	-13478	-3030	-1966
-11921	-2680	-1591	-10453	-2350	-1170	-8985	-2020	-842	-7428	-1670	-655	-5960	-1340	-93
-4448	-1000	280	-2980	-670	655	-1467	-330	1076	0	0	1591			

TENSION HOLD CYCLE, TEST 10 - CYCLE 5 -

LOAD (N)	LOAD (LB)	STRAIN (με)	LOAD (N)	LOAD (LB)	STRAIN (με)	LOAD (N)	LOAD (LB)	STRAIN (με)	LOAD (N)	LOAD (LB)	STRAIN (με)	LOAD (N)	LOAD (LB)	STRAIN (με)
1645	370	1966	3247	730	2340	4893	1100	2808	6583	1480	3136	8273	1860	3698
9919	2230	4072	11609	2610	4540	13300	2990	4681	14901	3350	5477	16591	3730	5758
18193	4090	6366	19883	4470	6741	21573	4850	7302	23219	5220	7864	24865	5590	8426
26511	5960	8941	28201	6340	9643	29847	6710	10018	29847	6710	10205	29847	6710	10439
29847	6710	10345	29802	6700	10018	29847	6710	10111	29802	6700	10064	29847	6710	10111
29847	6710	10345	29847	6710	10205	29802	6700	10158	29847	6710	10111	29847	6710	10111
29847	6710	10064	29802	6700	10205	29847	6710	10252	29802	6700	10252	29802	6700	10018
29847	6710	10064	29802	6700	10252	29802	6700	10205	29847	6710	10018	29802	6700	10018
29802	6700	10158	29802	6700	10064	29847	6710	10158	29802	6700	10111	29802	6700	10018
29847	6710	10018	29847	6710	10205	28201	6340	9643	26555	5970	9269	24998	5620	8988
23442	5270	8426	21840	4910	8239	20239	4550	7724	18637	4190	7349	17081	3840	6881
15479	3480	6600	13878	3120	6179	12277	2760	5711	10675	2400	5196	9074	2040	4728
7472	1680	4494	5871	1320	4072	4270	960	3230	2713	610	3183	1067	240	2855
-444	-100	2387	-2046	-460	1732	-3603	-810	1498	-5204	-1170	983	-6761	-1520	421
-8451	-1900	-140	-9963	-2240	-655	-11609	-2610	-1123	-13211	-2970	-1732	-14812	-3330	-2200
-16413	-3690	-2574	-18015	-4050	-3511	-16458	-3700	-2855	-14901	-3350	-2434	-13433	-3020	-1919
-11965	-2690	-1732	-10453	-2350	-1263	-8940	-2010	-889	-7428	-1670	-655	-5960	-1340	-140
-4448	-1000	280	-2980	-670	702	-1467	-330	889	0	0	1310			

TENSION HOLD CYCLE, TEST 10 - CYCLE 200 -

LOAD (N)	LOAD (LB)	STRAIN (με)	LOAD (N)	LOAD (LB)	STRAIN (με)	LOAD (N)	LOAD (LB)	STRAIN (με)	LOAD (N)	LOAD (LB)	STRAIN (με)	LOAD (N)	LOAD (LB)	STRAIN (με)
1645	370	3464	3247	730	4166	4893	1100	4447	6672	1500	5009	8273	1860	5336
9963	2240	6038	11609	2610	6600	13255	2980	7162	14901	3350	7724	16591	3730	8332
18237	4100	9081	19927	4480	9643	21618	4860	10486	23264	5230	11001	24865	5590	11797
26511	5960	12356	28157	6330	13201	29847	6710	13763	29802	6700	13997	29847	6710	13903
29847	6710	14044	29802	6700	14090	29847	6710	13950	29802	6700	14044	29802	6700	13903
29847	6710	14184	29802	6700	13997	29802	6700	13903	29847	6710	13997	29847	6710	13950
29847	6710	13809	29802	6700	13903	29847	6710	13950	29802	6700	13763	29847	6710	13716
29847	6710	14090	29802	6700	14044	29847	6710	13856	29847	6710	13903	29847	6710	13856
29847	6710	13950	29847	6710	13950	29802	6700	13903	29847	6710	13997	29847	6710	13763
29847	6710	14044	29802	6700	13950	28157	6330	13295	26555	5970	13060	24998	5620	12826
23442	5270	12311	21796	4900	12077	20239	4550	11609	18637	4190	11141	17081	3840	10813
15479	3480	10392	13878	3120	9924	12277	2760	9456	10675	2400	9222	9029	2030	8566
7517	1690	8332	5916	1330	7583	4314	970	7209	2668	600	6694	1067	240	6273
-355	-80	5570	-2001	-450	5383	-3558	-800	4634	-5115	-1150	4072	-6805	-1530	3230
-8362	-1880	2668	-9963	-2240	1919	-11565	-2600	1217	-13211	-2970	561	-14812	-3330	-93
-16369	-3680	-655	-17970	-4040	-1872	-16413	-3690	-1170	-14856	-3340	-842	-13433	-3020	-421
-11876	-2670	93	-10408	-2340	140	-8896	-2000	795	-7428	-1670	936	-5916	-1330	1357
-4448	-1000	1872	-2935	-660	2293	-1467	-330	2621	0	0	2761			

CONTINUOUS CYCLE, TEST 11A - CYCLE 1 -

LOAD (N)	LOAD (LB)	STRAIN (με)	LOAD (N)	LOAD (LB)	STRAIN (με)	LOAD (N)	LOAD (LB)	STRAIN (με)	LOAD (N)	LOAD (LB)	STRAIN (με)	LOAD (N)	LOAD (LB)	STRAIN (με)
1378	310	244	2713	610	636	4136	930	1077	5515	1240	1615	6939	1560	1762
8362	1880	1958	9741	2190	2497	11120	2500	2888	12543	2820	3280	13967	3140	3525
15301	3440	4112	16769	3770	4357	18104	4070	4896	19527	4390	5092	20906	4700	5581
22329	5020	6022	23708	5330	6511	25132	5650	6903	23664	5320	6218	22374	5030	6365
21039	4730	6022	19705	4430	5630	18326	4120	5336	16992	3820	4798	15657	3520	4553
14278	3210	4112	12988	2920	3867	11654	2620	3427	10319	2320	3182	8940	2010	2790
7606	1710	2448	6271	1410	2056	4893	1100	1811	3558	800	1566	2224	500	1028
889	200	783	-400	-90	489	-1734	-390	97	-3024	-680	-195	-4359	-980	-587
-5782	-1300	-930	-7117	-1600	-1321	-8451	-1900	-1664	-9786	-2200	-1909	-11120	-2500	-2203
-12499	-2810	-2741	-13833	-3110	-3280	-15168	-3410	-3574	-13878	-3120	-3133	-12588	-2830	-2839
-11342	-2550	-2594	-10097	-2270	-2154	-8762	-1970	-1909	-7561	-1700	-1517	-6316	-1420	-1077
-5070	-1140	-930	-3780	-850	-587	-2490	-560	-244	-1245	-280	48	-44	-10	489

CONTINUOUS CYCLE, TEST 11A - CYCLE 2 -

LOAD (N)	LOAD (LB)	STRAIN (με)	LOAD (N)	LOAD (LB)	STRAIN (με)	LOAD (N)	LOAD (LB)	STRAIN (με)	LOAD (N)	LOAD (LB)	STRAIN (με)	LOAD (N)	LOAD (LB)	STRAIN (με)
1289	290	832	2668	600	1370	4136	930	1370	5515	1240	1664	6894	1550	2105
8362	1880	2399	9741	2190	2839	11120	2500	3329	12543	2820	3476	13922	3130	3916
15346	3450	4259	16725	3760	4700	18059	4060	5043	19527	4390	5434	20906	4700	5777
22241	5000	6316	23708	5330	6511	25132	5650	6952	23664	5320	6413	22374	5030	6267
20995	4720	6022	19661	4420	5483	18371	4130	5140	16947	3810	4749	15613	3510	4602
14323	3220	4308	12988	2920	3770	11654	2620	3427	10319	2320	3084	8940	2010	2741
7606	1710	2497	6271	1410	2105	4893	1100	1762	3603	810	1321	2179	490	1028
889	200	783	-400	-90	489	-1734	-390	48	-3024	-680	-293	-4359	-980	-636
-5693	-1280	-979	-7117	-1600	-1224	-8451	-1900	-1468	-9741	-2190	-2007	-11120	-2500	-2399
-12499	-2810	-2790	-13833	-3110	-3084	-15168	-3410	-3574	-13878	-3120	-2986	-12588	-2830	-2790
-11342	-2550	-2399	-10097	-2270	-2154	-8807	-1980	-1811	-7561	-1700	-1517	-6316	-1420	-1175
-5070	-1140	-783	-3780	-850	-538	-2490	-560	-195	-1289	-290	-48	-44	-10	538

CONTINUOUS CYCLE, TEST 11A - CYCLE 3 -

LOAD (N)	LOAD (LB)	STRAIN (με)	LOAD (N)	LOAD (LB)	STRAIN (με)	LOAD (N)	LOAD (LB)	STRAIN (με)	LOAD (N)	LOAD (LB)	STRAIN (με)	LOAD (N)	LOAD (LB)	STRAIN (με)
1334	300	783	2713	610	979	4092	920	1419	5515	1240	1762	6894	1550	2252
8318	1870	2350	9741	2190	2839	11164	2510	3182	12543	2820	3476	13922	3130	4014
15301	3440	4504	16769	3770	4700	18148	4080	5092	19483	4380	5385	20906	4700	5826
22329	5020	6316	23664	5320	6658	25132	5650	6952	23664	5320	6609	22329	5020	6218
21039	4730	5924	19661	4420	5630	18326	4120	5238	16947	3810	4847	15613	3510	4553
14323	3220	4161	12988	2920	3916	11609	2610	3623	10275	2310	3133	8940	2010	2839
7606	1710	2399	6316	1420	2056	4937	1110	1811	3647	820	1517	2224	500	1028
889	200	783	-444	-100	538	-1734	-390	195	-3069	-690	-195	-4359	-980	-636
-5738	-1290	-881	-7072	-1590	-1273	-8451	-1900	-1615	-9786	-2200	-2056	-11120	-2500	-2252
-12499	-2810	-2790	-13789	-3100	-3280	-15168	-3410	-3574	-13878	-3120	-3133	-12588	-2830	-2839
-11342	-2550	-2399	-10052	-2260	-2154	-8762	-1970	-1762	-7561	-1700	-1468	-6316	-1420	-1126
-5070	-1140	-930	-3736	-840	-538	-2490	-560	-342	-1245	-280	48	-44	-10	440

CONTINUOUS CYCLE, TEST 11A - CYCLE 4 -

LOAD (N)	LOAD (LB)	STRAIN (με)	LOAD (N)	LOAD (LB)	STRAIN (με)	LOAD (N)	LOAD (LB)	STRAIN (με)	LOAD (N)	LOAD (LB)	STRAIN (με)	LOAD (N)	LOAD (LB)	STRAIN (με)
1334	300	832	2713	610	1175	4092	920	1321	5471	1230	1762	6939	1560	2154
8318	1870	2497	9741	2190	2937	11120	2500	3231	12543	2820	3427	13922	3130	3965
15346	3450	4455	16725	3760	4749	18104	4070	5140	19527	4390	5434	20906	4700	5777
22329	5020	6316	23708	5330	6658	25132	5650	6952	23708	5330	6511	22374	5030	6365
21039	4730	5924	19661	4420	5532	18371	4130	5287	16992	3820	4994	15657	3520	4749
14323	3220	4308	12988	2920	3965	11609	2610	3525	10319	2320	3231	8896	2000	2937
7606	1710	2448	6271	1410	2105	4937	1110	1713	3514	790	1468	2224	500	1224
889	200	783	-400	-90	440	-1734	-390	97	-3069	-690	-293	-4359	-980	-538
-5693	-1280	-930	-7072	-1590	-1175	-8451	-1900	-1566	-9786	-2200	-1958	-11164	-2510	-2301
-12499	-2810	-2790	-13833	-3110	-2986	-15168	-3410	-3427	-13878	-3120	-3084	-12588	-2830	-2692
-11342	-2550	-2399	-10052	-2260	-2203	-8762	-1970	-1860	-7517	-1690	-1517	-6316	-1420	-1077
-5070	-1140	-832	-3736	-840	-636	-2535	-570	-342	-1245	-280	97	0	0	489

CONTINUOUS CYCLE, TEST 11A - CYCLE 5 -

LOAD (N)	LOAD (LB)	STRAIN (με)	LOAD (N)	LOAD (LB)	STRAIN (με)	LOAD (N)	LOAD (LB)	STRAIN (με)	LOAD (N)	LOAD (LB)	STRAIN (με)	LOAD (N)	LOAD (LB)	STRAIN (με)
1334	300	881	2713	610	1175	4136	930	1370	5471	1230	1664	6894	1550	2056
8362	1880	2399	9741	2190	2888	11120	2500	3329	12543	2820	3574	13967	3140	3916
15346	3450	4406	16725	3760	4749	18104	4070	5189	19527	4390	5532	20906	4700	5826
22329	5020	6511	23708	5330	6658	25132	5650	7050	23708	5330	6609	22329	5020	6316
20995	4720	6120	19661	4420	5581	18371	4130	5189	16903	3800	4896	15657	3520	4651
14323	3220	4357	12988	2920	3867	11654	2620	3427	10275	2310	3182	8940	2010	2888
7561	1700	2594	6271	1410	2105	4937	1110	1909	3603	810	1517	2135	480	1077
934	210	783	-400	-90	587	-1734	-390	97	-3069	-690	-244	-4359	-980	-587
-5782	-1300	-881	-7117	-1600	-1126	-8407	-1890	-1713	-9786	-2200	-2056	-11120	-2500	-2350
-12543	-2820	-2692	-13833	-3110	-3084	-15212	-3420	-3672	-13878	-3120	-3231	-12588	-2830	-2839
-11342	-2550	-2350	-10097	-2270	-2056	-8807	-1980	-1811	-7517	-1690	-1517	-6316	-1420	-1126
-5070	-1140	-783	-3780	-850	-489	-2490	-560	-244	-1245	-280	48	-44	-10	391

CONTINUOUS CYCLE, TEST 11A - CYCLE 1000 -

LOAD (N)	LOAD (LB)	STRAIN (με)	LOAD (N)	LOAD (LB)	STRAIN (με)	LOAD (N)	LOAD (LB)	STRAIN (με)	LOAD (N)	LOAD (LB)	STRAIN (με)	LOAD (N)	LOAD (LB)	STRAIN (με)
1334	300	881	2757	620	1273	4136	930	1468	5426	1220	1860	6939	1560	2350
8318	1870	2790	9786	2200	3133	11120	2500	3427	12588	2830	4014	13922	3130	4308
15301	3440	4651	16725	3760	5238	18104	4070	5679	19572	4400	6169	20906	4700	6560
22329	5020	7050	23708	5330	7638	25087	5640	8176	23708	5330	7833	22374	5030	7344
21039	4730	7050	19705	4430	6707	18371	4130	6413	16992	3820	6071	15657	3520	5532
14323	3220	5287	12988	2920	4945	11609	2610	4700	10319	2320	4210	8940	2010	3965
7606	1710	3623	6271	1410	3182	4937	1110	2888	3603	810	2399	2224	500	2252
889	200	1811	-400	-90	1126	-1690	-380	1028	-3024	-680	587	-4359	-980	48
-5782	-1300	-293	-7117	-1600	-783	-8451	-1900	-1175	-9786	-2200	-1566	-11120	-2500	-2105
-12499	-2810	-2546	-13833	-3110	-3035	-15168	-3410	-3476	-13833	-3110	-3133	-12588	-2830	-2741
-11298	-2540	-2497	-10052	-2260	-2203	-8807	-1980	-1909	-7561	-1700	-1566	-6227	-1400	-1126
-5026	-1130	-1028	-3736	-840	-636	-2490	-560	-195	-1289	-290	48	-44	-10	342

TENSION-COMPRESSION HOLD CYCLE, TEST 11B - CYCLE 1 -

LOAD (N)	LOAD (LB)	STRAIN (με)	LOAD (N)	LOAD (LB)	STRAIN (με)	LOAD (N)	LOAD (LB)	STRAIN (με)	LOAD (N)	LOAD (LB)	STRAIN (με)	LOAD (N)	LOAD (LB)	STRAIN (με)
1645	370	587	3247	730	1028	4848	1090	1321	6538	1470	1811	8229	1850	2301
9875	2220	2790	11609	2610	3329	13255	2980	3819	14856	3340	4210	16591	3730	4798
18193	4090	5336	19838	4460	5875	21573	4850	6462	23219	5220	7001	24865	5590	7833
26511	5960	8323	28201	6340	9008	29802	6700	9792	29802	6700	9939	29758	6690	9939
29802	6700	10037	29758	6690	9939	29758	6690	9939	29802	6700	9939	29802	6700	9988
29802	6700	9988	29802	6700	9988	29802	6700	10037	29802	6700	9988	29802	6700	10037
29802	6700	10037	29802	6700	9988	29758	6690	9988	29802	6700	9988	29758	6690	10037
29758	6690	10037	29802	6700	9988	29802	6700	10037	29758	6690	10037	29802	6700	9988
29802	6700	10037	29802	6700	10037	29802	6700	10037	29802	6700	9988	29802	6700	9988
29802	6700	10037	29802	6700	9988	28157	6330	9694	26511	5960	9204	24954	5610	8715
23397	5260	8323	21796	4900	8029	20150	4530	7540	18593	4180	7148	17036	3830	6707
15390	3460	6316	13744	3090	5875	12232	2750	5434	10631	2390	4994	9029	2030	4553
7472	1680	4210	5916	1330	3867	4270	960	3280	2668	600	2692	1067	240	2203
-444	-100	1811	-2046	-460	1176	-3647	-820	783	-5204	-1170	342	-6761	-1520	-391
-8451	-1900	-1028	-10008	-2250	-1517	-11654	-2620	-2105	-13255	-2980	-2741	-14812	-3330	-3280
-16413	-3690	-3965	-18015	-4050	-4700	-18059	-4060	-4700	-18015	-4050	-4749	-18015	-4050	-4700
-18059	-4060	-4700	-18059	-4060	-4798	-18059	-4060	-4798	-18015	-4050	-4798	-18015	-4050	-4749
-18104	-4070	-4847	-18015	-4050	-4749	-18015	-4050	-4798	-18059	-4060	-4749	-18015	-4050	-4798
-18015	-4050	-4749	-18059	-4060	-4798	-18015	-4050	-4749	-18015	-4050	-4847	-18015	-4050	-4798
-18015	-4050	-4798	-18015	-4050	-4749	-17970	-4040	-4749	-18059	-4060	-4798	-18059	-4060	-4798
-18015	-4050	-4798	-18015	-4050	-4749	-18015	-4050	-4798	-18015	-4050	-4896	-18015	-4050	-4798
-18059	-4060	-4896	-16458	-3700	-4259	-14945	-3360	-4112	-13478	-3030	-3623	-12010	-2700	-3133
-10453	-2350	-2888	-8940	-2010	-2350	-7472	-1680	-1958	-5960	-1340	-1664	-4448	-1000	-1321
-2980	-670	-832	-1512	-340	-636	0	0	-146						

TENSION-COMPRESSION HOLD CYCLE, TEST 11B - CYCLE 2 -

LOAD (N)	LOAD (LB)	STRAIN (με)	LOAD (N)	LOAD (LB)	STRAIN (με)	LOAD (N)	LOAD (LB)	STRAIN (με)	LOAD (N)	LOAD (LB)	STRAIN (με)	LOAD (N)	LOAD (LB)	STRAIN (με)
1556	350	440	3247	730	832	4848	1090	1224	6583	1480	1664	8184	1840	2301
9919	2230	2741	11609	2610	3329	13166	2960	3770	14856	3340	4210	16547	3720	4896
18193	4090	5483	19838	4460	6022	21529	4840	6658	23175	5210	7393	24820	5580	7931
26466	5950	8518	28112	6320	9302	29802	6700	9841	29802	6700	10037	29758	6690	10037
29802	6700	9988	29758	6690	10086	29758	6690	10086	29758	6690	10086	29802	6700	10086
29758	6690	10135	29802	6700	10184	29758	6690	10086	29802	6700	10086	29802	6700	10135
29802	6700	10086	29802	6700	10086	29802	6700	10135	29758	6690	10086	29758	6690	10086
29758	6690	10086	29802	6700	10086	29758	6690	10086	29758	6690	10086	29802	6700	10135
29802	6700	10135	29758	6690	10086	29758	6690	10135	29758	6690	10184	29758	6690	10135
29802	6700	10135	29802	6700	10135	28157	6330	9694	26511	5960	9351	24998	5620	8911
23397	5260	8470	21796	4900	8078	20194	4540	7784	18593	4180	7246	17036	3830	6854
15435	3470	6609	13789	3100	6120	12232	2750	5483	10631	2390	5140	9029	2030	4798
7472	1680	4357	5827	1310	3965	4270	960	3378	2668	600	2986	1067	240	2399
-444	-100	1860	-2046	-460	1321	-3603	-810	881	-5204	-1170	342	-6850	-1540	-293
-8451	-1900	-881	-10008	-2250	-1468	-11654	-2620	-2056	-13255	-2980	-2643	-14812	-3330	-3133
-16413	-3690	-3867	-18059	-4060	-4553	-18015	-4050	-4700	-18015	-4050	-4651	-18015	-4050	-4651
-18059	-4060	-4749	-18015	-4050	-4700	-18015	-4050	-4798	-18059	-4060	-4749	-18015	-4050	-4700
-18059	-4060	-4798	-18059	-4060	-4798	-18015	-4050	-4749	-18059	-4060	-4798	-18015	-4050	-4798
-18015	-4050	-4798	-18015	-4050	-4749	-18015	-4050	-4749	-18015	-4050	-4700	-18015	-4050	-4700
-18015	-4050	-4749	-18059	-4060	-4749	-18059	-4060	-4798	-18015	-4050	-4700	-18059	-4060	-4798
-18059	-4060	-4749	-18015	-4050	-4749	-18059	-4060	-4798	-18015	-4050	-4798	-18059	-4060	-4847
-18059	-4060	-4749	-16413	-3690	-4259	-14945	-3360	-3916	-13478	-3030	-3525	-11965	-2690	-3133
-10453	-2350	-2790	-8985	-2020	-2399	-7472	-1680	-2105	-5960	-1340	-1615	-4492	-1010	-1370
-3024	-680	-979	-1467	-330	-587	-44	-10	-195						

TENSION-COMPRESSION HOLD CYCLE, TEST 11B - CYCLE 3 -

LOAD (N)	LOAD (LB)	STRAIN (με)	LOAD (N)	LOAD (LB)	STRAIN (με)	LOAD (N)	LOAD (LB)	STRAIN (με)	LOAD (N)	LOAD (LB)	STRAIN (με)	LOAD (N)	LOAD (LB)	STRAIN (με)
1601	360	469	3247	730	783	4848	1090	1824	6538	1470	1615	8184	1840	2350
9830	2210	2692	11476	2580	3280	13122	2950	3672	14768	3320	4161	16413	3690	4749
18059	4060	5336	19705	4430	5973	21351	4800	6560	22997	5170	7246	24865	5590	7833
26466	5950	8617	28157	6330	9155	29802	6700	9792	29758	6690	9988	29758	6690	9988
29758	6690	9988	29802	6700	10086	29758	6690	10037	29802	6700	10086	29758	6690	10086
29802	6700	10135	29802	6700	10086	29802	6700	10135	29758	6690	10086	29802	6700	10135
29758	6690	10135	29802	6700	10184	29802	6700	10135	29758	6690	10135	29758	6690	10184
29758	6690	10086	29713	6680	10037	29758	6690	10135	29802	6700	10135	29758	6690	10184
29802	6700	10135	29802	6700	10135	29802	6700	10086	29758	6690	10184	29758	6690	10135
29802	6700	10184	29758	6690	10135	28157	6330	9743	26511	5960	9351	24998	5620	8959
23397	5260	8519	21796	4900	8176	20150	4530	7686	18593	4180	7344	16992	3820	6903
15390	3460	6511	13789	3100	6169	12232	2750	5679	10631	2390	5043	9029	2030	4700
7472	1680	4455	5871	1320	3916	4270	960	3378	2668	600	2986	1067	240	2448
-444	-100	1909	-2046	-460	1321	-3603	-810	879	-5204	-1170	391	-6850	-1540	-195
-8451	-1900	-832	-10052	-2260	-1370	-11654	-2620	-1858	-13211	-2970	-2546	-14812	-3330	-3231
-16413	-3690	-3672	-18015	-4050	-4357	-18015	-4050	-4602	-18015	-4050	-4602	-18015	-4050	-4504
-18059	-4060	-4700	-18015	-4050	-4651	-18059	-4060	-4651	-18059	-4060	-4749	-18015	-4050	-4651
-18015	-4050	-4749	-18059	-4060	-4700	-18015	-4050	-4749	-18015	-4050	-4847	-18015	-4050	-4700
-18015	-4050	-4700	-18015	-4050	-4700	-18059	-4060	-4798	-18015	-4050	-4749	-18059	-4060	-4700
-18059	-4060	-4749	-18015	-4050	-4749	-18015	-4050	-4798	-18059	-4060	-4798	-18015	-4050	-4749
-18015	-4050	-4847	-18015	-4050	-4798	-18015	-4050	-4798	-18015	-4050	-4798	-18015	-4050	-4749
-18015	-4050	-4749	-16413	-3690	-4308	-14945	-3360	-3819	-13478	-3030	-3574	-11921	-2680	-3084
-10453	-2350	-2790	-8940	-2010	-2399	-7428	-1670	-2007	-5960	-1340	-1713	-4448	-1000	-1321
-2935	-660	-734	-1467	-330	-636	0	0	-244						

TENSION-COMPRESSION HOLD CYCLE, TEST 11B - CYCLE 4 -

LOAD (N)	LOAD (LB)	STRAIN (με)	LOAD (N)	LOAD (LB)	STRAIN (με)	LOAD (N)	LOAD (LB)	STRAIN (με)	LOAD (N)	LOAD (LB)	STRAIN (με)	LOAD (N)	LOAD (LB)	STRAIN (με)
1601	360	440	3247	730	881	4893	1100	1824	6583	1480	1762	8184	1840	2399
9830	2210	2643	11520	2590	3231	13122	2950	3672	14723	3310	4210	16413	3690	4749
18015	4050	5434	19661	4420	5875	21351	4800	6560	22997	5170	7295	24643	5540	7784
26244	5900	8470	27890	6270	9155	29580	6650	9694	29802	6700	9988	29802	6700	10037
29758	6690	10037	29802	6700	10135	29802	6700	10086	29802	6700	10184	29802	6700	10135
29758	6690	10135	29802	6700	10184	29758	6690	10184	29713	6680	10232	29758	6690	10135
29802	6700	10184	29802	6700	10232	29802	6700	10184	29802	6700	10184	29802	6700	10184
29802	6700	10135	29802	6700	10232	29802	6700	10135	29802	6700	10184	29802	6700	10135
29758	6690	10184	29802	6700	10184	29802	6700	10135	29802	6700	10232	29802	6700	10184
29758	6690	10232	29802	6700	10184	28112	6320	9743	26555	5970	9400	24998	5620	9057
23397	5260	8617	21751	4890	8176	20194	4540	7735	18548	4170	7344	17036	3830	6903
15390	3460	6511	13833	3110	6169	12232	2750	5679	10631	2390	5238	9029	2030	4847
7472	1680	4455	5871	1320	4014	4270	960	3427	2624	590	3035	1067	240	2399
-444	-100	2056	-2046	-460	1468	-3647	-820	979	-5204	-1170	489	-6850	-1540	-244
-8451	-1900	-783	-9963	-2240	-1370	-11609	-2610	-1860	-13255	-2980	-2546	-14812	-3330	-3182
-16413	-3690	-3623	-18015	-4050	-4455	-18015	-4050	-4602	-18015	-4050	-4700	-18015	-4050	-4553
-18059	-4060	-4553	-18015	-4050	-4651	-18015	-4050	-4504	-18015	-4050	-4651	-18015	-4050	-4700
-18015	-4050	-4700	-18015	-4050	-4602	-18015	-4050	-4602	-18015	-4050	-4700	-18015	-4050	-4504
-18015	-4050	-4553	-18015	-4050	-4651	-18015	-4050	-4602	-18015	-4050	-4553	-17970	-4040	-4749
-18015	-4050	-4602	-18015	-4050	-4553	-18059	-4060	-4504	-18015	-4050	-4602	-18015	-4050	-4602
-18015	-4050	-4602	-18015	-4050	-4553	-18015	-4050	-4602	-18059	-4060	-4602	-18015	-4050	-4651
-18015	-4050	-4602	-16413	-3690	-4210	-14901	-3350	-3770	-13478	-3030	-3427	-11965	-2690	-3035
-10497	-2360	-2692	-8985	-2020	-2252	-7428	-1670	-1909	-5960	-1340	-1566	-4492	-1010	-1224
-3024	-680	-538	-1467	-330	-489	0	0	-97						

TENSION-COMPRESSION HOLD CYCLE, TEST 11B - CYCLE 5 -

LOAD (N)	LOAD (LB)	STRAIN (με)	LOAD (N)	LOAD (LB)	STRAIN (με)	LOAD (N)	LOAD (LB)	STRAIN (με)	LOAD (N)	LOAD (LB)	STRAIN (με)	LOAD (N)	LOAD (LB)	STRAIN (με)
1601	360	536	3247	730	1028	4893	1100	1524	6538	1470	1811	8184	1840	2448
9830	2210	2790	11520	2590	3280	13166	2960	3819	14768	3320	4259	16413	3690	4945
18059	4060	5434	19705	4430	6022	21351	4800	6658	22997	5170	7393	24598	5530	8029
26244	5900	8617	27890	6270	9253	29536	6640	9890	29758	6690	10135	29802	6700	10135
29802	6700	10135	29758	6690	10184	29802	6700	10281	29802	6700	10232	29802	6700	10184
29802	6700	10232	29802	6700	10330	29802	6700	10330	29758	6690	10330	29802	6700	10379
29802	6700	10281	29802	6700	10281	29758	6690	10281	29802	6700	10184	29802	6700	10281
29802	6700	10330	29758	6690	10281	29802	6700	10281	29758	6690	10232	29802	6700	10330
29802	6700	10281	29758	6690	10330	29802	6700	10330	29802	6700	10281	29802	6700	10330
29802	6700	10330	29802	6700	10330	28112	6320	9890	26555	5970	9547	24954	5610	9008
23397	5260	8666	21707	4880	8274	20150	4530	7882	18593	4180	7491	17081	3840	7050
15435	3470	6609	13789	3100	6218	12232	2750	5826	10631	2390	5287	9029	2030	4945
7426	1670	4602	5871	1320	4014	4225	950	3525	2624	590	3084	1067	240	2643
-489	-110	2105	-2001	-450	1419	-3603	-810	1077	-5204	-1170	538	-6850	-1540	-195
-8407	-1890	-685	-10052	-2260	-1126	-11609	-2610	-1960	-13211	-2970	-2546	-14812	-3330	-3133
-16413	-3690	-3721	-18059	-4060	-4357	-18015	-4050	-4504	-18015	-4050	-4455	-18015	-4050	-4504
-18015	-4050	-4504	-18015	-4050	-4602	-18015	-4050	-4553	-18015	-4050	-4357	-18015	-4050	-4602
-18059	-4060	-4553	-18015	-4050	-4553	-18015	-4050	-4553	-18015	-4050	-4553	-18059	-4060	-4602
-17970	-4040	-4553	-18015	-4050	-4602	-18015	-4050	-4553	-18015	-4050	-4455	-18015	-4050	-4504
-17970	-4040	-4651	-18059	-4060	-4651	-18015	-4050	-4651	-18015	-4050	-4553	-18015	-4050	-4602
-17970	-4040	-4651	-18015	-4050	-4504	-18015	-4050	-4602	-18015	-4050	-4455	-18015	-4050	-4749
-18015	-4050	-4651	-16458	-3700	-4161	-14901	-3350	-3867	-13478	-3030	-3378	-11921	-2680	-2986
-10453	-2350	-2594	-8940	-2010	-2154	-7428	-1670	-1811	-5960	-1340	-1468	-4448	-1000	-1175
-3024	-680	-734	-1467	-330	-440	0	0	97						

TENSION-COMPRESSION HOLD CYCLE, TEST 11B - CYCLE 120 -

LOAD (N)	LOAD (LB)	STRAIN (με)	LOAD (N)	LOAD (LB)	STRAIN (με)	LOAD (N)	LOAD (LB)	STRAIN (με)	LOAD (N)	LOAD (LB)	STRAIN (με)	LOAD (N)	LOAD (LB)	STRAIN (με)
1690	380	587	3281	740	930	4937	1110	1517	6583	1480	2007	8229	1850	2497
9830	2210	2986	11476	2580	3525	13166	2960	4014	14768	3320	4700	16458	3700	5532
18059	4060	6022	19705	4430	6756	21573	4850	7638	23219	5220	8568	24865	5590	9106
26466	5950	10037	28201	6340	10673	29847	6710	11505	29758	6690	11701	29758	6690	11652
29758	6690	11652	29802	6700	11652	29847	6710	11701	29802	6700	11701	29847	6710	11750
29802	6700	11799	29847	6710	11750	29758	6690	11799	29847	6710	11848	29802	6700	11848
29802	6700	11848	29802	6700	11848	29802	6700	11799	29802	6700	11897	29802	6700	11848
29802	6700	11848	29802	6700	11799	29802	6700	11848	29802	6700	11897	29802	6700	11799
29802	6700	11848	29802	6700	11799	29802	6700	11897	29802	6700	11897	29802	6700	11848
29847	6710	11848	29802	6700	11848	28201	6340	11457	26555	5970	10967	25043	5630	10624
23397	5260	10281	21751	4890	9792	20239	4550	9302	18593	4180	8959	17081	3840	8568
15435	3470	8029	13833	3110	7686	12321	2770	7098	10631	2390	6707	9029	2030	6316
7472	1680	5826	5871	1320	5336	4270	960	4945	2757	620	4455	1067	240	3770
-355	-80	3329	-1957	-440	2741	-3558	-800	2105	-5204	-1170	1517	-6805	-1530	832
-8362	-1880	244	-9918	-2230	-538	-11609	-2610	-1175	-13122	-2950	-2154	-14768	-3320	-2790
-16324	-3670	-3476	-17926	-4030	-4406	-17926	-4030	-4602	-17970	-4040	-4553	-17970	-4040	-4553
-17970	-4040	-4553	-17926	-4030	-4455	-18015	-4050	-4700	-17970	-4040	-4602	-17926	-4030	-4553
-17926	-4030	-4553	-17970	-4040	-4602	-17970	-4040	-4602	-17970	-4040	-4651	-17970	-4040	-4700
-17970	-4040	-4700	-17970	-4040	-4651	-17970	-4040	-4651	-17970	-4040	-4749	-18015	-4050	-4798
-17926	-4030	-4700	-17970	-4040	-4651	-17926	-4030	-4700	-17970	-4040	-4651	-17926	-4030	-4553
-17970	-4040	-4651	-17926	-4030	-4651	-17926	-4030	-4602	-17970	-4040	-4700	-17926	-4030	-4602
-17926	-4030	-4749	-16369	-3680	-4357	-14901	-3350	-3867	-13433	-3020	-3427	-11876	-2670	-3084
-10453	-2350	-2741	-8896	-2000	-2350	-7384	-1660	-1909	-5918	-1330	-1517	-4403	-990	-1126
-2935	-660	-734	-1467	-330	-195	0	0	48						

MULTI-STEP CREEP TEST, TEST 12 - LOAD = 29891 N (6720 LB) -

TIME (SEC)	STRAIN (με)	TIME (SEC)	STRAIN (με)	TIME (SEC)	STRAIN (με)	TIME (SEC)	STRAIN (με)	TIME (SEC)	STRAIN (με)
50	9104	100	9104	150	8906	200	9055	250	9055
300	9154	350	9055	400	9005	450	8857	500	8857
550	8906	600	8956	650	8906	700	8906	750	8708
800	8807	850	8758	900	8560	950	8758	1000	8906
1050	8857	1100	8857	1150	8857	1200	9005	1250	8857
1300	8857	1350	8807	1400	8906	1450	8956	1500	9005
1550	8857	1600	9055	1650	9104	1700	9055	1750	9104
1800	9104	1850	9203	1900	9104	1950	9253	2000	9154
2050	9154	2100	9104	2150	9154	2200	9154	2250	9203
2300	9302	2350	9352	2400	9352	2450	9302	2500	9401
2550	9302	2600	9500	2650	9549	2700	9401		

MULTI-STEP CREEP TEST, TEST 12 - LOAD = 30826 N (6930 LB) -

TIME (SEC)	STRAIN (με)	TIME (SEC)	STRAIN (με)	TIME (SEC)	STRAIN (με)	TIME (SEC)	STRAIN (με)	TIME (SEC)	STRAIN (με)
2750	9698	2800	9698	2850	9797	2900	9797	2950	9747
3000	9747	3050	9747	3100	9747	3150	9797	3200	9797
3250	9648	3300	9747	3350	9797	3400	9747	3450	9698
3500	9698	3550	9698	3600	9747	3650	9747	3700	9747
3750	9747	3800	9846	3850	9896	3900	10044	3950	10044
4000	10094	4050	10143	4100	10292	4150	10242	4200	10292
4250	10391	4300	10341	4350	10341	4400	10391	4450	10341
4500	10341	4550	10242	4600	10242	4650	10292	4700	10292
4750	10292	4800	10391	4850	10440	4900	10490	4950	10440
5000	10490	5050	10539	5100	10490	5150	10638	5200	10539
5250	10539	5300	10638	5350	10589	5400	10589	5450	10589
5500	10688	5550	10688	5600	10688	5650	10688	5700	10688
5750	10737	5800	10737	5850	10688	5900	10638	5950	10737
6000	10786	6050	10885	6100	10737	6150	10836	6200	10737
6250	10786	6300	10786	6350	10638				

MULTI-STEP CREEP TEST, TEST 12 - LOAD = 31804 N (7150 LB) -

TIME (SEC)	STRAIN (με)	TIME (SEC)	STRAIN (με)	TIME (SEC)	STRAIN (με)	TIME (SEC)	STRAIN (με)	TIME (SEC)	STRAIN (με)
6400	10836	6450	10984	6500	10836	6550	10836	6600	10935
6650	10836	6700	10786	6750	10885	6800	10885	6850	10935
6900	10885	6950	10885	7000	10786	7050	10984	7100	10885
7150	10935	7200	10935	7250	10984	7300	10935	7350	10984
7400	11034	7450	11083	7500	11034	7550	11083	7600	11133
7650	11133	7700	11133	7750	11133	7800	11232	7850	11133
7900	11133	7950	11182	8000	11133	8050	11133	8100	11232
8150	11281	8200	11232	8250	11232	8300	11182	8350	11232
8400	11182	8450	11182	8500	11281	8550	11133	8600	11182
8650	11133	8700	11479	8750	11331	8800	11281	8850	11281
8900	11232	8950	11430	9000	11331	9050	11281	9100	11331
9150	11281	9200	11281	9250	11331	9300	11331	9350	11281
9400	11331	9450	11331	9500	11380	9550	11380	9600	11281

MULTI-STEP CREEP TEST, TEST 12 - LOAD = 32736 N (7360 LB) -

TIME (SEC)	STRAIN (με)	TIME (SEC)	STRAIN (με)	TIME (SEC)	STRAIN (με)	TIME (SEC)	STRAIN (με)	TIME (SEC)	STRAIN (με)
9650	11430	9700	11677	9750	11628	9800	11727	9850	11677
9900	11677	9950	11727	10000	11677	10050	11776	10100	11826
10150	11776	10200	11776	10250	11826	10300	11875	10350	11875
10400	11875	10450	11974	10500	11974	10550	11925	10600	12024
10650	12024	10700	11826	10750	12073	10800	11974	10850	12123
10900	11974	10950	12073	11000	11974	11050	12073	11100	12073
11150	12073	11200	12123	11250	12123	11300	12073	11350	12073
11400	12024	11450	11925	11500	12024	11550	12024	11600	12073
11650	12073	11700	12024	11750	12123	11800	12123	11850	12024
11900	12123	11950	12024	12000	12172	12050	12172	12100	12320
12150	12271	12200	12172	12250	12221	12300	12271	12350	12320
12400	12419	12450	12469	12500	12370	12550	12320	12600	12419
12650	12419	12700	12370	12750	12370	12800	12419	12850	12469
12900	12469	12950	12469	13000	12419	13050	12320	13100	12469
13150	12419	13200	12419	13250	12518	13300	12518	13350	12518
13400	12568	13450	12518	13500	12617	13550	12617	13600	12667
13650	12617	13700	12667	13750	12617	13800	12667	13850	12617
13900	12716	13950	12766	14000	12766	14050	12716	14100	12766
14150	12865	14200	12766	14250	12865	14300	12865	14350	12766
14400	12766	14450	12815	14500	12766	14550	12716	14600	12766
14650	12766	14700	12766	14750	12766	14800	12815	14850	12815
14900	12815	14950	12815	15000	12865	15050	12914	15100	12914
15150	12914	15200	12914	15250	12964	15300	12865	15350	12914
15400	12964								

MULTI-STEP CREEP TEST, TEST 12 - LOAD = 33361 N (7500 LB) -

TIME (SEC)	STRAIN (με)	TIME (SEC)	STRAIN (με)	TIME (SEC)	STRAIN (με)	TIME (SEC)	STRAIN (με)	TIME (SEC)	STRAIN (με)
15450	13063	15500	13063	15550	13013	15600	13013	15650	13063
15700	13063	15750	13063	15800	13063	15850	13112	15900	13013
15950	13063	16000	13112	16050	13063	16100	13112	16150	13063
16200	13063	16250	13063	16300	13063	16350	13013	16400	13063
16450	13063	16500	13013	16550	13013	16600	13063	16650	13162
16700	13162	16750	13112	16800	13162	16850	13063	16900	13261
16950	13162	17000	13112	17050	13211	17100	13211	17150	13211
17200	13261	17250	13310	17300	13310	17350	13261	17400	13261
17450	13162	17500	13211	17550	13162	17600	13112	17650	13211
17700	13162	17750	13162	17800	13162	17850	13112	17900	13162
17950	13162								

MULTI-STEP CREEP TEST, TEST 12 - LOAD = 34117 N (7670 LB) -

TIME (SEC)	STRAIN (με)	TIME (SEC)	STRAIN (με)	TIME (SEC)	STRAIN (με)	TIME (SEC)	STRAIN (με)	TIME (SEC)	STRAIN (με)
18000	13459	18050	13409	18100	13409	18150	13409	18200	13459
18250	13557	18300	13557	18350	15933	18400	15933	18450	15834
18500	15834								